Synthesis, Structure and Magnetic Properties of Polynuclear Lanthanide Complexes

A Thesis
Submitted for the degree of
DOCTOR OF PHILOSOPHY

by

Amaleswari Rasamsetty

(11CHPH10)

School of Chemistry
University of Hyderabad
Hyderabad 500 046
Telangana
India

December, 2016

Dedicated

to

My Grandmother

STATEMENT

I hereby declare that the matter embodied in the thesis entitled **"*Synthesis, Structure and Magnetic Properties of Polynuclear Lanthanide Complexes*"** is the result of investigations carried out by me in the School of Chemistry, University of Hyderabad, India under the supervision of **Dr. Viswanathan Baskar**.

In keeping with the general practice of reporting scientific investigations, the acknowledgements have been made wherever the work described is based on the findings of other investigators. Any omission or error that might have crept in is regretted. This work is also free from plagiarism. I hereby agree that my thesis can be submitted in Shodhganga/INFLIBNET

December 2016 **Amaleswari Rasamsetty**

(11CHPH10)

Dr. Viswanathan Baskar
Associate Professor
School of Chemistry
University of Hyderabad
Telangana
Hyderabad-500 046, India

Phone: +91-40-2313 4825 (O)
Fax: +91-40-2301 2460
E-mail: vbsc@uohyd.ac.in
baskarviswanathan@gmail.com

CERTIFICATE

Certified that the work embodied in the thesis entitled **"*Synthesis, Structure and Magnetic Properties of Polynuclear Lanthanide Complexes*"** has been carried out by **Ms. Amaleswari Rasamsetty** under my supervision and the same has not been submitted elsewhere for any degree.

Viswanathan Baskar
(Thesis Supervisor)

Dean
School of Chemistry
University of Hyderabad

Acknowledgement

This thesis embodies the results of last few years' work whereby I have been accompanied and supported by many people. It is an honor and very pleasant opportunity to be able to express my gratitude to all of them.

I invariably fall short of words to express my heartfelt gratitude to my supervisor Dr. Viswanathan Baskar. His unerring support, coherence of scientific thoughts, insightful guidance along with great enthusiasm for research navigated me during the finest moments and the darkest hours of scholarly tenure.

I would like to express my sincere thanks to my doctoral committee members, Dr. R. Nagarajan and Dr. R. Balamurugan for their timely support.

Words are inadequate to express my heartiest obligation to Dr. Maheshwaran Shanmugam, Dr. Floriana Tuna and Dr. E. Carolina Sañudo for their help in Magnetic studies.

I wish to express my deep sense of indebtedness to Prof. M. Durga Prasad, Dean School of Chemistry and M. V. Rajasekharan, former Dean School of Chemistry.

I wish to express my deep sense of appreciation to the technical staff working in NMR and X-ray Diffraction facility of the school.

With utmost sincerity, I thank my senior colleagues- Dr. Anand Kumar Jami, Dr. P. V. V. N. Kishore, Dr. Sanathana Raj Prabu and Dr. N. Kumar for their generous help, critical suggestions and able guidance.

I sincerely thank all my present lab mates- U. Ugandhar, Junaid Ali, G. Narsimahulu and Suman Mondal for creating a cordial environment during my stay in Lab. Their assistance during the tenure of my work is gratefully acknowledged.

My special thanks to friends and colleagues- Kishore, Shruthi, Ranjani, Geetha, Showkat, Jyothi, Prabhu anna, Chinmoy Das, Ramakrishna, Indravath Krishna Naik, Sakthivel, Ram Kumar, Suman, Naveen, Sathiesh, Leela, Swathi, Swapna, Paulami, Harathi, Tamilarsi, Arumugam, Anif, Bhasha, Jagjeet, Nagamaiah and Sudheer for their camaraderie, constant support and helping me whenever necessary.

It is pleasure to thankfully acknowledge my school friends- Durga, Geetha, Chandrika, Swathi, Sarojini, Susmitha, B.Sc and M.Sc friends Sukanya, Kavitha, Sravanthi, Bhanu,

Divya, Lavanya, Priyanka, Madhu, Anitha, Prasanna, Kishore, Vinay, Kiran, Srinivas and Harish for being there at rough patches of my life.

I will not be sincere in my acknowledgements if I will not extend it to my Cousins-Mounika, Soniya Narayan, Bhrgavi, Vijaya, Murali anna, Suman, Honey, Padma, Durga Prasad, Kavitha akka, Rakesh, Leela, Uncles-Bhapanarao, Baburao, Ganesh and Aunts Devi, Kumari, Suguna and Sathya for their love and encouragement.

The close association of Neelima, Raji, Revathi, Sridevi akka and her family is unforgettable.

I have no words to express my heartfelt gratitude and respect towards my father Naga Hanuman and mother late Parvathi for their blessings, endless love and for teaching me the essence of education and integrity.

I heartily thank my beloved brother Leela Sankar and sister Lavanya whose unconditional love and affection has always been my strength.

My deepest gratitude goes to my grandmothers late Laksmi Dhaneswari and Late Savithri for their love and support.

Amaleswari Rasamsetty

CONTENTS

Title	Page No
Statement	ii
Certificate	iii
Acknowledgements	iv
Synopsis	xii
Chapter 1:- Introduction	1-59
1.1 General Introduction to Magnetism	1
1.2 Basic Principle of Magnetism	3
1.3 Introduction to Magneto chemistry	3
1.3.1 Magnetic Susceptibility	3
1.3.2 Magnetic Induction	4
1.3.3 Effect of temperature-Curie and Curie-Weiss Law	4
1.3.4 Magnetic hysteresis loop	5
1.4 Single Molecule Magnets (SMMs)	6
1.4.1 Magnetic anisotropy	7
1.4.2 Characterization techniques and important terms of SMMs	9
1.5 First SMM Mn_{12}-OAc	12
1.6 Transition Metal based SMMs:	13
1.6.1 SMMs Based on Manganese	14
1.6.2 SMMs Based on Iron	16
1.6.3 SMMs Based on Cobalt	18
1.6.4 SMMs Based on Nickel	19
1.7 SMMs with 3d-4f metal ions	19
1.8 Why lanthanides preferred over transition metals?	22

1.8.1 Lanthanide Chemistry 23

1.9 First 4f based SMM 24

1.10 General structural topologies in lanthanide cluster chemistry 26

1.11 Highlights from Ln based SMMs 27

1.11.1 Mononuclear SMMs 27

1.12 Multi-nuclear Lanthanide complexes 29

1.12.1 Dinuclear Lanthanide SMMs 29

1.12.2 Trinuclear Lanthanide SMMs 31

1.12.3 Tetranuclear Lanthanide SMMs 32

1.12.4 Pentanuclear Lanthanide SMMs 34

1.12.5 Higher nuclearity Lanthanide SMMs 35

Table 1.1 Some of the reported high nuclearity SMMs 36

1.13 Magnetocaloric Effect (MCE): Origin 36

1.13.1 Basic Theory 37

1.13.2 Measurement of the magnetocaloric effect 39

1.14 3*d*-Based molecular magnetic coolants 40

1.15 3*d*-4*f*-Based molecular magnetic coolants 42

1.16 4*f*-Based molecular magnetic coolants 44

Table 1.2 Some of the reported 4*f* -based magnetic coolants 46

1.17 Motivation for the work carried out 47

1.18 References 48

Chapter 2:- Hexanuclear lanthanide clusters encapsulating a μ_6-CO_3^{2-} ion displaying an unusual binding mode 61-79

2.1 Introduction 62

2.2 Experimental Section 63

2.2.1 General methods and Procedures 63

2.2.2 Instrumentation 63

2.2.3 General Synthetic procedure 64

2.3. Results and Discussion 64

2.3.1 Description of crystal structure 65

2.4. Magnetism studies 68

2.5. Conclusion 69

2.6. References 74

Chapter 3:- Effect of Coordination geometry on the Magnetic properties of a series of Di and Tetra nuclear Lanthanide Hydroxo Clusters 81-113

3.1. Introduction 82

3.2. Experimental Section 84

3.2.1 General information and Instrumentation 84

3.2.2 General Synthetic procedure for compounds 3.1-3.6 84

3.3 Results and Discussion 86

3.3.1 Structural Description for 3.1-3.3 86

3.3.2 Structural Description for 3.4-3.6 88

3.4 Magnetic properties 89

3.4.1 Static Magnetic Susceptibility 89

3.4.2 Ac magnetic susceptibility studies 92

3.4.3 Estimation of MCE efficiency 97

3.5 Conclusion 99

3.6 References 107

Chapter 4:- Triketone Assisted Self-Assembly of Lanthanide oxo/hydroxo clusters: Synthesis, Structure and Magnetic properties 115-139

4.1 Introduction 116

4.2 Experimental Section 118

4.2.1 General Information and Instrumentation 118

4.2.2 General synthetic procedure 118

4.2.3 X ray Crystallography 119

4.3 Results and Discussion 119

4.3.1 Description of the Crystal Structure for 4.1-4.4 120

4.3.2 Description of crystal structure of 4.4 120

4.4 Magnetic Properties 122

4.4.1 Static Magnetic Properties of 4.1-4.4 122

4.4.2 Dynamic Magnetic Properties 124

4.5 Conclusion 126

4.6 References 132

Chapter 5:- Unprecedented Octanuclear Ln(III) Clusters 141-156

5.1 Introduction 142

5.2 Experimental Section 143

5.2.1 General information 143

5.2.2 Synthesis 143

5.2.3 Instrumentation 144

5.3 Results and Discussion 144

5.4 Magnetic Measurements 146

5.5 Conclusion 148

5.6 References 153

Future Scope of the Thesis 157

List of Publications 158

Poster and Oral Presentations / Workshops 159

Abbreviations

SMM	single molecule magnet
MCE	magnetocaloric effect
cho	anion of chlorohydroxo pyridine
thf	tetrahydrofuran
hfac	hexafluoroacetylacetonate
H_3tpa	tris(pyrrolyl-α-methyl)amine
Mes	mesityl
iPr	isopropyl
$HBpz_3^-$	hydrotris(pyrazolyl)borate $HBpz_3^-$
ovn	o-vanillin
avnH_2	aldol-vanillin
DMF	dimethylformamide
H_2ovph	o-vanillin picolinoylhydrazone
acac	acetylacetone
tpaH	triphenylacetic acid
H_2EDDC	(*N′,N″,E,N′,N″,E*)-*N′,N″*- (ethane-1,2-diylidene)dipyrazine-2-carbohydrazide
H_2phendox	1,10-phenanthroline-2,9-dicarbaldehyde dioxime
DEA	diethanolamine
DMC	N, N-dimethylcarbamic acid anions

SYNOPSIS

This thesis is entitled as "Synthesis, Structure and Magnetic Properties of Polynuclear Lanthanide Complexes". It is divided into 5 chapters and details of each chapter are given below.

Chapter 1

Introduction: Detailed literature survey on Single molecule magnets (SMMs), Magnetocaloric effect (MCE) and synthesis of various Lanthanide oxo/hydroxo clusters. The introduction part concludes with the motivation for the present work that has been carried out in this thesis.

Chapter 2

Hexanuclear Lanthanide Clusters Encapsulating a μ_6-CO_3^{2-} Ion Displaying an Unusual Binding Mode

This chapter deals with the synthesis, characterization and magnetic properties of a series of hexanuclear lanthanide oxo clusters. These were synthesized by treating hydrated lanthanum halides with a functionalized β-diketone {[1-(2-HydroxyPhenyl)-3-(2-thienyl)-1,3-Propanedione]} in presence of a base. Single crystal X-ray diffraction reveals that cluster **2.1**-**2.3** are isostructural hexanuclear lanthanide clusters templated by μ_6-CO_3^{2-} introduced *via* spontaneous fixation of atmospheric carbon dioxide displaying a new coordination mode of binding. Magnetism studies carried out on **2.2** and **2.3** are also discussed in detail.

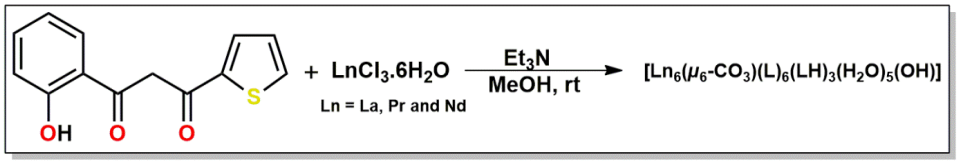

Scheme1

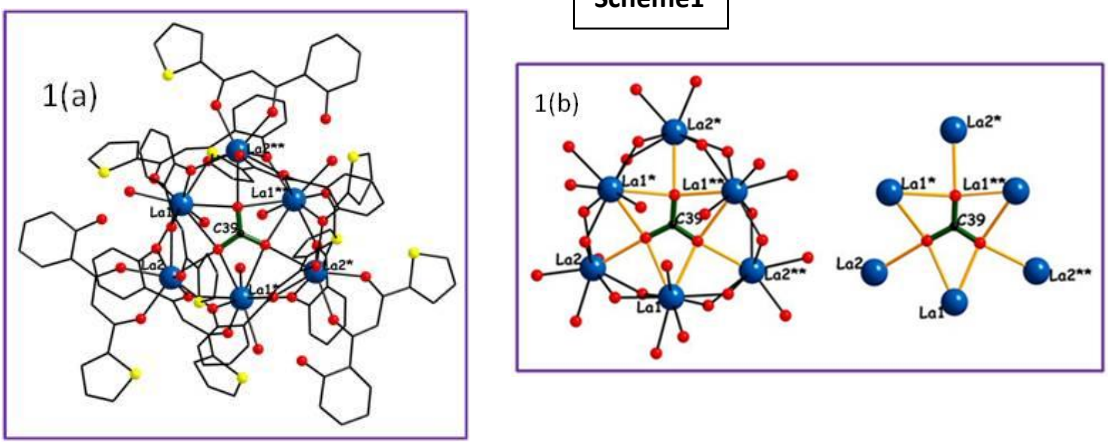

Figure. **(**1a) Solid state structure of compound **2.1** (1b) Core of the cluster showing coordination mode of CO_3^{2-} (μ_6-η^1:η^2:η^1:η^2:η^1:η^2).

Chapter 3

Effect of Coordination geometry on the Magnetic properties of a series of Di and Tetra nuclear Lanthanide Hydroxo Clusters

This chapter deals with the synthesis and characterization of two separate series of Ln(III) complexes achieved under ambient conditions. Of the two series one consists of three new compounds which are isostructural shows a distorted cubane like tetranuclear $[Ln_4(\mu_3\text{-}OH)_4(L)_4(\mu_2\text{-piv})_4(MeOH)_4]$ (Ln = Gd **3.1**, Dy **3.2** and Ho **3.3**) frameworks where as another series is represented by discrete dinuclear $[Ln_2(L)_4(\mu_2\text{-}LH_2')_2].4DMF/CH_3CN$ (Ln = Gd **3.4**, Dy **3.5** and Ho **3.6**) structural entities. Under similar reaction conditions, type of the co-ligand used has a profound role to play for deciding the final outcome of the reaction Magnetic studies were performed on all the complexes and the details are given in this chapter.

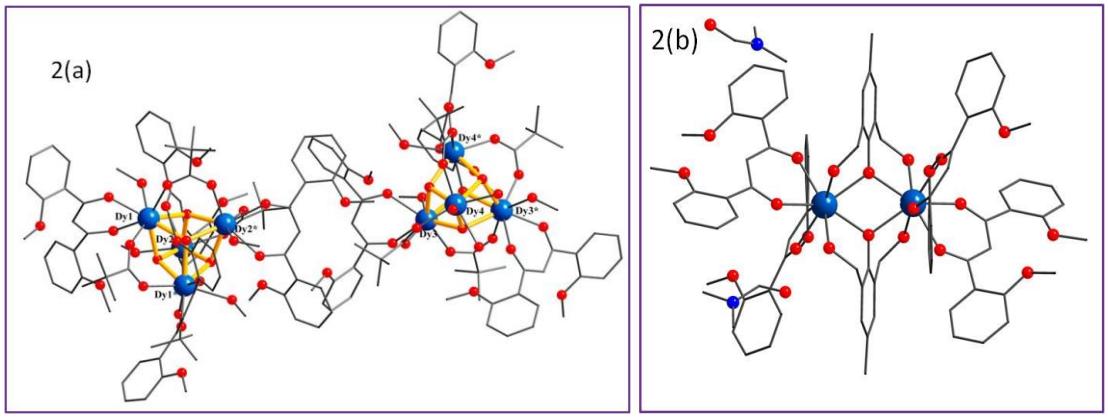

Figure. **(**2a) Solid state structure of compound **3.1**. (2b) Solid state structure of compound **3.5**.

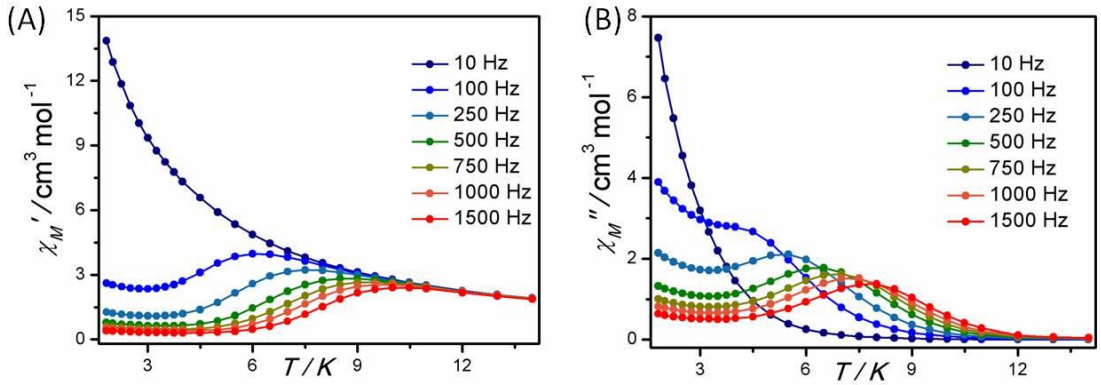

Figure 3. Ac magnetic susceptibility data for **3.5** at frequencies between 9 and 1500 Hz. in-phase (χ') signal vs T (A) and out of phase signal (χ'') vs T (B).

Chapter 4

Triketone Assisted Self-Assembly of Lanthanide oxo/hydroxo Clusters: Synthesis, Structure and Magnetic measurements

This chapter deals with the synthesis and characterization of a series of tetranuclear Ln(III) clusters (**1-3** $[Ln_4(\mu_3\text{-}OH)_2(phpt)_6(MeOH)_2].6CHCl_3$ (Ln=Dy(**4.1**) and Ho(**4.2**)), $[Dy_4(\mu_3\text{-}OH)_2(hfht)_6(MeOH)_2].2Et_3N.4CH_3OH$ (**4.3**)) which have been isolated by the reaction of triketones (1,5-diphenylpentane-1,3,5-trione(H2phpt), 1,1,1,7,7,7-Hexafluoroheptane-2,4,6-trione(H_2hfht)) with $Ln(NO_3)_3.6H_2O$ (Ln(III) = Dy and Ho) in presence of triethylamine as a base. Using acetylacetone (acac) as co-ligand along with H_2hfht resulted in the isolation of a tetranuclear cluster **4.4** ($[Dy_4(\mu_3\text{-}OH)_2(acac)_4(hfht)_6].2CHCl3$) similar to **4.1-4.3**. Single cystal X-ray diffraction reveals that all the complexes are isostructural. Magnetic studies were performed on all the complexes and the details are given in this chapter.

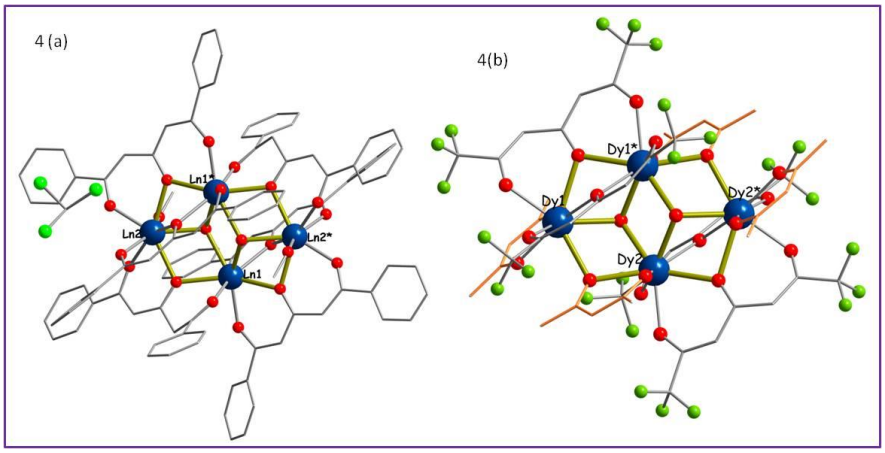

Figure. **(**4a) Solid state structure of compound **4.1** (2b) Solid state structure of compound **4.4**.

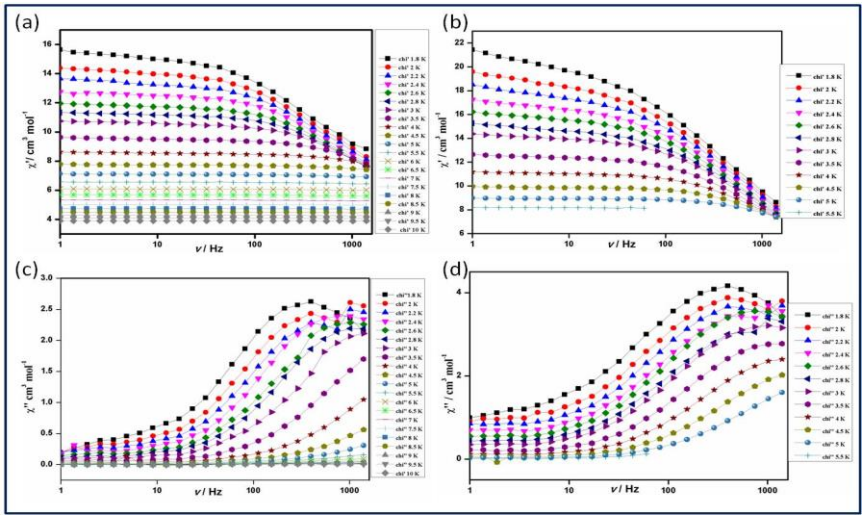

Figure 5. Alternating current magnetic susceptibility measurement performed on polycrystalline samples of **3** and **4** showing the frequency dependent in-phase (χ_M') [(a) and (b)] and out-of-phase susceptibility signals (χ_M'') in applied magnetic field of 1000 Oe [(c) and (d)].

Chapter 5

Unprecedented Octanuclear Ln(III) clusters: Synthesis, Structure and Magnetic measurements

This chapter deals with the synthesis and characterization of a series of novel octanuclear Ln(III) clusters $[Ln_8(\mu_2\text{-}\eta^1\text{:}\eta^1 cyc PO_2)_{12}(NO_3)_6(OH)_2]4OH$ {Ln = Gd(**5.1**), Dy(**5.2**) and Y(**5.3**)}. These are the first examples of organophosphinate based Ln(III) clusters. These complexes have been synthesized by the reaction of 1,1,2,3,3-pentamethyltrimethylenephosphinic acid ($cyc PO_2H.2H_2O$) with $Ln(NO_3)_3.6H_2O$ in presence of base under refluxion. Single crystal X-ray structural elucidation reveals the formation of octanuclear clusters with nitrate coordination. The details of the synthesis, structural characterization and magnetic studies are given in detail in this chapter.

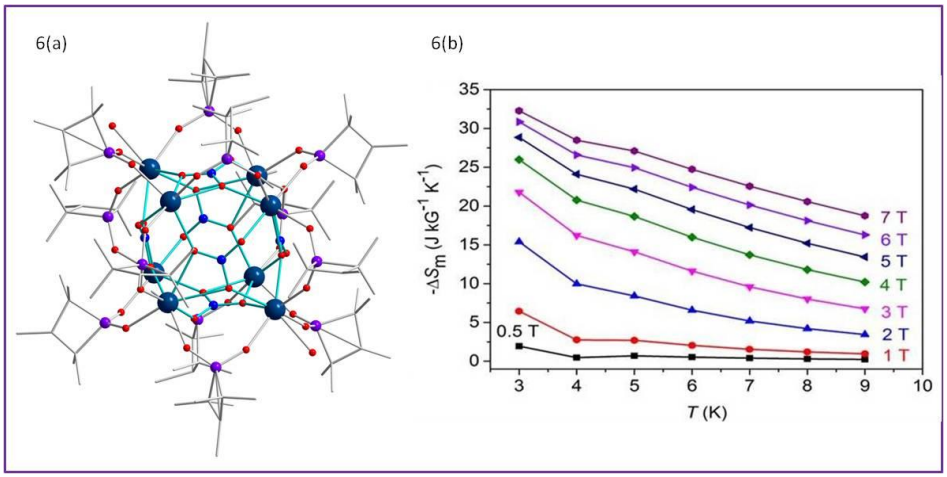

Figure. **(**6a) Solid state structure of compound **5.1 (**6b) $-\Delta S_m$ calculated by using the magnetization data of **5.1** at different fields and temperatures.

**********The end of Synopsis**********

Introduction

CHAPTER 1

1.1 General Introduction Magnetism

The phenomenon of 'magnetism' owes its origin to pre-historic times from the ancient Greek city of magnesia. Though ancient Greeks were first to start accessing the magnetic properties of Iodestone (Fe_2O_3) which they were commonly using for removing nails from sandals, Chinese were able to use its properties for developing compass for the first time. However, both these civilizations were completely unaware of the underlying physical forces giving birth to this unusual behaviour. Though there was a clear lacuna between these fascinating properties of this material and their respective interpretation at that time, the detailed study of magnetism became of prime importance and interest in 19^{th} and 20^{th} century. The progressive study of magnetic properties finally started culminating in the characterization of a number of magnetic materials which have become indispensible in modern technological world. Many appliances which are in common use mostly rely on magnetic properties of inorganic transition or lanthanide metal oxides. Simplest examples being medical instruments, loud speakers, microphones, sensors, data storage devices, switches etc.

In presence of external magnetic field, properties of all materials are governed by electronic configuration of their atoms and ions. In case of a diamagnetic material, electrons are exactly spin paired, whereas there is presence of unpaired electrons for paramagnetic one and if these paramagnetic centers are in vicinity, interactions between metal centers become of prime importance which further give rise to ferro-, anti-ferro- and ferrimagnetism (figure 1.1).

a) Diamagnetism: All electrons are spin paired thereby causing their individual magnetic fields to cancel. When in an external magnetic field, the magnetic moment opposes the applied field resulting in a weak negative magnetic susceptibility which will not be retained when field is removed.

b) Paramagnetism: Due to presence of unpaired electrons, their magnetic moment augments the external magnetic field and hence gives rise to small positive susceptibility which is lost when external field is removed.

c) Ferromagnetism: Like paramagnetic substances, ferromagnetic materials have unpaired electrons. However, in addition to the tendency of intrinsic magnetic moment of electrons to be parallel to applied field, these magnetic moments orient parallel to each other and hence there is presence of net magnetic moment which is retained even in absence of the external field. Each and every ferromagnetic material shows the ferromagnetic behavior up to a characteristic temperature called the Curie temperature or Curie point.

d) Anti-ferromagnetism: The neighbouring electrons having the intrinsic magnetic moment that tends to point in opposite direction and each neighbour is anti-parallel. Hence there is a zero net magnetic moment. Generally it exists at sufficiently low temperature and above a certain temperature called the Neel temperature, it shows paramagnetism.

e) Ferrimagnetism: The electron spins of adjacent electrons are oppositely directed and these materials retain their magnetic properties even on removal of external magnetic field. Though like antiferromagnetic substances, in ferrimagnets all adjacent spins are aligned antiparallel but adjacent magnetic moments are not equal in strength which leads to non-zero residual magnetic moment even at absolute zero Kelvin.

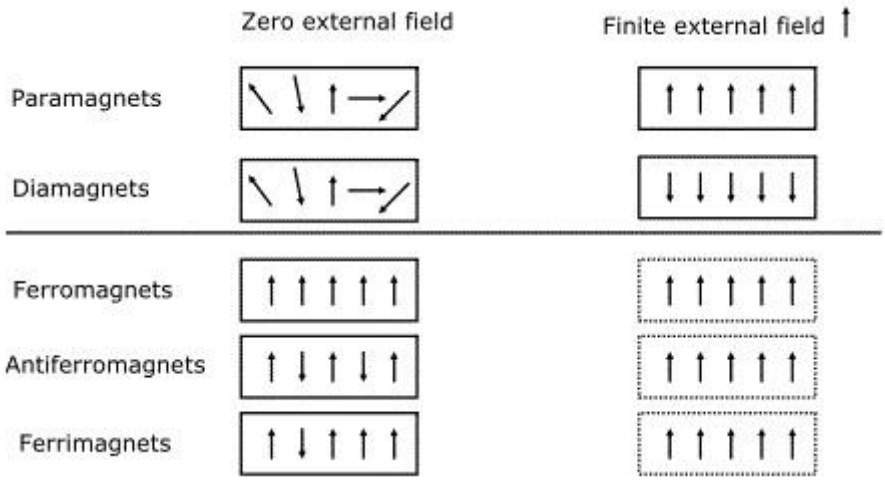

Figure 1.1. Types of Magnetic behaviour

1.2 Basic Principle of Magnetism

Individual magnetic moment of the spinning electrons, which is a combination of the orbital angular momentum and its intrinsic angular momentum, is the cause of the magnetism for magnetic materials. As per the laws of electrodynamics, motion of any charged particle like electron around the nucleus gives rise to orbital magnetic moment which can be described as shown in equation 1.1

$$\mu_{\mathrm{L}} = -\frac{e}{2m}L \qquad (1.1)$$

where *m*, e and L denotes mass, charge and orbital angular momentum of electron respectively.

Likewise the magnetic moment, μ-spin(or μ_S) which arises because of the intrinsic spin of the electron and contributes to its total magnetic moment, can be calculated as

$$\mu_{\mathrm{s}} = -\frac{e}{m}S \qquad (1.2)$$

where *S* denotes spin angular momentum

Hence, $$\mu_{\mathrm{total}} = \mu_{\mathrm{L}} + \mu_{\mathrm{s}} \qquad (1.3)$$

1.3 Introduction to Magneto chemistry

The study of the variations in magnetic properties of compounds corresponding to their structural alterations arising from the spin and orbital angular momentum of electrons is known as magnetochemistry.

As far as electronic structure and magnetic exchange interactions in metal complexes are concerned magnetic measurements are very important source to unravel the corresponding information.

1.3.1 Magnetic Susceptibility:

The magnetic susceptibility is the most important and prime measurement in magneto chemistry that quantifies the strength of interaction of any compound with an external magnetic field and is represented as χ given by the equation:

$$\mathrm{M} = \chi \times \mathrm{H} \qquad (1.4)$$

where M is magnetization (magnetic dipole moment per unit volume), H is magnetic field strength.

1.3.2 Magnetic Induction:

For a substance in an external magnetic field (H), the density of magnetic lines of force known as magnetic induction or magnetic flux density (B). As magnetic field density and the magnetic field (H) are co-related by permeability (μ_0)

$$B = \mu H \tag{1.5}$$

$$B = \mu_0 H + \mu_0 M \tag{1.6}$$

where μ_0 is permeability of free space, $\mu_0 H$ and $\mu_0 M$ are respective inductions contributed by field and sample respectively.

$$\text{Since } \chi = \frac{M}{H}, \text{ therefore } \mu = \mu_0 (1 + \chi) \text{ or } \mu/\mu_0 = (1 + \chi) \tag{1.7}$$

where μ/μ_0 is called relative permeability

1.3.3 Effect of temperature-Curie and Curie-Weiss Law:

Many paramagnetic substances especially at higher temperature follow Curie law which accounts for their molar susceptibility and is described as

$$\chi = \frac{C}{T} \tag{1.8}$$

where C is the curie constant which depends upon spin multiplicity of ground state while T is temperature.

In case of ferro and anti-ferromagnetic substances where there are spontaneous interactions between adjacent spins, magnetic susceptibility could be described by modified Curie law known as Curie-Weiss law

$$\chi = \frac{C}{T - \theta} \tag{1.9}$$

where C, T and θ are Curie constant, temperature and the Weiss constant or Weiss temperature respectively. Positive θ indicates ferromagnetic interactions while negative θ

indicates anti-ferromagnetic interactions between metal centres and the behaviour is shown in figure 1.2(a).

Magnetic susceptibility is measured as a function of temperature and data is plotted as χ *vs* T. In case of diamagnetic substances, magnetic susceptibility is invariant with temperature and for paramagnetic substances it is inversely proportional to temperature. Ferromagnetic substances have characteristic Curie temperature (T_C) above which it behaves as a simple paramagnet but below this temperature χ increases rapidly. Likewise anti-ferromagnetic substances possess a characteristic temperature known as Neel-temperature (T_N) above which it acts as a paramagnet and below this temperature χ decreases with decreasing temperature as shown in figure 1.2(b).

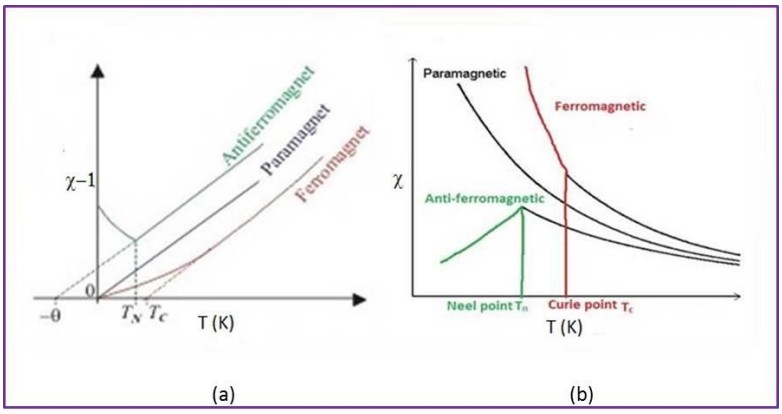

Figure 1.2. (a) Comparison of susceptibility (χ^{-1}) *vs* temperature (b) χ *vs* T plot for the ferromagnetic, antiferromagnetic and paramagnetic materials.

1.3.4 Magnetic hysteresis loop:

This property is exhibited by ferro- or ferrimagnetic substances. When these substances are subjected to an external magnetic field, the domains of these species align parallel to the field and the substance become magnetized and reaching a saturation point of its magnetization. When external magnetic field is removed, magnetization does not reach zero because some of the domains do not change their alignment and the residual magnetization is called as remenant magnetization (M_r). In order to bring magnetization back to zero, field needs to be applied in the opposite direction called coercieve field (H_c). Saturation of magnetization is also achieved by applying an opposite field and then decreasing the field and reversing it again in the opposite direction completes the loop after going through a point with zero magnetization. This spontaneous magnetization after

a magnetic field is applied and removed is known as hysteresis (figure 1.3). A narrow loop suggests a soft magnet (low $H_{c)}$ and a broad loop suggest hard magnet (large H_c) or permanent magnet. Due to its bistability or magnetic memory, hysteresis is a desirable quality of a magnetic material for device applications.

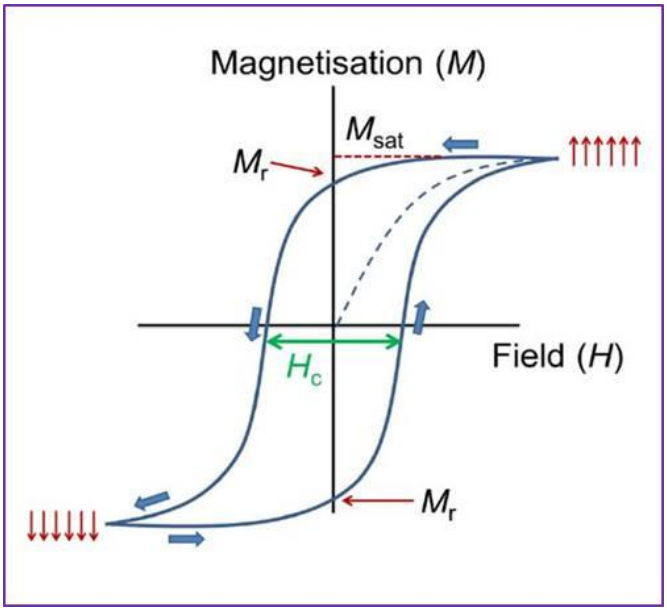

Figure 1.3. Representation of a hysteresis loop, showing the remnant magnetization M_r and the coercive fields +/- H_c.

The magnetic behavior of any material is primarily decided by presence of unpaired electrons. The magnetic field that a magnetic substance displays is the consequence of an electrical charge in motion, particularly the spin and orbital angular moment of the electrons within atoms of a material. These materials are called as atom-based magnets. In 1990's the development of a novel class of molecular magnetic materials, known as Single Molecule Magnets (SMMs) was one of the exciting discoveries.[1,2] The ability to scale down the size of magnetic devices by virtue of single molecules to behave as potential bulk magnets is an exciting field for researchers working in this field.

1.4 Single Molecule Magnets (SMMs)

In general, single molecule magnets (SMMs) are discrete polynuclear complexes comprised of a magnetic core (exchange coupled core) surrounded by organic moieties which prevents the core from interacting with neighbouring spins by minimizing the intermolecular interactions. The magnetic core is responsible for the observed magnetic

moment associated with molecule. These molecules become magnetized upon introduction of an external magnetic field and retain their magnetization even after removal of the field for a significant period of time. In addition these molecules show magnetic hysteresis below a certain temperature called blocking temperature T_B and their magnetic behaviour is purely molecular in origin. In general, double well potential energy diagram is used to explain relaxation process and magnetization. SMMs exhibit a special feature of bistability which results from separating opposite spin projection along the easy axis. Anisotropy barrier which prevents reorientation of the spins of molecules is called as effective energy barrier represented as U_{eff}. SMMs have attracted attention from physicists, materialists and chemists owing to their potential applications in spintronic devices,[3] high density information storage devices[4] and in quantum computing.[5]

The two essential properties for molecules to exhibit SMM behaviour are 1) large negative uniaxial magnetic anisotropy and 2) a doubly degenerate non-zero ground state ($S \neq 0$). Combination of these two results in an energy barrier U which is equal to $S^2|D|$ for an integer spin and $(S^2\text{-}1/4)|D|$ for half integer spins respectively.

1.4.1 Magnetic anisotropy:

It is the most important concept to be understood while studying SMMs. Magnetic anisotropy can be described as the directional dependence of magnetic properties of a material. In the absence of external magnetic field, if a molecule is isotropic the magnetic moment doesn't align in any direction but if a molecule is having anisotropy, the magnetic moment will prefer to align in a particular direction called as easy axis and is assigned z-direction and the plane perpendicular to it is called as hard plane. Spin-orbit coupling and zero-field splitting are responsible for the magnetic anisotropy of a system. Electrons possess spin and therefore angular momentum exists known as spin angular momentums (S), orbitals of an atom also possess angular momentum known as orbital angular momentum (L). The interaction of spin and orbital angular momentum is called as spin-orbit coupling (LS coupling). The total angular momentum is denoted by J which takes values from (L+S) to (L-S) (figure 1.4).

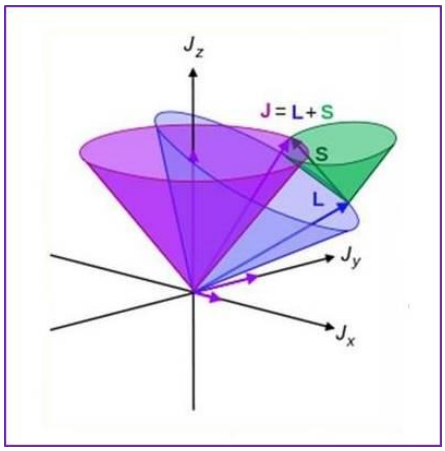

Figure 1.4. Graphical representation of spin-orbit coupling (Russel-Saunders coupling). Spin angular momentum (*S*, green) is summed with orbital angular momentum (*L*, blue) to give resulting overall angular momentum (*J*, purple). Adapted from ref 6a

The ground state term of an atom is denoted as $^{2S+1}L_J$ where S is the total spin angular momentum of all the electrons which possess $m_s = \pm 1/2$ and $2S+1$ is the spin multiplicity which accounts the number of spin-orbit states. *L* is the total orbital angular momentum and will change which is represented by S, P, D, F, etc., corresponding to the values of *L* = 0, 1, 2, 3 and onwards. *J* is the total angular momentum of the system which can be calculated as follows: if the free metal ion is less than half-filled it takes the value of *L*-*S* and if metal ion is more than half filled it takes the value of *L*+*S*, different values of *J* indicates different energy levels. If metal ion is exactly half filled (example in case of isotropic metal ion like Mn^{+2} and Gd^{+3}) *L* = 0, then *J* = *S*.

While studying the magnetic properties of transition and inner transition metal ions, spin-orbit coupling is an important parameter. In case of 3d metal ions, spin-orbit coupling is usually reduced by ligand field and as a result quenches orbital angular momentum and anisotropy of the system,[7] However it is true only when coordination number of metal ion is large. The contribution of ligand field weakens when coordination number of metal ion is reduced and in such cases spin-orbit coupling acts as the primary force affecting the magnetic anisotropy. In 2009, Riordan and co-workers reported that a sulphur-ligated Fe(II) complex with only four donor atoms possess a pseudo-tetrahedral geometry and has a large negative zero field splitting parameter (D = -33 cm^{-1}).[8] This splitting was attributed to the spin-orbit coupling of the the lowest lying orbitals having energy gap small enough to allow mixing. In 2010, Long and co-workers reported that octahedral Cr(II) and Cr(III)

complexes show enhanced anisotropy due to spin-orbit coupling resulting from bulky auxillary groups (*i.e*. Cl, Br and I) in the ligands.[9] Spin-orbit coupling is more pronounced when studying heavy metal ions like lanthanides, which possess valence electrons in 4*f* orbitals which are shielded by 6s and 5d electrons so the effective nuclear charge increases. Spin-orbit coupling increases if effective nuclear charge increases, therefore heavier lanthanides particularly Tb(III) and Dy(III) show strong spin-orbit coupling and gap between ground and first excited states is large enough to makes them useful candidates to act as single molecule magnets.

Zero field splitting (ZFS) affects the magnetic anisotropy (denoted by *D*) which refers to the loss of degeneracy in M_s or M_j levels even in the absence of external magnetic fields. It arises due to spin –orbit interactions, overall symmetry of the molecule, coordination geometry of the metal centre and bulk crystal packing. In other words it is splitting of 2S+1 microstates (when S≥1/2) in the absence of external magnetic field. The most important aspect is its sign, a negative value of *D* (easy-axis anisotropy) stabilizes the highest $\pm M_s$ levels resulting in the observation of an energy barrier for the slow relaxation of magnetization and a positive *D* value (easy-plane anisotropy) stabilizes the lowest $\pm M_s$ states (*i.e*. *M*s=0 in an integer or *M*s=±1/2 in a half integer spin system respectively) which precludes the observation of energy barrier (figure 1.5).

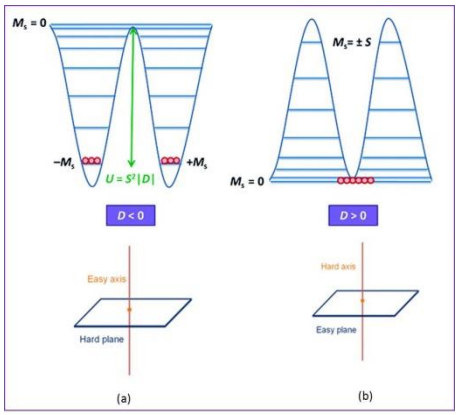

Figure 1.5. Schematic representation of the double-well energy diagram for two different cases where *D* is negative (a) or positive (b).

1.4.2 Characterization techniques and important terms of SMMs:

A helium cooled super conducting quantum interference device (SQUID) magnetometer is used to measure extremely subtle magnetic fields as low as 5 x 10^{-8} T. Unlike in traditional magnetometer, the coils are inductively coupled to super conducting loop (SQUID) which

can detect tiny magnetic flux. There are two different types of SQUID magnetometers, one is direct current (dc) and the other one is alternating current (ac) operated by direct and alternative currents respectively. All paramagnetic materials exhibit an in-phase magnetic susceptibility (χ') signal, but the evidence for SMM behaviour is the observation of an out-of-phase susceptibility (χ'') response with varying frequencies, temperature and applied fields and the observation of hysteresis loop. Since in many cases, hysteresis loop is observed below instrument level, majority of SMMs are characterized by ac measurements. The relaxation rates can be measured by using ac susceptibility measurements which will be carried out at very low temperatures (below 50 K) since the blocking temperature has not exceeded 15 K till date. To study the ac magnetic susceptibility data and to derive energy barrier for spin reversal, commonly used plots are χ'' *vs.* T or χ'' *vs.* ν along with Arrhenius plot ln(τ) *vs.* 1/T. The main characteristic feature of SMM includes not only a signal in the χ'' *vs.* T or χ'' *vs.* ν plot but also shifting of peaks at different temperatures or different frequencies. In χ'' *vs.* T plot, the frequencies range from 0.1 to 1500 Hz (limits of commonly used SQUID magnetometers). In this plot, intermolecular interactions could be regarded as negligible when there is an increase in the intensity of peaks which are shifting towards lower temperature. However increase in the intensity of peaks initially and then followed by a decrease at lower temperatures indicates significant intermolecular interactions within the sample. It is an important characteristic feature of SMM that intermolecular interactions should be minimized and the magnetic behaviour must be purely molecular in origin. Often the observed increase at the end of the curves (Figure 1.6a) is attributed to quantum tunneling pathways (QTM) through the energy barrier for spin reversal. If the available thermal energy is lesser than the height of energy barrier, the energy barrier will oppose the reorientation of the magnetization and hence relaxation of magnetization will be slow. Recently, χ'' *vs.* ν plots are being used to analyze ac data which gives more information and more reliable data due to the accuracy with which the frequency can be controlled as opposed to the temperature.

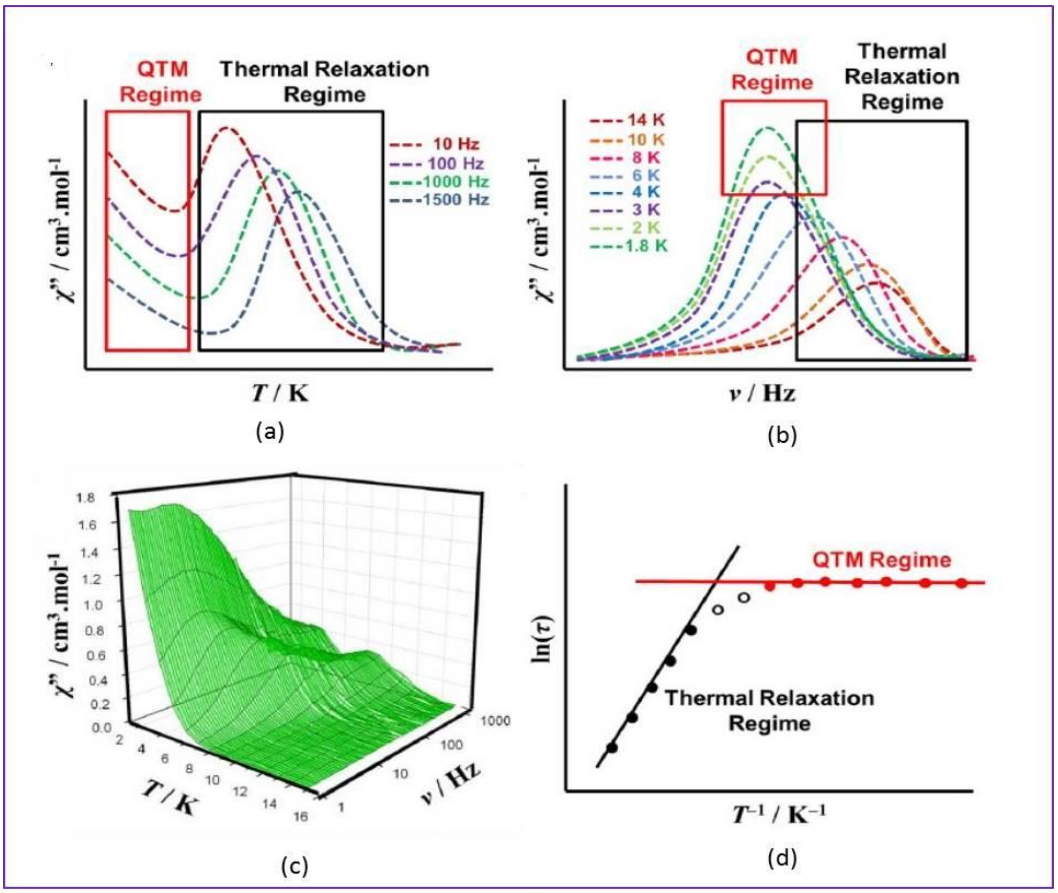

Figure 1.6. Alternating current (ac) data plots (a) Out-of-phase magnetic susceptability χ'' *vs.* temperature (b) Out-of-phase magnetic susceptability χ'' *vs.* frequency where both quantum tunneling and thermal relaxation regimes were shown (c) 3-D plot using both temperature and frequency dependence of χ'' d) Arrhenius plot.

Figure 1.6 (c) shows combination of both the sets of data in a 3-D plot and allows revealing hidden peaks when only one X-axis is used. Using this plot, we can visualize how and where the two peaks become one when the x-axis is frequency. In χ'' *vs.* ν plot, the peaks at different temperature corresponds to $\tau = (2\pi\nu)^{-1}$ and by using this formula, relaxation time (τ_0) at that particular temperature can be obtained by calculating frequency at which the peak occurs using a simple Gaussian fit. The relaxation process of an SMM follows Arrhenius principle, for a thermal activation process to overcome the energy barrier with $\tau = \tau_0 \exp(U_{eff}/KT)$n or $\ln(\tau) = \ln(\tau_0) + U_{eff}/KT$(Figure 1.6d represents the Arrhenius plot). Where K represents Boltzmann constant, T is temperature and τ_0 is pre-exponential factor. In the Arrhenius plot, the slope of the strait line (thermal relaxation regime) will give the U_{eff} and Intercept gives the pre exponential factor (τ_0).

1.5 First SMM Mn_{12}-OAc

The very first and the most studied SMM discovered is the $[Mn_{12}O_{12}(CH_3COO)_{16}(H_2)_4]\cdot 2CHO_3COOH\cdot 4H_2O$ cluster commonly called as Mn_{12}-OAc, whose structure is shown in figure 1.7a. Though this molecule was synthesized by Lis in 1980,[10] until 1990 its magnetic properties were not studied. However in 1993, Sessoli, Gatteschi and Caneschi reported that magnetic moment of the molecule could be retained after the removal of an external magnetic field.[11] The demonstration of retention of magnetization or slow magnetic relaxation in a zero-dimensional molecule gave birth to the field of single molecule magnetism. The Mn_{12}-OAc cluster contains four tetrahedral Mn(IV) ions (S = 3/2) (a central Mn_4O_4 cubane) surrounded by eight octahedral Mn(III) ions (S = 2) bridged via oxygen atoms which define a crown-like geometry around the Mn_4O_4 cubane (figure 1.7b). All the eight Mn(III) ions in the outer crown and four Mn(IV) ions in the central cubane are ferromagnetically coupled among themselves and at low temperatures they are antiferromagnetically coupled resulting in an S = 10 ground state. Magnetic anisotropy in this complex arises due to the alignment of all the Jahn-Teller axes of Mn(III) ions in the same direction which gives rise to the large and negative axial anisotropy.

Axial anisotorpy within the molecule induces splitting of ground state with $2S+1$ fold degeneracy. For an S = 10 ground state, 21 microstates are possible with $m_s = \pm 10, \pm 9, \pm 8, \pm 7 \ldots\ldots 0$ as depicted in figure 1.7c. In the absence of external magnetic field, $m_s = \pm 10$ states are in lowest energy and $m_s = 0$ state highest energy leading to an energy barrier for the reversal of spin magnetization. Electron paramagnetic resonance (EPR) measurements made by Hill and co-workers found that the D value was -0.47 cm^{-1} confirming that D was negative which supports that ground state was $m_s \pm 10$. The potential energy barrier for the reversal of spin depends on zero field splitting parameter (D) and the ground state spin (S) by using relation $U_{eff} = S^2 \mid D \mid$, where U_{eff} is the anisotropy barrier for the reorientation of spin from ms = +10 to ms = -10 or vice versa. For Mn_{12}-OAc, the experimental energy barrier value is 44 cm^{-1} which is significantly lower than the expected theoretical value of 52cm^{-1}. The ac susceptibility measurements show that there were frequency depend out-of-phase signals indicating slow magnetic relaxation. In the hysteresis loop it was noticed that a curve with sharp steps at regular interval times was observed instead of smooth

curve. Finally it was concluded that the steps observed are due to relaxation occurring through quantum tunnelling mechanism.

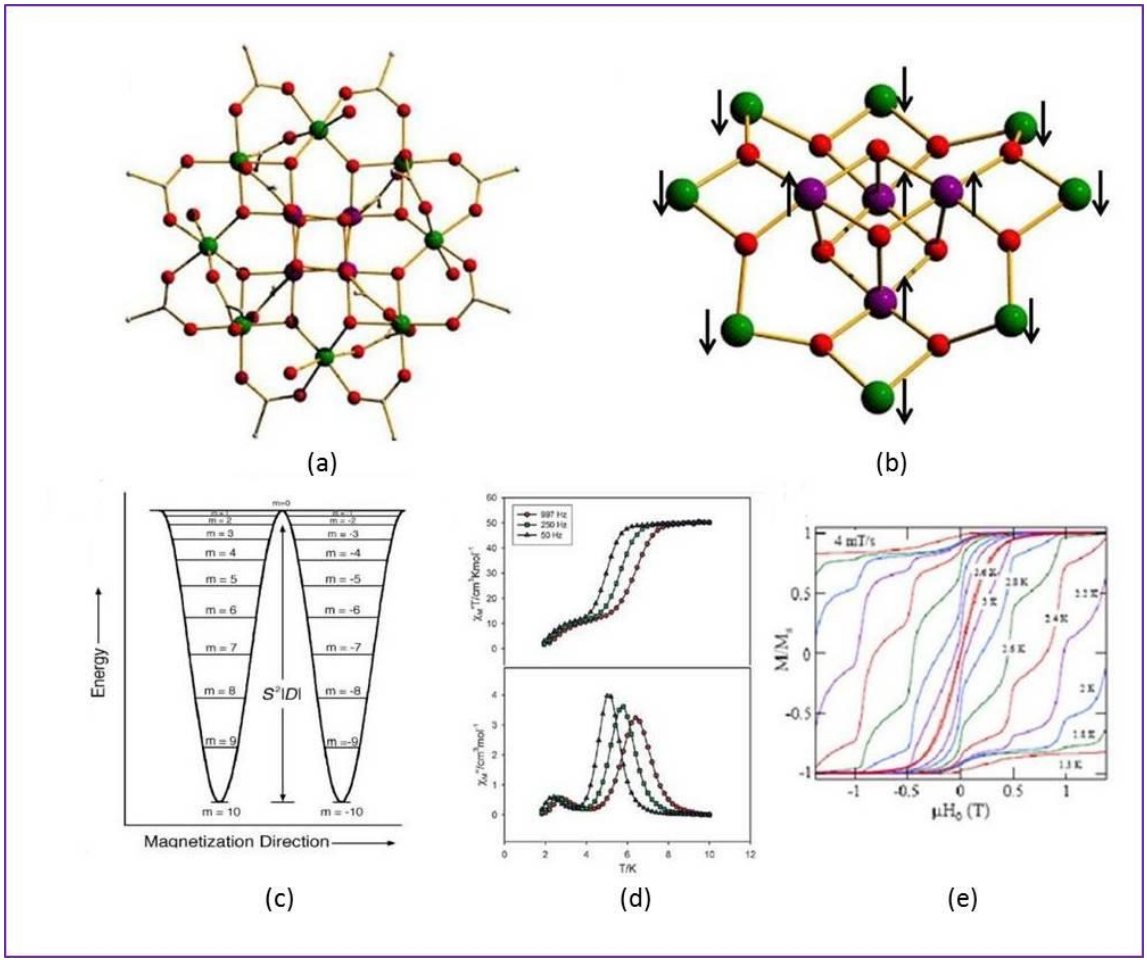

Figure 1.7. (a) Ball and stick representation of Mn_{12}-OAc (b) core of Mn_{12}-OAc with spin orientations (c) Schematic representation of the low lying energy diagram of Mn_{12}-OAc. (d) In-phase and out–phase ac susceptibility of Mn12-Ac. (e) Hysteresis loop

1.6 Transition Metal based SMMs

After the discovery of Mn_{12}-OAc as SMM, most of the efforts have been devoted to make polynuclear metal clusters containing 3d metal ions as central metals to achieve large energy barriers for slow relaxation of magnetization. [12] Among these Manganese (Mn), Iron (Fe), Cobalt (Co) and Nickel (Ni) based SMMs have been studied extensively.

1.6.1 SMMs Based on Manganese:

Manganese is widely used metal for making SMMs because of two fundamental reasons 1) Manganese exhibits variable oxidation states such as Mn^{+2}, Mn^{+3} and Mn^{+4} in polynuclear metal complexes, due to which it leads to antiferromagnetic interactions between the nearest metals. Moreover possessing different number of unpaired electrons results in the stabilization of non-zero ground state. Complexes containing Manganese (Mn) are likely to have large ground state (*S*) compared to other 3d transition metal ions. 2) Jahn –Teller distortion in Mn^{+3} (d^4) ions lead to increased magnetic anisotropy (*D*) of the complexes due to reduction in the symmetry from $Oh \rightarrow D_{4h}$. Combination of these two factors result in appreciable energy barriers. A large number of manganese based complexes with nuclearity ranging from Mn_1 to Mn_{84}[13] have been reported with *S* values ranging from 3/2 to 83/2. Since it is easy to prepare, large number of Mn_{12}-derivatives have been extensively prepared using different ligands like carboxylates,[14] sulfonates,[15] phosphinates,[16] nitrates,[17] and dicarboxylates.[18] In order to obtain large energy barriers, initially research was focused on increase number of metal centres to provide large spins (*S*).

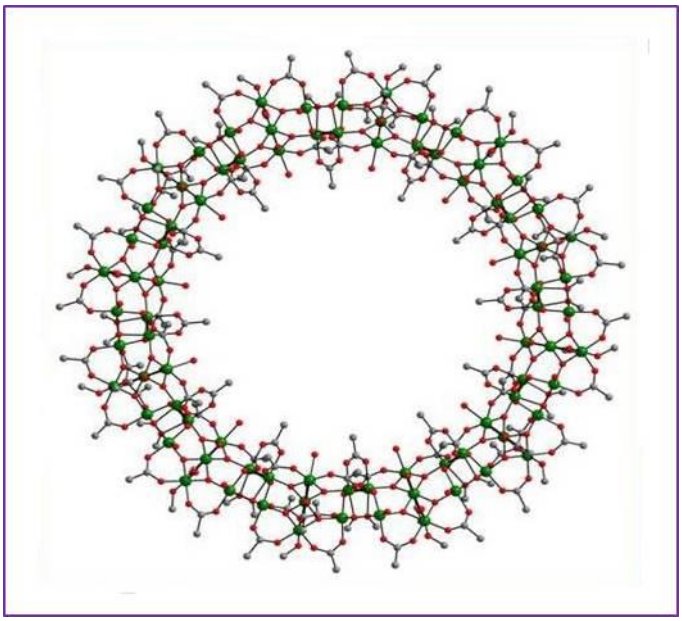

Figure 1.8. Molecular structure of Mn_{84}

In this regard, Christou and co-workers reported a giant wheel like manganese complex $[Mn_{84}O_{72}(O_2CCH_3)_{78}(OCH_3)_{24}(OH)_6(CH_3OH)_{12}(H_2O)_{42}]$ (figure 1.8) which has been synthesized by the reaction of Mn_{12}-OAc precursor with $NBu^n_4MnO_4$ in a mixture of MeOH and glacial acetic acid at room temperature.[13s] Despite its massive size it shows

small spin ground state ($S \approx 6$) due to dominant antiferromagnetic interactions between the metal ions. The observed energy barrier for the reversal of spin magnetization is only 18 K which is smaller than the Mn_{12}-OAc and its analogues. In 2006, Christou group reported a bromoacetate analogue ($[Mn_{12}O_{12}(O_2CCH_2Br)_{16}(H_2O)_4]$) of Mn_{12} family showing highest energy barrier (74.4 K) and blocking temperature (T_B) up to 3.5 K.[13t]

In 2006, Powell and co-workers have reported a Mn_{19} cluster formulated as $[Mn^{III}_{12}Mn^{II}_{7}(\mu_4\text{-}O)_8(\mu3,\eta^1\text{-}N_3)_8(HL)_{12}(CH_3CN)_6]$ with highest spin ground state $S = 83/2$. It was synthesized by the reaction of $MnCl_2.4H_2O$ with H_3L [2,6-bis(hydroxyl methyl)-4 methyl phenol)] in presence of NaN_3 in Methanol and NaO_2CMe in acetonitrile at room temperature.[13d] It is an interesting structure in which two Mn_9 fragments are connected through one Mn(II) metal centre (figure 1.9a). The use of organic and azido ligands which bridge multiple metal centers resulted in a Mn_{19} cluster which possess dominant ferromagnetic interactions which in turn gives the maximum spin ground state ($S = 83/2$). However the complex shows hysteresis at very low temperature (0.5 K) and doesn't show high energy barrier for the reversal of magnetization. Eventhough Mn(III) centers show greater degree of Jahn-Teller distortions, their strong ferromagnetic interactions between spin carriers and geometrical arrangement lead to a system with very low anisotropy which resulted in low values of U_{eff} and T_B. Brechin and co-workers reported a family of hexanuclear manganese complexes $[Mn^{III}_6O_2(sao)_6(O_2CR)_2L_4]$ (where R = H, Me, Ph etc, sao^{-2} is the dianion of salicylaldoxime, L= MeoH or EtoH) (figure 1.9b).[13r] They found that it is possible to alter the spin ground state (from $S = 4$ to $S = 12$) by changing the substitutents on salicylaldoxime ligand. They reported a new family of SMMs with bulky substituents on bridging ligands resulting in structural distortions in the core which further leads to twisting in oxime moiety and increase in torsion angles of Mn-N-O-Mn (an average of $\alpha_v = 36.5°$). It was found that there would be a switch from antiferromagnetic to ferromagnetic interactions between metal centers when torsion angle increases above 31.3°. One of the complex synthesized was $[Mn^{III}_6O_2(Et\text{-}sao)_6(O_2CPh(Me)_2)_2(EtOH)_6]$ with largest energy barrier $U_{eff} = 86.4$ K and $T_B = 5$ K is.[13u] Recently Christou and co-workers reported a Mn_{16} cluster (figure 1.9c) formulated as $[Mn_{16}O_{10}(OH)_3(OMe)_8(O_2CPh^{tBu})_{17}(MeOH)_5]$,[13v] which has been synthesized by the reaction of 4-^{tBu}benzoic acid in CH_2Cl_2/MeOH with $N^nBu_4MnO_4$ at room temperature. Core of the cluster shows an unusual layer-like structure 1:2:3:4:3:2:1 with W-shaped pleated

topology (figure 1.9d). This molecule possesses high magnetic anisotropy which is reflected in the magnitude of zero field splitting parameter (D = -0.16 cm^{-1}) due to parallel alignment of Jahn-Teller elongation axes of Mn^{+3} ion. Ac in-phase susceptibility measurements confirm the spin ground state value (S=12), as determined from dc data. The appearance of frequency dependent out-of-phase signals confirm the presence of SMM behaviour and the fits of ac data by using Arrhenius equation gave energy barrier value 49.7 K with a relaxation time of 4.32×10^{-9} s.

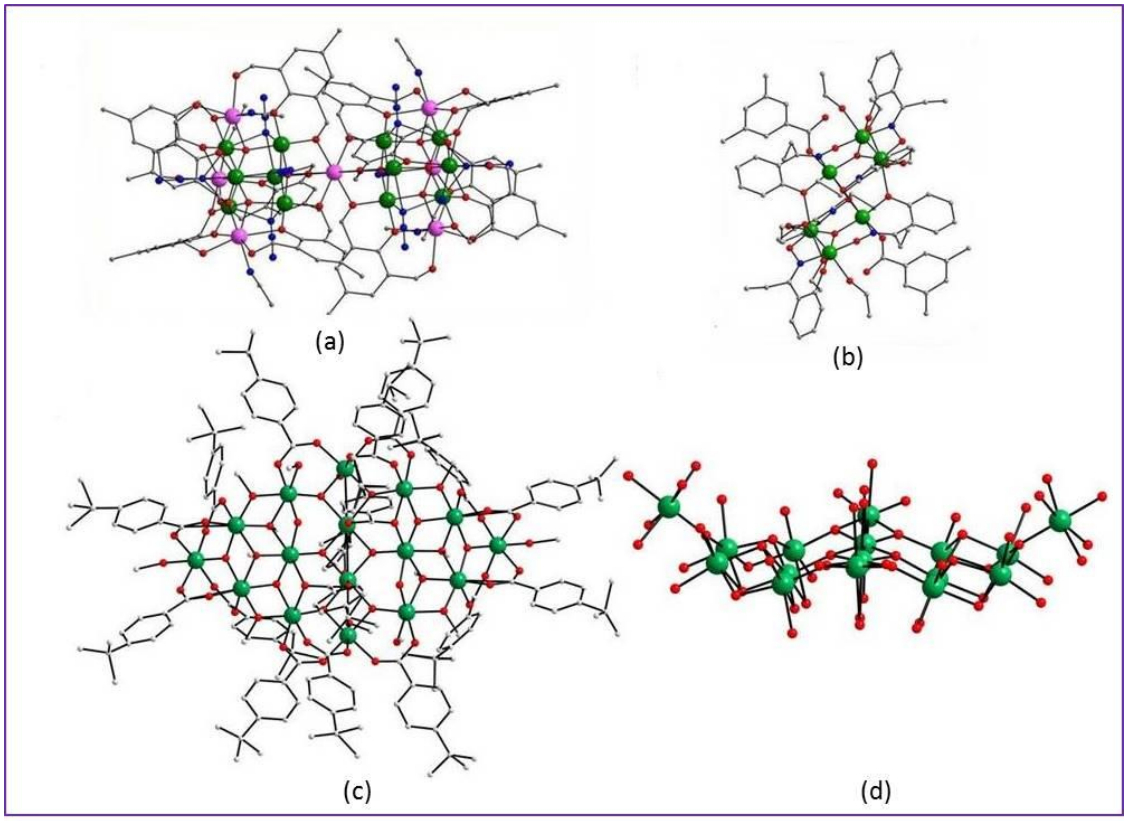

Figure 1.9. Molecular structure of a) Mn_{19} b) Mn_6 c) Mn_{16} d) core of Mn_{16}

1.6.2 SMMs Based on Iron:

Iron complexes (in their +2 and +3 oxidation states) with various ligand systems exhibited SMM features and make up the second largest family behind manganese. $[Fe_4(OMe)_6(dpm)_6]$ (where dpm = 2,2,6,6-tetramethylheptane-3,5-dionate) is the smallest iron cluster showing slow relaxation of magnetization with U_{eff} = 3.5 K at very low temperatures.[19a] One of the famous complex $[Fe_8O_2(OH)_{12}(tacn)_6]^{8+}$ where tacn = 1,4,7 triazacyclononane[19b] generally referred as Fe_8Br-cluster was reported by Wieghardt *et.al*, in 1984 and this was the second molecule found to exhibit SMM feature after Mn_{12}-OAc.

In similarity with Mn_{12}-OAc, magnetic properties of Fe_8Br-cluster were also studied a decade later its discovery. The antiparallel spin projection of the two iron atoms out of eight resulted in ferromagnetic coupling between all the metal ions which gave spin ground sate S = 10 with an anisotropic parameter D = -0.34 cm^{-1} and it exhibits relaxation below 0.36 K which shows the presence of pure QTM. Other than Fe_8, there are number of SMMs reported with different structural topologies like cubane, star and wheel type. Among these ferric stars conventionally prepared by using dpm ligand combined with trimethylol derivatives or with simple alkoxides exhibit S = 5 spin ground state with anisotropic parameter (D) varying from -0.20 to -0.445. A number of Fe(III) based SMMs are reported with different nuclearities such as Fe_9, Fe_{10}, Fe_{13}, and Fe_{19}.[20] Mindiola and co-workers reported the first single centre Fe(III) complex to exhibit slow relaxation of the magnetization in zero applied field.[21a] In an air stable Fe(III) complex [(PNP)$FeCl_2$] (PNP = N[2-P($CHMe_2$)2-4-methylphenyl]$_2^-$), which was prepared by one electron oxidation of [(PNP)FeCl] with $ClCPh_3$, dc measurements show unexpected spin ground state S=3/2 to 5/2 and the ac measurements reveal that it exhibits frequency dependent out-of-phase signal at zero field with an effective energy barrier of 32 K. Apart from Fe(III), Fe(II) also acts as an ideal candidate to show SMM features due to its single-ion magnetic anisotropy combined with a large spin (S=2). For theoretical interpretation Fe(II) complexes are very much important since they are very sensitive to the ligand field environment, magnetic field and temperature. Goodwin *et al*. reported a high nuclearity complex, $[Fe_{19}(metheidi)_{10}(OH)_{14}O_6(H_2O)_{12}](NO_3)\cdot 24H_2O$ (H_3metheidi = N-(1-hydroxymethylethyl)iminodiacetic acid, having a large ground state spin S = 33/2.[21b] The field dependence of magnetization shows saturation at 32.5 μ_B which is consistent with the theoretical value for S = 33/2 and g = 2, Arrhenius plot gave the energy barrier of 15 K. In 2008, Sanakis and co-workers reported a Fe(II) complex $[Fe_9(X)_2(O_2CMe)_8\{(2\text{-}py)_2CO_2\}_4]$ (where, X=OH(1), N_3(2), and NCO(3)).[21c] Magnetic measurements show that ground state is not well isolated from excited state due to moderate exchange between Fe(II)-Fe(II). Ac measurements show out-of-phase signal which suggests that these complexes exhibit a slow relaxation of magnetization and the fit from Arrhenius law gave effective energy barriers of 41 K (when X=N_3) ($\tau_0=3.4\times10^{-12}$ s) and 44 K (when X=NCO) ($t0=2.0\times10^{-11}$ s). Mononuclear Fe(II) complexes are also showing SMM behaviour. High spin trigonal Fe(II) complexes show varying degrees of slow relaxation upon application of dc field.[21d] Long and co-workers reported the first example of a mononuclear transition

metal based SMM, a trigonal pyramidal Fe(II) complex K[(tpa$^{Mes)}$Fe][21e] whose dc measurements confirm $S = 2$. The ground state spin of the complex and the fit to the data afforded an axial zero field splitting parameter D = -39.6 cm^{-1}. Ac susceptibility measurements show out-of-phase signal in presence of an applied magnetic field. Fit from Arrhenius law gave U_{eff} = 42 cm^{-1} with a relaxation time $\tau_0 = 2\times10^{-9}$ s. The absence of slow relaxation at zero field is likely be attributed to quantum tunneling of magnetization (QTM) through the spin reversal barrier. Several mononuclear transition metal complexes show Single ion magnetism (SIM) behaviour. Among them, coordinatively unsaturated iron complexes display high energy barriers up to U_{eff} = 186 cm^{-1} in $[Fe\{N(SiMe_3)(Dipp)\}_2]$[21f] (Dipp = C_6H_3-2,6-iPr) and U_{eff} = 226 cm^{-1} in $[Fe(C(SiMe_3)_3)_2]^{-}$[21g] which originates due to high orbital contribution.

1.6.3 SMMs Based on Cobalt:

The first example of Co(II) complex which displays slow relaxation of magnetization was $[Co_4(hmp)_4(MeOH)_4(Cl)_4]$ (where, hmp = hydroxyl methyl pyridine) reported in 2002.[22a] Magnetic data reveals ferromagnetic interactions between the metal ions. As temperature decreased out-of-phase susceptibility increases towards 1.8 K which is consistent with slow relaxation of magnetization. This complex shows hysteresis below 1.2 K and the loops show very little dependence on sweep rate due to significant interactions between ligand and MeOH ligands on adjacent clusters which suggest that QTM is hindered. In 2008, two Co(II) cubane complexes were reported $[GuH]_8[Co_4(cit)_4]$ (Gu = guanidine and H4cit = citric acid).[22b,c] Citrate ligands are bridging Co(II) ions, carboxylate ions are capping the metal ions and all the metal ions are hexa-coordinated. Carboxylate ions impart a twisted trigonal-prismatic geometry around each metal ion. Dynamic susceptibility measurements show frequency dependent out-of-phase signal and Arrhenius analysis gives an energy barrier of 24 K with a relaxation time 3.4×10^{-8} s. There are other Co(II) SMMs with different structural topologies and nuclearities such as Co_4 molecular squares, Co_5 square pyramids, cubane based Co_6, Co_7 disc type , Co_8 systems and Co_{12} systems from the Co_4 subunits.[22d] In 2015, Gao and co-workers have reported an Co(II)-Co_3(III) complex with only one paramagnetic ion Co(II) which is present in approximate D_3 coordination environment.[22e] This compound is air stable and dynamic susceptibility measurements confirm the presence of slow relaxation of magnetization with energy barrier as high as 109 K in zero applied magnetic field.

1.6.4 SMMs Based on Nickel:

In 2001, Winpenny and co-workers reported the first Ni(II) based SMM, a cyclic dodecanuclear complex $[Ni_{12}(chp)_{12}(O_2CMe)_{12}(thf)6(H_2O)_6]$ (chp = anion of chlorohydroxo pyridine) which was prepared by the reaction of Hchp with $Ni(O_2CMe)_2.xH_2O$ under reflux conditions.[23a]Isothermal magnetization studies show that the complex saturates at 25.5 μ_B which suggests S = 12 ground state and anisotropic parameter D = -0.05cm^{-1}. Ac susceptibility measurements shows frequency dependent out-of-phase signal, characterstic of SMMs, Arrhenius law gave energy barrier of 9.6 K for reorientation of magnetization.

Hendrickson and co-workers reported three Ni_4 cubanes,[23b] (Ni_4O_4). In these cubanes all the four nickel centers are ferromagnetically coupled resulting in spin ground state S = 4 and D value varies from -0.43 to 0.60. There are numerous examples of $[Ni_4O_4]$ cubanes with S = 4 ground state which have been studied and their anisotropy can be tuned by changing the ligand field.[23c-j] Ni_{10} cluster $[Ni_{10}(tmp)_2(N_3)_8(acac)_6(MeOH)_6]\cdot H_2O$ (H_3tmp = 1,1,1-tris(hydroxymethyl)propane) has been shown to exhibit ferromagnetic interactions between metal ions which leads to a spin ground state S = 10 with appreciable zero field splitting. Ac susceptibility measurements show out-of-phase susceptibility signal below 2.5 K and Arrhenius analysis gives an energy barrier of 14 K for the reversal of spin magnetization.[23k] There are other Ni(II) SMMs with different structural topologies and nuclearities such as $[Ni_{12}(chp)_{12}(O_2CMe)_{12}(thf)_6(H_2O)_6]$, $[Ni(hmp)(ROH)Cl]_4$, $[Ni(H_2thme)(MeCN)]_4(NO_3)_4$, $[Ni_{21}(cit)_{12}(OH)_{10}(H_2O)_{10}]Na_2(NMe_4)_{14}]$, and $[Ni_8Na_2(N_3)_{12}(^tBuPhCO_2)_2(mpo)_4(Hmpo)_6(EtOAc)_6]$.[23l-p] A heptanuclear Ni(II) complex $[Ni_7(OH)_8(hfac)_6(py)_6]\cdot$py has been synthesized from a tetranuclear complex and pyridine at high temperature.[23q] The EPR study confirms ground state S = 6 and dynamic susceptibility measurements reveal that only heptanuclear complex shows slow relaxation of magnetization at very low temperatures.

1.7 SMMs with 3d-4f metal ions

Since the discovery of first SMM Mn_{12}-OAc, there has been considerable interest towards synthesizing polynuclear transition metal complexes. To achieve high energy barriers, heterometallic 3*d*-4*f* complexes have attracted much attention with the idea of combining high spin-states of 3d metal ions with the large magnetic anisotropy of lanthanides. After

the discovery of first example of heterometallic 3*d*-4*f* Cu-Gd complex[24a] large number of 3d-4f complexes with varying nuclearities and 3d metal ions and 3d/4f ion ratios have been synthesized and investigated successfully.

Manganese exhibits variable oxidation states such as Mn(II), Mn(III) and Mn(IV) with $3d^5$, $3d^4$ and $3d^3$configurations respectively. Mn(II) and Mn(III) ions display simple paramagnetism, while Mn(IV) ion in octahedral geometry shows Jahn-Teller elongation thus Mn(III) ion is a good candidate for constructing SMMs. A large number of Mn-Ln clusters which are exhibiting SMM behaviour are reported.[24b-e] Iron exhibits two different oxidation states Fe(II) and Fe(III) and according to Hund's rule Fe(II), a d^6 system is not as stable as Fe(III), a d^5 system hence more Fe(III)-Ln systems have been isolated.[24f –l] Cobalt also exhibits two different oxidation states Co(II) and Co(III) and in most of the circumstances, these Co(II)/(III) ions adopt octahedral or tetrahedral coordination modes. When high spin Co(II) ions are in octahedral environment orbital angular momentum is not quenched, which makes it more suitable for magnetic materials.[24m] Nickel generally appears as Ni(II) which shows paramagnetism in octahedral field (high spin) and diamagnetism in square-planr filed (low-spin). A large number of heterometallic 3*d*-4*f* complexes containing Ni(II) are reported.[24n] Zinc(II) also has been used to study the magnetic interactions between different spin carriers in heterometallic 3*d*-4*f* complexes.[24o,p]

Numerous examples of 3*d*-4*f* complexes are reported with different nuclearities including di, Tri, tetra, penta, hexa, hepta, octa and high nuclearity clusters. Among trinuclear 3*d*-4*f* complexes, triangular trinuclear complexes where metal ions are bridged by μ_3-oxide ions doesn't show SMM behaviour.[25a-e] Due to the differential nature of 3*d* metal ions, all the known heterometallic 3*d*-4*f* complexes can be categorized into two: those with paramagnetic 3*d* ions and those with diamagnetic 3*d* ions. As compared with former, later complexes can be used as magnetic dilution agents due to the diamagnetic nature to efficiently increase the energy barrier for the reversal of spin magnetization in two different manners. Quantum tunneling of magnetization (QTM) generated by 4*f* ions can be suppressed by the diamagnetic 3*d* ion and diamagnetic 3d metal ion can produce large charge polarization on the bridged atoms there by inducing strong electrostatic interaction between 4*f* metal ions which eventually leads to large energy gap between ground and the

first excited state. For the construction of high performance 3*d*-4*f* SMMs, metal ions such as Co(III) and Zn(II) have been used as best candidates due to their diamagnetic nature.

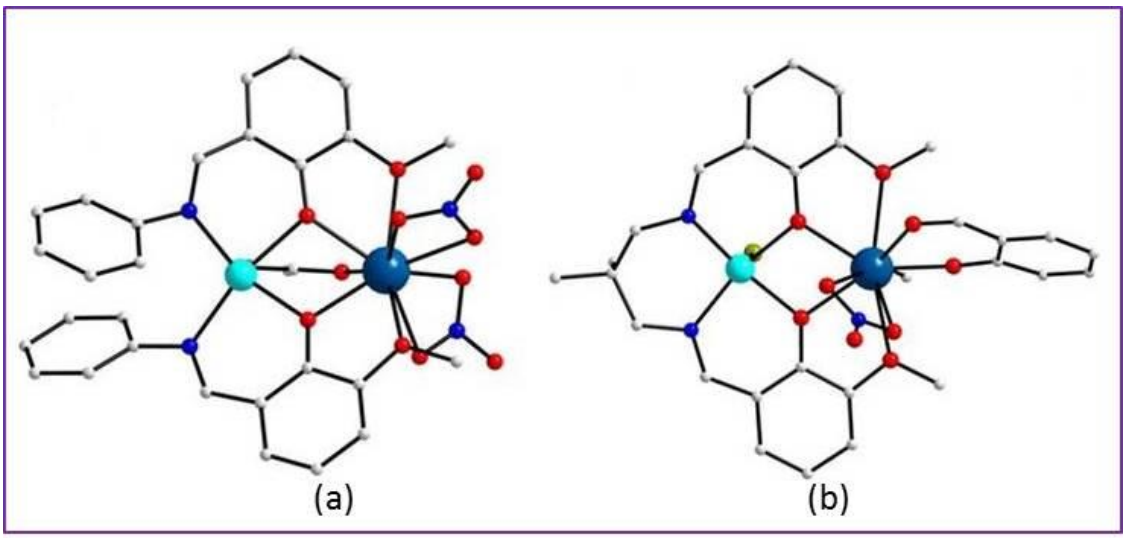

Figure 1.10. (a) Molecular structure of $[ZnDy(NO_3)_2(L)_2(CH_3CO_2)]$ (b) Molecular structure of [BrZn-Dy]

Tang and co-workers reported that replacing transition metal ion in 3*d*-4*f* complexes with a diamagnetic 3*d* ion improves the magnetic properties.[25f] In a propeller like M(III) $Dy(III)_3$ complex $[FeDy_3(HBpz_3)_6(dto)_3]\cdot 4CH_3CN\cdot 2CH_2Cl_2$ by replacing the Fe(II) ion (S=½) with diamagnetic Co(III) ion (S=0), a slower relaxation of magnetization has been observed with larger energy gap. Linear fit of the experimental data gave U_{eff} 15 K with a relaxation time (τ_0) of 1.5×10^{-6} s for $\{FeDy_3\}$ and 52 K, τ_0 3.6×10^{-8} s for $\{CoDy_3\}$.[25g] Shanmugam and co-workers reported a fivefold increase in the energy barrier by introducing diamagnetic Zn(II) ion, energy barrier for mononuclear Dy(III) complex is 16 cm^{-1} and for the {ZnDy} complex it is 83 cm^{-1} (figure 1.10a).[25f] In another report replacement of paramagnetic Cu(II) metal ion by diamagnetic Zn(II) shows energy barrier for the spin reversal increases greatly from 32 K to 333 K under an applied field of 1.0 KOe (figure 1.10b).[25h] Very recently, Zhao and co-workers used tetra-coordinated Ni(II) as a diamagnetic ion to synthesize a new oxime derived 3*d*-4*f* complex, $\{Dy_4Ni_6\}$ which exhibits a field induced Single molecule magnetic behaviour.[25i]

1.8 Why lanthanides preferred over transition metals?

Though large number of transition metal based SMMs have been reported, their energy barriers for reversal of spin magnetization and blocking temperatures are low when compared with the first lanthanide based SMM [$LnPc_2$] reported by Ishikawa *et. al*, in 2003.[26] Lanthanide based SMMs have been reported with different structural topologies and nuclearities ranging from monomer to Ln_2 to Ln_{60}. The favorable factors associated with lanthanides over transition metals, are large ground state spin (*S*) and high negative uniaxial magnetic anisotropy (*D*). In case of transition metal ions, in order to obtain large ground state term, it is necessary to bring multiple paramagnetic metal centers together which show ferro or ferri magnetic arrangement of spins. The splitting of ground state (*S*) into their individual m_s levels provide energy barrier for the reversal of spin magnetization. This energy also depends on the anisotropy of individual spincenters present in the complex/clusters and the orientation of anisotropy axis on individual metal centers. Eventhough they have good magnetic interactions between metal ions, due to lack of spin-orbit coupling [notable exception Co(II)] transition metal ions failed to provide large anisotropies (*D* varies between 0.5 to 0.9 cm^{-1}).

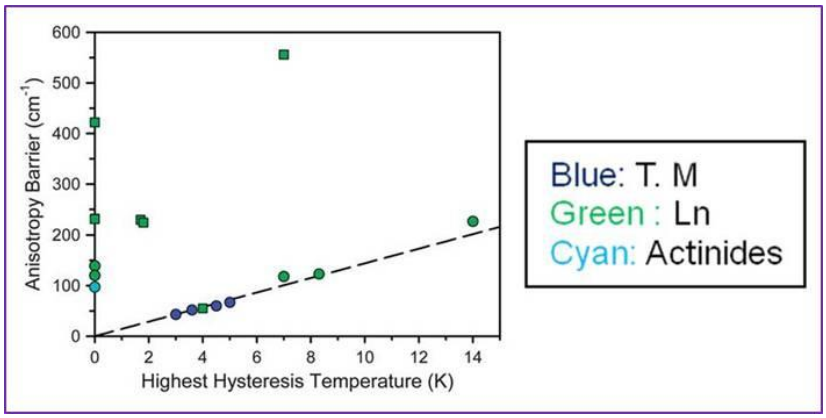

Figure 1.11: Plot of the highest recorded hysteresis temperature vs. the anisotropy barrier for the selected single molecule magnets.[6b]

Magnetic properties of lanthanides are different from transition elements, because the 4*f* electrons are not involved in bonding since they are shielded by 5*s* and 5*p* orbitals. There is no effect of ligand field on 4*f* orbitals, resulting in a weak crystal field splitting and weak magnetic exchange interaction between metal ions. Due to the complete degeneracy of 4*f* orbitals, they provide large unquenched orbital angular momentum which makes them perfect choice to obtain improved SMM parameters. Due to strong spin-orbit

coupling, lanthanides have large magnetic anisotropy particularly for Tb, Dy and Ho and the ground state term for lanthanides given by ground state term *J*. Large magnetic moments in these ions are due to large *J* values. Since for lanthanides after gadolinium *J*= *L*+*S* is the lowest energy term and which leads to ground states with large *J* value which in turn result in large magnetic moments. The splitting of ground state term into individual *mj* levels results in an energy barrier for the spin reversal. So the magnitude of energy barrier depends on the factors which control the splitting. In this regard, the crystal field in which lanthanide ions are situated has a significant effect on the electronic structure of the lanthanide ions. The crystal field interacts with the ground state, removes the 2*J*+1degeneracy of the ground state which influences the magnetic properties of lanthanide ions. Finally the relaxation of lanthanide ions depends on the spin-orbit coupling and local crystal field. Because of these intrinsic properties, lanthanide ions are chosen as best candidates to construct the SMMs with improved parameters.

1.8.1 Lanthanide Chemistry:

Lanthanides represent a set of fifteen elements known as rare earth elements. The most common oxidation state of lanthanides is +3. These ions have comparatively large ionic radii and hence they are largely electropositive. As atomic number increases, the 4*f* orbitals become more stable than the 5*d* orbitals so the electronic configuration is given as $[Xe]4f^n6s^2$ (n=3-14 for Pr-Yb except Gd). As atomic number increases, there is a smooth decrease in the ionic radii of lanthanide elements due to the progressive addition of electrons to the same subshell, thus increasing charge density resulting in the so-called lanthanide contraction. Similar shrinkage is observed in transition elements also but in case of lanthanides, the decrease in ionic radii is nearly 22% (1.061Å for La^{3+} to 0.848 Å for Lu^{3+}) and this decrease influences the coordination number and geometry of lanthanide elements.

The physical and chemical properties of lanthanides are different from transition elements because of the shielding of 4*f* elements by 5*s* and 5*p* orbitals. These deeply buried 4*f* orbitals can not overlap with the ligand orbitals and hence do not participate in bonding. Magnetic and spectroscopic properties of lanthanides are independent of ligand field but the steric bulk of ligands are more important than crystal field effects, when compared with transition elements crystal field splitting of lanthanide complexes is small. Due to

their large atomic radii, lanthanides exhibit high coordination numbers generally 6-12. In contrast to transition elements where the bonding is strong, the bonding between lanthanides and ligands is basically electrostatic and it depends upon the electronegativity of ligands.

1.9 First 4f based SMM

In 3*d*-metal ions, the energy barrier (U_{eff}) for the reversal of spin magnetization corresponds to the total ground sate spins (*S*) and easy axis magnetic anisotropy (*D*) but in case of highly anisotropic metals like lanthanides, it fails to represent accurate barriers. In addition to *D*, more anisotropic terms are needed to explain the U_{eff} for lanthanide based SMMs and also it depends on the ligand field in which lanthanide ion resides. In 2003 Ishikawa *et al*. reported first lanthanide based SMM pthalocyanin double decker complex, $[Ln(III)Pc_2].TBA^+$ (Ln(III) = Tb and, Dy,; Pc = phthalocyanine dianion; TBA^+ = $N(C4H9)^+$) (figure 1.12).[26]

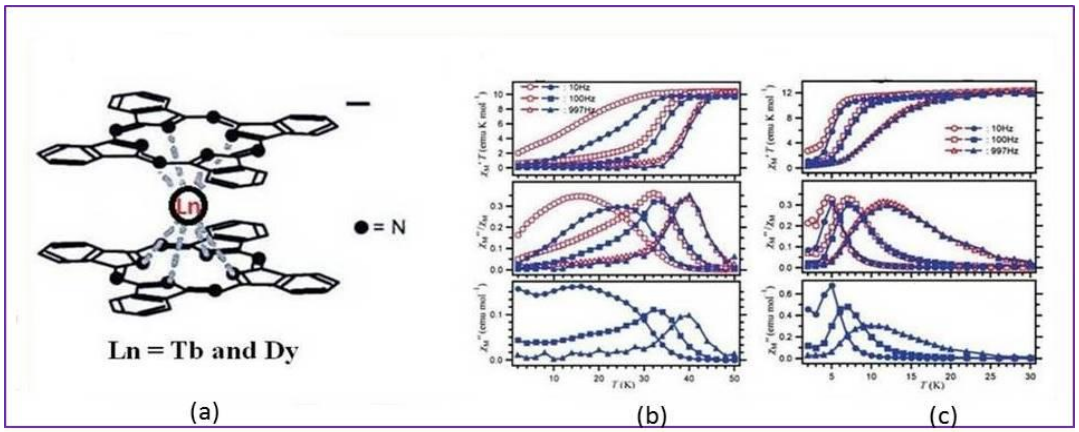

Figure 1.12. (a) Structure of $[LnPc_2]^-$ (b) χ′T versus T (top), χ″ /χM versus T (middle), and χ″ versusT for a powdered sample of 1 (open points), and for Tb derivative diluted in diamagnetic $[Bu_4N][Pc_2Y]$ (filled points) (c) χ′T versus T (top), χ″ /χM versus T (middle), and χ″ versusT for Dy derivative (open marks) and that diluted in $[Bu_4N][Pc_2Y]$ (b) χ′T versus T.

Lanthanide ions were sandwiched between two phthalocyanine molecules and the metal ions are octacoordinated with C_{4v} symmetry. Alternating-Current (AC) susceptibility measurements were carried on Tb(III) and Dy(III) analogues. Below 50 K, Tb(III) analogue exhibits frequency dependent out-of-phase signal without applied dc field, whilst Dy(III) analogue shows more diminished behaviour. Ac-susceptibility measurements were performed on diluted samples of Tb(III) doped with diamagnetic

matrix [Y(III)Pc_2. TBA^+] to prove this magnet like behaviour is not due to long range ordering or intermolecular interactions. The shifting of in-phase (χ') and out-of-phase (χ'') curves towards higher temperature clearly demonstrates that SMM behaviour is intrinsic to the molecule and the shifting is due to the removal of intermolecular interactions. The effective energy barriers are 230 cm^{-1} and 28 cm^{-1} for Tb(III) and Dy(III) respectively.

Since the discovery of lanthanide phthalocyanine double-decker $[LnPc_2]^-$ complex, there has been a growing interest in the synthesis of lanthanide based SMM's. Lanthanide complexes can be prepared either by rational or by using self-assembly approach. In order to synthesize a Ln-SMM with predictable magnetic properties, a greater understanding is required between structure and magnetic properties. In this regard, mononuclear complexes are very important due to their structural simplicity which makes magneto-structural correlations more understandable. Many reported mononuclear complexes were synthesized by using rational design approach with high energy barriers and with high blocking temperatures.

Serendipitous approach depends on self-assembly of metal ions with flexible ligands to potentially isolate polynuclear metal complexes. In this method, resulting products can vary by changing the metal to ligand ratio, reaction conditions, solvent used for the reaction, metal salts and ligands used. More number of metal ions can be incorporated by increasing the number of donor groups on the ligand. Empty coordination sites at the metal centres are filled when alcohol based solvents such as methanol and ethanol are used. In this approach, metal salts in organic solvents were reacted with flexible ligands in presence of base. Lanthanide ions (hard acids based on HSAB concept) will form stable complexes with ligands in which oxygen and nitrogen (hard bases) act as donor atoms. On the basis of this approach, a large number of lanthanide oxo-hydroxo clusters have been reported by the utilization of wide variety of ligand systems like β-diketones,[27] carboxylates,[28] alkoxides,[29] aminoacids,[30] Schiff bases,[31]o-vanillin based Schiff bases,[32] phosphonates,[33] calixarenes,[34] polyoxometalates[35] and radical ligands.[36] In all these complexes, lanthanide ions were connected either by oxido or hydroxide bridges. Chloirde ion (Cl^-), pyrazines, carboxylates and triazoles have also been employed as bridging ligands for the synthesis of lanthanide complexes/clusters/coordination polymers having significant energy barriers and blocking temperatures. The lanthanide metal ion precursors starting from simple hydrated lanthanum chlorides/nitrates/acetates, previously occupied

coordinated complexes such as $Ln(acac)_3.2H_2O$/$Ln(hfac)_3.2H_2O$, and organometallic lanthanide precursors such as Cp_2Ln have been used as metal source. A large number of lanthanide complexes with different nuclearites have been prepared by using above mentioned metal precursors and ligand systems.

Among lanthanides, Dysprosium plays a crucial role in the synthesis of lanthanide-based SMMs with high energy barriers due to its intrinsic magnetic anisotropy. According to Russel-Saunders scheme, the ground state of free lanthanide ion can be given as $^{2S+1}L_J$, where *S* and *L* are the spin and orbital angular quantum number respectively and *J* varies from |*L*-*S*| to |*L*+*S*|. For a lanthanide ion ($4f^n$), ground state is the lowest possible *J* when n<7 i.e. |*L*-*S*| and conversely the ground state is highest possible *J* when n>7 i.e. |*L*+*S*|. The electronic configuration of Dy (III) ion is [Xe] $4f^9$ and spin orbit coupling leads to ground state $^6H_{15/2}$. In presence of ligand field, the ground state of a metal ion will split in to 2*J*+1 states but in case of lanthanides it is due to spin-parity effect. Dy(III) ion is with 16 fold degeneracy (2x15/2+1) and due to the spin-parity effect, the degeneracy is removed into new sublevels i.e. doubly degenerate ± m_j states. For Dy(III) ion *mj* states are ±15/2, ±13/2, ±11/2, ±9/2, ±7/2, ±5/2, ±3/2, ±1/2 and these doublets are called as kramers doublets. There is large separation between the ground and first excited states due to strong spin-orbit coupling which is responsible for high energy barrier required for the reversal of spin magnetization in Dy-based SMMs.

1.10 General structural topologies in lanthanide cluster chemistry

Lanthanide oxo/hydroxo clusters are generally synthesized through self-assembly approach and cluster topologies like dimeric, triangular, tetranuclear cores (butterfly cubanes and rarely tetrahedral), square-based-pyramid and hourglass were repeatedly encountered (chart-1.1). In dimeric lanthanide core, two metal ions were bridged through two μ_2-OH groups. In triangle type lanthanide core, two μ_3-OH bridges connect all three metal ions. Three types of structural topologies were observed in tetranuclear complexes in which most common were butterfly and cubane core. Four lanthanide ions connected through two μ_3-OH along with four μ_2-OH bridges and four metal centers connected through the four μ_3-OH bridges were observed in former and later case. The other and rare structural topology in tetranuclear series is a tetrahedral type core in which all the four metal centres are connected through one μ_4-OH and five μ_2-OH bridges. In case of

pentanuclear clusters, most frequently observed structural topology is square-based-pyramid where all metal centres are connected through one μ_4–OH and four μ_3-OH bridges. In case of nonanuclear clusters, hour glass/sand glass like topology is observed frequently which actually is constructed through two square based pyramidal units via the apical metal centre and all metal ions are connected through two μ_4 –OH and eight μ_3-OH bridges (chart 1.1).

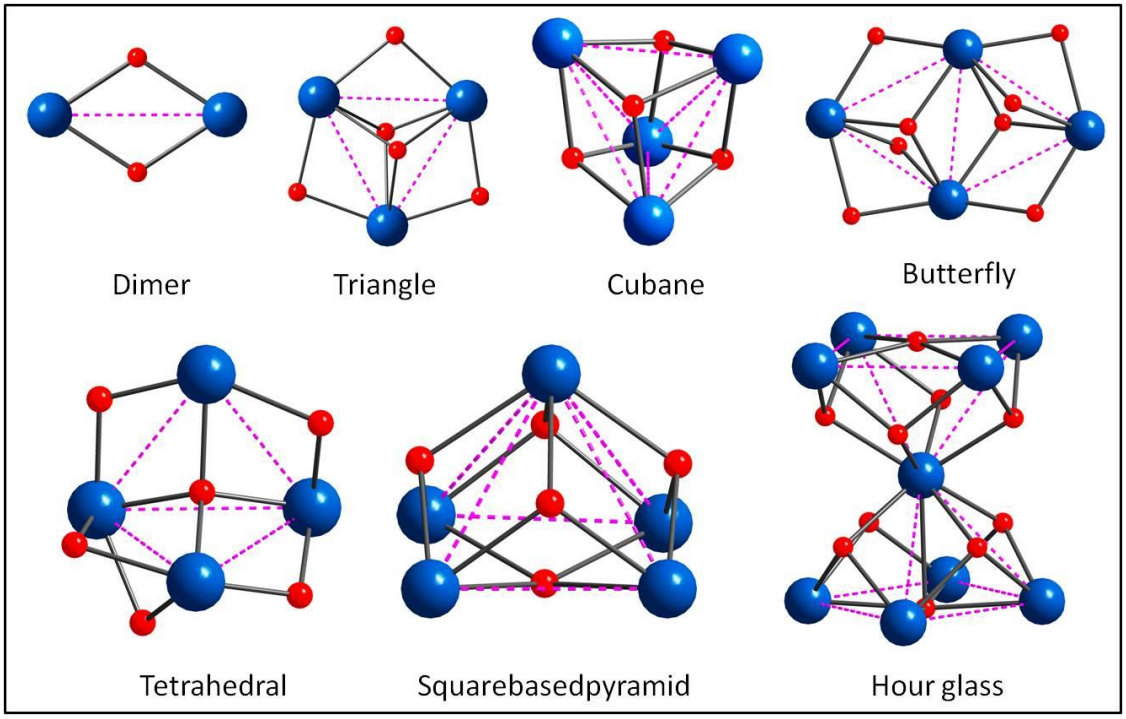

Chart 1.1: Frequently observed lanthanide oxo-hydroxo cluster structural topologies.

1.11 Highlights from Ln based SMMs

1.11.1 Mononuclear SMMs:

To understand spin-relaxation in lanthanides, mononuclear complexes are very important due to their structural simplicity. They represent the smallest possible magnetic units and have applications in molecular-scale electronics.[37a,b] Since the discovery of $[LnPc_2]^-$, lanthanide Single Ion Magnets (SIMs) are frequently studied because they often exhibit remarkably high blocking temperature (T_B) particularly when ligands with high symmetry are used.[37c,d] In 2007, Ishikawa and co-workers reported the two electron oxidation of $TbPc_2^-$ where they observed a significant jump in the energy barrier due to the oxidation of ligands and introduction of OEt groups causing longitudinal contraction of the coordination sphere around Tb(III) ion.[37e] Strong interaction between the electron density

of metal ion with the ligand field which increase the splitting between ground and the first excited states, results in an increase in the energy barrier. In 2013, Torres and co-workers demonstrated the effect of various terminal substituents on Pc ligands and on the SMM behaviour of corresponding complexes.[37f] Hetereroleptic [TbPcPc'] system which is substituted with *tert*-butylphenoxy substituent shows some structural advantages: a) presence of bulky substituent on ligand facilitates the isolation of molecules from each other there by favouring their behaviour as SMM b) N-Tb distance increases due to the presence of substituent on one of the Pc ring and due to the bulkiness of substituent it forces the metal ion towards bare Pc ring and therefore lifting the interaction between metal ion and unsubstituted ring. This complex exhibits highest SIM anisotropy barriers for reversal of magnetization (U_{eff} = 939 K).[37e] Introduction of organometallic chemistry is another important advance in the field of Lanthanide SIMs. A heteroleptic Er(III) complex sandwiched with Cp* (1,2,3,4,5-pentamethylcyclopentadienyl) and COT (cyclooctatetraenyl) rings is one of the first reported organometallic SIMs (figure 1.13a).[37b] High local symmetry is believed to be generated by the ligands and is responsible for the observed magnetic properties. Ac susceptibility measurements show the presence of two thermally activated magnetic relaxation processes with the energy barriers as high as 197 and 323 K and it shows a butterfly shaped hysteresis at 1.8 K up to even 5 K. Recently, Tong and co-workers reported a Dy(III) complex with quasi D_{5h} geometry that exhibits the record SIM blocking temperature of 11 K (figure 1.13b).[37c] Certain crystal field parameters which result in QTM, were prevented by the high local symmetry in the vicinity of spin carrier and it demonstrates the benefit of high symmetry in promoting Ising type magnetic anisotropy in Ln-SIMs.

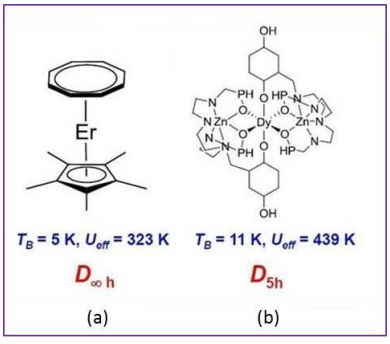

Figure 1.13. (a) (Cp*)Er(COT), (b) $[Zn_2DyL_2(MeOH)]NO_3.3MeOH.H_2O$, L=2,2',2'-(((nitrilo-tris(ethane-2,1-diyl))tris(azanediyl)tris(methylene)tris-(4-bromo-phenol).

1.12 Multi-nuclear Lanthanide complexes

Lanthanide SMMs exhibit highest blocking temperatures to date.[38] This is despite the fact that even at very low temperatures many polymetallic lanthanide SMMs exhibit single ion magnetic relaxation dynamics due to a unified spin ground state. The major challenge with Ln-SMMs is the poor overlapping of *4f*-orbitals with ligand orbitals resulting in poor magnetic exchange interactions. Tremendous effort has been put into overcoming this limitation with a particular focus on di-nuclear lanthanide complexes.

1.12.1 Dinuclear Lanthanide SMMs:

Dinuclear lanthanide complexes are very important:1) as they provide simplest molecular motif to study the magnetic interactions between two lanthanide ions/spin carriers[39a] 2) they are crucial for understanding the relationship between single ion relaxation and relaxation of a molecular entity[39b] 3) In a dinuclear system, it is easy to determine the possible orientation of anisotropy.[39c] Recent studies reveal that for a lanthanide SMM, ligand field and the coordination geometry around metal ion exerts great impact on magnetic anisotropy.[39d,e] Strong exchange coupling between metal ions helps to suppress QTM, as potentially leads to larger ground state. Since lanthanides are oxophilic in nature, majority of lanthanide complexes reported were oxo-bridged (phenolates, o-vanillin based and carboxylates) and these ligands are responsible for magnetic interactions between lanthanide ions. The slow relaxation of magnetization in monometallic complexes like Tb(III) phthalocyanine and polyoxometallate Er(III) complex shows that the symmetry and strength of crystal field is probably the most significant factor in controlling relaxation of the single ions. These observation lead to examine ligands other than N- or O- which produce strong crystal field. Winpenny and Layfield reported organometallic lanthanide complexes with general formula $[(\eta^5\text{-Cp})_2\text{Ln}(\mu\text{-X})]$ where heteroatom bridges include bta (benzatriazolide), Cl and $SSiPh_3$.[39f] All these complexes were showing axial character of kramers ground state which is evidenced by *ab initio* calculations and these calculations revealed there is a weak Ln-Ln interaction in bta- and Cl-bridged complexes, whereas much softer sulphur atoms in the thiolate bridged dimer $[(\eta\text{-}C_5H_4Me)_2Dy(\mu\text{-}SSiPh_3)]_2$ resulted in strong exchange interactions and high energy barriers (U_{eff} = 133 cm^{-1}) out of the series.

To achieve strong exchange interactions between lanthanide ions, radical-bridges are the best ligand systems. Insertion of a radical bridge between two Ln ions force an antiferromagnetic interaction between metal and ligand and therefore results in strong ferromagnetic exchange between Ln ions as shown in figure 1.14.

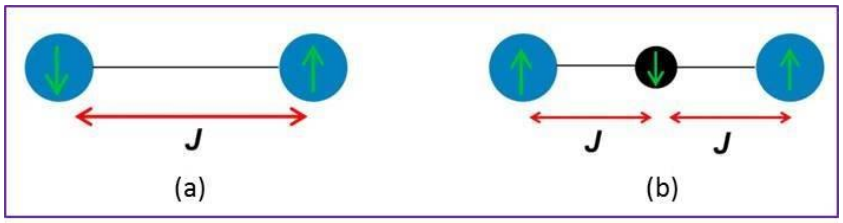

Figure 1.14. Graphical representation of the typical spin alignment between lanthanide ions (a) bridged by a neutral ligand and (b) a radical-containing ligand. Blue circles represent Ln(III) ions and black circle represents a radical spin.

In 2007, Sessoli and co-workers have illustrated the strategy of controlled ferromagnetic coupling between Ln ions using a Dy(III) nitronyl-nitroxide complex.[40a] Recently, Long group demonstrated that introducing a radical bridge between Ln ions not only increases ferromagnetic interactions but also increases the exchange coupling (*J*).

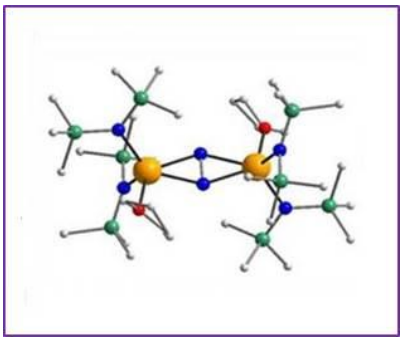

Figure 1.15: Molecular structure of $\{[(Me_3Si)_2N]_2(THF)Tb_2(\mu\text{-}\eta^2\text{:}\eta^2\text{-}N_2)$

The best example is dinuclear Tb(III) complex bridged by azide (N_2^{3-}) radical,[38c] K(18-crown-6)$(THF)_2$][{$[(Me_3Si)_2N]_2(THF)Tb\}_2(\mu\text{-}\eta^2\text{:}\eta^2\text{-}N_2)$] (figure 1.15), which has been synthesized from the reduction of N_2^{2-} bridged {$[(Me_3Si)_2N]_2(THF)Ln\}_2(\mu\text{-}\eta^2\text{:}\eta^2\text{-}N_2)$ (Ln = Tb Ho Er)} complexes in presence of potassium graphite [KC_8]. The remarkable feature of this complex is that it holds the highest exchange coupling (*J*) due to the diffused spin orbitals on the bridging ligands which penetrate the 4*f* orbitals. As a result of combining this strong exchange coupling with single ion anisotropy, resulted in high energy barrier and high blocking temperature up to 14 K. However, in some radical bridged Ln

complexes, there is no SMM behaviour which may be due to slight differences in symmetry.[40b]

1.12.2 Trinuclear Lanthanide SMMs:

Among series of lanthanide clusters, trinuclear clusters are limited in number and most of the trinuclear SMMs reported are with dysprosium. Based on structural arrangement, trinuclear lanthanide complexes are subdivided into two types- triangular and linear. Dy_3 triangles have gained considerable amount of attention due to their slow magnetic relaxation despite their non-magnetic ground state. In 2006, Powell and co-workers reported two similar triangular Dy(III) compounds $[Dy_3(\mu_3\text{-}OH)_2(H_2O)_5L_3Cl]Cl_5$ and $[Dy_3(\mu_3\text{-}OH)_2(H_2O)_5L_3Cl]Cl_3$ (where HL= *o*-vanillin) which display a complex and unprecedented magnetic behaviour.[41a] Crystal structure consist of a triangle of Dy(III) ions which are capped by three μ_3-hydroxides and they are bridged by deprotonated *o*-vanillins as depicted in figure 1.16. All the Dy(III) ions are octa-coordinated and the overall symmetry of the molecule is close to C_{3h}. The magnetization (M_B) versus field (H) confirms the presence of a diamagnetic ground state. Both experimental and theoretical studies reveal that canting of the anisotropy axis of the Dy(III) ions leading to a toroidal alignment of the local magnetization vectors and this alignment is considered as a form of vortex spin chirality. As magnetization vectors are having two opposite rotations, it is essential to cross an energy barrier to convert one into another. Ac susceptibility measurements show out-of-phase signal below 20 K with substantial energy barriers of 36 K at zero applied field and 120 K at an applied field of 3 kG. This study reveals that information can be stored even in a non-magnetic ground state. In perspective of the unusual magnetic behaviour of these complexes, considerable efforts have been made to prepare Dy_3 triangles.[41b-e] In another report, coupling of two Dy(III) triangles through hydrogen bonding leads to dramatic enhancement of thermal energy barrier up to 198 K.[41f] In 2009, Powell and co-workers reported a nearly linear Dy_3 complex $[Dy_3L_2(HL)_4(EtOH)_2](ClO_4)$ (where HL=*o*-vanillin oxime) in which the central Dy(III) ion show a geometry close to ideal dodecahedron whereas terminal ions show geometry in between dodecahedral and square-antiprismatic.[41g] Dc measurements reveal that there is ferromagnetic interactions between Dy(III) ions below 20 K and ac susceptibility measurements display more than two maxima indicating complex relaxation behaviour. The best fit from Arrhenius analysis gave two energy barriers with U_{eff} = 28 K and U_{eff} =

67.2 K and ac measurements in presence of applied magnetic field led to the conclusion that QTM is less prominent when compared with the reported Dy_3 triangles.

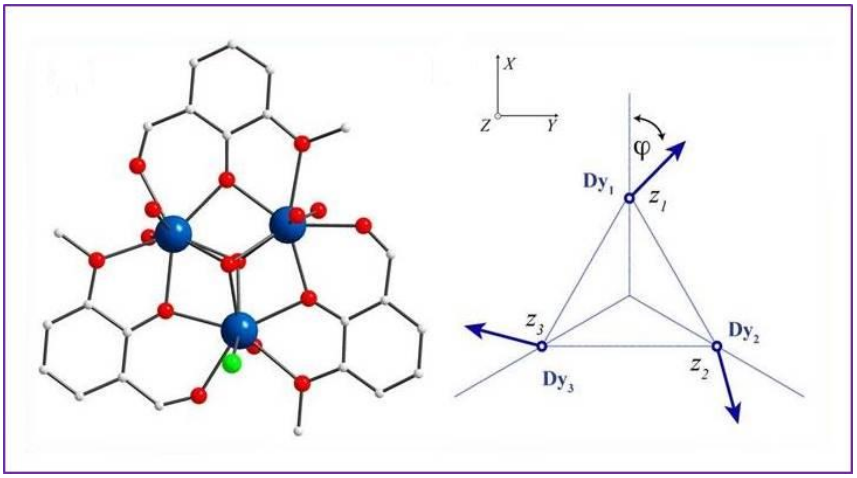

Figure 1.16. (a) Molecular structure of $[Dy_3(\mu_3\text{-}OH)_2L_3Cl(H_2O)_5]Cl_3$ triangle (b) Scheme of the spin structure of the $\{Dy_3\}$ complex and of the local easy axes orientation in respect of the laboratory XYZ reference frame.

1.12.3 Tetranuclear Lanthanide SMMs:

Tetranuclear Ln complexes display different geometries with respect to metal centers. These geometries include 1D linear and zig-zag chains, squares and rhomboidal/butterfly arrangement of Ln ions and 3D cubes and tetrahedral. Among these the most common topologies observed are butterfly and cubane. In 2010, Tang and co-workers reported the synthesis of a linear tetranuclear Dy(III) complex $[Dy_4(L)_4(CH_3OH)_6]2CH_3OH$ by the reaction of $DyCl_3.6H_2O$ with H_3L (2-hydroxy-3-methoxybenzoic acid [(2-hydroxy-3-methoxyphenyl)methylene] hydrazide) in methanol/acetonitrile as a solvent and in presence of a base.[42a] The centrosymmetric core has near linear geometry characterized by Dy-Dy-Dy angles of 149.9(1)°. The two internal Dy(III) ions are eight-coordinated and occupy distorted bicapped trigonal prismatic geometry and the two terminal Dy(III) ions are nine-coordinated and display monocapped square antiprismatic geometry. Ac susceptibility measurements show the occurrence of two distinct peaks in out-of-phase ac signals. The sow relaxation process gives U_{eff} = 173 K and fast relaxation gives U_{eff} = 19.18 K figure 1.17a. Recently, Shanmugam and co-workers reported a series of Ln_4-squares with general formula $[Ln_4(\mu_4\text{-}OH)(HL)(H_2L)_3(H_2O)_4]Cl_2$.[42b] The structures are described as hydroxo-centered squares of Ln(III) ions with each edge bridged by doubly deprotonated H_4L Ligand (where H_4L=2-(2-hydroxy-3-methoxybenzylidene)amino)-2-

(hydroxymethyl)propane-1,3-diol). Ac susceptibility measurements of the Dy(III) analogue shows frequency dependent out-of-phase signal at zero field with U_{eff} 29 K and 100 K for fast and slow relaxation processes respectively (figure 1.17b). In 2009, Murugesu and co-workers reported a tetranuclear complex $[Dy_4(\mu_3\text{-}OH)_2(bmh)_2(msh)_4Cl_2]$ (where H_2bmh=1,2-bis(2-hydroxy-3-methoxybenzylidene) hydrazone and Hmsh=3-methoxysalicylaldehyde hydrazone).[42c] The complex has a defect-dicubane central core and the four Dy(III) ions are bridged by two μ_3-hydroxide ligands. Each metal ion is octca-cordinated and occupies square-antiprismatic geometry. Ac susceptibility measurements show out-of-phase signals and the fit from Arrhenius plot gave energy barriers of U_{eff} = 170 K and 9.7 K for high and low temperature dynamics respectively and this complex holds the highest energy barrier among tetranuclear butterfly complexes (figure 1.17c). It has been reported that tetrametallic Dy(III) cubane complexes are likely to be SMMs when the Dy-O-Dy angles are greater than 99° and there are some evidences to support this hypothesis. Very few Dy_4-cubane complexes are reported as SMMs[42d-g] and among these the one reported by Chandrasekhar and co-workers shows highest energy barrier upto 74 K.[42h]

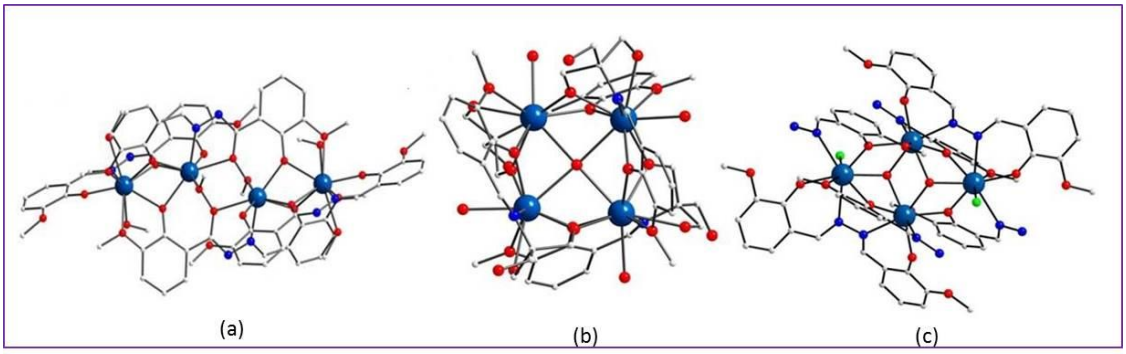

Figure 1.17. (a) Molecular structure of $[Dy_4(L)_4(MeOH)_6]\cdot$ 2MeOH (b) Molecular structure of $[Dy_4(\mu_4\text{-}OH)(HL)(H_2L)_3(H_2O)_2(MeOH)_2]Br_2$ (c) Molecular structure of $[Dy_4(\mu_3\text{-}OH)_2(bmh)_2(msh)_4Cl_2]$

Recently, Winpenny and co-workers reported tetranuclear Ln(III) complexes $[Ln_4K_2O(O^tBu)_{12}].C_6H_{14}$ bridged by alkoxide ions and their doped yttrium analogues (figure 1.18). They demonstrated that the relaxation via higher excited states in Dy-analogue is due to strong axial crystal field which led to higher values of energy barrier (U_{eff}). Ac susceptibility measurements show two distinct frequency dependent out-of-

phase signals and Arrhenius plot of these data gives U_{eff} = 692 and 316 K respectively and the Dy-doped Y-complexes reach even more high energy barriers (U_{eff} >800 K).[43]

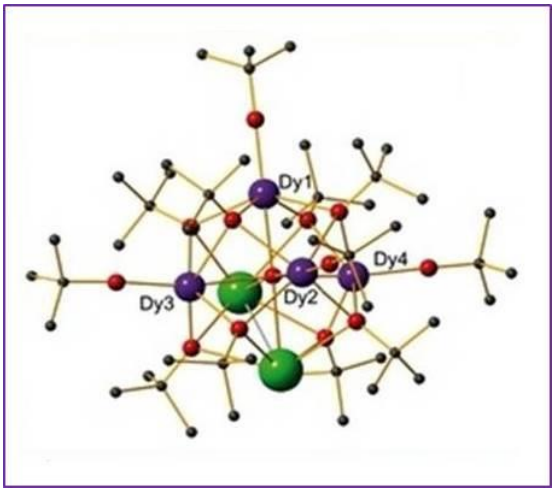

Figure 1.18. Molecular structure of $[Dy_4K_2O(O^tBu)_{12}]$

1.12.4 Pentanuclear Lanthanide SMMs:

Among different series of lanthanide SMMs, pentanuclear Ln-SMMs are very rarely encountered. Winpenny and co-workers reported an iso-propoxide bridged dysprosium square based pyramid $[Dy_5O(O^iPr)_{13}]$ (figure 20). This complex was synthesized by the reaction of $DyCl_3$ with freshly generated KO^iPr in O^iPrH/toluene with a stoichiometric amount of water. All the Dy(III) ions are held together by oxide/alkoxide and all the ions are hexa-coordinated and the geometry around each ion is octahedral.[44a] The interesting feature of this complex is lanthanide ions are away from the central μ_5-oxide bridge and shifted towards terminal alkoxides and as a result all the lanthanide ions are approximately in C_{4v} symmetry. This high symmetry is responsible for substationally high energy barrier for spin relaxation. Observation of frequency dependent out-of-phase signals at 40 K from ac susceptibility measurements indicate its SMM behaviour, Arrhenius plot produced energy barrier of U_{eff} = 528 K (figure 1.19).

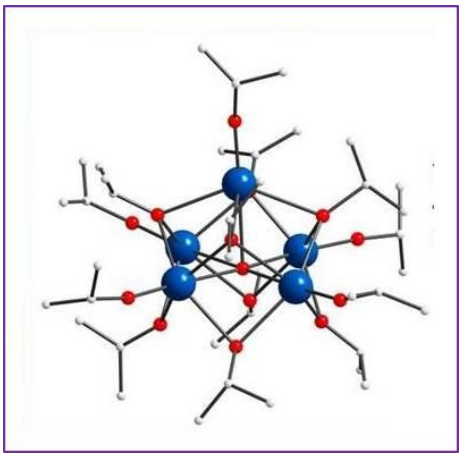

Figure 1.19. Molecular structure of $[Dy_5(\mu\text{-}O)(O^iPr)_{13}]$

In contrast to this the isostructural Tb (non-kramers ion) or Er (Kramers ion) analogue doesn't show any SMM properties. However the Ho analogue $[Ho_5(\mu_5\text{-}O)(\mu_3\text{-}O^iPr)4(\mu\text{-}O^iPr)_4(O^iPr)_5]$ shows frequency dependent signal without any maxima. In an applied field of H_{dc} = 3.5 kOe, an anisotropy barrier of U_{eff} = 389 K was calculated, indicating an efficient QTM in the absence of applied magnetic field. Eventhough the pyramidal structure of $[Dy_5(\mu_4\text{-}OH)(\mu_3\text{-}OH)_4(Ph_2acac)_{10}]$ is similar to that of preceding Dy_5 complex but it shows less pronounced SMM behaviour which may be due to lack of four–fold symmetry. Below 8 k it shows out-of-phase signal with a relaxation energy barrier U_{eff} = 32.2 K.[44b]

1.12.5 Higher nuclearity Lanthanide SMMs:

Polymetallic lanthanide clusters with six or more than six metal ions were investigated to study the magnetic properties but these were found to possess less SMM behaviour which may be due to fast and significant QTM at low temperatures . Number of Dy-based high nuclearity clusters were reported with different nuclearities like Dy_6,[45] Dy_7,[46] Dy_8,[47] Dy_9,[48] Dy_{10},[49] Dy_{11},[47d,50] Dy_{12},[51] Dy_{14}[52] and Dy_{24}[53] of which very few clusters are displaying interesting magnetic properties (Table1.1).

Table 1.1 Some of the reported high nuclearity SMMs

Ln-SMM	U_{eff}/K	ref
$[Dy_6(\mu_3\text{-}OH)_4(ovn)_2(L_1')_2Cl(H_2O)_9]^{5+}$	200	32
$[Dy_6(\mu_3\text{-}CO_3)_2\ (ovph)_4(Hovph)_2Cl_4(H_2O)_2]$	56	45e
$[Dy_6(\mu_3\text{-}OH)(ovh)_4(avn)_2(NO_3)_4(H_2O)_4][NO_3]_2$	9.6	45f
$[Dy_7(OH)_6(thmeH_2)_5(thmeH)(tpa)_6(MeCN)_2][NO_3]_2$	140	46b
$[Dy_8(\mu_4\text{-}CO_3)_4(L_2')_8(H_2O)_8]$	74.2	46g
$[Dy_8(\mu_3\text{-}OH)_8(DEA)_4Cl_4$	49.3(5 K Oe)	47b
$[Dy_{11}(OH)_{11}(phendox)_6(phenda)_3(OAc)_3][OH]$	3	45h
$[2Cl\subset Dy_{12}(OH)_{16}(phenda)_8(H_2O)_8][OH]_2$	3	51
$[Dy_{14}(EDDC)_4(opch)_4(O_3PC_{10}H_7)_{10}(OAc)_6(H_2O)_4]xH_2O$	74	52c
$[Dy_{24}(DMC)_{36}(\mu_4\text{-}CO_3)_{18}(\mu_3\text{-}H_2O)_2]_nH_2O$	Weak SMM behaviour without clear maxima	53

H_2L_1' = 2-hydroxymethyl-6-methoxyphenol; H_2L_2' = (E)-N′-(2-hyborxy-3-methoxybenzylidene) pyrazine-2-carbohydrazide; H2ovph, o-vanillin picolinoylhydrazone.

1.13 Magnetocaloric Effect (MCE): Origin

In addition to single molecule magnetism, polynuclear metal complexes can exhibit a property called magnetocaloric effect. In simplest terms, it is a temperature change (*i.e.*, heating or cooling) in the complex caused by introduction or removal of external magnetic field (*H*). In 1881, Warburg discovered MCE effect in case of iron[54] and it was explained independently by Giauque and Debye. They demonstrated its first practical use in attaining temperatures lower than liquid Helium via adiabatic demagnetization. This effect can be used as an alternative technology for refrigeration termed as Magnetic refrigeration which acts as environmentally benign and highly energy efficient refrigeration compared to traditional gas compression refrigerators. Exploration of MCE effect has attracted immense interest in recent years due to its applications in different areas such as medicine and industrial research.[55]The rising cost and scarcity of ^{3}He-isotope is the primary reason for researching molecular magnetic refrigerants and enhanced the desire for alternative techniques for cooling at cryogenic temperatures. Lanthanide containing alloys like $Gd_3Ga_5O_{12}$ (gadolonium gallium garnet GGG) are used for cryogenic cooling and research is continuously going on to see if these discrete molecules could act as similarly efficient refrigerants.

1.13.1 Basic Theory:

Though MCE effect is an intrinsic property of all magnetic materials, its intensity depends upon properties of particular material. MCE generates when the magnetic sublattice couples with applied magnetic field (*H*), there by changing the magnetic contribution to the total entropy of the material.[56] Since MCE effect is directly related to adiabatic temperature change (ΔT_{ad}) and isothermal change in magnetic entropy (ΔS_m), thermodynamics is used to explain this, in terms of magnetic variables (magnetic field *H* and magnetization *M*) with relation to entropy S_E and temperature *T*. The magnitude of total entropy (S_t) of a ferromagnetic substance at constant pressure depends on both temperature (*T*) and applied magnetic field (*H*), whose contributions are magnetic entropy (S_m) a function of temperature and field, lattice (S_{lat}) and electronic entropies (S_{el}) which are the functions of temperature.

$$S_{t(T,\,H)} = S_{m(T,\,H)} + S_{lat(T)} + S_{el(T)} \qquad (1.10)$$

The change in magnetic entropy (ΔS_m) and change in adiabatic temperature (ΔT_{ad}) are the two parameters which quantify MCE efficacy and both these processes are strongly dependent on initial temperature and magnetic field variation (ΔH) and are depicted in figure 1.20 (a) and (b). The total entropy of a magnetic material is unchanged ($\Delta S_t = 0$) in case magnetic coolant is magnetized adiabatically in reversible conditions. Equation 1.1 explains the figure 1.20 (c) where A → B describes the adiabatic magnetization/demagnetization. In this process, the total entropy of the system does not change. However, on subjecting magnetic material to the external magnetic field, all the spins get aligned parallel to the direction of external field thus decreasing magnetic entropy. Since it is adiabatic process, due to lack of heat exchange, the decrease in S_m is accompanied by increase in other entropy *i.e.* S_{lat} which implies the system should heat up. Under adiabatic removal of magnetic field, magnetic entropy increases as there is no heat exchange. This increase is accompanied by a decrease in lattice entropy resulting in a change in temperature and this is known as adiabatic temperature change ($\Delta T_{ad} = T_1 - T_0$). A → C describes isothermal magnetization/demagnetization. Upon introduction of external magnetic field, electronic and lattice entropies remain constant since temperature is constant. However magnetic entropy decreases as the spins align parallel with the field which results in a net decrease of total entropy of the system (ΔS_m). Spins again re-

randomize upon removal of the external magnetic field, the lattice and electronic entropies experience a decrease and reduction of these entropy terms lead to a temperature colder than initial.

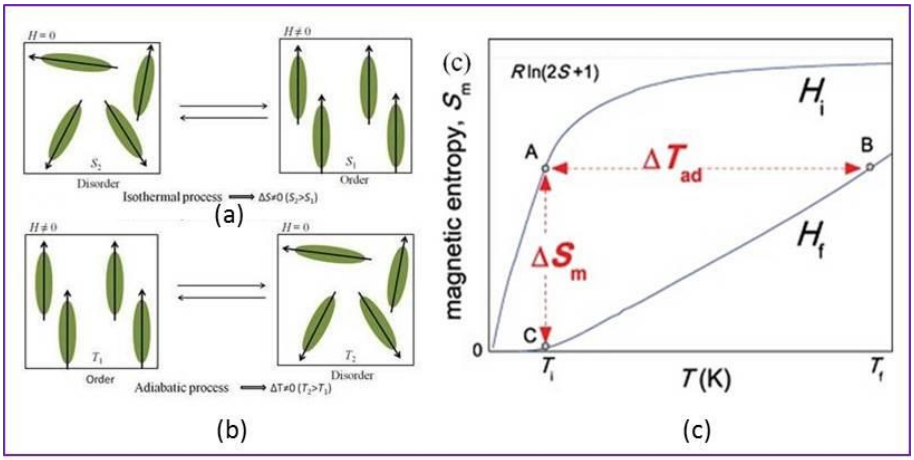

Figure 1.20. Schematic representation showing two basic processes of the MCE when a magnetic field is applied or removed in a magnetic system: (a) isothermal process leading to an entropy change (b) adiabatic process which yields a variation in temperature (c) Solid lines represent the total entropy in two different magnetic fields (H_i=0, H_f>0). The horizontal arrow shows ΔT_{ad} and the vertical arrow shows ΔS_m when the magnetic field is changed from H_i to H_f (H_i=$H_{initial}$ and H_f=H_{final})

The relationship between magnetic field (H), magnetization of a material (M) and temperature (T), MCE-related values ΔT_{ad} (T, ΔH) and ΔS_m (T, ΔH) is given by one of the Maxwell relation (1.11)

$$\left(\frac{\partial S(T,H)}{\partial H}\right)_T = \left(\frac{\partial M(T,H)}{\partial T}\right)_H \tag{1.11}$$

Which for an isothermal and adiabatic process led to:

$$\Delta S_m(T,\Delta H) = \int_{H_i}^{H_f}\left[\frac{\partial M\,(T,H)}{\partial T}\right]_H \mathrm{d}H \tag{1.12}$$

Equation 1.12 shows the relationship between change in magnetic entropy to the magnetization with respect to temperature at constant field and to the field variation.

For more practical applications, the requirement for an efficient magnetic coolant is that it should possess substantially high MCE at low magnetic fields. In other words, it should

respond quickly to magnetization and demagnetization. The advantage of using molecules as refrigerants over ordered ferro or ferri-magnets lie on the facile manipulation of chemical composition and ideal mono-dispersity in size. In addition to accessibility to fine tuning magnetothermal properties, previous studies have shown that enhancement of MCE requires some specific properties which include a) negligible magnetic anisotropy b) large metal-to-ligand ratio and c) moderate to weak ferromagnetic interactions results in large spin ground state value of *S*. High ground state would render high entropy change and temperature change. In addition to this, low-lying excited states and weak ferromagnetic interactions also contributes to the magnetic entropy.

$$S_m = n\mathrm{R}\ln(2S+1) \tag{1.13}$$

Where n represents the number of paramagnetic ions in the system.

1.13.2 Measurement of the magnetocaloric effect:

MCE efficiency can be measured by two methods which include direct and indirect. Direct method involves the measurement of initial and final temperature with change in magnetic field. In this case the adiabatic temperature change is quantified by

$$\Delta T_{ad}(T_0, H_F{-}H_0) = T_F - T_0 \tag{1.14}$$

These measurements can be performed using contact and non-contact techniques controlled by temperature sensor whether it is connected to sample or not. These measurements should be accompanied by a rapid alteration in the magnetic field and the accuracy depends on the errors in field settings, thermometry and quality of thermal insulation of the sample and is also effected by non-adiabatic measurement technique. Considering all these factors the accuracy of direct measurements is in the range of 5-10%. Only few molecular magnetic coolants have been measured by using this technique which include $[\{Gd(OAc)_3(H2O)_2\}_2]\cdot 4H_2O$ and $[Gd(HCOO)_3]_n$ and the results are in good agreement with the heat capacity measurements.[57]

In indirect method MCE efficiency can be calculated either by heat capacity or magnetization measurments, former case allows the calculation of both adiabatic temperature change (ΔT_{ad}) and magnetic entropy change (ΔS_m), whereas in later case magnetic entropy change (ΔS_m) is the only parameter possible to measure. The accuracy of

the magnetization measurements relies on the magnetic moment, temperature and magnetic field. The error in ΔS_m values (T, ΔH) lies in the range of 20-30%. Whereas better accuracy is found when heat capacity measurements are used to calculate MCE. However because of the accumulation of experimental errors at near room temperature in the total entropy functions, the errors arising in MCE evaluation are almost same whether calculated from direct or indirect magnetization measurements.

Knowing the requirements for high performance molecular magnetic coolants, synthetic chemists look towards isotropic metal ions. The most common metal ions used are Mn(II), Fe(III) with $d^5$and Gd(III) with f^7electronic configuration. Based upon the respective magnitudes of 3*d*–3*d*, 3*d*–4*f*, and 4*f*–4*f* coupling values, 3d complexes which are ferromagnetically-coupled and well-isolated 4f ions [especially Gd(III)] are promising candidates for applicability at sub-milli-Kelvin and elevated temperatures respectively. Whereas 3d–4f complexes find applications at intermediate temperatures. The ΔS_m values for 3*d* metal ions are not good due to unavoidable zero-field splitting and strong coupling between metal ions. Several alternatives have been proposed to achieve high MCE efficiency. The existence of appreciably large spin ground state along with low-lying excited states is important for a significant MCE as previously described. For the sake of enhancing the number of metal ions in a single entity, several authors have synthesized different polydenatate ligands. One important family of ligands used are organophosphates or organophosphonates.[58] Introducing small ferromagnetic interactions which induce fast response of the spins to the applied field results in quick magnetization at lower fields which is an important requirement for efficient and low-cost magnetic cooling devices. Due to ferromagnetic interactions, 3*d*-4*f* complexes have gained remarkable attention. Another important factor to achieve maximum entropy is negligeble magnetic anisotropy. Gd(III) has small intrinsic anisotropy due to the shielding of *f* orbitals by the larger 5*s* and 5*p* orbitals, this weakens interactions between adjacent metal ions. Hence, Gd(III) based complexes are regarded as promising candidates for magnetic refrigerators.

1.14 3*d*-Based molecular magnetic coolants:

Molecular magnetic coolants were first observed in famous SMMs Mn_{12} and Fe_8, both having ground state S = 10 and appreciable magnetic anisotropy.[10, 20b] In absence of external magnetic field, system retains its magnetization because of the extreme magnetic

anisotropy and these molecules does not show the entropy change as predicted by −R ln(2*S* + 1). Later Winpenny and co-workers reported an anti-ferromagnetically coupled ring, {Cr_7Cd} complex[59a] with magnetic cooling properties having a diamagnetic Cd(II) and seven Cr(III) ions which are bridged by fluoride and pivalate counter anions. Entropy change is not so high because of the lower ground state value *S* =3/2, which in turn suggests that the molecule has high-spin but isotropic metal ions act as good candidate for molecular coolers. Later McIness and co-workers reported a large high spin Fe_{14} cluster with *S* = 25 having a hexa-capped hexagonal bipyramid core of Fe^{3+} centres.[59b] Both ferro and anti-ferromagnetic interactions co-exist in the molecule and the large MCE (ΔS_m = 17.6 J $kg^{-1}K^{-1}$) exhibited by this molecule is because of its high density along with low-lying excited states which originate from magnetic frustration. Another example is pure Fe(III) based cluster Fe_{17}, reported by Evangelisti with a ground state *S* = 35/2[59c] and having a very small zero-field splitting parameter (*D* = -0.023 cm^{-1}). This low zero-field splitting along with lack of magnetic ordering suggests that Fe_{17} molecular nanomagnet can be used as magnetic refrigerant. Manoli *et al*. reported a mixed valent $Mn^{II}_6Mn^{III}_4$ supertetrahedral molecule {Mn_{10}} which was found to be a very good magnetic coolant. Due to T_d symmetry, this molecule possess a vanishing zero field splitting[59d] and magnetic studies show that it has a large ground state *S* = 22. Heat capacity measurements show that the entropy change (ΔS_m) reaches a maximum of 13.0 J $kg^{-1}K^{-1}$ at around 2.2 K. In addition, several 3d complexes with high spin ground states including {Mn_{10}} (*S*=28±1),[59e] {Na_2Mn_{15}}(*S*=32) ,[59f] {Mn_{19}}(with record spin ground state *S*=83/2)[59g] were reported but because of their large ground state spins, very low values for MCE were observed. Recently Tong and co-workers studied the comparison between a 3D coordination polymer $[Mn(II)(glc)_2]_n$ and discrete mononuclear $[Mn(II)(glc)_2(H_2O)_2]$.[59h] The maximum $-\Delta S_m$ value increased from a small value of 6.9 J $kg^{-1}K^{-1}$ to a huge value of 60.3 J $kg^{-1}K^{-1}$ (figure 1.21). Water molecules break polymeric framework into monomeric pieces which changes the magnetic structure and largely reduces magnetic interactions. This study finally cocludes that the effect of magnetic coupling on MCE is most prominent when compared to other factors such as magnetic density for 3*d*-type magnetic refrigerants. The draw-back of using 3*d* SMMs as magnetic coolants are as follows: (1) the presence of a magnetic hysteresis loop results in loss of energy and hence effects the performance of MCE (2) the magnetic anisotropy results in smaller $-\Delta S_m$ value and (3)

finally though a high spin state is attained through strong interaction, maximum value of $-\Delta S_m$ is lower than the one without interactions.

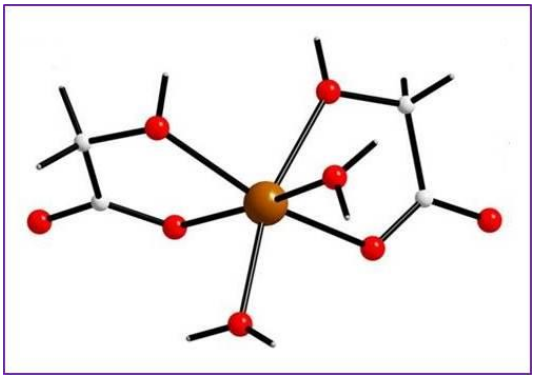

Figure 1.21. Molecular structure of $[Mn(II)(glc)_2(H_2O)_2]$

1.15 3*d*-4*f*-Based molecular magnetic coolants:

High spin density 3d ions in combination with weak exchange 4*f* ions can result in generating weak magnetic interactions. Among 3*d* metal ions, isotropic Cr(III) (d^3), Mn(II) (d^5) and Fe(III) (d^5) are preferred than anisotropic ions. Brechin and co-workers reported first 3*d*-4*f* mixed metal cluster $\{Mn_4Gd_4\}$ using calix[4]arene complex and described its magnetic properties which demonstrate typical interactions between Mn(III) and Gd(III) which are weak ferromagnetic in nature. In this complex, entropy change values to 19 J kg^{-1} K^{-1} at 4 K with ΔH = 7 T and it acts as magnetic refrigerant at low temperatures (figure 1.22).[60a] Some of the reported Mn–Gd species including $\{Mn_4Gd_6\}$ and $\{Mn_9Gd_9\}$[60b] clusters have recently been documented. Synthesis of oxydiacetate (oda) bridged Mn(II)–Gd(III) 3D MOF and its MCE evaluation through both magnetization and heat capacity measurements showed entropy change of 50.1 J kg^{-1} K^{-1} for ΔH=70 kG.[60c] Furthermore, weak ferromagnetic interactions and low molecular mass generates appreciable entropy change even at lesser field strengths (42.6 J $kg^{-1}K^{-1}$with ΔH = 30 kOe and 26.7 J $kg^{-1}K^{-1}$with ΔH = 10 kOe) which eventually prove this complex as an effective coolant under low field conditions. So far, many 3d-4f magnetic coolants have been reported with different ligand systems like alkoxides, phosphonates and carboxylates.[60d-f]

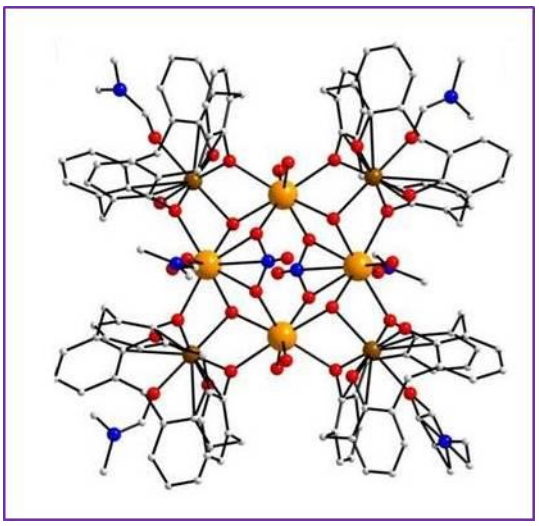

Figure 1.22. Molecular structure of [Mn_4Gd_4]

Among 3*d*-4*f* clusters, Cu-Gd comprises a large proportion of molecular magnetic coolants. Murray and co-workers reported an unusual but elegant {Cu_5Gd_4} cluster composed of a series of vertex- and face-sharing {$GdCu_3$} tetrahedra.[60g]The weak ferromagnetic interactions between Cu(II)−Gd(III), low molecular mass and an inbuilt weak exchange of lanthanide ions, populate numerous *S* states even at the lowest temperatures which lifts the MCE with $-\Delta S_m$ value larger than 30 J kg^{-1} K^{-1}.

Long and co-workers reported a structurally fascinating 48-metal cluster complex {$Gd_{36}Ni_{12}$}, resulting from self-assembly of metal ions in presence of mixed anionic species.[61a] Magnetic studies show a remarkable change in entropy (36.3 J kg^{-1} K^{-1}) at lower temperature (3 K) with respect to changes in the magnetic field (70 kOe). The significantly large values of MCE may be attributed to large metal/ligand ratio along with use of small acetate ligand. In another report two 3*d*-4*f* coordination polymers [{$Gd_{42}Ni_{10}$}and {$Gd_{42}Co_{10}$}] were synthesized by making use of similar light acetate ligands. These polymers have a bowl-like core made of {Gd_8(III) },{Gd_6(III) M_2}, and {M_4} subunits gauged by perchlorate (ClO_4^-) and carbonate (CO_3^{2-}) anions.[61b] Magnetic studies revealed {$Gd_{42}Ni_{10}$} complex showing entropy change of 38.2 J $kg^{-1}K^{-1}$with ΔH = 70 kOe at 2.0 K and for {$Gd_{42}Co_{10}$} it is 41.3 J $kg^{-1}K^{-1}$, which are less than theoretical values and the reason can be attributed to the presence of intra-cluster antiferromagnetic interactions and crystal-field effects. The larger $-\Delta S_m$ value for Co(II) complex compared with Ni(II) can be explained on the basis of larger ground-state spin for Co(II) relative to Ni(II).

The near isotropy of Cr(III) d^3 and Fe(III) d^5 makes them efficient candidates for 3*d*-4*f* low temperature molecular magnetic coolants. A couple of Cr(III)-Gd(III) complexes {Cr_2–Gd_2} and {Cr_2–Gd_3}were prepared by using fluoride as bridging ligand.[61c] Magnetic studies reveal that MCE value of {Cr_2–Gd_2} complex is relatively small (11.4 J $kg^{-1}K^{-1}$ at 4.1 K with ΔH = 90 kOe.) due to strong antiferromagnetic interactions between metal ions. However the magnetic coupling and relatively small ZFS in {Cr_2–Gd_3} makes it a good candidate for MCE where change in entropy reaches to 28.7 J $kg^{-1}K^{-1}$at 2.2 K with ΔH = 90 kOe.

1.16 4*f*-Based molecular magnetic coolants:

The first pure 4*f* based magnetic coolant is disc shaped {Gd_7} reported by Collison and co-workers very recently (figure 1.23). The molecule comprises of a central Gd(III) which is surrounded by a Gd_6 hexagon with μ_3-hydroxy groups and it has a C_3 symmetry.[62a] The core of the cluster is surrounded by ligands including triphenylacetate and tris(hydroxymethyl)ethane. Entropy change of 23 J $kg^{-1}K^{-1}$ for ΔH = 7 T at 3 K was calculated from magneto thermal studies. A square-based pyramid {$Gd_5O(O^iPr)_{13}$} reported by Winpenny and co-workers shows entropy change of 34 J kg^{-1} K^{-1} which is lesser than the theoretical value of 55 J kg^{-1} K^{-1}. This may be due to strong magnetic interactions between metal ions.[62b] Evangelisti and co-workers reported a gadolinium acetate dimer {Gd_2} with an exceptionally high MCE value (40 J kg^{-1} K^{-1}) at extremely low temperature where the intramolecular ferromagnetic exchange favours field dependent enhancement of the MCE.[62c] Later, Tong and co-workers expanded this acetate-bridging structure into a tetramer [$Gd_4(OAc)_4(acac)_8(H_2O)_4$] and a linear chain $[Gd(OAc)_3(H_2O)_{0.5}]_n$,[62d] These complexes show different magnetic coupling due to difference in Gd-O-Gd angles. In tetramer, the Gd-O-Gd angles are larger showing ferromagnetic interactions whereas in linear chain the angles are smaller resulting in antiferromagnetic interactions and show highest magnetic density due to lower M_w/N_{Gd} ratio and exhibits high MCE (40 J kg^{-1} K^{-1}) than the tetramer. Later, many 4*f* based magnetic coolants were reported some of them are listed below (Table 1.2).

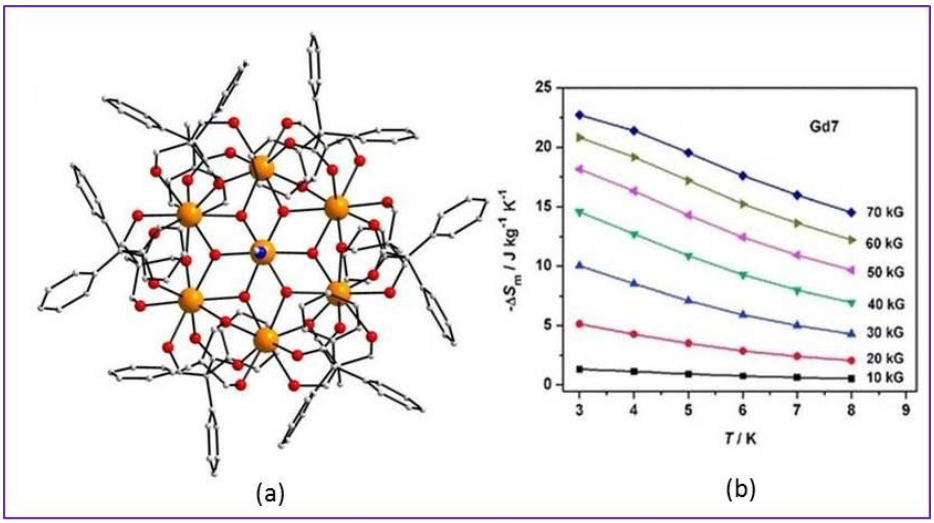

Figure 1.23. (a) Molecular structure of $[Gd_7(OH)_6(thmeH_2)_5(thmeH)(tpa)_6(MeCN)_2](NO_3)_2$ (b) Temperature-dependency of $-\Delta S_m$

Table 1.2 Some of the reported 4*f* -based magnetic coolants

	$-\Delta S_m$ ($J\ Kg^{-1}\ K^{-1}$)	ΔH(T)	T_{max} (k)	Ref
$[Gd_7(OH)_6(thmeH_2)_5(thmeH)(tpa)_6(MeCN)_2](NO_3)_2$	23	7	3	46a
$[Gd_5O(O^iPr)_{13}]$	34	7	3	62b
$[Gd_{24}(DMC)_{36}(CO_3)_{18}(H_2O)_2]\ 6H_2O$	46.1	7	2.5	63a
$[\{Gd(OAc)_3(H_2O)_2\}_2]\cdot 4H_2O$	40	7	2	57a
$[Gd_4(OAc)_4(acac)_8(H_2O)_4]$	30.7	7	2.4	62d
1D				
$[Gd_2(OAc)_3(MeOH)]_n$	45	7	2	63b
$[Gd_2(OAc)_3(H_2O)_{0.5}]_n$	47	7	2	63b
$[Gd(HCOO)(OAC)_2(H_2O)_2]_n$	45.9	7	1.8	63c
2D				
$[Gd(C_4O_4)(OH)(H_2O)_4]_n$	47.3	9	3	63c
3D				
$[Gd_2(fum)_3(H_2O)_4]_n.3nH_2O$	20.7	7.5	5	63d
$[Gd_2(N\text{-}BDC)_3(DMF)_4]_n$	29	7	2	63b
$[Gd_5Zn(BPDC)_3(H_2O)_{10}(OH)_6]_n$	30.7	7	3	63e
$[Gd_{36}(NA)_{36}(OH)_{49}(O)_6(NO_3)_6]_n$	40	7	3	63f
$[Gd_2(OH)_2(suc)_2(H_2O)]_n$	42.8	7	1.8	63g
$[Gd_6(OH)_8(suc)_5(H_2O)_2]_n$	48	7	1.8	63g
$[Gd(HCOO)(C_8H_4O_4)]_n$	47	9	2.3	63h
$[Gd(HCOO)_3]_n$	59	7	3	57b
$[Gd(OH)CO_3]_n$	66.4	7	1.8	63i

1.17 Motivation for the work carried out:

In light of the increasing demand for molecules with better SMM and MCE properties efforts were directed towards the synthesis of lanthanide based polynuclear clusters with different types of ligands. The work embodied in this thesis mainly focused on synthesis, structural characterization and detailed study of magnetic properties of lanthanide clusters. Studies were extended to understand the effect of different ligand systems on the nuclearity and magnetic properties of resulting clusters.

Though there are ample reports of Lanthanide β-diketone clusters in literature, use of functionalized β-diketones and triketones as ligands is scarcely reported. In this backdrop, orthosubstituted β-diketones with and without coligands were used for the synthesis of lanthanide clusters, whose synthesis, structural characterization and magnetic properties were discussed in chapter 2 and 3.

Further extension to this work was done and triketones as such or in presence of β-diketone were used as ligands. The effect of increasing the number of donar site on ligand from di to triketones and its effect on coordinating ability of the ligand were studied and the results obtained are discussed in chapter 4.

Though phosphorous based ligands like organophosphonates and organophosphates have been used for the synthesis of lanthanide clusters with large MCE values, there are no reports with phosphinic acids as ligands for such study. Cyclic phosphinic acid was used as ligand for the first time and the results are discussed in chapter 5.

1.18 References:

(1) Gatteschi, D.; Sessoli, R.; Villain, J. Molecular Nanomagnets, *Oxford University Press.* **2006**.

(2) (a) Christou, G.; Gatteschi, D.; Hendrickson, D. N.; Sessoli, R. *MRS Bull*. **2000**, *25*, 66. (b) Gatteschi, D.; Sessoli. R. *Angew. Chem. Int. Ed.* **2003**, *43*, 268. (c) Aromi, G.; Brechin, E. K. *Struct. Bonding*. **2006**, *122*, 1. (d) Bagai, R.; Christou, G. *Chem. Soc. Rev.* **2009**, *38*, 1011.

(3) Frost, J. M.; Harriman, K. L. M.; Murugesu, M. *Chem. Sci*. **2016**, *7*, 2470.

(4) Mannini, M.; Pineider, F.; Sainctavit, P.; Danieli, C.; Otero, E.; Sciancalepore, C.; Talarico, A.M.; Arrio, M.-A.; Cornia, A.; Gatteschi, D.; Sessoli, R. *Nature Mater*. **2009**, *8*, 194.

(5) (a) Thiele, S.; Balestro, F.; Ballou, R.; Klyatskaya, S.; Ruben, M.; Wernsdorfer. W. *Science*. **2014**, *344*, 1135. (b) Bogani, L.; Wernsdorfer, W. *Nat. Mater*. **2008**, *7*, 179. (c) Affronte, M.; Troiani, F.; Ghirri, A.; Candini, A.; Evangelisti, M.; Corradini, V.; Carretta, S.; Santini, P.; Amoretti, G.; Tuna, F.; Timco, G.; Winpenny. R. E. P. *J. Phys. D*: *Appl. Phys*. **2007**, *40*, 2999. (d) Wernsdorfer, W. *Nat. Mater*. **2007**, *6*, 174. (e) Timco, G. A.; Carretta, S.; Troiani, F.; Tuna, F.; Pritchard, R. J.; Muryn, C. A.; McInnes, E. J. L.; Ghirri, A.; Candini, A.; Santini, P.; Amoretti, G.; Affronte, M.; Winpenny, R. E. P. *Nat. Nanotechnol*. **2009**, *4*, 173.

(6) (a) https://upload.wikimedia.org/wikipedia/commons/3/30/LS_coupling.svg, Creative Commons Licence. (b) Rinehart, J. D.; Long, J. R. chem. Sci. 2011, 2, 2078.

(7) Kahn, O. *Molecular Magnetism*, Wiley-VCH, Publishers Inc.: New York, 1993

(8) Popescu, C. V.; Mock, M. T.; Stoian, S. A.; Dougherty, W. G.; Yap, G. P. A.; Riordan, C. G. *Inorg. Chem*. **2009**, *48*, 8317.

(9) Karunadasa, H. I.; Arquero, K. D.; Berben, L. A.; Long, J. R. *Inorg. Chem*. **2010**, *49*, 4738.

(10) Lis,T. *Acta Crystallogr., Sect. B: Struct. Crystallogr. Cryst. Chem*. **1980**, *36*, 2042.

(11) (a) Sessoli, R.; Gatteschi, D.; Caneschi, A.; Novak, M. A. *Nature* **1993**, *365*, 141. (b) Sessoli, R.; Tsai, H. L.; Schake, A. R.; Wang, S. Y.; Vincent, J. B.; Folting, K.; Gatteschi, D.; Christou, G.; Hendrickson, D. N. *J. Am. Chem. Soc*. **1993**, *115*, 1804.

(12) (a) Milios, C. J.; Vinslava, A.; Wernsdorfer, W.; Moggach, S.; Parsons, S.; Perlepes, S. P.; Christou, G.; Brechin, E. K. *J. Am. Chem. Soc*. **2007**, *129*, 2754. (b) Rinehart, J. D.;

Fang, M.; Evans, W. J.; Long, J. R. *Nat. Chem*. **2011**, *3*, 538. (c) Rinehart, J. D.; Fang, M.; Evans, W. J.; Long, J. R. *J. Am. Chem. Soc*. **2011**, *133*, 14236. (d) Blagg, R. J.; Ungur, L.; Tuna, F.; peak, J.; Comar, P.; Collison, D.; Wernsdorfer, W.; Mclnnes, E. J. L.; Chibotaru, L. F.; Winpenny, R. E. P. *Nat. Chem*. **2013**, *5*, 673.

(13) (a) Tsai, H.-L.; Chen, D.-M.; Yang, C.-I.; Jwo, T.-Y.; Wur, C.-S.; Lee, G.-H.; Wang, Y.; *Inorg. Chem. Commun*. **2001**, *4*, 511.(b) Jones, L. F.; Rajaraman, G.; Brockman, J.; Murugesu, M.; Raftery, J.; Teat, S. J.; Wernsdorfer, W.; Christou, G.; Brechin, E. K.; Collison, D. *Chem*. *Eur. J*. **2004**, *10*, 5180. (c) Murugesu, M.; Habrych, M.; Wernsdorfer, W.; Abboud, K. A.; Christou, G. *J. Am. Chem. Soc*. **2004**, *126*, 4766. (d) Ako, A. K.; Hewitt, I. J.; Mereacre, V.; Clérac, R.; Wernsdorfer, W.; Anson, C. E.; Powell, A. K. *Angew. Chem. Int. Ed*. **2006**, *45*, 4926. (e) Yang, C.-I.; Lee, G.-H.; Wur, C.-S.; Lin, J.-G.; Tsai, H.-L. *Polyhedron* **2005**, *24*, 2215. (f) Brechin, E. K.; Sanudo, E. C.; Wernsdorfer, W.; Boskovic, C.; Yoo, J.; Hendrickson, D. N.; Yamaguchi, A.; Ishimoto, H.; Concolino, T. E.; Rheingold, A. L.; Christou, G. *Inorg.Chem*. **2005**, *44*, 502. (g) Piligkos, S.; Rajaraman, G.; Soler, M.; Kirchner, N.; Slageren, J.; Bircher, R.; Parsons, S.; Guedel, H. U.; Kortus, J.; Wernsdorfer, W.; Christou, G.; Brechin, E. K. *J. Am. Chem. Soc*. **2005**, *127*, 5572. (h) Gatteschi, D.; Sessoli, R.; Cornia, A. *Chem. Commun*. **2000**, 725. (i) Accorsi, S.; Barra, A.-L.; Caneschi, A.; Chastanet, G.; Cornia, A.; Fabretti, A. C.; Gatteschi, D.; Mortalò, C.; Olivieri, E.; Parenti, P.; Rosa, P.; Sessoli, R.; Sorace, L.; Wernsdorfer, W.; Zobbi, L. *J. Am. Chem. Soc*. **2006**, *128*, 4742. (j) Murrie, M.; Teat, S. J.; Stoeckli-Evans, H.; Güdel, H. U. *Angew. Chem. Int. Ed*. *42* **2003** 4653. (k) Ochsenbein, S. T.; Murrie, M.; Rusanov, E.; Stoeckli-Evans, H.; Sekime, C.; Güdel, H. U. *Inorg. Chem*. **2002**, *41*, 5133. (l) Aromí, G.; Parsons, S.; Wernsdorfer, W.; Brechin, E. K.; McInnes, E. J. L. *Chem. Commun*. **2005**, 5038. (m) Oshio, H.; Nihei, M.; Koizumi, S.; Shiga, T.; Nojiri, H.; Nakano, M.; Shirakawa, N.; Akatsu, M. *J. Am. Chem. Soc*. **2005**, *127*, 4568. (n) Schelter, E. J.; Prosvirin, A.V.; Dunbar, K. R. *J. Am. Chem. Soc*. **2004**, *126*, 15004. (o) Zaleski, C. M.; Depperman, E. C.; Kampf, J. W.; Kirk, M. L.; Pecoraro, V. L. *Angew. Chem. Int. Ed*. **2004**, *43* 3912. (p) Mishra, A. Wernsdorfer, W.; Abboud, K. A.; Christou, G. *J. Am. Chem. Soc*. **2004**, 126, 15648. (q) Eppley, H. J.; Tsai, H.-L.; de Vries, N.; Folting, K.; Christou, G.; Hendrickson, D. N. *J. Am. Chem. Soc*. **1995**, *117*, 301. (r) Milios, C. J.; Raptopoulou, C. P.; Terzis, A.; Lloret, F.; Vicente, R.; Perlepes, S. P.; Escuer, A. *Angew. Chem., Int. Ed*. **2004**, *43*, 210. (s) Tasiopoulos, A. J.; Vinslava, A.; Wernsdorfer, W.; Abboud, K.

A.; Christou, G. *Angew. Chem. Int. Ed*. **2004**, *43*, 2117. (t) Chakov, N. E.; Lee, S.-C.; Harter, A. G.; Kuhns, P. L.; Reyes, A. P.; Hill, S. O.; Dalal, N. S.; Wernsdorfer, W.; Abboud, K. A.; Christou, G. *J. Am. Chem. Soc*. **2006**, *128*, 6975. (u) Milios, C. J.; Inglis, R.; Vinslava, A.; Bagai, R.; Wernsdorfer, W.; Parsons, S.; Perlepes, S. P.; Christou, G.; Brechin, E. K. *J. Am. Chem. Soc*. **2007**, *129*, 12505. (v) Thuijs, A. E.; King, P.; Abboud, K. A.; Christou, G. *Inorg. Chem*. **2015**, *54*, 9127.

(14) Eppley, H. J.; Tsai, H.-L.; de Vries, N.; Folting, K.; Christou, G.; Hendrickson, D. N. *J. Am. Chem. Soc*. **1995**, *117*, 301.

(15) Chakov, N. E.; Wernsdorfer, W.; Abboud, K. A.; Hendrickson, D. N.; Christou, G. *Dalton Trans*. **2003**, 2243.

(16) Boskovic, C.; Pink, M.; Huffman, J. C.; Hendrickson, D. N.; Christou, G. *J. Am. Chem. Soc*. **2001**, *123*, 9914.

(17) Artus, P.; Boscovic, C.; Yoo, J.; Streib, W. E.; Brunel, L. C.; Hendrickson, D. N.; Christou, G. *Inorg. Chem*. **2001**, *40*, 4199.

(18) (a) Pacchioni, M.; Cornia, A.; Fabretti, A. C.; Zobbi, L.; Bonacchi, D.; Caneschi, A.; Chastanet, G.; Gatteschi, D.; Sessoli, R. *Chem. Commun*. **2004**, 2604. (b). Bagai, R.; Christou, G. *Chem. Soc. Rev*. **2009**, *38*, 1011.

(19) (a) Barra, A. L.; Caneschi, A.; Cornia, A.; Fabrizi de Biani, F.; Gatteschi, D.; Sangregorio, C.; Sessoli, R.; Sorace, L. *J. Am. Chem. Soc*. **1999**, *121*, 5302. (b) Wieghardt, K.; Pohl, K.; Jibril, I.; Huttner, G. *Angew. Chem. Int. Ed*. **1984**, 23, 77.

(20) (a) Boudalis, A. K.; Sanakis, Y.; Clemente-Juan, J. M.; Donnadieu, B.; Nastopoulos, V.; Mari, A.; Coppel, Y.; Tuchagues, J.- P.; Perlepes, S. P. *Chem. Eur. J*. **2008**, *14*, 2514. (b) Taft, K. L.; Delfs, C. D.; Papaefthymiou, G. C.; Foner, S.; Gatteschi, D.; Lippard, S. J. *J. Am. Chem. Soc*. **1994**, *116*, 823. (c) Benelli, C.; Cano, J.; Journaux, Y.; Sessoli, R.; Solan, G. A.; Winpenny, R. E. P. *Inorg. Chem*. **2001**, *40*, 188. (d) Hoshino, N.; Ako, A. M.; Powell, A. K.; Oshio, H. *Inorg. Chem*. **2009**, *48*, 3396. (e) Powell, A. K.; Heath, S. L.; Gatteschi, D.; Pardi, L.; Sessoli, R.;Spina, G.; Delgiallo, F.; Pieralli, F. *J. Am. Chem. Soc*. **1995**, *117*, 2491.

(21) (a) Mossin, S.; Tran, B. L.; Adhikari, D.; Pink, M.; Heinemann, F. W.; Sutter, J. P.; Szilagyi, R. K.; Meyer, K.; Mindiola, D. J. *J. Am. Chem. Soc*. **2012**, *134*, 13651. (b) Goodwin, J. C.; Sessoli, R.; Gatteschi, D.; Wernsdorfer, W.; Powell, A. K.; Heath, S. L. *Dalton Trans*. **2000**, 1835. (c) Boudalis, A. K.; Sanakis, Y.; Clemente-Juan, J. M.; Donnadieu, B.; Nastopoulos, V.; Mari, A.; Coppel, Y.; Tuchagues, J.-P.; Perlepes, S.

P. *Chem. Eur. J*. **2008**, *14*, 2514. (d) Lin, P.-H.; Smythe, N. C.; Gorelsky, S. I.; Maguire, S.; Henson, N. J.; Korobkov, I.; Scott, B. L.; Gordon, J. C.; Baker, R. T.; Murugesu, M. *J. Am. Chem. Soc*. **2011**, *133*, 15806. (e) Harman, W. H.; Harris, T. D.; Freedman, D. E.; Fong, H.; Chang, A.; Rinehart, J. D.; Ozarowski, A.; Sougrati, M. T.; Grandjean, F.; Long, G. J.; Long, J. R.; Chang, C. J. *J. Am. Chem. Soc*. **2010**, *132*, 18115. (f) Zadrozny, J. M.; Atanasov, M.; Bryan, A. M.; Lin, C.-Y.; Rekken, B. D.; Power, P. P.; Neese, F.; Long, J. R. *Chem. Sci*. **2013**, *4*, 125. (g) Zadrozny, J. M.; Xiao, D. J.; Atanasov, M.; Long, G. J.; Grandjean, F.; Neese, F.; Long, J. R. *Nat. Chem*. **2013**, *5*, 577.

(22) (a) Yang, E. C.; Hendrickson, D. N.; Wernsdorfer, W.; Nakano, M.; Zakharov, L. N.; Sommer, R. D.; Rheingold, A. L.; Ledezma-Gairaud, M.; Christou, G. *J. Appl. Phys*. **2002**, *91*, 7382. (b) Galloway, K. W.; Whyte, A. M.; Wernsdorfer, W.; Sanchez-Benitez, J.; Kamenev, K. V.; Parkin, A.; Peacock, R. D.; Murrie, M. *Inorg. Chem*. **2008**, *47*, 7438. (c) Moubaraki, B.; Murray, K. S.; Hudson, T. A.; Robson, R. *Eur. J. Inorg. Chem*. **2008**, 4525. (d) Murrie, M. *Chem. Soc. Rev*. **2010**, *39*, 1986. (e) Zhu, Y.-Y.; Zhang, Y.-Q.; Yin, T.-T.; Gao, C.; Wang, B.-W.; Gao, S. *Inorg. Chem*. **2015**, *54*, 5475.

(23) (a) Cadiou, C.; Murrie, M.; Paulsen, C.; Villar, V.; Wernsdorfer, W.; Winpenny, R. E. P. *Chem. Commun*. **2001**, 2666. (b) Yang, E.-C.; Wernsdorfer, W.; Hill, S.; Edwards, R. S.; Nakano,M.; Maccagnano, S.; Zakharov, L. N.; Rheingold, A. L.; Christou, G.;Hendrickson, D. N. *Polyhedron* **2003**, *22*, 1727. (c) Moragues-Canovas, M.; Helliwell, M.; Ricard, L.; Rivière, E.; Wernsdorfer, W.; Brechin, E.; Mallah, T. *Eur. J. Inorg. Chem*. **2004**, 2219. (d) Bell, A.; Aromi, G.; Teat, S. J.; Wernsdorfer, W.; Winpenny, R. E. P. *Chem. Commun*. **2005**, 2808. (e) Aromi, G.; Parsons, S.; Wernsdorfer, W.; Brechin, E. K.; McInnes, E. J. L. *Chem. Commun*. **2005**, 5038. (f) Aromi, G.; Bouwman, E.; Burzuri, E.; Carbonera, C.; Krzystek, J.; Luis, F.; Schlegel, C.; van Slageren, J.; Tanase, S.; Teat, S. J. *Chem. Eur. J*. **2008**, *14*, 11158. (g) Ferguson, A.; Lawrence, J.; Parkin, A.; Sanchez-Benitez, J.; Kamenev, K. V.; Brechin, E. K.; Wernsdorfer, W.; Hill, S.; Murrie, M. *Dalton Trans*. **2008**, 6409. (h) Serna, Z.; De la Pinta, N.; Urtiaga, M. K.; Lezama, L.; Madariaga, G.; Clemente-Juan, J. M.; Coronado, E.; Cortes, R. *Inorg. Chem*. **2010**, *49*, 11541. (i) Ferguson, A.; Schmidtmann, M.; Brechin, E. K.; Murrie, M. *Dalton Trans*. **2011**, *40*, 334. (j) Zhang, S. H.; Li, N.; Ge, C. M.; Feng, C.; Ma, L. F. *Dalton Trans*. **2011**, *40*, 3000. (k) Aromí,

G.; Parsons, S.; Wernsdorfer, W.; Brechin, E. K.; McInnes, E. J. L. *Chem. Commun*. **2005**, 5038. (l) Cadiou, C.; Murrie, M.; Paulsen, C.; Villar, V.; Wernsdorfer, W.; Winpenny, R. E. P. *Chem. Commun*. **2001**, 2666. (m) Yang, E. C.; Wernsdorfer, W.; Hill, S.; Edwards, R. S.; Nakano, M.; Maccagnano, S.; Zakharov, L. N.; Rheingold, A. L.; Christou, G.; Hendrickson, D. N.; *Polyhedron* **2003**, *22*, 1727. (n) Moragues-Cánovas, M.; Helliwell, M.; Ricard, L.; Riviefe, E.; Wernsdorfer, W.; Brechin, E. K.; Mallah, T. *Eur. J. Inorg. Chem*. **2004**, 2219. (o) Ochsenbein, S. T.; Murrie, M.; Sekine, C.; Stoeckli-Evans, H.; Rusanov, E.; Güdel, H. U. *Inorg. Chem*. **2002**, *41*, 5133. (p) Bell, A.; Aromí, G.; Teat, S. J.; Wernsdorfer, W.; Winpenny, R. E. P. *Chem. Commun*. **2005**, 2808. (q) Petit, S.; Neugebauer, P.; Pilet, G.; Chastanet, G.; Barra, A. L.; Antunes, A. B.; Wernsdorfer, W.; Luneau, D. *Inorg. Chem*. **2012**, *51*, 6645.

(24) (a) Costes, J.-P.; Dahan, F.; Dupuis, A.; Laurent, J.-P. *Inorg. Chem*. **1996**, *35*, 2400. (b) Rinck, J.; Novitchi, G.; Heuvel, W. V.; Ungur, L.; Lan, Y.; Wernsdorfer, W.; Anson, C. E.; Chibotaru, L. F.; Powell, A. K. *Angew. Chem., Int. Ed*. **2010**, *49*, 7583. (c) Xiang, H.; Lu, W.-G.; Zhangc, W.-X.; Jiang, L. *Dalton Trans*. **2013**, *42*, 867. (d) Yamashita, A.; Watanabe, A.; Akine, S.; Nabeshima, T.; Nakano, M.; Yamamura, T.; Kajiwara, T. *Angew. Chem. Int. Ed*. **2011**, *50*, 4016. (e) Watanabe, A.; Yamashita, A.; Nakano, M.; Yamamura, T.; Kajiwara, T *Chem.- Eur. J*. **2011**, *17*, 7428. (f) Saalfrank, R. W.; Scheurer, A.; Bernt, I.; Heinemann, F. W.; Postnikov, A. V.; Schünemann, V.; Trautwein, A. X.; Alam, M. S.; Rupp, H.; Müller, P. *Dalton Trans*. **2006**, 2865 (g) Ako, A. M.; Waldmann, O.; Mereacre, V.; Klöwer, F.; Hewitt, I. J.; Anson, C. E.; Güdel, H. U.; Powell, A. K. *Inorg. Chem*. **2007**, *46*, 756. (h) Saalfrank, R. W.; Deutscher, C.; Sperner, S.; Nakajima, T.; Ako, A. M.; Uller, E.; Hampel, F.; Heinemann, F. W. *Inorg. Chem*. **2004**, *43*, 4372. (i) Rumberger, E. M.; Zakharov, L. N.; Rheingold, A. L.; Hendrickson, D. N. *Inorg. Chem*. **2004**, *43*, 6531. 6 (j) Ungur, L.; Langley, S. K.; Hooper, T. N.; Moubaraki, B.; Brechin, E. K.; Murray, K. S.; Chibotaru, L. F. *J. Am. Chem. Soc*. **2012**, *134*, 18554. (k) Langley, S. K.; Moubaraki, B.; Murray, K. S. *Polyhedron*, **2013**, *64*, 255. (l) Langley, S. K.; Moubaraki, B.; Murray, K. S. *Inorg. Chem*. **2012**, *51*, 3947. (m) Chandrasekhar, V.; Pandian, B. M.; Vittal, J. J.; Clérac, R. *Inorg. Chem*. **2009**, *48*, 1148. (n) Chandrasekhar, V.; Pandian, B. M.; Boomishankar, R.; Steiner, A.; Vittal, J. J.; Houri, A.; Clérac, R. *Inorg. Chem*. **2008**, *47*, 4918. (o) Palacios, M. A.; Titos-Padilla, S.; Ruiz, J.; Herrera, J. M.; Pope, S. J.; Brechin, E. K.; Colacio, E. *Inorg. Chem*. **2014**, *53*, 1465 (p) Titos-Padilla, S.; Ruiz,

J.; Herrera, J. M.; Brechin, E. K.; Wersndorfer, W.; Lloret, F.; Colacio, E. *Inorg. Chem*. **2013**, *52*, 9620.

(25) (a) Stamatatos, T. C.; Efthymiou, C. G.; Stoumpos, C. C.; Perlepes, S. P. *Eur. J. Inorg.Chem*. **2009**, *18*, 336. (b) Tasiopoulos, A. J.; Perlepes, S. P. *Dalton Trans*. 2008, *37*, 553. (c) Papaefstathiou, G. S.; Perlepes, S. P. *Inorg. Chem*. **2002**, *23*, 249. (d) Stoumpos, C. C.; Rubeau, O.; Aromi, G.; Tasiopoulos, A. J.; Nastopoulos, V.; Escuer, A.; Perlepes, S. P. *Inorg. Chem*. 2010, *49*, 359. (e) Georgopoulou, A. N.; Efthymiou, C. G.; Papatriantafyllopoulou, C.; Psycharis, V.; Raptopoulou, C. P.; Manos, M.; Tsiopoulos, A. J.; Escuer, A.; Perlepes, S. P. *Polyhedron* **2011**, *30*, 2978. (f) Upadhyay, A.; Singh, S. K.; Das, C.; Mondol, R.; Langley, S. K.; Murray, K. S.; Rajaraman, G.; Shanmugam, M. *Chem. Commun*. **2014**, *50*, 8838. (g) Xu, G.-F.; Gamez, P.; Tang, J.; Clerac, R.; Guo, Y.-N.; Guo, Y. *Inorg. Chem*. **2012**, *51*, 5693. (h) Kajiwara, T.; Nakano, M.; Takahashi, K.; Takaishi, S.; Yamashita, M. *Chem. – Eur. J*. **2011**, *17*, 196. (i) Dong, H.-M.; Li, Y.; Liu, Z.-Y.; Yang, E.-C.; Zhao X.-J. *Dalton Trans*. **2016**, *45*, 11876.

(26) (a) Ishikawa, N.; Sugita, M.; Ishikawa, T.; Koshihara, S.; Kaizu, Y.; *J. Am. Chem. Soc*. **2003**, *125*, 8694.

(27) (a) Wu, Y.; Morton, S.; Kong, X.; Nichol, G. S.; Zheng, Z. *Dalton Trans.* **2011,** *40*, 1041-1046. (b) Andrews, P. C.; Gee, W. J.; Junk, P. C.; MacLellan, J. G. *Dalton Trans.* **2011,** *40*, 12169-12179. (c) Yadav, M.; Mondal, A.; Mereacre, V.; Jana, S. K.; Powell, A. K.; Roesky, P. W. *Inorg. Chem.* **2015,** *54*, 7846-7856. (d) Thielemann, D. T.; Wagner, A. T.; Lan, Y.; Oña-Burgos, P.; Fernãndez, I.; Rösch, E. S.; Kölmel, D. K.; Powell, A. K.; Bräse, S.; Roesky, P. W. *Chem. -Eur. J.* **2015,** *21*, 2813-2820.

(28) (a) Zhao, X.-Q.; Zhao, B.; Shi, W.; Cheng, P.; Liao, D.-Z.; Yan, S.-P. *Dalton Trans.* **2009,** 2281. (b) fang, S.-M.; Sañudo, E. C.; Hu, M.; Zhang, Q.; Ma, S. T.; Jia, L.-R.; Wang, wang, C.; Tang, J.-Y.; Liu, C.-S. *Cryst. Growth Des.* **2011**, *11*, 811.

(29) (a) Blagg, R. J.; Muryn, C. A.; McInnes, E. J. L.; Tuna, F.; Winpenny, R. E. P. *Angew. Chem. Int. Ed.* **2011,** *50*, 6530. (b) kritikos, M.; Moustiakimov, M.; Westin, G. *Inorg. Chim. Acta* **2012,** *384*, 125. (c) Blagg, R. J.; Ungur, L.; Tuna, F.; Speak, J.; Comar, P.; Collison. D.; Wernsdorfer, W.; McInnes, E. J. L.; Chibotaru, L. F.; Winpenny, R. E. P. *Nat. Chem.* **2013,** *5*, 673.

(30) (a) Wang, R.; Selby, H. D.; Liu, H.; Carducci, M. D.; Jin, T.; Zheng, Z.; Anthis, J. W.; Staples, R. J. *Inorg. Chem.* **2002,** *41*, 278. (b) Kong, X.-J.; Wu, Y.; Long, L.-S.;

Zheng, L.-S.; Zheng, Z. *J. Am. Chem. Soc*. **2009**, *131*, 6918. (c) Zheng, Z. *Chem. Commun.* **2001,** 2521. (d) Thielemann, D. T.; Fernández, I.; Roesky, P. W. *Dalton Trans.* **2010,** *39*, 6661.

(31) (a) Zhao, L. Xue, S.; Tang, J. *Inorg. Chem*. **2012,** *51*, 5994. (b) Lin, P.-H.; Burchell, T. J.; Clérac, R.; Murugesu, M. *Angew. Chem. Int. Ed.* **2008,** *47*, 8848. (c) Xue, S.; Zhao, L.; Guo, Y.-N.; Zhang, P.; Tang, J. *Chem. Commun.* **2012,** *48*, 8946. (d) Chandrasekhar, V. ; Hossain, S.; Das, S.; Biswas, S.; Sutter, J.-P. *Inorg. Chem.* **2013,** *52*, 6346. (e) Lin, P.-H.; Burchell, T. J.; Ungur, L.; Chibotaru, L. F.; Wernsdorfer, W.; Murugesu, M. *Angew. Chem. Int. Ed.* **2009,** *48*, 9489. (f) Tian, H.; Zhao, L.; Lin, H.; Tang, J.; Li, G. *Chem. – Eur. J.* **2013,** *19*, 13235.

(32) Hewitt, I. J.; Tang, J.; Madhu, N. T.; Anson, C. E.; Lan, Y.; Luzon, J.; Etienne, M.; Sessoli, R.; Powell, A. K. *Angew. Chem. Int. Ed.* **2010,** *49*, 6352-6356.

(33) Liao,W.; Wang, X.; Deng, R.; Zhang, H.; Gao, S. *Inorg. Chem*. **2009**, *48*, 11743.

(34) (a) Bi, Y.; Wang, X.; Liao, W.; Wang, X.; Deng, R.; Zhang, H.; Gao, S. *Inorg. Chem.* **2009,** *48*, 11743. (b) Liu, C.; Zhang, D.; Hao, X.; Zhu, D. *Cryst. Growth Des.* **2012,** *12*, 2948.

(35) (a) Ritchie, C.; Speldrich, M.; Gable, R. W.; Sorace, L.; Kogerler, P.; Boskovic, C. *Inorg. Chem*. *2011*, **50**, 7004. (b) AlDamen, M. A.; Cardona-Serra, S.; Clemente-Juan, J. M.; Coronado, E.; Gaita-Arino, A.; Martı-Gastaldo, C.; Luis, F.; Montero, O. *Inorg. Chem*. **2009**, *48*, 3467.

(36) (a) Wang, X.; Bao, X.; Xu, P.; Li, L. *Eur. J. Inorg. Chem.*, **2011**, 3586. (c) Wang, X.; Li, L.; Liao, D. *Inorg. Chem.*, **2010**, *49*, 4735. (d) Coronado, E.; Gimenez-Saiz, C.; Recuenco, A.; Tarazon, A.; Romero, F. M.; Camon, A.; Luis, F. *Inorg. Chem.*, **2011**, *50*, 7370. (e) Lopez, N.; Prosvirin, A. V.; Zhao, H.; Wernsdorfer, W.; Dunbar, K. R. *Chem. Eur. J.*, **2009**, *15*, 11390. (f) Wang, X.; Tian, H.; Ma, Y.; Yang, P.; Li, L.; Liao, D. *Inorg. Chem. Comm.*, **2011,** *14*, 1728. (g) Mei, X.; Liu, R.; Wang, C.; Yang, P.; Li, L.; Liao, D. *Dalton Trans.*, **2012**, *41*, 2904. (h) Poneti, G.; Bernot, K.; Bogani, L.; Caneschi, A.; Sessoli, R.; Wernsdorfer, W.; Gatteschi, D. *Chem. Commun.*, **2007**, *18*, 1807.

(37) (a) Thiele, S.; Balestro, F.; Ballou, R.; Klyatskaya, S.; Ruben, M.; Wernsdorfer. W. *Science* **2014**, *344*, 1135. (b) Mannini, M.; Bertani, F.; Tudisco, C.; Malavolti, L.; Poggini, L.; Misztal, K.; Menozzi, D.; Motta, A.; Otero, E.; Ohresser, P.; Sainctavit, P.; Condorelli, G. G.; Dalcanale, E.; Sessoli. R. *Nat. Chem*. **2013**, *5*, 4582. (c) Jiang,

S.-D.; Wang, B.-W.; Sun, H.-L.; Wang, Z.-M.; Gao. S. *J. Am. Chem. Soc*. **2011**, 133, 4730. (d) Liu, J.-L.; Chen, Y.-C.; Zheng, Y.-Z.; Lin, W.-Q.; Ungur, L.; Wernsdorfer, W.; Chibotaru, L. F.; Tong, M.-L. *Chem. Sci*. **2013**, *4*, 3310. (e) Takamatsu, S.; Ishikawa, T.; Koshihara, S.-Y.; Ishikawa. N. *Inorg. Chem*. **2007**, *46*, 7250. (f) Ganivet, C. R.; Ballesteros, B.; Torre, G.; Clemente-Juan, J. M.; Coronado, E.; Torres, T. *Chem.- Eur. J*. **2013**, *19*, 1457.

(38) (a) Lin, P.-H.; Burchell, T. J.; Ungur, L.; Chibotaru, L. F.; Wernsdorfer, W.; Murugesu, M.; *Angew. Chem. Int. Ed*. **2009**, *48*, 9489. (b) Blagg, R. J.; Tuna, F.; McInnes, E. J. L.; Winpenny, R. E. P. *Chem. Commun*. **2011**, *47*, 10587. (c) Rinehart, J. D.; Fang, M.; Evans, W. J.; Long, J. R. *J. Am. Chem. Soc*. **2011**, *133*, 14236. (d) Guo, Y.-N.; Xu, G.-F.; Gamez, P.; Zhao, L.; Lin, S.-Y.; Deng, R.; Tang, J.; Zhang, H.-J. *J. Am. Chem. Soc*. **2010**, *132*, 8538. (e) Demir, S.; Zadrozny, J. M.; Nippe, M.; Long, J. R. *J. Am. Chem. Soc*. **2012**, *134*, 18546.

(39) (a) Yang, F.; Zhou, Q.; Zeng, G.; Li, G.; Gao, L.; Shi, Z.; Feng, S. *Dalton Trans.* **2014**, *43*, 1238. (b) Rinehart, J. D.; Fang, M.; Evans, W. J.; Long, J. R. *Nat. Chem.* **2011**, *3*, 538. (c) Venugopal, A.; Tuna, F.; Spaniol, T. P.; Ungur, L.; Chibotaru, L. F.; Okuda, J.; Layfield, R. A. *Chem. Commun.*, **2013**, *49*, 901. (d) Sessoli, R.; Powell, A. K. *Coord. Chem. Rev.*, **2009**, *253*, 2328. (e) Suzuki, K.; Sato, R.; Mizuno, N. *Chem. Sci.*, **2013**, *4*, 596. (f) Zhang, P.; Zhang, L.; Tang, J. *Dalton Trans.* **2015**, *44*, 3923. (f) Tuna, F.; Smith, C. A.; Bodensteiner, M.; Ungur, L.; Chibotaru, L. F.; McInnes, E. J. L.; Winpenny, R. E. P.; Collison, D.; Layfield, R. A. *Angew*. *Chem. Int. Ed*. **2012**, *51*, 6976.

(40) (a) Poneti, G.; Bernot, K.; Bogani, L.; Caneschi, A.; Sessoli, R.; Wernsdorfer, W.; Gatteschi, D. *Chem. Commun*. **2007**, 1807. (b) Demir, S.; Nippe, M.; Gonzalez, M. I.; Long. J. R. *Chem. Sci.* **2014**, *5*, 4701.

(41) (a) Tang, J.; Hewitt, I.; Madhu, N. T.; Chastanet, G.; Wernsdorfer, W.; Anson, C. E.; Benelli, C.; Sessoli, R.; Powell, A. K. *Angew*. *Chem. Int. Ed*. **2006**, *45*, 1729. (b) Tian, H.; Guo, Y.-N.; Zhao, L.; Tang, J.; Liu, Z. *Inorg. Chem*. **2011**, *50*, 8688. (c) Ke, H.; Zhao, L.; Guo, Y.; Tang, J. *Eur. J. Inorg. Chem*. **2011**, 4153. (d) Ke, H.; Xu, G.-F.; Zhao, L.; Tang, J.; Zhang, X. Y.; Zhang, H. J. *Chem.- Eur. J*. **2009**, *15*, 10335. (e) Novitchi, G.; Pilet, G.; Ungur, L.; Moshchalkov, V. V.; Wernsdorfer, W.; Chibotaru, L. F.; Luneau, D.; Powell, A. K. *Chem. Sci*. **2012**, *3*, 1169. (f) Hewitt, I. J.; Tang, J.; Madhu, N. T.; Anson, C. E.; Lan, Y.; Luzon, J.; Etienne, M.; Sessoli, R.; Powell, A. K.

Angew. Chem. Int. Ed. **2010**, *49*, 6352. (g) Hewitt, I. J.; Lan, Y.; Anson, C. E.; Luzon, J.; Sessoli, R.; Powell, A. K. *Chem. Commun*. **2009**, 6765.

(42) (a). Guo, Y.-N.; Xu, G.-F.; Gamez, P.; Zhao, L.; Lin, S.-Y.; Deng, R.; Tang, J.; Zhang, H.-J. *J. Am. Chem. Soc*. **2010**, *132*, 8538. (b) Das, C.; Vaidya, S.; Gupta, T.; Frost, J. M.; Brechin, E. K.; Righi, M.; Affronte, M.; Rajaraman, G.; Shanmugam, M. *Chem. Eur. J*. **2015**, *21*, 15639. (c) Lin, P.-H.; Burchell, T. J.; Ungur, L.; Chibotaru, L. F.; Wernsdorfer, W.; Murugesu. M. *Angew. Chem. Int. Ed*. **2009**, *48*, 9489. (d) Gao, Y. J.; Xu, G. F.; Zhao, L.; Tang, J.; Liu, Z. L. *Inorg. Chem*. **2009**, *48*, 11495. (e) Ke, H. S.; Gamez, P.; Zhao, L.; Xu, G. F.; Xue, S. F.; Tang, J. *Inorg. Chem*. **2010**, *49*, 7549. (f) Liu, C.-M.; Zhang, D.-Q.; Hao, X.; Zhu, D.-B. *Cryst. Growth Des*. **2012**, *12*, 2948. (g) Li, Y. ; Yu, J.-W.; Liu, Z.-Y.; Yang, E.-C.; Zhao, X.-J. *Inorg. Chem.* **2015**, *54*, 153. (h) Das, S.; Dey, A.; Biswas, S.; Colacio, E.; Chandrasekhar, V. *Inorg. Chem*. **2014**, *53*, 3417.

(43) Blagg, R. J.; Ungur, L.; Tuna, F.; Speak, J.; Comar, P.; Collison, D.; Wernsdorfer, W.; McInnes, E. J. L.; Chibotaru L. F.; Winpenny, R. E. P. *Nat. Chem*. **2013**, *5*, 673.

(44) (a) Blagg, R. J.; Muryn, C. A.; McInnes, M. J. L.; Tuna, F.; Winpenny, R. E. P. *Angew. Chem. Int. Ed.* **2011,** *50*, 6530. (b) Gamer, M. T.; Lan, Y.; Roesky, P. W.; Powell, A. K.; Clerac, R. *Inorg. Chem*. **2008**, *47*, 6581.

(45) (a) Mukherjee, S.; Chaudhari, A. K.; Xue, S.; Tang, J .; Ghosh, S. K. *Inorg. Chem. Commun*. **2013**, *35*, 144. (b) She, S.; Chen, Y.; Zaworotko, M. J.; Liu, W.; Cao, Y.; Wua, J.; Li, Y. *Dalton Trans*. **2013**, *42*, 10433. (c) Baniodeh, A.; Magnani, N.; Bräse, S.; Ansonb, C. E.; Powell, A. K. *Dalton Trans*. **2015**, *44*, 6343. (d) Bi, Y. F.; Xu, G. C.; Liao, W. P.; Du, S. C.; Deng, R. P.; Wang, B. W. *Sci. China Chem***. 2012** , *55* , 967. (l) Tian, H.; Wang, M.; Zhao, L.; Guo, Y. N.; Guo, Y.; Tang, J.;Liu, Z. *Chem.-Eur. J.* **2012** , *18* , 442. (e) Guo, Y. N.; Chen, X. H.; Xue, S.; Tang, J. *Inorg. Chem.* **2012**, *51*, 4035. (f) Hussain, B.; Savard, D.; Burchell, T. J.; Wernsdorfer, W.; Murugesu, M. *Chem. Commun*. **2009**, 1100. (g) Tian, H.; Zhao, L.; Guo, Y.-N.; Guo, Y.; Tang, J.; Liu, Z. *Chem. Commun*. **2012**, *48*, 708. (h) Miao, Y. L.; Liu, J. L.; Li, J. Y.; Leng, J. D.; Ou, Y. C.; Tong, M. L. *Dalton Trans*. **2011**, *40*, 10229.

(46) (a) Mazarakioti, E. C.; Poole, K. M.; Cunha-Silva, L.; Christou, G.; Stamatatos, T. C. (b) Sharples, J. W.; Zheng, Y.-Z.; Tuna, F.; McInnes, E. J. L.; Collison, D. *Chem. Commun*. **2011**, *47*, 7650. (c) Tian, H.; Bao, S.-S.; Zheng, L.-M. *Chem. Commun*. **2016**, *52*, 2314.

(47) (a) Tian, H.; Zhao, L.; Guo, Y. N.; Guo, Y.; Tang, J.; Liu, Z. *Chem. Commun.* **2012** , *48*, 708. (b) Bala, S.; Bishwas, M. S.; Pramanik, B.; Khanra, S.; Fromm, K. M.; Poddar, P.; Mondal, R. *Inorg. Chem.* **2015**, *54*, 8197. (c) Alexandropoulos, D. I.; Cunha-Silva, L.; Pham, L.; Bekiari, V.; Christou, G.; Stamatatos, T. C. *Inorg. Chem.* **2014**, *53*, 3220. (d) Miao, Y.-L.; Liu, J.-L.; Li, J.-Y.; Leng, J.-D.; Oua, Y.-C.; Tong. M.-L. *Dalton Trans*. **2011**, *40*, 10229. (e) Yang, P.; Gao, X.; Song, H.; Zhang, S.; Mei, X.; Li, L.; Liao, D. *Inorg. Chem*. **2011**, *50*, 720. (f) Savard, D.; Lin, P.-H.; Burchell, T. J.; Korobkov, I.; Wernsdorfer, W.; Clerac, R.; Murugesu, M. *Inorg. Chem*. **2009**, *48*, 11748.

(48) (a) Alexandropoulos, D. I.; Mukherjee, S.; Papatriantafyllopoulou, C.; Raptopoulou, C. P.; Psycharis, V.; Bekiari, V.; Christou, G.; Stamatatos, T. C. *Inorg. Chem.* **2011,** 50, 11276. (b) Greisch, J.-F.; Chmela, J.; Harding, M. E.; Klopper, W.; Kappes, M. M.; Schooss, D. *Inorg*. *Chem*. **2016**, *55*, 3316.

(49) (a) Ke, H.; Xu, G. F.; Zhao, L.; Tang, J.; Zhang, X. Y.; Zhang, H. J. *Chem.-Eur. J.* **2009**, *15*, 10335. (b) Wu, Z.-L.; Dong, J.; Ni, W.-Y.; Zhang, B.-W.; Cui, J.-Z.; Zhao, B. *Dalton Trans*. **2014**, *43*, 16838. (c) Su, K.; Jiang, F.; Qian, J.; Pang, J.; Hu, F.; Bawaked, S. M.; Mokhtar, M.; AL-Thabaiti, S. A.; Hong. M. *Inorg*. *Chem. Commun*. **2015**, *54*, 34.

(50) Miao, Y.-L.; Liu, J.-L.; Li, J.-Y.; Leng, J.-D.; Oua, Y.-C.; Tong. M.-L. *Dalton Trans*. **2011**, *40*, 10229.

(51) Miao, Y. L.; Liu, J. L.; Leng, J. D.; Lina, Z. J.; Tong, M. L. *CrystEngComm*. **2011**, *13*, 3345.

(52) (a) Chesman, A. S. R.; Turner, D. R.; Moubaraki, B.; Murray, K. S.; Deacon, G. B.; Batten, S. R. *Dalton Trans*. **2012**, *41*, 10903. (b) Li, X.-L.; He, L.-F.; Feng, X.-L.; Song, Y.; Hu, M.; Han, L.-F.; Zheng, X.-J.; Zhang, Z.-H.; Fang, S.-M. *CrystEngComm*, **2011**, *13*, 3643. (c) Tian, H.; Bao, S.-S.; Zheng. L.-M. *Chem. Commun*. **2016**, *52*, 2314.

(53) Li , W.; Xiong. G. *Inorg. Chem. Commun*. **2015**, *59*, 1.

(54) Warburg, E. *Ann. Phys (Leipzig)*, **1881**, *13*, 141.

(55) (a) Pecharsky, V. K.; Gschneider, Jr,. K. A. *J. Magn. Magn. Mater*. **1999**, *200*, 44. (b) Gschneider, Jr., K. A.; Pecharsky, V. K. *J. Appl. Phys*. **1999**, *85*, 5365.

(56) (a) Sessoli, R. *Angew. Chem. Int. Ed*. **2012**, *51*, 43. (b) Evangelisti, M.; Brechin, E. K. *Dalton Trans*. **2010**, *39*, 4672.

(57) (a) Evangelisti, M.; Roubeau, O.; Palacios, E.; Camín, A.; Hooper, T. N.; Brechin, E. K.; Alonso, J. J. *Angew. Chem. Int. Ed*. **2011**, *50*, 6606. (b) Lorusso, G.; Sharples, J. W.; Palacios, E.; Roubeau, O.; Brechin, E. K.; Sessoli, R.; Rossin, A.; Tuna, F.; McInnes, E. J. L.; Collison, D.; Evangelisti, M. *Adv. Mater*. **2013**, *25*, 4653.

(58) (a) Accorsi, S.; Barra, A.; Caneschi, A.; Chastanet, G.; Cornia, A.; Fabretti, A. C.; Gatteschi, D.; Mortalo, C.; Olivieri, E.; Parenti, F.; Rosa, P.; Sessoli, R.; Sorace, L.; Wernsdorfer, W.; Zobbi, L. *J. Am. Chem. Soc*. **2006**, *126*, 4742. (b) Stamatatos, T. C.; Efthymiou, C. G.; Stoumpos, C. C.; Perlepes, S. P. *Eur. J. Inorg. Chem*. **2009**, *23*, 3361. (c) Manoli, M.; Johnstone, R. D. L.; Parsons, S.; Murrie, M.; Affronte, M.; Evangelisti, M.; Brechin, E. K. *Angew. Chem. Int. Ed*. **2007**, *46*, 4456.

(59) (a) Affronte, M.; Ghirri, A.; Carretta, S.; Amoretti, G.; Piligkos, S.; Timco, G. A.; Winpenny, R. E. P. *Appl. Phys. Lett*., **2004**, *84*, 3468. (b) Low, D. M.; Jones, L. F.; Bell, A.; Brechin, E. K.; Mallah, T.; Rivière, E.; Teat, S. J.; McInnes, E. J. L. *Angew. Chem., Int. Ed*., **2003**, *42*, 3781. (c) Gass, I. A.; Brechin, E. K.; Evangelisti, M. *Polyhedron*, **2013**, *52*, 1177. (d) Manoli, M.; Johnstone, R. D. L.; Parsons, S.; Murrie, M.; Affronte, M.; Evangelisti, M.; Brechin, E. K. *Angew. Chem. Int. Ed*. **2007**, *46*, 4456. (e) Nayak, S.; Evangelisti, M.; Powell, A. K.; Reedijk, J. *Chem.–Eur. J*. **2010**, *16*, 12865. (f) Liu, J.-L.; Leng, J.-D.; Lin, Z.; Tong, M.-L. *Chem.–Asian J*. **2011**, *6*, 1007. (g) Ako, A. M.; Hewitt, I. J.; Mereacre, V.; Clerac, R.; Wernsdorfer, W.; Anson, C. E.; Powell, A. K. *Angew. Chem. Int. Ed*. **2006**, *45*, 4926. (h) Chen, Y.-C.; Guo, F.-S.; Liu, J.-L.; Leng, J.-D.; Vrábel, P.; Orendáč, M.; Prokleška, J.; Sechovský, V.; Tong, M.-L. *Chem. Eur. J*. **2014**, *20*, 3029.

(60) (a) Karotsis, G.; Evangelisti, M.; Dalgarno, S. J.; Brechin, E. K. *Angew. Chem. Int. Ed*. **2009**, *48*, 9928. (b) Zheng, Y.-Z.; Pineda, E. M.; Helliwell, M.; Winpenny, R. E. P. *Chem. Eur. J*. **2012**, *18*, 4161. (c) Guo, F.-S.; Chen, Y.-C.; Liu, J.-L.; Leng, J.-D.; Meng, Z.-S.; Vrábel, P.; Orendáč, M.; Tong, M.-L. *Chem. Commun*. **2012**, *48*, 12219. (d) Karotsis, G.; Kennedy, S.; Teat, S. J.; Beavers, C. M.; Fowler, D. A.; Morales, J. J.; Evangelisti, M.; Dalgarno, S. J.; Brechin, E. K. *J. Am. Chem. Soc*. **2010**, *132*, 12983. (e) Liu, K.; Shi, W.; Cheng, P. *Coord. Chem. Rev*. **2015**, *74*, 289, (f) Peng, J. B.; Zhang, Q. C.; Kong, X. J.; Ren, Y. P.; Long, L. S.; Huang, R. B.; Zheng, L. S.; Zheng, Z. *Angew. Chem. Int. Ed*. **2011**, *50*, 10649. (g) Langley, S. K.; Chilton, N. F.; Moubaraki, B.; Hooper, T.; Brechin, E. K.; Murray, K. S. *Chem. Sci*. **2011**, *2*, 1166.

(61) (a) Peng, J.-B.; Zhang, Q.-C.; Kong, X.-J.; Ren, Y.-P.; Long, L.-S.; Huang, R.-B.; Zheng, L.-S.; Zheng, Z. *Angew. Chem. Int. Ed*. **2011**, *50*, 10649. (b) Peng, J.-B.; Zhang, Q.-C.; Kong, X.-J.; Zheng, Y.-Z.; Ren, Y.-P.; Long, L.-S.; Huang, R.-B.; Zheng, L.-S.; Zheng, Z. *J. Am. Chem. Soc*. **2012**, *134*, 3314. (c) Thuesen, C. A.; Pedersen, K. S.; Schau-Magnussen, M.; Evangelisti, M.; Vibenholt, J.; Piligkos, S.; Weihe, H.; Bendix, J. *Dalton Trans*. **2012**, *41*,11284. (d) Birk, T.; Pedersen, K. S.; Thuesen, C. A.; Weyhermüller, T.; Schau-Magnussen, M.; Piligkos, S.; Weihe, H.; Mossin, S.; Evangelisti, M.; Bendix, J. *Inorg. Chem*. **2012**, *51*, 5435.

(62) (a) Sharples, J. W.; Zheng, Y.-Z.; Tuna, F.; McInnes, E. J. L.; Collison, D. *Chem. Commun*. **2011**, *47*, 7650. (b) Blagg, R. J.; Tuna, F.; McInnes, E. J. L.; Winpenny, R. E. P. *Chem. Commun*. **2011**, *47*, 10587. (c) Evangelisti, M.; Roubeau, O.; Palacios, E.; Camón, A.; Hooper, T. N.; Brechin, E. K.; Alonso, J. J. *Angew. Chem. Int. Ed*. **2011**, *50*, 6606. (d) Guo, F. S.; Leng, J. D.; Liu, J. L.; Meng, Z. S.; Tong, M. L. *Inorg. Chem*. **2012**, *51*, 405.

(63) (a) Chang, L.-X.; Xiong, G.; Wang, L.; Cheng, P.; Zhao, B. *Chem. Commun*. **201**3, *49*, 1055. (b) Lorusso, G.; Palacios,M. A.; Nichol, G. S.;Brechin, E. K.; Roubeau, O.; Evangelisti, M. *Chem,. Commun*. **2012**, *48*, 7592. (c) Biswas, S.; Adhikary, A.; Goswami, S.; Konar, S. *Dalton Trans*. **2013**, *42*, 13331. (d) Sedláková, L.; Hanko, J.; Orendáčová, A.; Orendáč, M.; Zhou, C. L.; Zhu, W. H.; Wang, B. W. Wang, Z. M.; Gao, S. *J. Alloys Compd*. **2009**, 425. (e) Shi, P. F.; Zheng, Y. Z.; Zhao, X. Q.; Xiong, G.; Zhao, B.; Wam, F. F.; Cheng, P. *Chem.–Eur. J*. **2012**, *18*, 15086. (f) Wu, M.; Jiang, F.; Kong, X.; Yuan, D.; Long, L.; Al-Thabaiti, S. A.; Hong, M. *Chem. Sci*. **2013**, *4*, 3104. (g) Chen, Y.-C.; Guo, F.-S.; Zheng, Y.-Z.; Liu, J.-L.; Leng, J.-D.; Tarasenko, R.; Orendáč, M.; Prokleška, J.; Sechovský, V.; Tong, M.-L. *Chem.–Eur. J*. **2013**, *19*, 14876. (h) Sibille, R.; Mazet, T.; Malaman, B.; Francois, M. *Chem.–Eur. J*. **2012**, *18*, 12970. (i) Chen, Y. C.; Meng, Z. S.; Qin, L.; Zheng, Y. Z.; Liu, J. L.; Guo, F. S.; Tarasenko, R.; Orendáč, M.; Proklesška, J.; Sechovský, V. ; Tong, M. L. *J. Mater. Chem. A*, **2014**, *2*, 9851.

Hexanuclear Lanthanide Clusters Encapsulating a μ_6-CO_3^{2-} ion Displaying an Unusual Binding Mode

CHAPTER 2

Abstract: Reaction of hydrated lanthanum halides (Ln = La, Pr and Nd) with LH_2 [1-(2-HydroxyPhenyl)-3-(2-thienyl)-1,3-Propanedione] in presence of excess triethylamine with methanol as a solvent resulted in the isolation and structural characterization of a series of novel hexanuclear lanthanide clusters. These clusters were templated by μ_6-CO_3^{2-}, introduced via spontaneous fixation of atmospheric carbon dioxide depicting a new coordination mode of binding. This particular mode of bridging is a first report of its kind in lanthanide clusters. Synthesis, structure and magnetic properties of **2.1**-**2.3** are discussed in this chapter.

2.1 Introduction:

Assembling lanthanide based high nuclearity clusters, where in lanthanides are bridged by an intervening 'O' or 'N' atom have received considerable attention in recent years owing to their potential applications in diverse fields like luminescence,[1] catalysis[2] and magnetism.[3] In general, polynuclear lanthanide oxo/hydroxo clusters have been synthesized by treating hydrated lanthanide salts with complexing ligands like carboxylates,[4] amino acids,[5] alkoxides,[6] β-diketones[7] or Schiff bases[8] in presence of excess base. This methodology has been extensively used to synthesize lanthanide oxo/hydroxo clusters displaying interesting magnetic properties. In recent years, using anions like nitrates and carbonates as template / ligands for constructing novel metal organic frameworks (MOF) and polynuclear clusters has started gaining momentum.[9] Carbonates have been inserted into molecular and supramolecular systems either by addition of carbonate source to the reaction mixture or by atmospheric fixation of carbon dioxide at room temperature. Recently Arikawa *et al*. have reported the utility of a ruthenium pincer complex for atmospheric fixation of carbon dioxide and have also successfully demonstrated the release of the absorbed carbonate by treating with a methylating reagent.[10] Transition metal complexes with zinc, copper, cobalt, nickel, platinum and iridium have also been found to be useful in atmospheric fixation of CO_2.[11] Literature on lanthanide complexes regarding fixation of atmospheric CO_2 is sparsely reported in comparison with transition metal based counterparts.[12] Some interesting examples include lanthanide oxo-hydroxo clusters templated by carbonate anion insertion via spontaneous fixation of atmospheric CO_2, like the dodecanuclear lanthanum cluster $[La_{12}(OH)_{12}(H_2O)_4(dbm)_{18}(phgly)_2(CO_3)_2]$ (dbm = dibenzoyl methane, phgly = phenyl glycine) templated by two CO_3^{2-} anions.[13] Another interesting report which needs to be mentioned is by Murray *et al*. wherein hexanuclear lanthanide clusters $[Ln_6(teaH)_2(teaH_2)_2(CO_3)(NO_3)_2(chp)_7(H_2O)]$ (where Ln = Tb and Dy; tea = triethanolamine, chp = 6-chloro-2-hydroxypyridine) with trapped carbonate ion, were found to exhibit SMM behavior.[14] Similarly, dysprosium clusters essentially templated by carbonate anions which show SMM behaviour have been reported with varying nuclearities like octa, hexa and tetranuclear clusters.[15] Isolation of Er_{26} and Dy_{26} clusters incorporating nitrate anion[16] and the spherical polycarbonate bound lanthanoid cluster along with a decanuclear cluster templated by carbonate ions indicate that anions other than hydroxides/oxides can as well be considered as promising candidates for assembling

novel molecular architectures.[17] These results pave a way for growing interest in synthesizing lanthanide clusters using CO_3^{2-} ions in a quest for achieving diverse molecular structures. In this background, synthesis, structural elucidation and magnetic properties of hexanuclear lanthanide oxo clusters templated by μ_6-CO_3^{2-} displaying a new coordination mode of binding are presented.

2.2 Experimental Section

2.2.1 General methods and Procedures:

All chemicals used were of analytical reagent grade and used as received without further purification. The ligand LH_2 [1-(2-HydroxyPhenyl)-3-(2-thienyl)-1,3-Propanedione] was prepared according to the literature procedure.[18] Lanthanum salts were prepared by neutralizing the corresponding lanthanum oxides with concentrated hydrochloric acid.

2.2.2 Instrumentation:

Elemental analyses were performed on a flash EA series 1112 CHNS analyzer. FT-IR spectra were recorded on a JASCO-5300 FT-IR spectrometer by using KBr pellets. ^{1}H and ^{13}C-NMR spectra were recorded on a BRUKER DRX 400 and 100 MHz instrument. Magnetic measurements were carried out in the Unitat de Mesures Magnètiques (Universitat de Barcelona) on polycrystalline samples (circa 30 mg) with a Quantum Design SQUID MPMS-XL magnetometer equipped with a 5 T magnet. Diamagnetic corrections were calculated using Pascal's constants and an experimental correction for the sample holder was applied. Single crystal X-ray diffraction measurement was carried out on a Bruker Smart Apex CCD area detector system (λ (Mo Kα) = 0.71073Å) at 100(2) K. Data processing was done by using SAINT program. The structures were solved by using SHELXS-97 program by direct methods and all non-hydrogen atoms were refined anisotropically by full matrix least squares on F^2 using the SHELXTL-14/7 program.[19] Hydrogen atoms were fixed by using riding model. Complete results of crystallographic analysis for compounds **2.1-2.3** are given in Table 2.1. DELU, SIMU, SADI and EADP instructions were used to restraint C1-C2 and C3-C4 in **2.1**, C1-C2, C25-C26, C27-C28 and C38-C39 in compound **2.2** and C1-C2 and C3-C4 in **2.3**. Dfix command was used to fix the distance between C2-C3 and C3-C4 in **2.2**.

2.2.3 General Synthetic procedure:

Reaction of 1 equivalent of hydrated lanthanum halide and 2 equivalents of LH_2 [1-(2-HydroxyPhenyl)-3-(2-thienyl)-1,3-Propanedione] in presence of excess triethylamine in methanol yielded a yellow precipitate which was collected and washed with methanol thoroughly. The solid was then dissolved in toluene, diffused with hexane and left undisturbed for crystallization. Yellow block shaped crystals suitable for X-ray diffraction were formed after two weeks.

Compound 2.1: $LaCl_3.6H_2O$ (0.1 g, 0.282 mmol), LH_2 (0.14g, 0.565 mmol), Et_3N (0.156 mL, 1.128 mmol). Yield: 0.190 g, 49.73% (based on La). Mp: 160 ˚C (dec). IR (KBr) cm^{-1}: 3441(br), 2252(w), 2125(w), 1611(w), 1584(s), 1561(s), 1522(s), 1502(s), 1463(m), 1407(m), 1337 (s), 1294(s), 1243(m), 1192(m), 1025(s), 1005(m), 925(m), 824(s), 760(s), 718(m). Anal. Calcd for $C_{118}H_{72}O_{36}S_9La_6$ (3187.75): C, 44.46; H, 2.28. Found: C, 44.36; H, 2.18%. ^{1}H NMR (400 MHz, $CDCl_3$, δ, ppm) 7.69 (d, 8H,), 7.58 (t, 13H), 7.38 (m, 8H), 7.21 (m, 9H), 7.11 (m, 6H), 6.998 (9H, s), 6.756 (12H, s), 6.59 (m, 4H). ^{13}C NMR (100 MHz, $CDCl_3$+DMSO, δ, ppm) 184.60, 177.75, 162.17, 148.31, 138.44, 133.48, 130.63, 129.76, 128.98, 128.58, 128.53, 126.07, 122.12, 119.0, 118.86, 93.51.

Compound 2.2: $PrCl_3.6H_2O$ (0.1 g, 0.281 mmol), LH_2 (0.14g, 0.565 mmol), Et_3N (0.156 mL, 1.128 mmol). Yield: 0.184 g, 48.61% (based on Pr). Mp: 175 ˚C (dec). IR (KBr) cm^{-1}: 3432(br), 2925(w), 1654(w), 1594(m), 1569(m), 1521(m), 1395(m), 1346(s), 1295(s), 1247(m), 1194(s), 1135(s), 1103(s), 1029(m), 1009(m), 854(s), 800(s), 754(s). Anal. Calcd for $C_{118}H_{72}O_{36}S_9Pr_6$ (3199.75); C, 44.29; H 2.27. Found: C, 44.25; H, 2.24%.

Compound 2.3: $NdCl_3.6H_2O$ (0.1 g, 0.278 mmol), LH_2 (0.137g, 0.55 mmol), Et_3N (0.156 mL, 1.128 mmol). Yield: 0.195 g, 51.2% (based on Nd). Mp: 172 ˚C (dec). IR (KBr) cm^{-1}: 3378(br), 1597(m), 1567(s), 1523(m), 1501(m), 1449(m), 1417(m), 1371(m), 1345(s), 1293(s), 1248(m), 1230(w), 1103(m), 1051(m), 1030(s), 1011(s), 755(s), 667(s). Anal. Calcd for $C_{118}H_{72}O_{36}S_9Nd_6$ (3219.73): C, 44.02; H 2.25. Found: C, 44.12; H, 2.18%.

2.3 Results and Discussion:

Synthetic procedure was adopted from literature studies. The hydrated lanthanum halides, ligand (LH_2) and triethylamine were reacted in methanol in 1:2:4 ratio, yielding the

product as yellow precipitate. The product was characterized by standard analytical and spectroscopic techniques. IR spectra of **2.1-2.3** show a characteristic band at around 1599 cm^{-1} corresponding to the C-O stretch of the deprotonated *β*-diketone and a peak at 1258 cm^{-1} which can be attributed to the phenolic oxygen stretching vibration. IR spectra also displayed a signal at 1521 cm^{-1} suggesting the presence of carbonate ions in **2.1-2.3**. Further ^{13}C-NMR spectrum of 2.**1** shows a signal at 177 ppm which is consistent with the signal observed for carbonate ions from literature reports suggesting the presence of carbonate ions in the synthesized cluster. Single crystal X-ray diffraction studies revealed the formation of hexanuclear lanthanide clusters $[Ln_6(\mu_6\text{-}CO_3)(L)_6(LH)_3(H_2O)_5(OH)]$ (Ln = La **2.1**, Pr **2.2**, Nd **2.3**) showing the presence of a carbonate anion obtained by fixation of atmospheric CO_2.

2.3.1 Description of crystal structure:

Single crystal X-ray analysis revealed that all the complexes are isostructural and crystallize in cubic space group *I-43d*. Cluster **2.1** is chosen as prototype for detailed structural description whose structure is shown in figure 2.1(a). The asymmetric unit contains one third of the cluster with a La dimer bridged by phenolic oxygen O7 and by μ2-oxygen of diketone O2. Three β-diketonate ligands are coordinated to the metal atoms out of which one is displaying both chelating as well as bridging while other two are displaying chelating mode of binding. Further La1 is coordinated to two water molecules and to one of the carbonate oxygen atom O8. Symmetric operation on O8 (y-1,z,x+1) generates the full unit. The hexanuclear cluster can be visualized to be built up of two triangular units La1, La2 and La1* bridged by one of the carbonate oxygen O8 and the other two oxygens O8*, O8** of the carbonate bridge another triangular unit La2**, La1** and La2*. Further oxo groups of diketone connect these two trinuclear units leading to the formation of a novel hexanuclear cluster which is structurally different from hexanuclear clusters reported so far in literature.[11h,14b] Carbonate anion is trapped in the centre of the cluster core and interestingly here the carbonate anion adapts a new bridging mode $\mu_6\text{-}\eta^1\text{:}\eta^2\text{:}\eta^1\text{:}\eta^2\text{:}\eta^1\text{:}\eta^2$ as shown in figure. 2.1(b) and chart-2.1. Assignment of bridging carbonate was further confirmed by careful observation of X-ray diffraction data. In cluster core, two different sets of metal atoms are present, one set is nine coordinated with two coordinated water molecules and the other set is eight coordinated with a chelating diketone and both these sets are present alternatively in the solid state structure. Out of the

nine ligands which are present in the peripheral part of the cluster, three ligand are acting as only chelating (monoanionic form) and the other six are acting as both chelating and bridging (dianionic form) by using their phenolic and diketone oxygens. For charge neutrality, one of the oxygen atoms bound to metal ion is considered as hydroxide ion. La1 is nine coordinated with two water molecules O9 and O10, two phenolic oxygens O7 and O3, three diketone oxygens O11, O12, O2* and two carbonate oxygen O8 and O8*. La2 is eight coordinated with one chelating diketone oxygens O4 and O5, two phenolic oxygen O7, O3 and three diketone oxygens O1, O2 and O12* and one carbonate oxygen O8*. The La-O phenolic, La-O chelating diketone oxygens and La-O bridging diketone oxygens bond distances are in the range of 2.416 to 2.418 Å, 2.505 to 2.629 Å and 2.410 to 2.463 Å respectively. La-O(water) and La-carbonate oxygen distances are in the range of 2.506 to 2.584 Å and 2.687 to 2.817 Å respectively which are consistent with the lanthanide carbonate compounds previously reported.[20] In case of Nd, the metal carbonate bonds are slightly longer than the earlier reports (2.927 Å). The bonding distance is at the extreme end of Ln-O bond lengths reported. The La-O-La angles fall in a wide range of 97.8 to 145.7°. Intramolecular La…La distances are in the order of 3.848 to 3.859 Å. The selected bond lengths (Å) and bond angles (°) for **2.1-2.3** are given in the Table 2.2-2.4. Continuous shape measurement using SHAPE software[21] indicates that the coordination sphere around La1 is Muffin geometry and La2 is in a triangular dodecahedron {figure 2.2(a)}. Complete results of geometric analysis are described in Table 2.5(a) and 2.5(b). Since no carbonate source was used in the synthetic pathway, the carbonate ion present in **2.1-2.3** is due to the fixation of atmospheric CO_2.

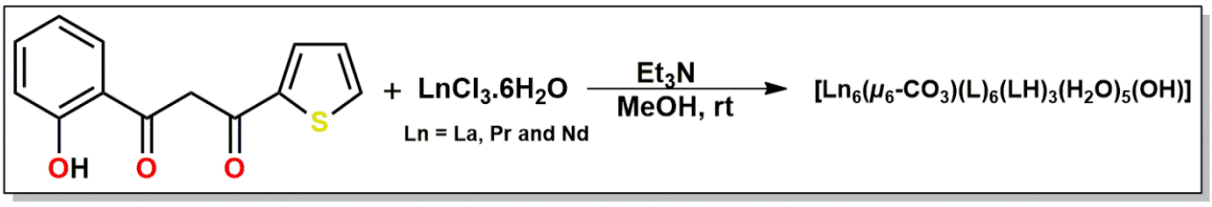

Scheme 2.1

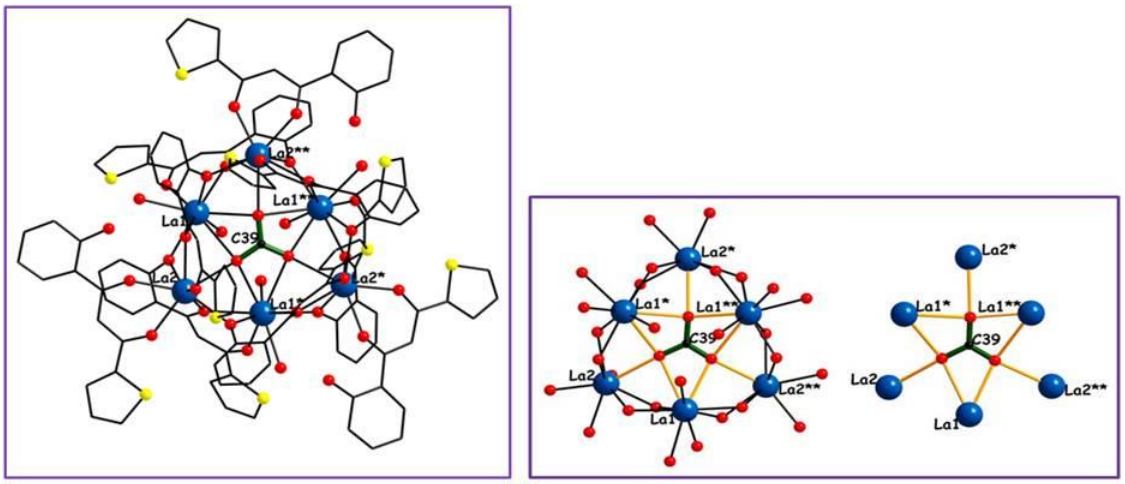

Figure 2.1(a): Molecular structure of compound **2.1**; **2.1(b)**: Core of the cluster showing coordination mode of CO_3^{2-} (μ_6-η^1:η^2:η^1:η^2:η^1:η^2)

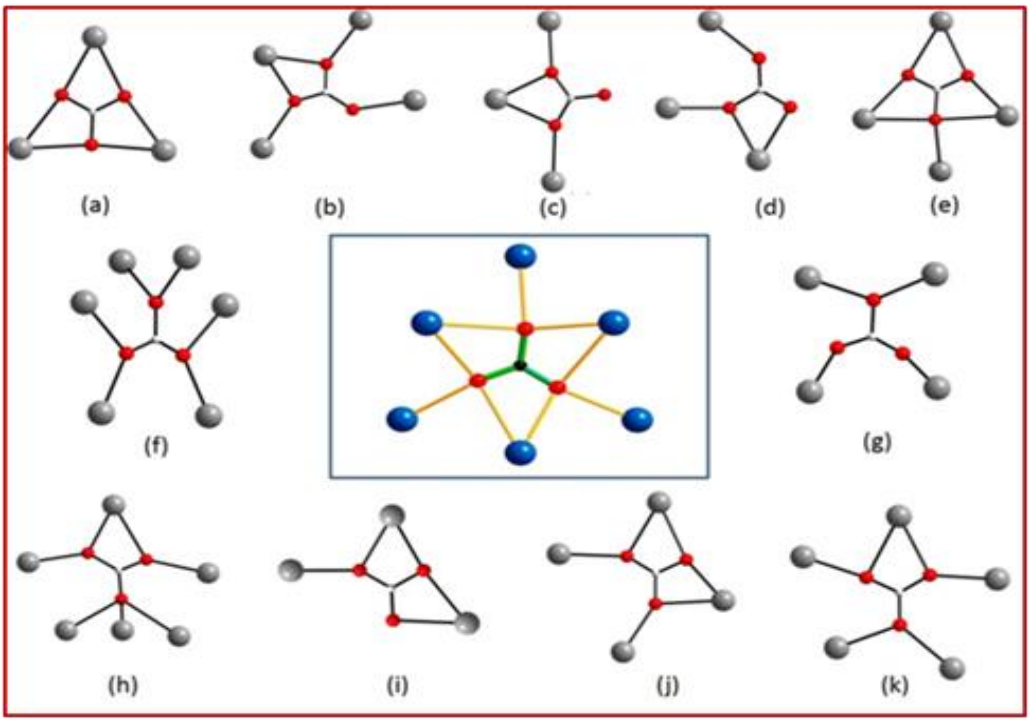

Chart 2.1: Represents various coordination modes of carbonate anion (a),[12a,c,d,e,f,g,I,14] (b),[15a] (c),[15b] (d),[15c] (e),[17] (f),[12h] (g),[12k] (h),[13] (i),[12b] (j),[12i] (k). [12j] The binding mode of carbonate observed in the present case is shown in the centre of the chart.

After identifying the presence of carbonate ions in **2.1**-**2.3** by IR, ^{13}C-NMR (in **2.1**) and structurally confirming its presence by single crystal X-ray diffraction studies, synthetic efforts were made to prepare carbonate inserted clusters directly. Despite several attempts, **2.1**-**2.3** could not be synthesized by any direct methods which involved the use of

carbonate based reagents in the synthetic pathway. Further, the crystallization process was carried out in a closed system which also failed to produce crystals worthy of diffraction quality. Hence, the carbonate anion found in **2.1-2.3** is due to fixation of atmospheric CO_2 in presence of basic medium created by excess quantity of triethylamine used in the reaction methodology. This is in concurrence to Murray's explanation for the formation of CO_3^{2-} ion from atmospheric CO_2 similar to the action of carbonic anhydrase.

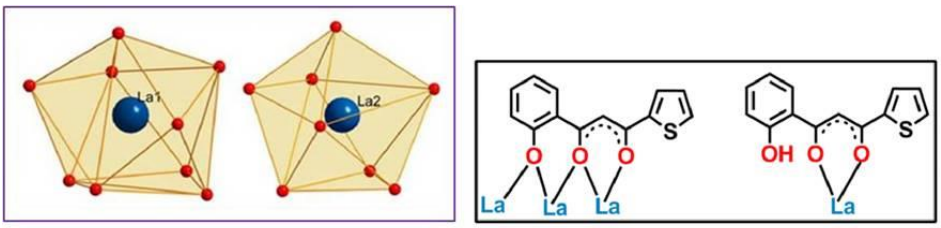

Figure 2.2(a): coordination geometry around La1 and La2 (in compound **2.1**); **2.2(b)**: different coordination modes of LH_2

2.4 Magnetism studies:

Susceptibility data was collected for **2.2** and **2.3** at 0.3 T applied field from 2 to 300 K. Below 30 K an additional data set was collected with an applied field of 0.02 T. As can be seen in Figure 2.3(a), both data sets overlap. The χT product for **2.2** at 300 K has a value of 8.46 cm^3 K mol^{-1} which is just below the expected value for six Pr(III) ion ($^3H_4$,1.5 cm^3 K mol^{-1} for one isolated Pr(III) ion, S = 1, L = 5, J=4 and gJ= 4/5). As temperature decreases, the χT product also decreases. The χT product for **2.3** at 300 K has a value of 8.73 cm^3 K mol^{-1}, just below the expected value for six Nd(III) ions (1.64 cm^3 K mol^{-1} for one Nd(III) S = 3/2, L = 6 J = 9/2 ; $^4I_{9/2}$, and gJ= 8/11). The decrease observed is mostly caused by the depopulation of the m_J states of the Ln(III) ion. At low temperature, the χT product for **2.2** is almost zero suggesting strong antiferromagnetic coupling in **2.2**, while **2.3** is paramagnetic. This is reflected in the magnetization vs. field plot at 2.0 K and is shown in figure 2.3(b). For **2.2** the magnetization does not reach saturation at 5 T and rises linearly with the applied field thereby indicating the population of the Zeeman split m_J levels and possibly an antiferromagnetically coupled ground state. The value observed is very low compared to the expected for six Pr(III) ions that are not interacting. The magnetization at 2 K for complex **2.3** does not saturate at 5 T and can be understood as the

paramagnetic behaviour of six Nd(III) ions that are practically isolated.

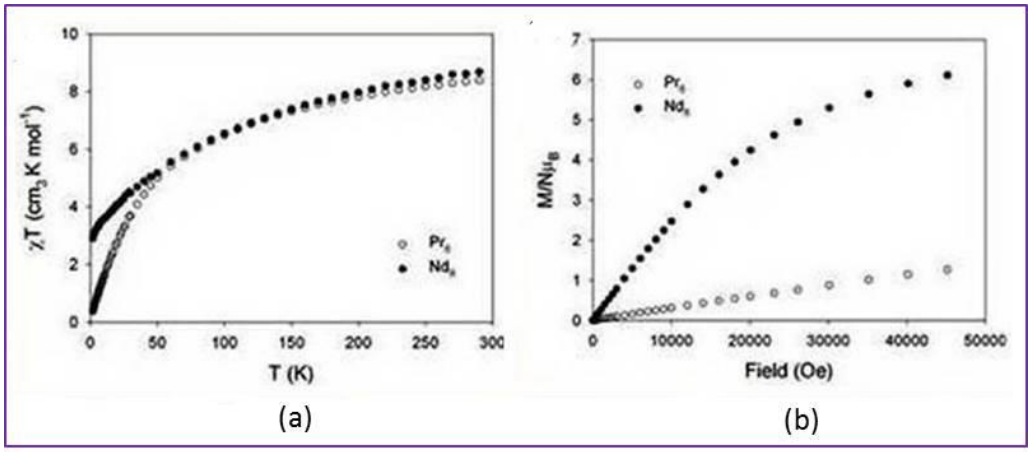

Figure 2.3a: Magnetic susceptibility as a function of temperature for compound **2.2** (Pr) and **2.3** (Nd); **2.3b**: Magnetization vs. field plot at 2.0 K for **2.2** and **2.3**.

2.5 Conclusion:

Hexanuclear lanthanide based oxo clusters [Ln = La(2.1), Pr(2.2), Nd(2.3)] templated by a carbonate anion introduced via spontaneous fixation of atmospheric CO_2 have been synthesized and structurally characterized. The carbonate anion displays a unique bridging mode μ_6-η^1:η^2:η^1:η^2:η^1:η^2 which is encountered for the first time in lanthanide chemistry. Magnetic studies on **2.2** and **2.3** reveal weak antiferromagnetic interactions between metal ions. Spontaneous fixation of atmospheric CO_2 leading to the formation of carbonate anions offers newer pathways towards designing novel carbonate bridged lanthanide clusters.

Table 2.1. Crystal data and structure refinement parameters for **2.1-2.3**

	2.1	**2.2**	**2.3**
Empirical formula	C_{118} H_{72} O_{36} S_9 La_6	C_{118} H_{72} O_{36} S_9 Pr_6	C_{118} H_{72} O_{36} S_9 Nd_6
Fw.g mol^{-1}	3187.76	3199.75	3219.74
Crystal system	Cubic	cubic	cubic
Space group	*I -4 3 d*	*I -4 3 d*	*I -4 3 d*
a/Å	39.4218(11)	39.2961(13)	39.1330(7)
b/Å	39.4218(11)	39.2961(13)	39.1330(7)
c/Å	39.4218(11)	39.2961(13)	39.1330(7)
α (°)	90	90	90
β (°)	90	90	90
γ(°)	90	90	90
v/Å^3	61265(3)	60680(6)	59927.9(19)
Z	16	16	16
ρ_c/Mg m^{-3}	1.382	1.401	1.427
μ/mm^{-1}	1.822	2.077	2.231
F(000)	24864	25056	25152
θ range(deg)	1.27 to 25.02	1.269 to 25.061	1.27 to 25.05
reflections collected	288498	268488	281176
Completeness to θ (%)	100.0	99.8	100.0
independent reflections/R_{int}	9039 /0.1333	8971/0.0878	8878 [R(int) = 0.0672]
GooF(F^2)	1.241	1.071	1.033
Final R indices (I>2σ(I))	R1 = 0.0745 wR2 = 0.2082	R1 = 0.0398 wR2 = 0.0955	R1 = 0.0389 wR2 = 0.1028
R indices (all data)	R1 = 0.0770 wR2 = 0.2100	R1 = 0.0428 wR2 = 0.0970	R1 = 0.0407 wR2 = 0.1045

Table 2.2. Selected Bond distances (Å) and Bond angles (º) for compound **2.1**

La(1)-O(8)	2.693(9)	O(3)-La(1)-O(8)	72.7(4)
La(1)-O(3)	2.421(11)	O(10)-La(1)-O(8)	74.9(5)
La(1)-O(11) *	2.622(10)	O(9)-La(1)-O(8)	149.4(5)
La(1)-O(10)	2.506(10)	O(2)-La(1)-O(8)	87.6(4)
La(1)-O(1)	2.409(9)	O(7) -La(1)-O(8)	70.2(4)
La(1)-O(9)	2.584(13)	O(11)-La(1)-O(8)	149.4(5)
La(1)-O(2)	2.516(9)	O(3)-La(1)-O(8)	102.5(4)
La(1)-O(7)	2.433(10)	O(10)-La(1)-O(8)	71.4(5)
La(1)-O(8)*	2.819(8)	O(12)-La(1)-O(8)	112.6(4)
La(2)-O(1)*	2.432(10)	O(9)-La(1)-O(8)	132.3(4)
La(2)-O(4)	2.461(10)	O(1) -La(2)-O(4)	104.6(5)
La(2)-O(11)	2.530(10)	O(4)-La(2)-O(3)	89.3(4)
La(2)-O(8)	2.746(9)	O(1)-La(2)-O(7)	142.9(5)
La(2)-O(5)	2.402(10)	O(4)-La(2)-O(7)	101.6(5)
La(2)-O(12)	2.398(11)	O(3)-La(2)-O(7)	128.4(5)
La(2)-O(2)	2.515(9)	O(1)-La(2)-O(5)	85.9(5)
La(2)-O(7)	2.426(10)	O(4)-La(2)-O(5)	68.1(5)
O(7)-La(1)-O(11)	95.29(5)	O(3)-La(2)-O(5)	148.0(5)
O(7)-La(1)-O(3)	138.6(5)	O(7)-La(2)-O(5)	79.9(5)
O(11)-La(1)-O(3)	105.5(4)	O(1)-La(2)-O(12)	144.4 (4)
O(7)-La(1)-O(10)	78.9(6)	O(4)-La(2)-O(12)	78.8(5)
O(11)-La(1)-O(10)	79.4(6)	O(3)-La(2)-O(12)	66.5(4)
O(3)-La(1)-O(10)	139.1(6)	O(7)-La(2)-O(12)	66.5(4)
O(7)-La(1)-O(12)	154.8(5)	O(5)-La(2)-O(12)	126.4(4)
O(11)-La(1)-O(12)	68.8(4)	O(1)-La(2)-O(2)	70.9(5)
O(3)-La(1)-O(12)	66.4(4)	O(4)-La(2)-O(2)	144.0(4)
O(10)-La(1)-O(12)	78.6(6)	O(3)-La(2)-O(2)	122.8(4)
O(7)-La(1)-O(9)	77.9(4)	O(7)-La(2)-O(2)	72.4(4)
O(11)-La(1)-O(9)	66.2(6)	O(5)-La(2)-O(2)	75.9(4)
O(3)-La(1)-O(9)	79.1(5)	O(12)-La(2)-O(2)	126.3(4)
O(10)-La(1)-O(9)	135.6(6)	O(1)-La(2)-O(8)	99.6(5)
O(12)-La(1)-O(9)	111.4(4)	O(4)-La(2)-O(8)	145.3(4)
O(7)-La(1)-O(2)	70.8(5)	O(3)-La(2)-O(8)	71.7(4)
O(11)-La(1)-O(2)	137.4(5)	La(2)-O(12)-La(1)	99.9(4)
O(3)-La(1)-O(2)	69.5(4)	La(1)-O(8)-La(1)*	146.1(5)
O(10)-La(1)-O(2)	133.1(5)	La(2)-O(8)-La(1)	88.1(5)
O(12)-La(1)-O(2)	134.0(4)	La(1)-O(3)-La(2)	105.2(5)
O(9)-La(1)-O(2)	71.4(5)	La(1)-O(7)-La(2)	105.1(5)

Table 2.3. Selected Bond distances (Å) and Bond angles (°) for compound **2.2**

Pr(1)-O(3)	2.385(10)	O(12)-Pr(1)-O(8)	67.2(3)
Pr(1)-O(11)	2.385(11)	O(10)-Pr(1)-O(8)	76.4(4)
Pr(1)-O(7)	2.397(9)	O(9)-Pr(1)-O(8)	148.5(5)
Pr(1)-O(12)	2.470(9)	O(2)-Pr(1)-O(8)	86.2(3)
Pr(1)-O(10)	2.476(13)	O(3)-Pr(1)-O(8)	103.7(3)
Pr(1)-O(9)	2.538(11)	O(11)-Pr(1)-O(8)	149.1(4)
Pr(1)-O(2)	2.577(9)	O(7)-Pr(1)-O(8)	68.9(3)
Pr(1)-O(8)	2.628(9)	O(12)-Pr(1)-O(8)	112. 6(3)
Pr(1)-O(8)*	2.884(9)	O(10)-Pr(1)-O(8)*	72.1(4)
Pr(2)-O(1)	2.343(11)	O(1)-Pr(2)-O(4)	103.3(4)
Pr(2)-O(4)	2.387(10)	O(1)-Pr(2)-O(3)	78.3(4)
Pr(2)-O(3)	2.392(9)	O(4)-Pr(2)-O(3)	86.8(3)
Pr(2)-O(7)	2.405(10)	O(1)-Pr(2)-O(7)	144.1(3)
Pr(2)-O(5)	2.439(10)	O(4)-Pr(2)-O(7)	100.8(3)
Pr(2)-O(12)	2.483(9)	O(3)-Pr(2)-O(7)	129.6(3)
Pr(2)-O(2)	2.481(9)	O(1)-Pr(2)-O(5)	84.9(4)
Pr(2)-O(8)	2.627(9)	O(4)-Pr(2)-O(5)	68.9(3)
O(3)-Pr(1)-O(11)	104.7(4)	O(3)-Pr(2)-O(5)	146.3(3)
O(3)-Pr(1)-O(7)	139.9(4)	O(7)-Pr(2)-O(5)	79.3(4)
O(11)-Pr(1)-O(7)	96.0 (3)	O(1)-Pr(2)-O(12)	144.1(3)
O(3)-Pr(1)-O(12)	66.2(3)	O(4)-Pr(2)-O(12)	77.8(3)
O(11)-Pr(1)-O(12)	69.3(3)	O(3)-Pr(2)-O(12)	65.9(3)
O(7)-Pr(1)-O(12)	153.8(3)	O(7)-Pr(2)-O(12)	67.3(3)
O(3)-Pr(1)-O(10)	139.0(4)	O(5)-Pr(2)-O(2)	75.2(2)
O(11)-Pr(1)-O(10)	78.7(4)	O(1)-Pr(2)-O(12)	126.7(3)
O(7)-Pr(1)-O(10)	78.2(4)	O(1)-Pr(2)-O(2)	72.4(3)
O(12)-Pr(1)-O(10)	77.7(4)	O(4)-Pr(2)-O(2)	144.3(3)
O(3)-Pr(1)-O(9)	79.0(3)	O(3)-Pr(2)-O(2)	125.0(3)
O(11)-Pr(1)-O(9)	66.2(4)	O(5)-Pr(2)-O(2)	75.5(3)
O(7)-Pr(1)-O(9)	78.6(2)	O(7)-Pr(2)-O(2)	72.5(3)
O(12)-Pr(1)-O(9)	112.3(3)	O(12)-Pr(2)-O(2)	126.8(3)
O(10)-Pr(1)-O(9)	135.1(5)	O(1)-Pr(2)-O(8)	100.7(4)
O(3)-Pr(1)-O(2)	138.0(2)	O(4)-Pr(2)-O(8)	143.9(3)
O(3)-Pr(1)-O(2)	70.8(3)	O(3)-Pr(2)-O(8)	72.1(3)
O(11)-Pr(1)-O(2)	138.2(3)	O(7)-Pr(2)-O(8)	73.4(3)
O(7)-Pr(1)-O(2)	70.9(3)	O(5)-Pr(2)-O(8)	140.3(3)
O(12)-Pr(1)-O(2)	134.5(3)	O(12)-Pr(2)-O(8)	67.1(3)
O(10)-Pr(1)-O(2)	132.8(4)	Pr(1)-O(8)-Pr(2)	92.1(3)
O(9)-Pr(1)-O(2)	72.2(3)	Pr(1)-O(8)*-Pr(2)	145.8(4)
O(3)-Pr(1)-O(8)	72.2(3)	Pr(2)-O(2)-Pr(1)	97.6(3)
O(11)-Pr(1)-O(8)	133.3(3)	Pr(1)-O(12)-Pr(2)	99.6(3)
O(7)-Pr(1)-O(8)	116.3(3)	Pr(1)-O(7)-Pr(2)	104.9(4)

Table 2.4. Selected Bond distances (Å) and Bond angles (º) for compound 2.**3**

Nd(1)-O(12)	2.359(12)	O(3)-Nd(1)-O(8)	72.5(3)
Nd(1)-O(7)	2.374(11)	O(11)-Nd(1)-O(8)	67.5(3)
Nd(1)-O(3)	2.381(11)	O(9)-Nd(1)-O(8)	77.7(4)
Nd(1)-O(11)	2.442(9)	O(10)-Nd(1)-O(8)	148.3(4)
Nd(1)-O(9)	2.509(14)	O(2)-Nd(1)-O(8)	85.0(3)
Nd(1)-O(10)	2.513(12)	O(12)-Nd(1)-O(8)	148.1(4)
Nd(1)-O(2)	2.546(10)	O(7)-Nd(1)-O(8)	69.2(3)
Nd(1)-O(8)*	2.590(10)	O(3)-Nd(1)-O(8)	103.9(4)
Nd(1)-O(8)	2.928(9)	O(11)-Nd(1)-O(8)	111.3(3)
Nd(2)-O(1)	2.331(12)	O(1)-Nd(2)-O(4)	102.9(4)
Nd(2)-O(3)	2.368(11)	O(1)-Nd(2)-O(3)	77.3(4)
Nd(2)-O(4)	2.380(11)	O(4)-Nd(2)-O(3)	85.9(4)
Nd(2)-O(7)	2.387(11)	O(1)-Nd(2)-O(7)	143.9(4)
Nd(2)-O(5)	2.410(11)	O(4)-Nd(2)-O(7)	100.9(24)
Nd(2)-O(2)	2.464(10)	O(3)-Nd(2)-O(7)	131.4(4)
Nd(2)-O(8)	2.618(10)	O(1)-Nd(2)-O(5)	84.6(4)
Nd(2)-O(11)	2.482(10)	O(4)-Nd(2)-O(5)	69.0(4)
O(12)-Nd(1)-O(7)	95.5(4)	O(3)-Nd(2)-O(5)	144.8(4)
O(12)-Nd(1)-O(3)	105.3(5)	O(7)-Nd(2)-O(5)	79.1(4)
O(7)-Nd(1)-O(3)	140.1(2)	O(1)-Nd(2)-O(2)	72.8(4)
O(12)-Nd(1)-O(11)	69.8(4)	O(4)-Nd(2)-O(2)	144.6(4)
O(7)-Nd(1)-O(11)	153.1(4)	O(3)-Nd(2)-O(2)	125.3(4)
O(3)-Nd(1)-O(11)	66.8(4)	O(7)-Nd(2)-O(2)	72.1(4)
O(12)-Nd(1)-O(9)	77.1(5)	O(5)-Nd(2)-O(2)	75.7(3)
O(7)-Nd(1)-O(9)	77.6(4)	O(1)-Nd(2)-O(11)	143.5(4)
O(3)-Nd(1)-O(9)	139.8(4)	O(4)-Nd(2)-O(11)	78.1(4)
O(11)-Nd(1)-O(9)	77.2(4)	O(3)-Nd(2)-O(11)	66.4(4)
O(12)-Nd(1)-O(10)	66.9(5)	O(7)-Nd(2)-O(11)	67.9(2)
O(7)-Nd(1)-O(10)	78. 5(4)	O(5)-Nd(2)-O(11)	127.6(3)
O(3)-Nd(1)-O(10)	79.0 (4)	O(2)-Nd(2)-O(11)	126.5(3)
O(11)-Nd(1)-O(10)	113.6(4)	O(1)-Nd(2)-O(8)	100.4(4)
O(9)-Nd(1)-O(10)	134.0(5)	O(4)-Nd(2)-O(8)	143.5(4)
O(12)-Nd(1)-O(2)	139.2(4)	O(3)-Nd(2)-O(8)	72.2(3)
O(7)-Nd(1)-O(2)	70.8(4)	O(7)-Nd(2)-O(8)	74.7(3)
O(3)-Nd(1)-O(2)	71.2(4)	O(5)-Nd(2)-O(8)	141.5(3)
O(11)-Nd(1)-O(2)	134.9(3)	Nd(2)-O(3)-Nd(1)	104.3(4)
O(9)-Nd(1)-O(2)	132.5(4)	Nd(1)-O(8)-Nd(2)	92.1(3)
O(10)-Nd(1)-O(2)	72.7(4)	Nd(1)-O(8)-Nd(1)*	146.0(4)
O(12)-Nd(1)-O(8)	134.0(4)	Nd(2)-O(8)-Nd(1)	85.7(3)
O(7)-Nd(1)-O(8)	115.6(3)	Nd(1)-O(7)-Nd(2)	105.1(4)

Table 2.5. Summary of SHAPE analysis for compound **2.1** around La1 (a) and La2 (b)

(a)

S.No.	Geometry	CShM value for La1
1	Enneagon (D9h)	33.492
2	Octagonal pyramid (C8v)	21.355
3	Heptagonal bipyramid (D7h)	15.875
4	Johnson triangular cupola J3 (C3v)	15.993
5	Capped cube J8 (C4v)	9.440
6	Spherical-relaxed capped cube (C4v)	8.187
7	Capped square antiprism J10 (C4v)	2.882
8	Spherical capped square antiprism (C4v)	2.293
9	Tricapped trigonal prism J51 (D3h)	4.090
10	Spherical tricapped trigonal prism (D3h)	3.282
11	Tridiminished icosahedron J63 (C3v)	11.319
12	Hula-hoop (C2v)	7.578
13	**Muffin (Cs)**	**1.582**

(b)

S.No.	Geometry	CShM value for La2
1	Octagon(D8h)	31.527
2	Heptagonal pyramid(C7v)	22.718
3	Hexagonal bipyrami(D6h)	15.974
4	Cube(Oh)	11.857
5	Square antiprism(D4d)	2.188
6	**Triangular dodecahedron(D2d)**	**1.562**
7	Johnson gyrobifastigium J26(D2d)	14.055
8	Johnson elongated triangular bipyramid J14(D3h)	27.022
9	Biaugmented trigonal prism J50(C2v)	3.081
10	Biaugmented trigonal prism(C2v)	2.553
11	Snub diphenoid J84(D2d)	3.888
12	Triakis tetrahedron(Td)	12.653
13	Elongated trigonal bipyramid(D3h)	23.105

2.6 References

(1) a) Natur, F. L.; Calvez, G.; Daiguebonne, C.; Guillou, O.; Bernot, K.; Ledoux, J.; Pollès, L. L.; Roiland, C. *Inorg. Chem*. **2013**, *52*, 6720. b) Bünzli, J. C. G. Eliseeva, S. V. *Chem. Sci*. **2013**, *4*, 1939. c) Biju, S.; Gopakumar, N.; Bünzli, J.-C. G.; Scopelliti, R.; Kim, H. K.; Reddy, M. L. P. *Inorg. Chem*. **2013**, *52*, 8750. d)

Eliseeva S. V.; Bünzli, J.-C. G. *Chem. Soc. Rev*. **2010**, *39*, 189. e) Sobieray, M.; Gode, J.; Seidel, C.; Poβ, M.; Feldmann, C.; Ruschewitz, U. *Dalton Trans*. **2015**, *44*, 6249.

(2) a) Pohlki, F.; Doye, S. *Chem. Soc. Rev*. **2003**, *32*, 104. b) Roesky, P. W.; Canseco-Melchor, G.; Zulys, A. *Chem. Commun*. **2004**, 738. c) Edelmann, F. T. *Chem. Soc. Rev*. **2009**, *38*, 2253. d) Gandara, F.; Enrique, G.-P.; Iglesias, M.; Snejko, N.; Monge, A. M. *Cryst. Growth Des*. **2010**, *10*, 128. (e) Weissa C. J.; Marks, T. J. *Dalton Trans*. **2010**, *39*, 6576.

(3) a) Woodruff, D. N.; Winpenny, R. E. P.; Layfield, R. A. *Chem. Rev*. **2013**, *113*, 5110. b) Neville, S. M.; Halder, G. J.; Chapman, K. W.; Duriska, M. B.; Moubaraki, B.; Murray, K. S.; Kepert, C. J. *J. Am. Chem. Soc*. **2009**, *131*, 12106. c) Ungur, L.; Langley, S. K.; Hooper, T. N.; Moubaraki, B.; Brechin, E. K.; Murray, K. S.; Chibotaru, L. F. *J. Am. Chem. Soc*. **2012**, *134*, 18554. d) Le Roy, J. J.; Ungur, L.; Korobkov, L.; Chibotaru, L. F.; Murugesu, M. *J. Am. Chem. Soc*. **2014**, *136*, 8003. e) Chilton, N. F.; Collison, D.; McInnes, E. J. L.; Winpenny, R. E. P.; Soncini, A. *Nat. Commun*. **2013**, *4*, 2551. f) Chandrasekhar, V.; Bag,; Colacio, E. *Inorg. Chem*. **2013**, *52*, 4562. g) Chandrasekhar, V.; Dey, A.; Das, S.; Rouzières, M.; Clérac, R. *Inorg. Chem*. **2013**, *52*, 2588. h) Goura, J.; Walsh, J. P. S.; Tuna, F.; Chandrasekhar, V. *Inorg. Chem*. **2014**, *53*, 3385. i) Goura, J.; Mereacre, V.; Novitchi, G.; Powell, A. K.; Chandrasekhar, V. *Eur. J. Inorg. Chem*. **2015**, 156. j) Baniodeh, A.; Mereacre, V.; Magnani, N.; Lan, Y.; Wolny, J. A;. Schünemann, V.; Anson, C. E.; Powell, A. K. *Chem. Commun*. **2013**, *49*, 9666. i) Baniodeh, A.; Magnani, N.; Bräse, S.; Anson, C. E.; Powell, A. K. *Dalton Trans*. **2015**, *44*, 6343.

(4) a) Das, M. C.; Ghosh, S. K.; Sanudo, E. C.; Bharadwaj, P. K. *Dalton Trans*. **2009**, 1644. b) Li, C.-J.; Lin, Z.-J.; Peng, M.-X.; Leng, J.-D.; Yang, M.-M.; Tong, M.-L. *Chem. Commun*. **2008**, 6348-6350; c) Li, C.-J.; Peng, M.-X.; Leng, J.-D.; Yang, M.-M.; Lin, Z.-J.; Tong, M.-L. *CrystEngComm*, **2008**, *10*, 1645. d) Gao, H.-L.; Yi, L.; Ding, B.; Wang, H.-S.; Cheng, P.; Liao, D.-Z.; Yan, S.-P. *Inorg. Chem*. **2006**, *45*, 481. e) Ghosh, S. K.; Bharadwaj, P. K. *Eur. J. Inorg. Chem*. **2005**, 4886. f) Zhao, X.-Q.; Zhao, B.; Shi, W.; Cheng, P. *Inorg. Chem.* **2009**, *48*, 11048. g) Zhao, X.-Q.; Zhao, B.; Shi, W.; Cheng, P.; Liao, D.-Z.; Yan, S.-P. *Dalton Trans*. **2009**,

2281.h) fang, S.-M.; Sañudo, E. C.; Hu, M.; Zhang, Q.; Ma, S. T.; Jia, L.-R.; Wang, C.; Tang, J.-Y.; Liu, C.-S. *Cryst. Growth Des*. **2011**, *11*, 811.

(5) a) Wang, R.; Liu, H.; Carducci, M. D.; Jin, T.; Zheng, C.; Zheng, Z. *Inorg. Chem*. **2001**, *40*, 2743. b) Wang, R.; Carducci, M. D.; Zheng, Z. *Inorg. Chem*. **2000**, *39*, 1836. c) Wang, R.; Zheng, Z.; Jin, T.; Staples, R. J. *Angew. Chem., Int. Ed*., **1999**, *38*, 1813. d) Wang, R.; Selby, H. D.; Liu, H.; Carducci, M. D.; Jin, T.; Zheng, Z.; Anthis, J. W.; Staples, R. J. *Inorg. Chem*. **2002**, *41*, 278. e) Kong, X.-J.; Wu, Y.; Long, L.-S.; Zheng, L.-S.; Zheng, Z. *J. Am. Chem. Soc*. **2009**, *131*, 6918. f) Zheng, Z. *Chem. Commun*. **2001**, 2521. g) Thielemann, D. T.; Fernández, I.; Roesky, P. W. *Dalton Trans*. **2010**, *39*, 6661.

(6) a) Kritikos, M.; Moustiakimov, M.; Wijk, M.; Westin, G. *Dalton Trans*. **2001**, 1931. b) Blagg, R. J.; Muryn, C. A.; McInnes, E. J. L.; Tuna, F.; Winpenny, R. E. P. *Angew. Chem., Int. Ed*. **2011**, *50*, 6530. c) kritikos, M.; Moustiakimov, M.; Westin, G. *Inorg. Chim*. *Acta*. **2012**, *384*, 125. d) Blagg, R. J.; Ungur, L.; Tuna, F.; Speak, J.; Comar, P.; Collison. D.; Wernsdorfer, W.; McInnes, E. J. L.; Chibotaru, L. F.; Winpenny, R. E. P. *Nat. Chem*. **2013**, *5*, 673.

(7) a) Andrews, P. C.; Deacon, G. B.; Frank, R.; Fraser, B. H.; Junk, P. C.; MacLellan, J. G.; Massi, M.; Moubaraki, B.; Murray, K. S.; Silberstein, M. *Eur. J. Inorg. Chem*. **2009**, *6*, 744. b) Baskar, V.; Roesky, P. W. *Z. Anorg. Allg. Chem*. **2005**, *631*, 2782. c) Baskar, V.; Roesky, P. W. *Dalton Trans*. **2006**, 676. d) Roesky, P. W.; CansecoMelchor G.; Zulys, A. *Chem. Commun*. **2004**, 738.e) Bürgstein, M. R.; Roesky, P. W. *Angew. Chem., Int. Ed*. **2000**, *39*, 549. f) Andrews, P. C.; Beck, T.; Fraser, B. H.; Junk, P. C.; Massi, M.; Moubaraki, B.; Murry, K. S.; Silberstein, M. *Polyhedron*, **2009**, *28*, 2123. g) Gamer, M. T.; Lan, Y.; Roesky, P. W.; Powell, A. K.; Clerac, R. *Inorg. Chem*. **2008**, *47*, 6581. h) Datta, S.; Baskar, V.; Li, H.; Roesky, P. W. *Eur. J. Inorg. Chem*. **2007**, 4216. i) Jami, A. K.; Kishore, P. V. V. N.; Baskar, V. *Polyhedron*, **2009**, *28*, 2284. j) Andrews, P. C.; Gee, W. J.; Junk, P. C.; MacLellan, J. G. *Dalton Trans*. **2011**, *40*, 12169. k) Andrews, P. C.; Gee, W. J.; Junk, P. C. MacLellan, J. G. *Polyhedron*, **2011**, *30*, 2837. (l) Yadav, M.; Mondal, A.; Mereacre, V.; Jana, S. K.; Powell, A. K.; Roesky, P. W. *Inorg. Chem*. **2015**, *54*, 7846. m) Hui, Y.-C.; Meng, Y.-S.; Li, Z.; Chen, Q.; Sun, H.-L.; Zhangd, Y.-Q.; Gao, S. *CrystEngComm*. **2015**, *17*, 5620. n) Thielemann, D. T.; Wagner, A. T.; Lan, Y.; Oña-Burgos, P.; Fernãndez, I.; Rösch, E. S.; Kölmel, D. K.; Powell, A.

K.; Bräse, S.; Roesky, P. W. *Chem. -Eur. J.* **2015**, *21*, 2813. o) Chilton, N. F.; Langley, S. K.; Moubaraki, B.; Soncini, A.; Batten, S. R.; Murray, K. S. *Chem. Sci*. **2013**, *4*, 1719.

(8) a) Chandrasekhar, V.; Hossain, S.; Das, S.; Biswas, S.; Sutter, J.-F. *Inorg. Chem.* **2013**, *52*, 6346. b) Das, S.; Dey, A.; Biswas, S.; Colacio, E.; Chnadrasekhar, V. *Inorg. Chem. 2014, 53*, 3417. c) Upadhyay, A.; Singh, S. K.; Das, C.; Mondal, R.; Langley, S. K.; Murray, K. S.; Rajaraman, G.; Shanmugam, M. *Chem. Commun*. **2014**, *50*, 8838. d) Ahmed, N.; Das, C.; Vaidya, S.; Langley, S. K.; Murray, K. S.; Shanmugam, M. *Dalton Trans*. **2014**, *43*, 17375. e) Ahmed, N.; Das, C.; Vaidya, S.; Langley, S. K.; Murray, K. S.; Shanmugam, M. *Chem. Eur. J*. **2014**, *20*, 14235. f) Yadav, M.; Mereacre, V.; Lebedkin, S.; Kappes, M. M.; Powell, A. K.; Roesky, P. W. *Inorg. Chem.* **2015**, *54*, 773.

(9) a) Sumida, K.; Rogow, D. L.; Mason, J. A.; McDonald, T. M.; Bloch, E. D.; Herm, Z. R.; Bae, T.-H.; Long, J. R. *Chem. Rev*. **2011**, *112*, 724. b) Karra, J. R.; Walton, K. S. *J. Phys. Chem. C*, **2010**, *114*, 15735. c) Xiang, Z.; Leng, S.; Cao, D. *J. Phys. Chem. C*, **2012**, *116*, 10573. d) Hao, G.-P.; Li, W.-C.; Lu, A.-H. *J. Mater. Chem.* **2011**, *21*, 6447. e) Southon, P. D.; Liu, L.; Fellows, E. A.; Price, D. J.; Halder, G. J.; Chapman, K. W.; Moubaraki, B.; Murray, K. S.; Letard, J.-F.; Kepert, C. J. *J. Am. Chem. Soc*. **2009**, *131*, 10998.

(10) Arikawa, Y.; Nakamura, T.; Ogushi, S.; Eguchi, K.; Umakoshi, K. Dalton Trans. **2015**, *44*, 5303.

(11) a) Escuer, A.; Vicente, R.; Kumar, S. B.; Solans, X.; Font-Bardía, M.; Caneschi, A. *Inorg. Chem*. **1996**, *35*, 3094. b) Schrodt, A.; Neubrand, A.; van Eldik, R. *Inorg. Chem*. **1997**, *36*, 4579. c) Fondo, M.; García-Deibe, A. M.; Ocampo, N.; Sanmartín, J.; Bermejo, M. R. *Dalton Trans*. **2004**, 2135. d) Fu, H.; Chen, W. L.; Fu, D. G.; Tong, M. L.; Chen, X. M.; Ji, L. N.; Mao, Z. W. *Inorg. Chem. Commun*. **2004**, *7*, 1285. e) Kong, L. Y.; Zhang, Z. H.; Zhu, H. F.; Kawaguchi, H.; Okamura, T.; Doi, M.; Chu, Q.; Sun, W. Y.; Ueyama, N. *Angew. Chem., Int. Ed*. **2005**, *117*, 4426. f) Kong, L. Y.; Zhu, H. F.; Huang, Y. Q.; Okamura, T.; . Lu, X. H; Song, Y.; Liu, G. X.; Sun, W. Y.; Ueyama, N. *Inorg. Chem*. **2006**, *45*, 8098. g) Chen, J.-M.; Wei, W.; Feng, X.-L.; Lu, T.-B. *Chem. -Asian J*. **2007**, *2*, 710. (h) Wild, A. A. C.; Fennell, K.; Morgan, G. G.; Hewage, C. M.; Malthouse, J. P. G. *Dalton Trans*.

2014, *43*, 13557. i) Sarkar, M.; Aromi, G.; Cano, J.; Bertolasi, V.; Ray, D. *Chem.–Eur. J*. **2010**, *16*, 13825.

(12) a) Jeong, K. S.; Kim, Y. S.; Kim, Y. J.; Lee, E.; Yoon, J. H.; Park, W. H.; Park, Y. W.; Jeon, S.-J.; Kim, Z. H.; Kim, J.; Jeong, N. *Angew. Chem., Int. Ed*. **2006**, *118*, 8134. b) Natarajan, L.; Pecaut, J.; Mazzanti, M. *Dalton Trans*. **2006**, 1002. c) Tang, X. L.; Wang, W. H.; Dou, W.; Jiang, J.; Liu, W. S.; Qin, W. W.; Zhang, G. L.; Zhang, H. R.; Yu, K. B.; Zheng, L. M. *Angew. Chem. Int. Ed*. **2009**, *48*, 3499. d) Bag, P.; Dutta, S.; Biswas, P.; Maji, S. K.; Flörke, U.; Nag, K. *Dalton Trans*., **2012**, *41*, 3414. e) Tian, H.; Wang, M.; Zhao, L.; Guo, Y.-N.; Guo, Y.; Tang, J.; Liu, Z. *Chem. -Eur. J*. **2012**, *18*, 442. f) Guo, Y.-N.; Chen, X.-H.; Xue, S.; Tang, J. *Inorg. Chem*. **2012**, *51*, 4035. g) Zhang, B.; Zheng, X.; Su, H.; Zhu, Y.; Du, C.; Song, M. *Dalton Trans*. **2013**, *42*, 8571. h) Ke, H.; Zhao, L.; Xu, G.-F.; Guo, Y.-N.; Tang, J.; Zhang, X.-Y.; Zhang, H.-J. *Dalton Trans*. **2009**, 10609. i) Huang, L.; Han, L.; Zhu, D.; Chen, L.; Xu, Y. *Inorg. Chem.Commun*. **2012**, *21*, 80. j) Chesman, A. S. R.; Turner, D. R.; Langley, S. K.; Moubaraki, B.; Murray, K. S.; Deacon, G. B.; Batten, S. R. *Inorg. Chem*. **2015**, *54*, 792. k) Sakamoto, S.; Yamauchi, S.; Hagiwara, H.; Matsumoto, N.; Sunatsuki, Y.; Re, N. *Inorg. Chem. Commun*. **2012**, *26*, 20.

(13) Andrews, P. C.; Beck, T.; Forsyth, C. M.; Fraser, B. H.; Junk, P. C.; Massi, M.; Roesky, P. W. *Dalton Trans*. **2007**, 5651.

(14) Langley, S. K.; Moubaraki, B.; Murray, K. S. *Inorg. Chem*. **2012**, *51*, 3947.

(15) a) Tain, H.; Zhao, L.; Guo, Y.-N.; Guo, Y.; Tang, J.; Liu, Z. *Chem Commun*. **2012**, *48*, 708. b) Tian, H.; Guo, Y.-N;. Zhao, L.; Tang, J.; Liu, Z. *Inorg. Chem*. **2011**, *50*, 8688. c) Gass, I. A.; Moubaraki, B.; Langley, S. K.; Btten, S. R.; Murry, K. S. *Chem Commun*. **2012**, *48*, 2089.

(16) Gu, X.; Xue, D. *Inorg. Chem*. **2007**, *46*, 3212.

(17) Chesman, A. S. R.; Turner, D. R.; Moubaraki, B.; Murray, K. S.; Deacon, G. B.; Batten, S. R. *Chem.- Eur. J*. **2009**, *15*, 5203.

(18) Stubbing, L. A.; Li, F. F.; Furkert, D. P.; Caprio, V. E.; Brimble, M. A. *Tetrahedron*, **2012**, *68*, 6948.

(19) a) Sheldrick, G. M. *SHELXS-97, Program for Crystal Structure Solution*; University of Göttingen, Göttingen, Germany, **1997**; b) Sheldrick, G. M.

Crystallogr. Sec. A: *Fundam. Crystallogr*. **2008**, *64*, 112; c) Sheldrick, G. M. *Acta Crystallogr. Sect. C: Cryst. Struct. Commun*. **2015**, *71*, 3.

(20) Hołyńska, M.; Clérac, R.; Rouzières, M. *Chem. -Eur. J*. **2015**, *21*, 13321.

(21) a) Alvarez, S.; Alemany, P.; Casanova, D.; Cirera, J.; Llunell, M.; Avnir, D. *Coord. Chem. Rev*. **2005**, *249*, 1693. (b) Casanova, D.; Llunell, M.; Alemany, P.; Alvarez, S. *Chem. -Eur. J*. **2005**, *11*, 1479.

Effect of Coordination Geometry on the Magnetic Properties of a Series of Di and Tetra nuclear Lanthanide Hydroxo Clusters

CHAPTER 3

Synthesis of two series of Ln(III) complexes was achieved under ambient conditions. One of the series consists of three new isostructurally distorted cubane like tetranuclear $[Ln_4(\mu_3\text{-}OH)_4(L)_4(\mu_2\text{-}piv)_4(MeOH)_4]$ {Ln = Gd **3.1**, Dy **3.2** and Ho **3.3**; LH = [1,3-Bis(o-methoxyphenyl)-propane-1,3-dione]; (Piv = pivallic acid)} frameworks, where as another series is represented by discrete dinuclear $[Ln_2(L)_4(\mu_2\text{-}LH_2')_2].4DMF/CH_3CN$ (Ln = Gd **3.4**, Dy **3.5** and Ho **3.6**; LH_3' = 2 6-Bis(hydroxymethyl)-p-cresol) structural entities. Under similar reaction conditions, type of the co-ligand employed has a profound role in deciding the structure of the end product. Synthesis, structure and magnetic properties of these complexes are discussed in this chapter.

3.1 Introduction

Lanthanide polyatomic complexes have been the epicentre of tremendous interest in recent times. Their peculiar structural features along with potential applications in numerous fields like luminescence,[1] catalysis[2] and molecular magnetism[3] (which includes single molecule magnets (SMMs) and molecular magnetic refrigerants) have in fact helped this emerging field to widen its horizons. Discrete molecules which exhibit slow relaxation of magnetization below certain temperature (blocking temperature, T_B) are referred as Single molecule magnet (SMM). It has been found that the factors governing SMM behaviour (overall ground state (S) and magnetic anisotropy (D)) in large polynuclear transition metal clusters counter balances each other. Such an act hampers increase of T_B significantly to a higher temperature. But lanthanide based SMMs attracted several researchers recently after the discovery of $[Tb(Pc)_2]^-$,[4] as the mentioned complex shows significantly large effective energy barrier (U_{eff}) compared to any transition metal cluster to date. A wide range of Ln(III) clusters with different topologies have been investigated, which include di,[5] tri,[6] tetra (linear, grids, cubanes, rhombous, Y-shaped, seasaw),[7] and polynuclear[8] clusters. Among transition metal complexes cubane cores are well known,[9] but in case of lanthanides they are still scarcely investigated[10] and so far, in few examples, magnetism has been investigated in detail.[10a-e] As far as magnetism is concerned, dinuclear Ln(III) complexes have been of much interest, owing to their simpler structural features which helps in better understanding of relaxation dynamics.[11] Apart from characteristic requirements for metal ions, the choice of organic ligands also has a deciding role to play. Aggregation of metal ions to polymetallic motifs and simultaneous exclusion of extensive polymerization and thermodynamic stability to the resulting complex are the important factors to be fulfilled by the ligands. Although the intrinsic orbital angular momentum constitutes large anisotropy, the resultant electronic structure of lanthanide ions is purely controlled by the ligand field, which lifts the degeneracy of the m_j levels. Ideal ligand field around certain lanthanide complexes along with suitable geometry and enhancing exchange interactions to quench the quantum tunnelling of magnetization are the factors which collectively help in enhancing T_B in lanthanide complexes.[12,13] Energy required for the reversal of magnetization could be modulated by changing the substituents on ligands which was shown by Murugesu and co-workers.[14] Due to their preferential bidentate chelating modes, β-diketones are attractive, as they strongly chelate to the Ln(III) ions and

provide suitable ligand field to fulfil the requirement for strong magnetic anisotropy and a favourable geometry (near D_{4d} geometry,) in majority of the complexes reported in the literature.[15,16,17] Even though β-diketones have been investigated in detail,[18] the use of functionalized β-diketones as ligands towards lanthanides are rare.[6a,19]

In addition to SMMs, Magnetic refrigeration is also emerging as one of the most important and leading application oriented field currently. The potential use of miniature molecular clusters for this purpose is evaluated in terms of their intrinsic magnetocaloric effect, i.e., change in temperature with the aid of external magnetic field. In context of finding new refrigerants, because of their efficient energy saving and environmentally benign properties, cryogenic molecular magnets are increasingly becoming a choice worth to hunt for. Isotropic molecular clusters are potentially targeted as magnetic coolants to achieve ultralow temperatures to replace the cryogenic liquid ^{3}He which is becoming rare and expensive.[20] Change in magnetic entropy ($-\Delta S_m$) and change in temperature (ΔT_{ad}) are the two parameters which quantify the MCE efficacy of a particular cluster. High magnetic density (high metal to ligand ratio),[21] negligible magnetic anisotropy (preferably isotropic in nature) and spin degeneracy are the key factors which play pivotal role in determining the MCE efficiency. The large spin ground state, negligible magnetic anisotropy, high magnetic density and ferromagnetic interactions associated with polymetallic Gd(III) complexes with suitable organic ligands authenticate their applicability as cryogenic molecule magnetic coolants.

With the aim of revealing new generation of SMMs and magnetic coolants, the use of bisortho-methoxy functionalized β-diketone (LH) ligand along with other co-ligands for the synthesis of Ln(III) clusters was investigated. The use of LH and pivallic acid (pivH as a co-ligand) resulted in successful isolation and characterization of three new tetranuclear clusters with distorted cubane core with the general formula $[Ln_4(\mu_3\text{-}OH)_4(L)_4(\mu_2\text{-}piv)_4(MeOH)_4]$ (Ln = Gd **3.1**, Dy **3.2**, Ho **3.3**). Similarly changing the pivallic acid (pivH) to a bulky co-ligand 2,6-Bis(hydroxymethyl)-p-cresol (LH_3') resulted in the isolation of three new dinuclear Ln(III) complexes with a general formula $[Ln_2(L)_4(\mu_2\text{-}LH_2')_2]4CH_3CN/DMF$ (Ln = Gd **3.4**, Dy **3.5** and Ho **3.6**) and their magnetic properties have been studied in detail.

3.2 Experimental Section

3.2.1 General information and Instrumentation:

The general reagents used were of analytical grade and used as received without further purification. LH was prepared according to the literature procedure.[22] Hydrated lanthanum trihalides were prepared from the corresponding oxides by neutralizing with concentrated HCl, followed by evaporation to dryness. Triethylamine, pivH, LH_3' and common organic solvents were purchased from commercial sources and used without further purification. Infrared spectra were recorded on a JASCO-5300 FT-IR spectrometer as KBr pellets. Thermo gravimetric analyses were carried out on SDT-Q600 supplied by Ta instruments. Elemental analysis was performed on a flash EA series 1112 CHNS analyzer. Magnetic measurements were carried out in Unitat de Mesures Magnètiques (Universitat de Barcelona) on polycrystalline samples (approximately 30 mg) with a Quantum Design SQUID MPMS-XL magnetometer equipped with a 5 T magnet. Diamagnetic corrections were calculated using Pascal's constants and an experimental correction for the sample holder was applied. Single crystal X-ray diffraction data for all the compounds was collected on a Bruker Smart Apex CCD area detector system (λ (Mo Kα) = 0.71073Å) at 100(2) K. Data processing was accomplished by using SAINT PLUS and the structures were solved by using SHELXS-97 and refined using SHELXL-2014/7 program.[23] All non-hydrogen atoms were refined anisotropically by full matrix least square cycles on F^2. Hydrogen atoms were introduced at calculated positions and refined as riding model. Crystal data parameters for complexes **3.1**-**3.6** are summarized in Table **3.1**.

3.2.2 General Synthetic procedure for compounds 3.1-3.6:

To a methanolic solution of ligand LH and pivH, $LnCl_3.6H_2O$ was added and stirred at room temperature for 10 minutes. To this solution, triethylamine was added dropwise and mixture was stirred for further 12h at room temperature resulting in a pale yellow precipitate which was washed with methanol, dried and re-dissolved in CH_3CN/MeOH for crystallization. Pale yellow block shaped crystals suitable for X-ray crystallography were obtained by slow evaporation of the solvent mixture under aerobic conditions. The same procedure was followed for the synthesis of **3.4**, **3.5** and **3.6** where LH_3' was used instead

of pivH. Crystals suitable for X-ray analysis were obtained by slow evaporation of solvent mixture DMF/MeOH.

Compound **3.1**: LH (0.150 g, 0.527 mmol), PivH (0.053 g, 0.527 mmol), $GdCl_3.6H_2O$ (0.196 g, 0.527 mmol), Et_3N (0.29 mL, 2.108 mmol). Yield: 0.450 g, 61.14% (based on Gd). Mp: 162 ˚C (dec). IR (KBr) cm^{-1}: 3599(b), 3073(w), 2959(s), 2865(w), 2832(m), 1610(w), 1561(m), 1506(m), 1478(s), 1396(m), 1308(s), 1237(s), 1177(m), 1023(s), 947(m), 892(m), 760(s). Anal. Calcd (%) for $C_{92}H_{116}O_{32}Gd_4$ (2362.85): C, 46.76; H, 4.94. Found: C, 46.45; H, 4.85.

Compound **3.2**: LH (0.150 g, 0.527 mmol), PivH (0.053 g, 0.527 mmol), $DyCl_3.6H_2O$ (0.198 g, 0.527 mmol), Et_3N (0.29 mL, 2.108 mmol). Yield: 0.450 g, 60.60% (based on Dy). Mp: 164 ˚C (dec). IR (KBr) cm^{-1}: 3583(b), 3073(w), 2953(s), 2865(w), 2837(m), 1604(w), 1544(m), 1511(m), 1478(s), 1391(m), 1308(s), 1237(s), 1182(m), 1018(s), 936(m), 821(m), 749(s). Anal.Calcd (%) for $C_{92}H_{116}O_{32}Dy_4$ (2369.53): C, 46.35; H, 4.90. Found: C, 46.27; H, 4.85.

Compound **3.3**: LH (0.150 g, 0.527 mmol), PivH (0.053 g, 0.527 mmol), $HoCl_3.6H_2O$ (0.200 g, 0.527 mmol), Et_3N (0.29 mL, 2.108 mmol). Yield: 0.320 g, 62.75% (based on Ho). Mp: 164 ˚C (dec). IR (KBr) cm^{-1}: 3583(b), 3073(w), 2953(s), 2865(w), 2832(m), 1599(w), 1550(m), 1506(m), 1478(s), 1396(m), 1308(s), 1232(s), 1182(m), 1018(s), 941(m), 821(m), 755(s). Anal.Calcd (%) for $C_{92}H_{116}O_{32}Ho_4$ (2393.56):C, 46.16; H, 4.88. Found: C, 46.05; H, 4.85.

Compound **3.4**: LH (0.1 g, 0.369 mmol), LH_3' (0.062g, 0.369 mmol), $GdCl_3.6H_2O$ (0.137 g, 0.369 mmol), Et_3N (0.20 mL, 1.476 mmol). Yield: 0.256 g, 60% (based on Gd). Mp: 162 ˚C (dec). IR (KBr) cm-1: 3599(b), 3075(w), 2995(s), 2840(w), 1668(s), 1609(s), 1561(s), 1515(m), 1486(s), 1396(m), 1237(s), 1177(m), 1023(s), 947(m), 892(m), 760(s). Anal. Calcd (%) for $C_{98}H_{106}N_4O_{26}Gd_2$(2070.36): C, 58.12; H, 4.67. Found: C, 58.05; H, 4.85.

Compound **3.5**: LH (0.1g, 0.369 mmpl), LH_3' (0.062g, 0.369 mmol), $DyCl_3.6H_2O$ (0.139 g, 0.369 mmol), Et_3N (0.20 mL, 1.476 mmol). Yield: 0.286 g, 64% (based on Dy). Mp: 173 ˚C (dec). IR (KBr) cm^{-1}: 3600(b), 3073(w), 2997(s), 2838(w), 1665(s), 1605(s), 1550(s), 1512(m), 1484(s), 1380(m), 1243(s), 1161(m), 1019(s), 945(m), 895(m), 750(s). Anal. Calcd (%) for $C_{98}H_{106}N_4O_{26}Dy_2$ (2080.86): C, 56.56; H, 5.13. Found: C, 56.05; H, 5.15.

Compound **3.6**: LH (0.1g, 0.369 mmpl), LH_3' (0.062g, 0.369 mmol), $HoCl_3.6H_2O$ (0.140 g, 0.369 mmol), Et_3N (0.20 mL, 1.476 mmol). Yield: 0.290 g, 65% (based on Ho). Mp: 164 ˚C (dec). IR (KBr) cm^{-1}: 3597(b), 3068(w), 2925(s), 2838(w), 1660(s), 1609(s), 1594(s), 1506(m), 1479(s), 1391(m), 1249(s), 1161(m), 1013(s), 949(m), 898(m), 756(s). Anal. Calcd (%) for $C_{98}H_{106}N_4O_{26}Ho_2$ (2085.72):C, 56.43; H, 5.12. Found: C, 56.05; H, 5.15.

3.3 Results and discussion

The clusters (**3.1-3.6**) were synthesized by using ligand controlled hydrolytic approach. Reaction between β-diketone (LH), pivH or LH_3' and the corresponding hydrated lanthanum chloride in methanol afforded neutral tetranuclear $[Ln_4(\mu_3\text{-}OH)_4(L)_4(\mu_2\text{-}piv)_4(MeOH)_4]$ (Ln = Gd **3.1**, Dy **3.2** and Ho **3.3**) and dinuclear $[Ln_2(L)_4(\mu_2\text{-}LH_2')_2]4CH_3CN/DMF$ (Ln = Gd **3.4**, Dy **3.5** and Ho **3.6**) lanthanide(III) complexes in good yields (60-65%). IR (KBr pellets) spectra of all the complexes show a broad band at 3000-3600 cm^{-1} confirming the presence of hydroxyl groups in the structure. A lack of characteristic band at 1675 or 1720 cm^{-1} (in **3.1**, **3.2** and **3.3**) indicates the deprotonation of carboxylic acid[10d] and a characteristic peak at 1599-1610 cm^{-1} corresponds to C-O stretching in coordinated β-diketone.

3.3.1 Structural Description for 3.1-3.3:

Single crystal X-ray diffraction analysis (collected at 100 K) reveal structurally identical nature of complexes **3.1-3.3** which crystallize in monoclinic space group *P2/n* with Z = 4. Due to their structural similarity, **3.2** is chosen as a prototype for discussion. Molecular structure of **3.2** $[Dy_4(\mu_3\text{-}OH)_4(L)_4(\mu_2\text{-}piv)_4(MeOH)_4]$ is depicted in figure 3.1(a). Single crystal X-ray diffraction reveals that, it is a tetrameric cluster and all the four Dy(III) ions occupy the alternate corners of a distorted cube. The asymmetric unit consists of two crystallographically distinct Dy_2-half units and hence one unit of these is considered for detailed discussion. As far as the constituents of this unit are concerned, it consists of a hydroxo bridged dysprosium dimer coordinated by two β-diketones, two pivallic acids and two methanol molecules. Bridging oxygen atoms O_{10} and O_{11} of μ_3-hydroxy groups generate the full cluster (distorted cubane motif). Overall the cubane core is surrounded by

four β-diketonates and four pivalates. Each β-diketonate binds to the metal in a chelating mode and further the cubane core is held together by four pivalate ligands. Each pivalate ligand binds to the metal in a *syn-syn* bridiging mode μ_2-η^1:η^1 [Figure 3.1(b)]. Each Dy(III) ion is octa-coordinated with 3 μ_3-OH anions, 2 oxygen atoms from β-diketonate ligand, 2 oxygen atoms from pivalic acids and finally the coordination is completed by a methanol molecule.

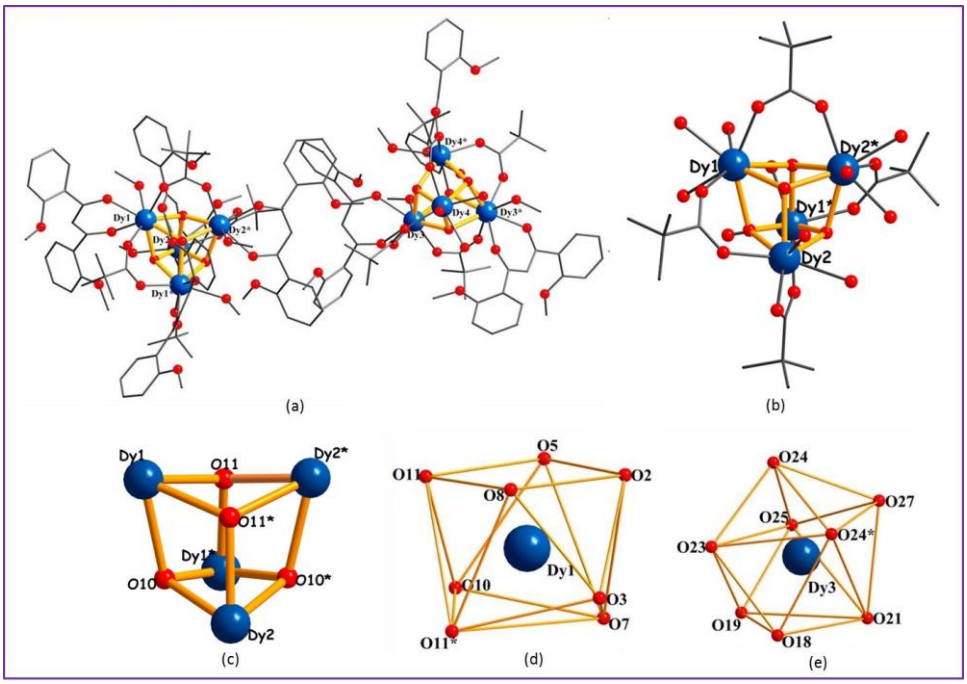

Figure 3.1 (a) Molecular structure of compound **3.2** (b) core of the cluster showing bridging mode of pivalate ligand (c) represents core of the cluster (d) and (e) represents coordination geometry around Dy(III) SAP and TDD.

Systematic analysis of the coordination geometries around the metal atoms using SHAPE 2.1[24] reveal that the octa-coordinated metal ions Dy1(III) and Dy2(III) adopt distorted square antiprismatic geometry with *pseudo* D_{4d} symmetry [Figure 3.1(d)]. Though a similar bonding perspective is observed in the second Dy2-half unit [Dy3(III) and Dy4(III)], but the Dy(III) ions in this unit exhibit triangular dodecahedron geometry with D_{2d} symmetry (Figure 3.1(e)) which rationalizes the presence of two crystallographically distinct Dy2-half units in the unit cell of all the complexes (**3.1**-**3.3**). The complete results of geometric analysis are described in the supporting information (Table 3.2). The Dy-O(diketone) and Dy-O(piv) bond lengths are in the range of 2.35-2.37 (3) Å and 2.29-2.33

(3) Å respectively. Four symmetry-related μ_3-OH^- groups aggregate four Dy(III) ions into a distorted cubic tetranuclear cluster with intra cluster metal-metal separation distances in the range of 3.74-3.83 (7) Å and Dy-O(μ_3-OH) distances are in the range of 2.35-2.38 (3) Å. The Dy-O-Dy angles are in the range of 104.54-108.51 (12)° which are close to tetrahedral geometry and the O-Dy-O angles are in the range of 69.22-144.29 (12)° due to geometrical strain. All the bond lengths and bond angles are consistent with the previously reported Ln-cubanes.[10]

3.3.2 Structural Description for 3.4-3.6:

Single crystal X-ray diffraction studies reveals that compounds **3.4-3.6** are dimeric lanthanide complexes and are structurally analogous to each other. Owing to their structural similarity, dysprosium analogue **3.5** is chosen for discussion [Figure 3.2(a)].

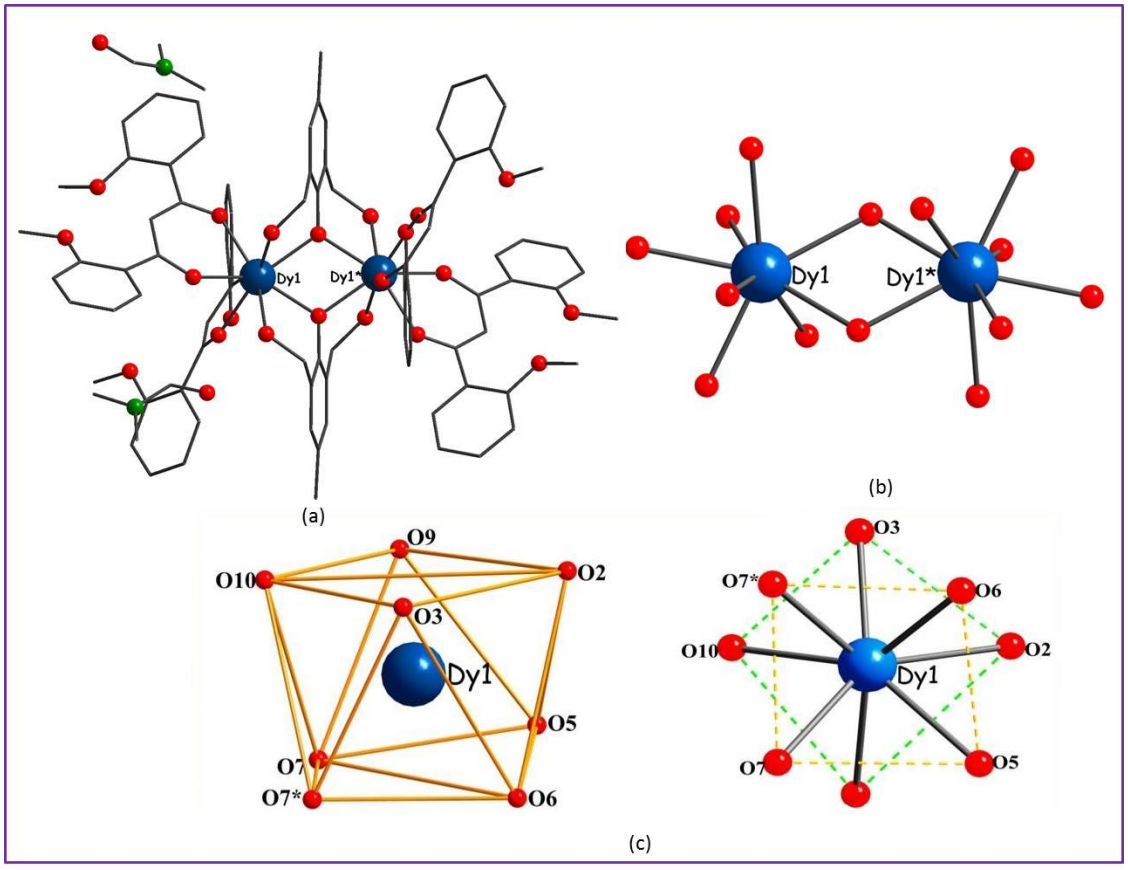

Figure 3.2. (a) Molecular structure of compound **3.5** (b) represents core of the cluster (c) coordination geometry around of Dy(III) ion.

All the three complexes crystallized in a triclinic, *P-1* space group. Only half of the molecule is presented in asymmetric unit and the remaining fragment of the molecule is generated by symmetry operation on O7 (inversion center). In the asymmetric unit, Dy(III) ion is surrounded by eight oxygen donors which are derived from two chelating β-diketones, two alkoxy oxygen atoms of LH_3 and two phenoxy oxygen LH_3'. The Dy-$O_{(diketone)}$, Dy-$O_{(alkoxyLH3)}$ and Dy-$O_{(phenoxyLH3)}$ bond lengths are of the order of 2.301-2.343 (2) Å, 2.313-2.438 (2) Å and 2.313-2.438 (2) Å respectively. The two Dy(III) ions in **3.5** are exclusively bridged by the phenoxy oxygen atom of LH_3 and the bond angle is found to be ∠Dy1-O6-Dy1* = 113.81°. The octa-coordinated Dy(III) ion exists in distorted square antiprism (with skew angle 39.5 which is slightly deviated from ideal value 45 ° for SAP) geometry with *pseudo* D_{4d} symmetry which was confirmed by CShM software[24] [Figure 3.2(c), Table 3.2]. The two dysprosium centers are separated by an intramolecular distance of 3.882 (3) Å. Selected bond distances and bond angles for all the compounds are given in the supporting information (Table 3.3-3.4).

3.4 Magnetic properties

3.4.1 Static Magnetic Susceptibility:

Variable temperature dc magnetic susceptibility data was collected for all the complexes at 1 kOe applied field from 300 to 2 K. As shown in Figure 3(a) the observed room temperature $\chi_M T$ values of 31.41 (**3.1**), 55.12 (**3.2**) and 52.60 cm3 K mol-1 (**3.3**) are slightly lower than the expected values of 31.5 cm^3 K mol^{-1} (g = 2.0; S = 7/2; L = 0, $^8S_{7/2}$ for Gd), 56.67 cm^3 K mol^{-1} (g = 4/3; S = 5/2; L = 5; $^6H_{15/2}$ for Dy), 56.25 cm^3 K mol^{-1} (g = 5/4; S = 2; L = 6; $^5I_8$ for Ho) for magnetically dilute Gd(III), Dy(III) and Ho (III) ions respectively. The $\chi_M T$ value for **3.1** remains constant from room temperature to T = 45 K. Below which it steadily decreases before precipitously falling below 35 K to a value of 14.89 cm^3 K mol^{-1} at 2.0 K. The $\chi_M T$ value for **3.3** gradually decreases from room temperature to T = 55 K, likely due to the depopulation of m_J levels. The $\chi_M T$ value drops rapidly below 45 K and reaches a value of 15.93 cm^3 K mol^{-1}(for **3.3**). On contrary, for **3.2**, the $\chi_M T$ value remains constant in the entire temperature range from room temperature to 42 K, upon decreasing temperature further, $\chi_M T$ value of **3.2** decreased rapidly and reaches a value of 43.2 cm^3 K mol^{-1} at 2 K. The low temperature decrease

in $\chi_M T$ value of all the three complexes is likely due to multiple factors such as magnetic anisotropy intra and intermolecular antiferromagnetic exchange interactions and intermolecular dipolar exchange interactions. Modelling the magnetic data of anisotropic metal complexes **3.2** and **3.3** is complicated by the first order orbital angular momentum and spin-orbit coupling effect. However, **3.1** serves as a surrogate marker to better understand the nature of coupling between the lanthanide ions (in **3.2** and **3.3**), if not quantitatively, at least qualitatively, as the electronic configuration of Gd(III) does not possess orbital angular momentum. Based on the crystal structure and cautious about the over parameterization, we have employed only one J value to model the magnetic data of **3.1**. This J represents the exchange interaction between the nearest neighbour in **3.1** [see inset of Figure 3.3(a)]. In order to extract the spin Hamiltonian parameters for **3.1** we employed the following Heisenberg Dirac Van-Vleck (HDVV) Hamiltonian, and the magnetic susceptibility data were fitted by matrix diagonalization using PHI software.[25]

$$\mathbf{H} = -2\mathbf{J_1}(\mathbf{S_{Gd_1}}.\mathbf{S_{Gd_{1a}}} + \mathbf{S_{Gd_1}}.+\mathbf{S_{Gd_1}}.\mathbf{S_{Gd_{2a}}} + \mathbf{S_{Gd_{1a}}}.\mathbf{S_{Gd_2}} + \mathbf{S_{Gd_{1a}}}.\mathbf{S_{Gd_{2a}}} + \mathbf{S_{Gd_2}}.\mathbf{S_{Gd_{2a}}}) + \mathbf{g}\,\boldsymbol{\mu_B} \quad (3.1)$$

The experimental data of **3.1** is very well reproduced with the following parameters J_1 = -0.055 cm^{-1} and g = 2.01 and the parameters extracted from fitting are consistent with literature reports.[26] Significantly small J_1 value is likely due to the large intra molecular distance between the two Gd(III) with buried valence 4f orbitals.

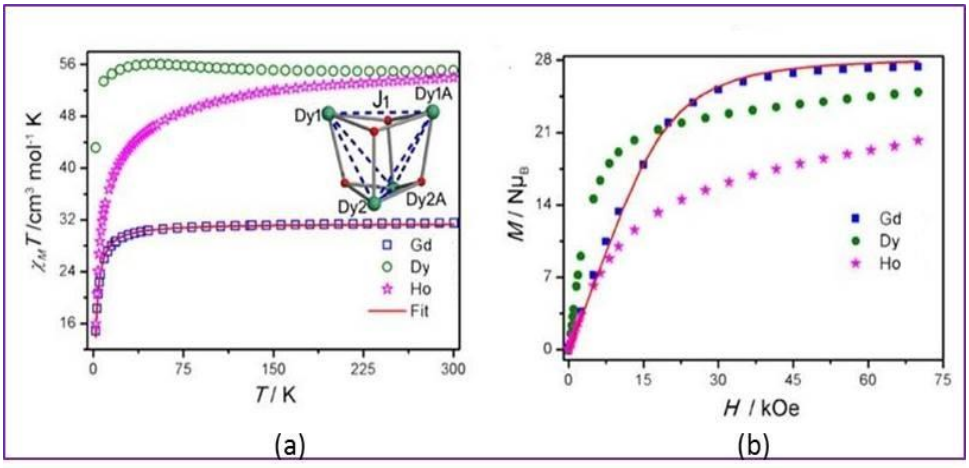

Figure 3.3 (a) Temperature dependence of the product of magnetic susceptibility and temperature (χ_MT) for **3.1**-**3.3** (b) field dependence of magnetization for **3.1**-**3.3**.

Isothermal magnetization was performed on polycrystalline sample of complexes **3.1**-**3.3** at 2.0K [Figure 3.3(b)]. Upon increasing the magnetic field, the magnetic moment sharply increases in all three complexes (**3.1**-**3.3**) and the magnetic moment of complexes **3.1**-**3.3** tend to saturate around 26.12, 25.14 and 19.76 NμB respectively at 70 kOe. For complex **3.1**, the saturation value is slightly lower than the expected saturation value (28 NμB). However, the magnetization plot of **3.1** is in good agreement with the simulated data using the parameters extracted from $\chi_M T$(T) fit of **3.1**. This exemplifies the reliability of the parameters extracted by modelling the magnetic data of **3.1**. In contrast for **3.2** and **3.3**, the saturation value is significantly lower than the expected value (40 NμB). This is in line with the literature precedents and is due to the presence of anisotropy associated with complexes **3.2** and **3.3**. It is further supported by the non-super imposable nature of reduced magnetization curves.

The $\chi_M T$ product for the Ln_2 complexes [Ln = Gd (**3.4**), Dy (**3.5**) and Ho (**3.6**)] at 300 K have values of 17.41, 28.62, and 27.65 cm^3 K mol^{-1} respectively. These values are in excellent agreement with the expected values for two non-interacting lanthanide ions, 7.9 cm^3 K mol^{-1} for one uncoupled Gd(III) ion ($^8S_{7/2}$, S = 7/2, L = 0, g = 2.0); 14.16 cm^3 K mol^{-1} for an uncoupled Dy(III) ion [$^6H_{15/2}$, S = 5/2, L = 5, J=15/2and g_J= 4/3); 14 cm^3 K mol^{-1} and the expected value for one isolated Ho (III) ion ($^5I_8$, S = 2, L = 6, J = 8 and g_J = 5/4)]. As temperature decreases, the $\chi_M T$ product for **3.4** remains constant until a sharp decrease is observed below 10 K. This phenomenon indicates that simple paramagnetic nature is witnessed in **3.4** from 300 K to 10 K and the observed $\chi_M T$ product is the sum of two isolated Gd(III) ions. The experimental magnetic data was fitted using the parameters J = -0.048 cm^{-1} and g = 1.99. The data clearly indicates the presence of weak antiferromagnetic exchange interaction and the extracted parameters are consistent with other reported complexes.[27] For **3.5** and **3.6** as temperature decreases, the $\chi_M T$ product slightly decreases as expected due to the depopulation of m_j sublevels of the ground J state. Below 25 K, the $\chi_M T$ product slightly rises for **3.6** indicating the onset of weak ferromagnetic coupling between two Ho(III) ions. For **3.5** the increase of $\chi_M T$ product below 25 K is more pronounced indicating stronger ferromagnetic coupling between two Dy(III) ions. The rapid rise observed for magnetization at 2 K for both **3.5** and **3.6** [Figure 3.4(a)] as a function of field confirms the population of a non-zero ground state.

The field dependence of magnetization is shown in Figure 3.4(b), the magnetization at 2K slowly increases and upon increasing the magnetic field, the magnetic moment sharply increases in all three complexes (**3.4**-**3.6**) and the magnetic moment of complexes tend to saturate at 50 kOe. For complex **3.4** the value of magnetic moment at 2.0 K is close to the expected value for an isotropic metal complex. The dc susceptibility data $\chi_M T(T)$ and $M(H)$ of **3.4** were fitted simultaneously using the HDVV Hamiltonian ($-2J_1(S_1.S_2) + g\mu_B S.H$).[25] The extracted parameters are in well agreement with the literature reports. While for complex **3.5** and **3.6** the saturation value is significantly lower than the expected value and the non-superimposition of reduced magnetization curves clearly suggesting the presence of anisotropy in these complexes.

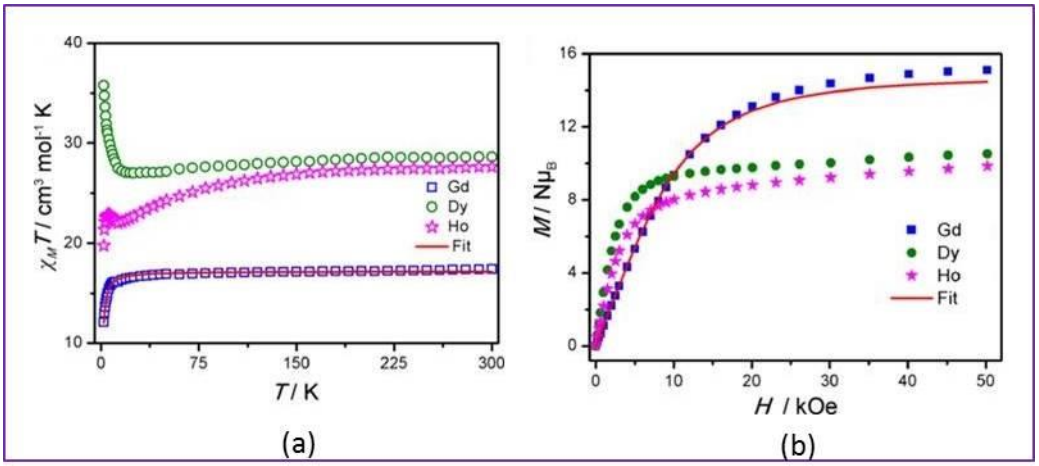

Figure 3.4. (a) Temperature dependence of the product of magnetic susceptibility and temperature ($\chi_M T$) for **3.4**-**3.6**. (b) field dependence of magnetization for **3.4**-**3.6**.

3.4.2 Ac magnetic susceptibility studies:

In order to check the magnetization relaxation dynamics, ac measurements were performed on selected polycrystalline samples complexes **3.2** and **3.5** with an applied oscillating field of 3.5 Oe with and without external magnetic field. Complex **3.2**, evidently shows frequency dependent out-of-phase susceptibility signals without any clear maxima (Figure **3.5**). This hampers us in extracting the effective energy barrier for the magnetization reversal of orientation. Evidently, Figure 3.5(a) shows that more than one relaxation is operational. This could be likely due to the distinct geometry shown by the Dy(III) in asymmetric unit of **3.2**. However, it is reported in literature that even a

mononuclear Dy(III) complexes such as $[ZnDy(L^{-})_2]^{3+}$ and [Dy(DOTA)] show more than one relaxation process such as Raman and Direct, apart from Orbach process.[28] In order to understand the relaxation dynamics completely, we need to replace one of the geometrically different Dy(III) with diamagnetic ion. However, attempts to isolate such isostructural complexes of **3.2** were not successful. Often the fast quantum tunneling of magnetization (QTM) is suppressed by applying the external bias magnetic field. However, there is no significant change observed in χ_M'' signals measured at 2 kOe compared to the zero bias field measurement. This may be due to the fast quantum tunneling relaxation of the magnetization (QTM) promoted by non-suitable ligand field environment and/or intermolecular dipolar interactions.

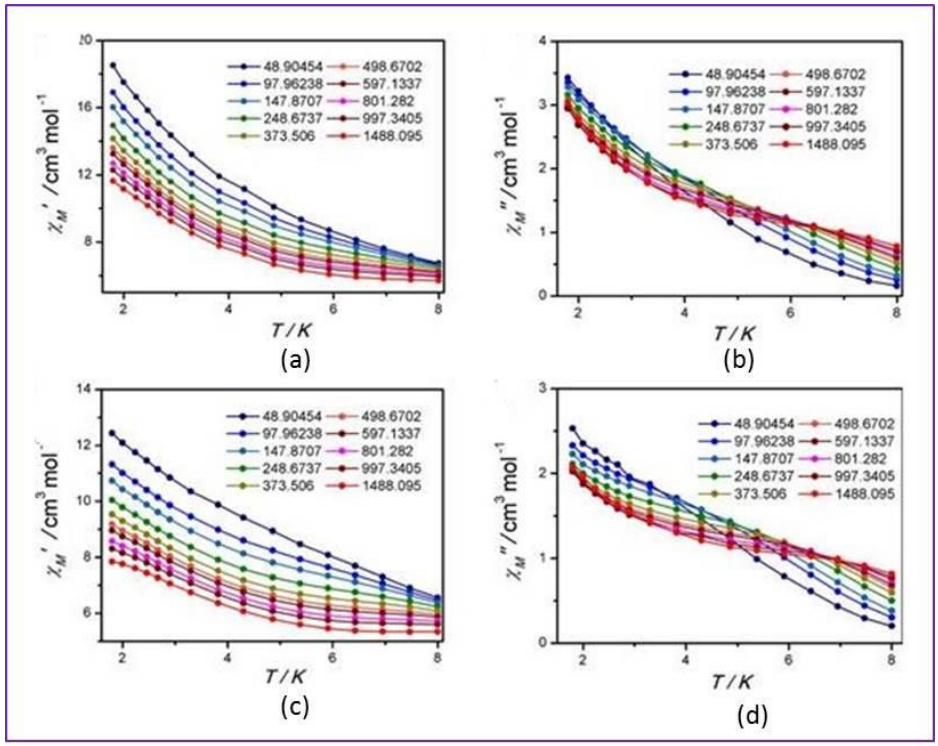

Figure 3.5. Alternating current magnetic susceptibility measurement performed on polycrystalline samples of **3.2** showing the frequency dependent in-phase (χ_M') and out-of-phase susceptibility signals (χ_M'') in absence of external magnetic field [(a) and (b)] or presence of external magnetic field of 2 kOe [(c) and (d)].

A complete survey on Dy cubanes revealed that better slow relaxations were observed in larger Dy–O–Dy angles in the range of 102.5 to 109.3°. In complex **3.2**, the Dy–O–Dy bond angles are between 104.54 to 108.51° which are very close to the reported cubane

SMMs except for the one that had bond angles of 99.20 to 115° which has the highest energy barrier reported in Ln cubanes (Table 3.5). In all these cases, geometry around the metal ions is either square antiprismatic or triangular dodecahedron but in present case the geometry around Dy(III) ions is different in two symmetric halves with one Dy(III) ion existing in square antiprism while the other Dy(III) ion exhibits triangular dodecahedron geometry.

On contrary to **3.2**, dinuclear complex **3.5** shows frequency dependent out-of-phase ac magnetic susceptibility signals at zero applied magnetic field (Figure 3.6). Evidently it shows more than one relaxation process, a slow relaxation process at higher temperature (4-11 K) and a fast relaxation such as QTM below 4 K. The observation of frequency dependent out-of-phase-susceptibility signals is characteristic signature of a single molecule magnet. In order to understand the influence of exchange interaction in **3.5**, we attempted to replace one of the Dy(III) ion with diamagnetic ion. Unfortunately, we were unable to isolate the complex of interest. This is likely due to the fact that one Dy(III) ion in **3.5** is related by inversion center to other. Hence 100 % replacement of one Dy(III) by a diamagnetic center is a chemically challenging task. The Dy(III) ions are octa-coordinated by eight oxygen donors in a sandwich-like environment with four oxygen donors above and four oxygen donors below the plane of the metal. This environment should provide strong axial anisotropy for an oblate ion like Dy(III) as reported by Long and co-workers.[29] An axial "sandwich" – type crystal field stabilizes the highest m_j level of the Kramers state resulting in slow magnetization of relaxation in **3.5** in absence of external bias magnetic field. In a recent report, Long and co-worker have pointed out the importance of enhancing exchange interaction to quench the QTM.[13] In the same vein, Murray and co-workers[30] and Shanmugam and co-workers[28a] have pointed out the importance of 3d metal ions in the vicinity of lanthanide coordination sphere to increase the super exchange interaction, thus effectively quenching fast relaxation processes such as QTM to a maximum extent in these complexes. Square antiprism geometry is a suitable ligand field for an oblate Dy(III) ion which has been experimentally proven and computationally rationalized in literature.[16,17] It has been noticed that the square antiprism geometry is observed for Dy(III) ions in both the complexes **3.2** and **3.5**. In complex **3.2**, however, the extent of deviation (distortion) from square antiprism geometry is larger (CShM value is 1.474) than in **3.5** (CShM value is 0.745).

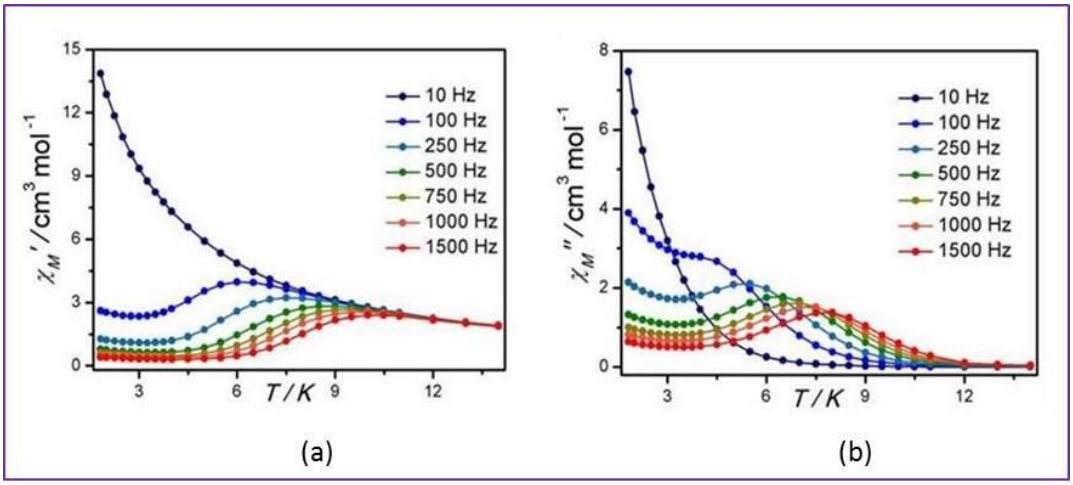

Figure 3.6. Ac magnetic susceptibility data for **3.5** at frequencies between 9 and 1500 Hz. (a) in-phase (χ_M') signal vs T and (b) out of phase signal (χ_M'') vs T

Further, as it is witnessed from the crystal structure that another crytollographically distinct Dy(III) in **3.2** exhibit further reduction in geometry [i.e. triangular dodecahedron geometry (TDD)]. Likely the combination of weak exchange interaction and distortion from ideal square antiprism geometry lead to significant transverse component which is likely to triggers the fast relaxation such as QTM in **3.2**. This is firmly supported by the fact that absence of frequency dependent out-of-phase susceptibility signals, either in the absence or presence of external magnetic field. On contrary, a favorable combination of suitable geometry and presence of exchange interaction facilitate to quench fast relaxation (such as QTM) to some extent which ultimately leads to slow relaxation of magnetization even in the absence of external magnetic field.

As pointed out earlier, the two crystallographically distinct Dy(III) ions in asymmetric unit of **3.2** possess different geometry (SAP and TDD geometry). To understand the influence of geometry on the g_z orientation of these Dy(III) ions (assuming mj of ±15/2 Krammers state stabilized) in **3.2**, electrostatic model developed by Chilton and Soncini was employed. Although there is a slight deviation in g_z orientation predicted from more accurate ab initio calculations, the deviation in g_z calculated by electrostatic model compared to the ab initio predicted orientation deviates marginally which is very well exemplified in the literature. The g_z orientation predicted for all the Dy(III) ion in **3.2**

using the electrostatic model is presented in Figure 3.7. The ground state Krammers g_z orientation of Dy2 ion deviates by 72° from g_z orientation of Dy1 ion in **3.2**. Further it is also noticed that g_z orientation of Dy1 (Dy2) deviates from its symmetrically related atom Dy1A (Dy2A) by 45° (48.5°). The significant deviation of g_z observed between the symmetry related Dy(III) ions (i.e., Dy1 and Dy1A & Dy2 and Dy2A) illustrate that charge density on the ligated atom distributed all around the Dy(III) ion. Further reduction in geometry in Dy2 (TDD) center compared to Dy1 (SAP) in **3.2** is likely the origin of larger deviation in g_z orientation in these two centers. The non-collinear orientation of g_z axis of each Dy(III) centers in **3.2** is likely to trigger the magnetization relaxation via the under-barrier mechanism in ground state itself rather than thermally assisted Orbach process. To understand further the role of distortion and g_z orientation of Dy(III) ion in **3.2**, g_z orientation of a Dy4 cubane complex with the molecular formula $[Dy_4(L)_4(Piv)_4]$ reported elsewhere by Chandrasekhar and co-workers was compared.[10d] Using the electrostatic model, g_z orientation for all the four Dy(III) ions in this complex were computed and it is shown in Figure 3.7B. This figure clarifies that g_z orientation of all the Dy(III) ions is in the same direction which are near collinear to each other (the average g_z deviation observed is 3-5°). This suggests that random orientation of g_z axis in **3.2** reduces the overall magnetic anisotropy resulting in faster relaxation in **3.2** compared to $[Dy_4(L)_4(Piv)_4]$.

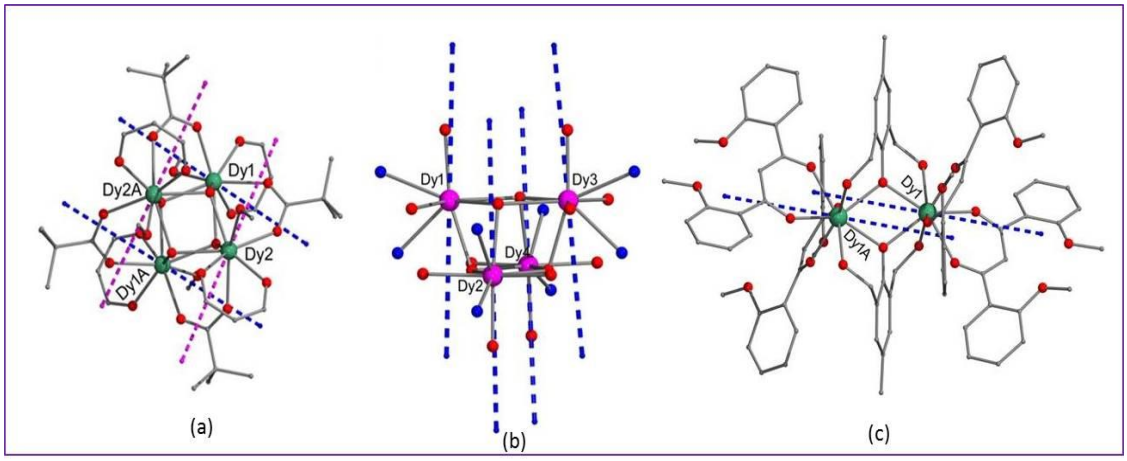

Figue 3.7. g_{zz} orientation observed in Dy(III) ion in both complexes **3.2**(a), $[Dy_4(L)_4(Piv)_4]$(b) and **3.5**(c) predicted using the electrostatic model.

In contrast to **3.2**, g_z orientation of the ground state (±15/2) Kramers doublet of Dy(III) ions in **3.5**, collinear with each other. The g_z anisotropic tensor of both the Dy(III) ions

orient towards the Dy…..Dy axis, which does not pass through Dy….Dy axis. The favorable ligand field around Dy(III) ions and the collinear arrangement of easy axis (g_z) on both Dy(III) ion along with the presence of ferromagnetic exchange interaction between the Dy(III) ion in **5** favors the relaxation of magnetization via other excited Krammers doublets resulting in thermally assisted slow relaxation of magnetization (Orbach process) predominantly rather an under barrier mechanism.

Arrhenius plot was constructed for Complex **3.5**, considering the maxima in χ_M'' plot as a function of temperature. The barrier for the reorientation of magnetization is estimated from Arrhenius plot (Figure 3.8) estimated to be U_{eff} = 32.52 K with an exponential factor τ_o = 1.987 × 10^{-6} s. It is a new example of a Dy2 SMM.

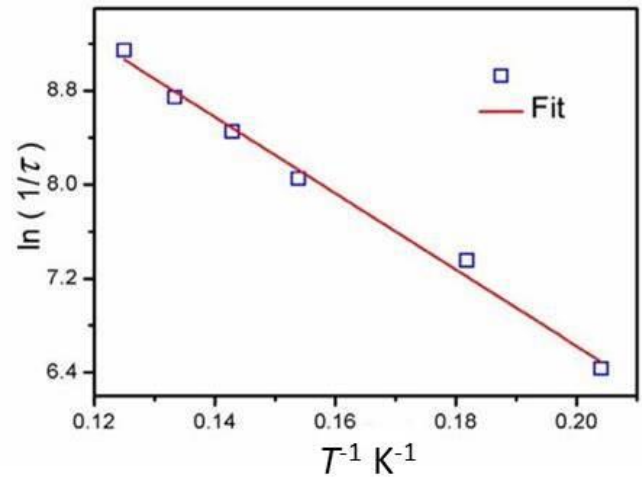

Figure 3.8. Arrhenius plot for complex **3.5**.

3.4.3 Estimation of MCE efficiency:

In order to understand the MCE efficiency of the isotropic metal complexes **3.1** and **3.4**, detailed isothermal field dependent magnetization measurements were performed on the polycrystalline samples From 2.0 to 15 K. The change in magnetic entropy (-ΔS_m) and change in adiabatic temperature (ΔT_{ad}) are the two salient thermodynamic parameters of magneto-caloric effect (MCE). Using the Maxwell's thermodynamic relation and from the detailed magnetization measurements of complexes, the change in magnetic entropy observed for these complexes were estimated.

$$-\Delta S_m(T,H) = \int_{H_i}^{H_f} \left[\frac{\partial M(T,H)}{\partial T}\right]_H dH \qquad 3.2$$

Where, H_i and H_f are the initial and final applied magnetic field, respectively.

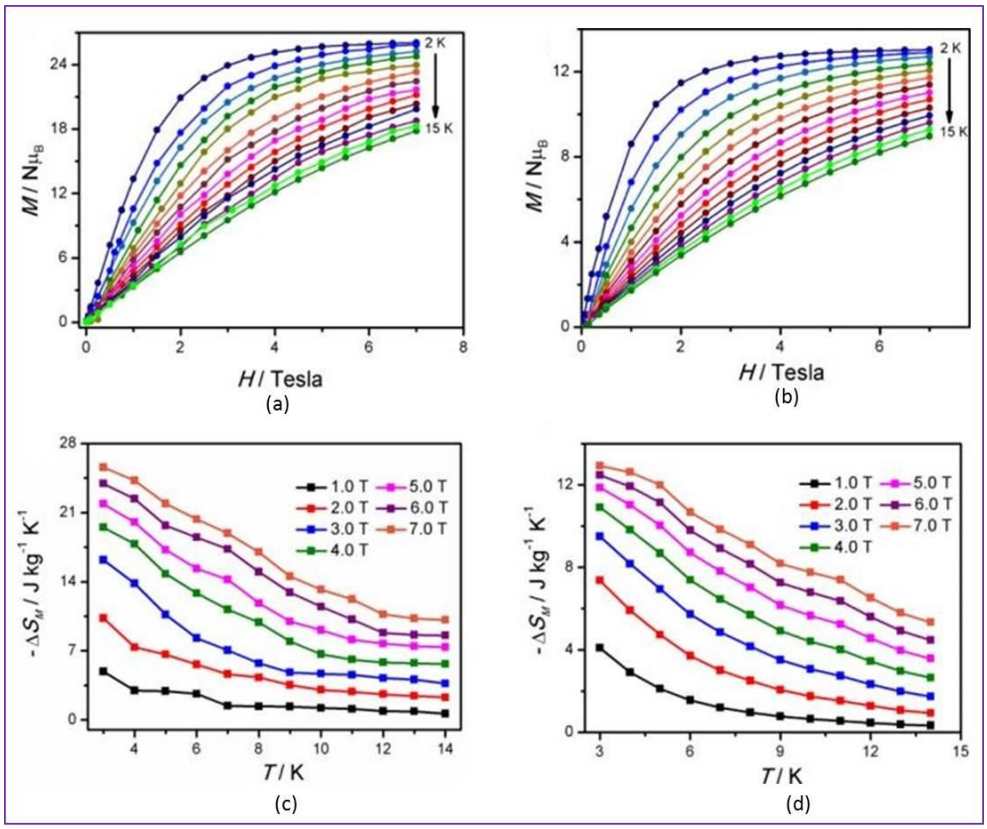

Figure 3.9. Detailed isothermal field dependent magnetization measurement performed on polycrystalline sample of **3.1** (a) and **3.4** (b) measured from 0-7 Tesla at the indicated temperatures. The magnetic entropy change ($-\Delta S_m$) for the complex **3.1** (c) and **3.4** (d) in the indicated magnetic field from 2-15 K temperature range.

The $-\Delta S_m$ value of 25.57 J Kg^{-1} K^{-1} at 3.0 K for ΔH = (0-7) Tesla [Figure 3.9(c)] for **3.1** is extracted from magnetization measurement. The extracted $-\Delta S_m$ value is comparable with other related structures reported in the literature.[26a] However, the observed $-\Delta S_m$ value for **3.1** is relatively low compared to a coordination polymeric chain of tetrameric Gd(III) complex.[31] This is due to the less mass density ratio observed in **3.1** compared to the polymeric chain. In fact importance of mass density ratio to reveal the better magnetic coolant material was elegantly reported by Evangelisti and co-workers and others recently.[32] Theoretically, the calculated full magnetic entropy content of Rln(8) = 17.3 J

mol^{-1} K^{-1} = 29.28 J Kg^{-1} K^{-1} per mole of Gd(III) involved, as it is expected from Rln(2S+1) and S=7/2 (where R is the universal gas constant).

Similar to **3.1**, in complex **3.4**, change in magnetic entropy is estimated using Maxwell's equation mentioned above with the value of 12.93 J Kg^{-1} K^{-1}[Figure 3.9(d)]. This value is slightly lower than the theoretically expected value of 16.71 J Kg^{-1} K^{-1} [Rln(8) and S=7/2]. This is likely due to the presence of exchange interaction between the molecules which lifts the degeneracy of the other energy level which prevents the easy polarization of the spin. Also, even in isotropic metal complexes like **3.1** and **3.4**, magnetic anisotropy originated due to the ligand field around the Gd(III).[33] The existence of magnetic anisotropy does not allow the easy polarization of spin orientation resulting in reduced magnetic coolant efficiency. The observed $-\Delta S_m$ value is comparable with the other related structures and some of the isotropic 3d-4f clusters reported in the literature.[34]

However, for both complexes (**3.1** and **3.4**) the observed $-\Delta S_m$ value is lower than the acetate bridged Gd(III) dimer,[32b] Co-Gd grid complexes reported by Winpenny and co-workers an extended three dimension GdF_3 complexes.[35] As pointed out earlier, the magnetic entropy is directly proportional to the overall spin ground state associated with the cluster. However there are clusters with large ground state registered with low $-\Delta S_m$ value compared to the complexes **3.1** and **3.4**.[36]

3.5 Conclusions

A family of tetranuclear lanthanide complexes were isolated and structurally characterized by single crystal X-ray diffraction with a general molecular formula of $[Ln_4(\mu_3\text{-}OH)_4(L)_4(\mu_2\text{-piv})_4(MeOH)_4]$ (Ln = Gd (**3.1**), Dy (**3.2**) and Ho (**3.3**) using substituted β-diketonate ligands. Using bulky coligand [2 6-Bis(hydroxymethyl)-p-cresol] in place of pivalic acid led to the isolation of a new series of dimeric complexes with the molecular formula of $[Ln_2(L)_4(\mu_2\text{-}LH_2')_2]$.4DMF/$CH_3CN$ (Ln = Gd (**3.4**), Dy (**3.5**) and Ho (**3.6**). Direct current magnetic susceptibility measurements were performed on polycrystalline sample of **3.1**-**3.6**. Complexes **3.1** and **3.4** shows existence of intramolecular antiferromagnetic coupling between Gd(III) ions which is strongly corroborated by the parameters extracted from magnetic data fit. On contrary, $\chi_M T(T)$ data unambiguously shows the existence of ferromagnetic coupling between Dy(III) ions in **3.5**. Magnetization relaxation dynamics was performed on selected complexes **3.2** and **3.5**. The tetrameric

complex **3.2** shows frequency dependent out-of-phase susceptibility signal without clearly resolved maxima. This is in contrast with the observation of complex **3.5** where zero field χ_M'' signals were observed with an effective energy barrier of 32.52 K and a pre-exponential factor (τ_o) = 1.987 × 10^{-6} s. The distinct magnetization relaxation behavior in **3.5** (compared to **3.2**) is correlated to the suitable ligand field and ideal square antiprism geometry around Dy(III), collinear arrangement of g_z orientation and ferromagnetic exchange coupling in **3.5** which quenches the under- barrier mechanism to some extent facilitating the Orbach process. Lack of such factors in complex **3.2** favors the under-barrier mechanism. These studies presented here clearly emphasize the influence of ligand field on the magnetization relaxation dynamics. The isotropic metal complexes **3.1** and **3.4** shows the change in magnetic entropy (-ΔS_m) of 25.57 and 12.93 J Kg^{-1} K^{-1} respectively. This study reiterates the fact that magnetic density is a crucial factor to increase the -ΔS_m value to design better magnetic refrigerants.

Table 3.1 Crystallographic data and structure refinement for **3.1-3.3**

	3.1	**3.2**	**3.3**
Empirical formula	$C_{92}H_{116}O_{32}Gd_4$	$C_{92}H_{116}O_{32}Dy_4$	$C_{92}H_{116}O_{32}Ho_4$
Fw.g mol^{-1}	2362.85	2383.85	2393.57
Crystal system	Monoclinic	Monoclinic	Monoclinic
Space group	P2/n	P2/n	P2/n
a/Å	25.191(4)	25.136(5)	25.118(3)
b/Å	14.292(3)	14.190(3)	14.1850(14)
c/Å	27.482(5)	27.383(5)	27.365(3)
α (°)	90	90	90
β (°)	101.401(3)	101.308(10)	101.334(2)
γ(°)	90	90	90
v/Å	9699(3)	9577(3)	9560.0(17)
Z	4	4	4
ρ_c/Mg m^{-3}	1.618	1.653	1.663
μ/mm^{-1}	2.778	3.165	3.354
F(000)	4720	4752	4768
θ range(deg)	1.00 to 24.77	1.23 to 25.00	1.01 to 25.09
reflns collected	89512	90520	91105
Completeness to θ (%)	99.7	99.9	99.7
ind refln/R_{int}	16610/ 0.0550	16853/0.0391	16947/0.0996
GooF(F^2)	1.051	1.072	1.111
Final R indices (I>2σ(I))	R_1 = 0.0366, wR_2 = 0.0887	R_1 = 0.0360 wR_2 = 0.0849	R1 = 0.0588 wR_2 = 0.0783
R indices (all data)	R_1 = 0.0430 wR_2 = 0.0922	R1 = 0.0398 wR_2 = 0.0869	R1 = 0.0783 wR_2 = 0.1173

Table 3.1 Crystallographic data and structure refinement for **3.4-3.6**

	3.4	**3.5**	**3.6**
Empirical formula	C_{98} H_{106} N_4 O_{26} Gd_2	C_{98} H_{106} N_4 O_{26} Dy_2	C_{98} H_{106} N_4 O_{26} Ho_2
Fw.g mol^{-1}	2070.36	2080.87	2085.73
Crystal system	Triclinic	Triclinic	Triclinic
Space group	P-1	P-1	P-1
a/Å	13.868(6)	13.859(12)	13.8538(14)
b/Å	13.939(6)	13. 906(12)	13.8879(14)
c/Å	15.1576(6)	15.079(12)	15.0749(15)
α (°)	64.652(2)	64.692(10)	64.6480(10)
β (°)	64.498(2)	64.850(10)	64.9470(10)
γ(°)	85.951(2)	85.947(10)	85.963(2)
v/Å	2366.7(18)	2356.3(4)	2352.6(4)
Z	1	1	1
ρ_c/Mg m^{-3}	1.453	1. 466	1.472
μ/mm^{-1}	1.467	1.652	1.748
F(000)	1058	1062	1064
θ range(°)	2.149 to 27.612	1.63 to 25.06	1.64 to 25.02
reflections collected	140134	22854	22692
Completeness to θ (%)	99.9	99.5	99.4
independent reflections/R_{int}	10960/ 0.0424	8327/0.0335	8264/ 0.0266
GooF(F^2)	1.051	1.047	1.045
Final R indices (I>2σ(I))	R_1 = 0.0182 wR_2 = 0.0448	R_1 = 0.0303 wR_2 = 0.0741	R_1 = 0.0266 wR_2 = 0.0679
R indices (all data)	R_1 = 0.0206 wR_2 = 0.0457	R_1 = 0.0323 wR_2 = 0.0752	R1 = 0.0274 wR2 = 0.0684

Table 3.2. Summary of **SHAPE** analysis for compound **3.2(a)** and **3.5(b)**.

(a)

S. No.	Geometry	Cshm value for Dy1	Cshm value for Dy3
1	Octagon(D8h)	30.499	30.354
2	Heptagonal pyramid(C7v)	23.324	23.230
3	Hexagonal bipyrami(D6h)	16.074	15.755
4	Cube(Oh)	11.044	11.458
5	**Square antiprism(D4d)**	**1.474**	1.410
6	**Triangular dodecahedron(D2d)**	1.607	**1.281**
7	Johnson gyrobifastigium J26(D2d)	14.578	13.992
8	Johnson elongated triangular bipyramid J14(D3h)	29.407	29.560
9	Biaugmented trigonal prism J50(C2v)	2.055	2.202
10	Biaugmented trigonal prism(C2v)	1.540	1.670
11	Snub diphenoid J84(D2d)	3.868	3.807
12	Triakis tetrahedron(Td)	11.794	12.090
13	Elongated trigonal bipyramid(D3h)	24.511	24.452

(b)

S. No.	Geometry	Cshm value for Dy1
1	Octagon(D8h)	30.595
2	Heptagonal pyramid(C7v)	22.709
3	Hexagonal bipyrami(D6h)	15.856
4	Cube(Oh)	10.0183
5	Square antiprism(D4d)	**0.745**
6	Triangular dodecahedron(D2d)	1.889
7	Johnson gyrobifastigium J26(D2d)	14.116
8	Johnson elongated triangular bipyramid J14(D3h)	27.296
9	Biaugmented trigonal prism J50(C2v)	2.507
10	Biaugmented trigonal prism(C2v)	1.828
11	Snub diphenoid J84(D2d)	4.552
12	Triakis tetrahedron(Td)	10.990
13	Elongated trigonal bipyramid(D3h)	22.665

Table 3.3. Selected Bond distances (Å) and Bond angles (°) for **3.1-3.3**

	Ln = Gd (3.1)	**Ln = Dy (3.2)**	**Ln = Ho (3.3)**
Ln(1)-O(8)	2.321(3)	2.331(3)	2.278(6)
Ln(1)-O(5)	2.338(3)	2.315(3)	2.295(5)
Ln(1)-O(10)	2.382(.3)	2.371(3)	2.341(5)
Ln(1)-O(3)	2.395(3)	2.364(3)	2.363(6)
Ln(1)-O(2)	2.421(3)	2.351(3)	2.364(6)
Ln(1)-O(10)*	2.400(3)	2.367(3)	2.359(5)
Ln(1)-O(11)	2.416(3)	2.372(3)	2.380(5)
Ln(1)-O(7)	2.504(3)	2.489(3)	2.469(6)
Ln(2)-O(6)*	2.339(3)	2.311(3)	2.299(5)
Ln(2)-O(9)	2.360(3)	2.295(3)	2.323(5)
Ln(2)-O(14)	2.379(3)	2.367(3)	2.347(5)
Ln(2)-O(11)	2.391(3)	2.353(3)	2.361(5)
Ln(2)-O(15)	2.397(3)	2.379(3)	2.343(6)
Ln(2)-O(10)	2.411(3)	2.382(3)	2.371(5)
Ln(2)-O(11)*	2.397(3)	2.382(3)	2.355(5)
Ln(2)-O(12)	2.516(3)	2.479(3)	2.477(6)
O(8)-Ln(1)-O(5)	101.58(12)	102.17(12)	100.4(2)
O(8)-Ln(1)-O(10)	85.68(11)	83.33(11)	86.34(19)
O(5)-Ln(1)-O(10)	142.85(11)	144.11(12)	143.42(19)
O(8)-Ln(1)-O(3)	79.90(12)	84.37(12)	84.84(19)
O(8)-Ln(1)-O(10)*	144.28(11)	144.29(11)	144.59(19)
O(5)-Ln(1)-O(10)*	83.56(11)	86.15(11)	84.21(18)
O(10)-Ln(1)-O(10)*	70.87(12)	70.97(13)	70.92(2)
O(3)-Ln(1)-O(10)*	134.55(11)	107.92(11)	108.77(18)
O(8)-Ln(1)-O(11)	77.30(12)	78.36(11)	77.38(19)
O(5)-Ln(1)-O(11)	76.73(11)	77.14(11)	76.76(18)
O(10)-Ln(1)-O(11)	69.37(11)	69.22(11)	69.70(17)
O(6)*1-Ln(2)-O(10)	77.07(11)	77.00(11)	77.34(18)
O(9)-Ln(2)-O(10)	78.05(11)	77.50(12)	78.52(19)

O(14)-Ln(2)-O(10)	138.30(11)	137.73(11)	136.49(17)
O(11)-Ln(2)-O(10)	69.32(11)	69.38(11)	69.52(17)
O(15)-Ln(2)-O(10)	136.27(11)	134.85(11)	137.48(18)
O(11)*-Ln(2)-O(10)	69.60(11)	69.27(11)	69.72(17)
O(14)-Ln(2)-O(12)	76.37(11)	76.70(11)	72.57(19)
O(11)-Ln(2)-O(12)	107.97(11)	68.10(11)	109.01(18)
O(15)-Ln(2)-O(12)	71.77(11)	73.22(12)	75.95(19)
O(11)*-Ln(2)-O(12)	67.34(11)	108.41(11)	67.29(17)
O(10)-Ln(2)-O(12)	134.73(11)	135.29(11)	134.52(18)
Ln(1)-O(10)-Ln(2)	108.18(12)	107.58(12)	108.20(2)
Ln(1)-O(11)-Ln(2)	107.74(12)	108.51(12)	107.27(19)
Ln(1)*-O(10)-Ln(2)	107.71(12)	107.89(12)	107.90(2)
Ln(1)-O(10)-Ln(1)*	104.85(12)	104.82(12)	104.71(19)
Ln(1)-O(11)-Ln(2)*	107.64(12)	107.72(12)	107.68(19)
Ln(2)-O(11)-Ln(2)*	105.02(12)	104.54(12)	104.45(19)

Table 3.4. Selected Bond distances (Å) and Bond angles (°) for **3.4-3.6**

	Ln = Gd (3.4)	**Ln = Dy (3.5)**	**Ln = Ho (3.6)**
Ln(1)-O(3)	2.375(11)	2.301(2)	2.294(2)
Ln(1)-O(6)	2.335(10)	2.321(2)	2.3128(18)
Ln(1)-O(6)*	2.356(10)	2.313(2)	2.3029(18)
Ln(1)-O(2)	2.332(11)	2.343(2)	2.3372(19)
Ln(1)-O(10)	2.357(11)	2.336(2)	2.3134(19)
Ln(1)-O(9)	2.350(11)	2.324(2)	2.323(2)
Ln(1)-O(5)	2.455(11)	2.438(2)	2.4216(19)
Ln(1)-O(7)	2.463(11)	2.436(2)	2.294(2)
O(3)-Ln(1)-O(6)*	146.94(4)	141.19(8)	141.15(7)
O(3)-Ln(1)-O(6)	140.19(4)	84.45(7)	84.24(7)
O(3)-Ln(1)-O(2)	71.78(4)	72.34(8)	72.69(7)
O(6)-Ln(1)-O(2)	84.50(4)	140.57(7)	145.69(7)
O(6)*-Ln(1)-O(2)	140.60(4)	145.94(7)	140.59(7)
O(3)-Ln(1)-O(10)	119.26(4)	69.74(8)	106.41(7)
O(6)-Ln(1)-O(10)	78.95(4)	78.80(7)	85.83(7)

O(6)*-Ln(1)-O(10)	79.05(4)	79.70(8)	142.88(7)
O(2)-Ln(1)-O(10)	69.58(4)	119.70(8)	75.58(7)
O(3)-Ln(1)-O(9)	75.80(4)	105.98(8)	69.85(8)
O(6)-Ln(1)-O(9)	142.720(4)	142.72(7)	79.66(7)
O(6)*-Ln(1)-O(9)	86.00(4)	85.86(7)	78.66(7)
O(2)-Ln(1)-O(9)	105.20(4)	75.65(8)	120.08(7)
O(10)-Ln(1)-O(9)	71.48(4)	72.03(8)	72.42(7)
O(3)-Ln(1)-O(5)*	75.87(4)	144.98(8)	144.75(7)
O(6)-Ln(1)-O(5)*	115.65(4)	115.84(7)	115.96(7)
O(6)*-Ln(1)-O(5)*	73.00(4)	73.40(7)	73.61(6)
O(2)-Ln(1)-O(5)*	146.10(4)	74.43(7)	73.93(7)
O(10)-Ln(1)-O(5)*	138.02(4)	139.08(8)	75.53(7)
O(9)-Ln(1)-O(5)*	75.85(4)	75.76(8)	139.32(7)
O(3)-Ln(1)-O(7)	74.14 (4)	80.18(8)	80.11(8)
O(6)-Ln(1)-O(7)	70.56(4)	70.86(7)	70.98(6)
O(6)*-Ln(1)-O(7)	111.45(4)	110.94(7)	110.90(7)
O(2)-Ln(1)-O(7)	80.20(5)	74.02(7)	73.82(7)
O(10)-Ln(1)-O(7)	138.71(4)	138.94(8)	145.04(7)
O(9)-Ln(1)-O(7)	145.92(4	145.39(7)	139.00(7)

Table 3.5. Bond distances (Å) and Bond angles (°) comparison table with literature reports

	Dy-$O_{hydroxy}$ Å	**Dy-O_{alkoxy} Å**	**Dy-Dy Å**	**Dy-O-Dy°**	***U_{eff}***
[$Dy_4(L)_4(\mu_2$-$\eta^1\eta^1$Piv)$_2$]·4H_2O·6CH_3OH		2.36-2.49	3.68-4.15	99.20-115.10	73 K[10d]
[$Dy_4(\mu_3$-$OH)_4$(isonicotinate)$_6$(py)($CH_3OH)_7$]($ClO_4)_2$·py·4CH_3OH	2.33-2.40		3.72-3.85	103.63-110.1	40.2 K[10a]
$Dy_8(HL)_{10}(C_6H_4NH_2CO O)_2(\mu_3$-	2.31-2.40		3.67-3.85	102.5-109.50	SMM[10]

$OH)_8(OH)_2(NO_3)_2(H_2O)_4$]				[b]
$[Dy_4(\mu_3$-$OH)_4(na)(pyzc)]n$	2.343-2.362	3.75-3.78	106.15-107.23	39.6 K[10e]
$[Dy_4(\mu_3$-$OH)_2(\mu_3$-$O)_2(cpt)_6(MeOH)_6(H_2O)]$	2.31-2.37	3.74-3.84	103.7-108.9	SMM [10f]
$[Dy_4(OH)_4(TBSOC)_2(H_2O)_4(CH_3OH)_4]\cdot 4H_2O$	2.33-2.36	2.57-2.73	105.7-107.9	22.9 K[10c]

3.6 References:

(1) (a) Eliseeva, S. V.; Bunzli, J.-C. G. *Chem. Soc. Rev*. **2010**, *39*, 189. (b) Heffern, M. C.; Matosziuk, L. M.; Meade, T. J. *Chem. Rev*. **2014**,*114*, 4496.

(2) (a) Schuetz, S. A.; Bowman, E. A.; Silvernail, C. M.; Day V. M.; Belot, J. A. *J. Organomet. Chem*. **2005**, *690*, 1011. (b) Veits G. K.; Read de Alaniz, J. *Tetrahedron* **2012**, *68*, 2015. (c) Sen, R.; Harza, D. K.; Koner, S.; Helliwell, M.; Mukherjee M.; Bhattacharjee, A. *Polyhedron* **2010**, *29*, 3183.

(3) (a) Woodruff, D. N.; Winpenny, R. E. P.; Layfield, R. A. *Chem. Rev*. **2013**, *113*, 5110. (b) Neville, S. M.; Halder, G. J.; Chapman, K. W.; Duriska, M. B.; Moubaraki, B.; Murray, K. S.; Kepert, C. J. *J. Am. Chem. Soc*. **2009**, *131*, 12106. (c) Ungur, L.; Langley, S. K.; Hooper, T. N.; Moubaraki, B.; Brechin, E. K.; Murray, K. S.; Chibotaru, L. F. *J. Am. Chem. Soc*. **2012**, *134*, 18554. (d) Le Roy, J. J.; Ungur, L.; Korobkov, L.; Chibotaru, L. F.; Murugesu, M. *J. Am. Chem. Soc*. **2014**, *136*, 8003. (e) Chilton, N. F.; Collison, D.; McInnes, E. J. L.; Winpenny, R. E. P.; Soncini A. *Nat. Commun*. **2013**, *4*, 2551. (f) Chandrasekhar, V.; Bag, P.; Colacio, E. *Inorg. Chem*. **2013**, *52*, 4562. (g) Chandrasekhar, V.; Dey, A.; Das, S.; Rouzières, M.; Clérac, R. *Inorg. Chem*. **2013**, *52*, 2588. (h) Goura, J.; Walsh, J.P. S.; Tuna, F.; Chandrasekhar, V. *Inorg. Chem*. **2014**, *53*, 3385. (i) Goura, J.; Mereacre, V.; Novitchi, G.; Powell, A. K.; Chandrasekhar, V. *Eur. J. Inorg. Chem*. **2015**, 156. (j) Baniodeh, A.; Mereacre, V.; Magnani, N.; Lan, Y.; Wolny, J. A.; Schünemann, V.; Anson, C. E.; Powell, A. K. *Chem. Commun*. **2013**, *49*, 9666. (k) Baniodeh, A.; Magnani, N.; Bräse, S.; Anson, C. E.; Powell, A. K. *Dalton Trans*. **2015**, *44*, 6343. (l) Hussain, B.; Savard, D.; Burchell, T. J.; Wernsdorfer W.; Murugesu, M. *Chem. Commun*. **2009**, 1100.

(4) Ishikawa, N.; Sugita, M.; Ishikawa, T.; Koshihara, S.-Y.; Kaizu, Y. *J. Am. Chem. Soc.* **2003**, *125*, 8694.

(5) (a) Katoh, K.; Asano, R.; Miura, A.; Horii, Y.; Morita, T.; Breedlove B. K.; Yamashita, M. *Dalton Trans*. **2014**, *43*, 7716. (b) Suzuki, K.; Sato R.; Mizuno, N. *Chem. Sci*. **2013**, *4*, 596. (c) Yang, F.; Zhou, Q.; Zeng, G.; Li, G.; Gao, L.; Shi Z.; Feng, S. *Dalton Trans*. **2014**, *43*, 1238. (d) Zhang, P.; Zhang, L.; Lin, S.-Y.; Xue S.; Tang, J. *Inorg. Chem*. **2013**, *52*, 4587. (e) Sun, W.-B.; Yan, B; Jia, L.-H.; Wang, B.-W.; Yang, Q.; Cheng, X.; Li, H.-F.; Chen, P.; Wang, Z.-M.; Gao, S. *Dalton Trans*. **2016**, *45*, 8790. (f) Long, J. R.; Habib, F.; Lin, P.-H.; Korobkov, I.; Enright, G.; Ungur, L.; Wernsdorfer, W.; Chibotaru, L.; Murugesu, M. *J. Am. Chem. Soc*. **2011**, *133*, 5319. g) Lin, P.-H.; Burchell, T. J.; Clérac, R.; Murugesu, M. *Angew. Chem., Int. Ed*. **2008**, *47*, 8848. (h) Layfield, R. A.; McDouall, J. J. W.; Sulway, S. A.; Tuna, F.; Collison, D.; Winpenny, R. E. P. *Chem. - Eur. J.* **2010**, *16*, 4442. (i) Xu, G.-F.; Wang, Q.-L.; Gamez, P.; Ma, Y.; Clerac, R.; Tang, J.; Yan, S.-P.; Cheng, P.; Liao, D.-Z. *Chem. Commun*. **2010**, *46*, 1506. (j) Ma, Y.; Xu, G.-F.; Yang, X. L.; Li, L.-C.; Tang, J.; Yan, S.-P.; Cheng, P.; Liao, D.-Z. *Chem. Commun*. **2009**, *46*, 8264-8266. (k) Sulway, S. A.; Layfield, R. A.; Tuna, F.; Wernsdorfer, W.; Winpenny, R. E. P. *Chem. Commun*. **2012**, *48*, 1508. (l) Lin, S.-Y.; Xu, G.-F.; Zhao, L.; Guo, Y.-N.; Guo, Y.; Tang, J. *Dalton Trans*. **2011**, *40*, 8213. (m) Lin, P. H.; Sun, W. B.; Yu, M. F.; Li, G. M.; Yan, P. F.; Murugesu, M. *Chem. Commun*. **2011**, *47*, 10993. (n) Guo, Y. N.; Chen, X. H.; Xue, S.; Tang, J. *Inorg. Chem.* **2011**, *50*, 9705. (o) Guo, Y.-N.; Xu, G.-F.; Wernsdorfer, W.; Ungur, L.; Guo, Y.; Tang, J.; Zhang, H. J.; Chibotaru, L. F.; Powell, A. K. *J. Am. Chem. Soc*. **2011**, *133*, 11948. (p) Pineda, E. M.; Chilton, N. F.; Marx, R.; Dorfel, M.; Sells, D. O.; Neugebauer, P.; Jiang, S. D.; Collison, D.; van Slageren, J.; McInnes, E. J. L.; Winpenny, R. E. P. *Nat. Commun.* **2014**, *5*, 5243. (q) Fatila, E. M.; Rouzières, M.; Jennings, M. C.; Lough, A. J.; Clérac, R.; Preuss, K. E. *J. Am. Chem. Soc*. **2013**, *135*, 9596. (r) Katoh, K.; Kajiwara, T.; Nakano, M.; Nakazawa, Y.; Wernsdorfer, W.; Ishikawa, N.; Breedlove, B. K.; Yamashita, M. *Chem.–Eur. J*. **2011**, 17, 117. (s) Bag, P.; Rastogi, C. K.; Biswas, S.; Sivakumar, S.; Mereacre, V.; Chandrasekhar, V. *Dalton Trans*. **2015**, *44*, 4328.

(6) (a) Andrews, P. C.; Deacon, G. B.; Frank, R.; Fraser, B. H.; Junk, P. C.; MacLellan, J. G.; Massi, M.; Moubaraki, B.; Murray K. S.; Silberstein, M. *Eur. J. Inorg. Chem*. **2009**, 744. (b) Tang, J.; Hewitt, I.; Madhu, N. T.; Chastanet, G.; Wernsdorfer, W.;

Anson, C. E.; Benelli, C.; Sessoli, R.; Powell, A. K. *Angew. Chem., Int. Ed*. **2006**, *45*, 1729. (c) Xue, S.; Zhao, L.; Guo, Y.-N.; Zhang P.; Tang, J. *Chem. Commun*. **2012**, *48*, 8946.

(7) Lin S.-Y.; Tang, J. *Polyhedron* **2014**, *83*, 185.

(8) (a) Blagg, R. J.; Muryn, C. A.; McInnes, E. J. L.; Tuna, F.; Winpenny, R. E. P. *Angew. Chem., Int. Ed*. **2011**, *50*, 6530. (b) Das, S.; Hossain, S.; Dey, A.; Biswas, S.; Sutter, J.-P.; Chandrasekhar, V. *Inorg. Chem*. **2014**, *53*, 5020. (c) Lin, S.-Y.; Wernsdorfer, W.; Ungur, L.; Powell, A. K.; Guo, Y.-N.; Tang, J.; Zhao, L.; Chibotaru, L. F.; Zhang, H.-J. *Angew. Chem., Int. Ed*. **2012**, *51*, 12767. (d) Sharples, J. W.; Zheng, Y.-Z.; Tuna, F.; McInnes, E. J. L.; Collison, D. *Chem. Commun*. **2011**, *47*, 7650.

(9) (a) Yang, E.-C.; Wernsdorfer, W.; Hill, S.; Edwards, R. S.; Nakano, M.; Maccagnano, S.; Zakharov, L. N.; Rheingold, A. L.; Christou, G.; Hendrickson, D. N. *Polyhedron* **2003**, *22*, 1727. (b) Moragues-Canovas, M.; Helliwell, M.; Ricard, L.; Riviere, E.; Wernsdorfer, W.; Brechin E.; Mallah, T. *Eur. J. Inorg. Chem.* **2004**, 2219. (c) Guedes, G. P.; Soriano, S.; Comerlato, N. M.; Speziali, N. L.; Lahti, P. M.; Novak M. A.; Vaz, M. G. F. *Eur. J. Inorg. Chem.* **2012**, 5642. (d) Oshio, H.; Hoshino, N.; Ito T.; Nakano, M. *J. Am. Chem. Soc.* **2004**, *126*, 8805. (e) Piga, F.; Moro, F.; Krivokapic, I.; Blake, A. J.; Edge, R.; McInnes, E. J. L.; Evans, D. J.; McMastera, J.; Slageren, J. V. *Chem. Commun.* **2012**, *48*, 2430. (f) Papadakis, R.; Rivière, E.; Giorgi, M.; Jamet, H.; Rousselot-Pailley, P.; Réglier, M.; Simaan A. J.; Tron, T. *Inorg. Chem.* **2013**, *52*, 5824. (g) Galloway, K. W.; Whyte, A. M.; Wernsdorfer, W.; Sanchez-Benitez, J.; Kamenev, K. V.; Parkin, A.; Peacock R. D.; Murrie, M. *Inorg. Chem.* **2008**, *47*, 7438. (h) Yang, E. C.; Wernsdorfer, W.; Zakharov, L. N.; Karaki, Y.; Yamaguchi, A.; Isidro, R. M.; Lu, G. D.; Wilson, S. A.; Rheingold, A. L.; Ishimoto, H.; Hendrickson, D. N. *Inorg. Chem.* **2006**, *45*, 529. (i) Isele, K.; Gigon, F.; Williams, A. F.; Bernardinelli, G.; Franz P.; Decurtins, S. *Dalton Trans*. **2007**, 332. (j) Venegas-Yazigi, D.; Cano, J.; Ruiz, E.; Alvarez, S. *Phys. Rev. B: Condens. Matter Mater. Phys*. **2006**, *384*, 123. (k) Gao, Y.; Zhao, L.; Xu, X.; Xu, G.-F.; Guo, Y.-N.; Tang J.; Liu, Z. *Inorg. Chem.* **2011**, *50*, 1304. (l) Aronica, C.; Chastanet, G.; Pilet, G.; Le Guennic, B.; Robert, V.; Wernsdorfer, W.; Luneau, D. *Inorg. Chem*. **2007**, *46*, 6108. (m) Zhao, X. Q.; Lan, Y. H.; Zhao, B.; Cheng, P.; Anson, C. E.; Powell, A. K. *Dalton Trans*. **2010**, *39*, 4911. (n) Nohra, B.; Mialane, P.; Dolbecq, A.; Riviere, E.; Marrot, J.; Secheresse, F. *Chem. Commun.* **2009**, 2703. (o) Das, A.; Klinke, F. J.; Demeshko, S.; Meyer, S.; Dechert, S.;

Meyer, F. *Inorg. Chem*. **2012**, *51*, 8141. (p) Petit, S.; Neugebauer, P.; Pilet, G.; Chastanet, G.; Barra, A.-L.; Antunes, A. B.; Wernsdorfer, W. Luneau, D. *Inorg. Chem.* **2012**, *51*, 6645.

(10) (a) Gao, Y. J.; Xu, G. F.; Zhao, L.; Tang, J.; Liu, Z. L. *Inorg. Chem*. **2009**, *48*, 11495. (b) Ke, H. S.; Gamez, P.; Zhao, L.; Xu, G. F.; Xue, S. F.; Tang, J. *Inorg. Chem*. **2010**, *49*, 7549. (c) Liu, C.-M.; Zhang, D.-Q.; Hao, X.; Zhu, D.-B. *Cryst. Growth Des*. **2012**, *12*, 2948. (d) Das, S.; Dey, A.; Biswas, S.; Colacio, E.; Chandrasekhar, V. *Inorg. Chem*. **2014**, *53*, 3417. (e) Li, Y. ; Yu, J.-W.; Liu, Z.-Y.; Yang, E.-C.; Zhao, X.-J. *Inorg. Chem.* **2015**, 54, 153. (f) Savard, D.; Lin, P.-H.; Burchell, T. J.; Korobkov, I.; Wernsdorfer, W.; Clérac, R.; Murugesu, M. *Inorg. Chem*. **2009**, *48*, 11748. (g) Kong, X.-J.; Long, L.-S.; Zheng, L.-S.; Wang, R.; Zheng, Z. *Inorg. Chem*. **2009**, *48*, 3268. (h) Gerasko, O. A.; Mainicheva, E. A.; Naumova, M. I.; Yurjeva, O. P. ; Alberola, A.; Vicent, C.; Llusar, R.; Fedin, V. P. *Eur. J. Inorg. Chem*. **2008**, 416. (i) Ma, B.-Q.; Zhang, D.-S.; Gao, S.; Jin, T.-Z.; Yan, C.-H.; Xu, G.-X. *Angew. Chem., Int. Ed*. **2000**, *39*, 3644. (j) Baskar, V.; Roesky, P. W. *Dalton Trans*., **2006**, 676. (k) Zheng, Z. P. *Chem. Commun.* **2001**, 2521. (l) Kong, X. J.; Wu, Y. L.; Long, L. S.; Zheng, L. S.; Zheng, Z. P. *J. Am. Chem. Soc*. **2009,** *131*, 6918. (m) Chesman, A. S. R.; Turner, D. R.; Moubaraki, B.; Murray, K. S.; Deacon, G. B.; Batten, S. R. *Dalton Trans*. **2012**, *41*, 3751.

(11) (a) Pointilart, F.; Le Guennic, B.; Golhen, S.; Cador, O.; Maury, O.; Quahab, L. *Chem. Commun*., **2013**, *49*, 615. (b) Habib, F.; Murugesu, M. *Chem. Soc. Rev*., **2013**, *42*, 3278. (c) Moreno Pineda, E.; Chilton, N. F.; Marx, R.; Dörfel, M.; Sells, D. O.; Neugebauer, P.; Jiang, S.-D.; Collison, D.; van Slageren, J.; McInnes, E. J. L.; Winpenny, R. E. P. *Nat. Commun*., **2014**, 5, 5243.

(12) (a) Liu, J.; Chen, Y.-C.; Liu, J.-L.; Vieru, V.; Ungur, L.; Jia, J.-H.; Chibotaru, L. F.; Lan, Y.; Wernsdorfer, W.; Gao, S.; Chen, X.-M.; Tong, M.-L. *J. Am. Chem. Soc*., **2016**, *138*, 5441. (b) Chen, Y.-C.; Liu, J.-L.; Ungur, L.; Liu, J.; Li, Q.-W.; Wang, L.-F.; Ni, Z.-P.; Chibotaru, L. F.; Chen, X.-M.; Tong, M.-L. *J. Am. Chem. Soc*., **2016**, 138, 2829.

(13) Rinehart, J. D.; Fang, M.; Evans, W. J.; Long, J. R. *J. Am. Chem. Soc*., **2011**, *133*, 14236.

(14) Habib, F.; Brunet, G.; Vieru, V.; Korobkov, I.; Chibotaru, L. F.; Murugesu, M. *J. Am. Chem. Soc*., **2013**, *135*, 13242.

(15) (a) Bernot, K.; Luzon, J.; Bogani, L.; Etienne, M.; Sangregorio, C.; Shanmugam, M. Caneschi, A.; Sessoli, R.; Gatteschi, D. *J. Am. Chem. Soc*., **2009**, *131*, 5573. (b) Jiang, S. D.; Wang, B. W.; Su, G.; Wang, Z. M.; Gao, S. *Angew.Chem. Int. Ed*., **2010**, *49*, 7448. (c) Li, D.-P.; Wang, T.-W.; Li, C.-H. S.; Liu, D.; Li, Y.-Z.; You, X.-Z. *Chem. Commun*., **2010**, *46*, 2929. (d) Ma, Y.; Xu, G.-F.; Yang, X.; Li, L.-C.; Tang, J.; Yan, S.-P.; Cheng, P.; Liao, D.-Z. *Chem. Commun*., **2010**, *46*, 8264.

(16) Chen, G.-J.; Gao, C.-Y.; Tian, J.-L.; Tang, J.; Gu, W.; Liu, X.; Yan, S.-P.; Liao, D.-Z.; Cheng, P. *Dalton Trans*. **2011**, *40*, 5579.

(17) Bi, Y.; Guo, Y.-N.; Zhao, L.; Guo, Y.; Lin, S.-Y.; Jiang, S. D.; Tang, J.; Wang, B. W.; Gao, S. *Chem. Eur. J*. **2011**, *17*, 12476.

(18) (a) Baskar, V.; Roesky, P. W. *Z. Anorg. Allg. Chem.* **2005**, *631*, 2782. (b) Baskar, V; Roesky, P. W. *Dalton Trans*. **2006**, 676. (c) Roesky, P. W.; CansecoMelchor, G.; Zulys, A. *Chem. Commun*. **2004**, 738. (d) Bürgstein, M. R.; Gamer, M. T.; Roesky, P. W. *J. Am. Chem. Soc*. **2004**, *126*, 5213. (e) Bürgstein, M. R.; Roesky, P. W. *Angew. Chem., Int. Ed*. **2000**, *39*, 549. (f) Addamo, M.; Bombieri, G.; Foresti, E.; Grillone, M. D.; Volpe, M. *Inorg. Chem*. **2004**, *43*, 1603. (g) Bombieri, G.; Clemente, D. A.; Foresti, E.; Grillone, M. D.; Volpe, M. *J. Alloys Compd*. **2004**, *374*, 382. (h) Andrews, P. C.; Beck, T.; Forsyth, C. M.; Fraser, B. H.; Junk, P. C.; Massi, M.; Roesky, P. W. *Dalton Trans*. **2007**, 5651. (i) Barash, E. H.; Coan, P. S.; Lobkovsky, E. B.; Streib, W. E.; Caulton, K. G. *Inorg. Chem.* **1993**, *32*, 497. (j) Wu, Y.; Morton, S.; Kong, X.; Nichol, G. S.; Zheng, Z. *Dalton Trans*. **2011**, *40*, 1041. (k) Andrews, P. C.; Gee, W. J.; Junk, P. C.; MacLellan, J. G. *Dalton Trans*. **2011**, *40*, 12169. (l) Andrews, P. C.; Gee, W. J.; Junk, P. C.; MacLellan, J. G. *Polyhedron* **2011**, *30*, 2837. (m) Yadav, M.; Mondal, A.; Mereacre, V.; Jana, S. K.; Powell, A. K.; Roesky, P. W. *Inorg. Chem.* **2015**, *54*, 7846. (n) Hui, Y.-C.; Meng, Y.-S.; Li, Z.; Chen, Q.; Sun, H.-L.; Zhangd, Y.-Q.; Gao, S. *CrystEngComm* **2015**, *17*, 5620. (o) Thielemann, D. T.; Wagner, A. T.; Lan, Y.; Oña-Burgos, P.; Fernãndez, I.; Rösch, E. S.; Kölmel, D. K.; Powell, A. K.; Bräse, S.; Roesky, P. W. *Chem. -Eur. J.* **2015**, *21*, 2813.

(19) (a) Andrews, P. C.; Deacon, G. B.; Frank, R.; Fraser, B. H.; Junk, P. C.; MacLellan, J. G.; Massi, M.; Moubaraki, B.; Murray, K. S.; Silberstein, M. *Eur. J. Inorg. Chem.*

2009, 744. (b) Tanase, S.; Viciano-Chumillas, M.; Smits, J. M. M.; Gelder, R. D.; Reedijk, J. *Polyhedron* **2009**, *28*, 457. (c) Aniscough, E.W.; Brodie, A. M.; Cresswell, R. J.; Waters, J. M. *Inorg. Chim. Acta* **1998**, *277*, 37-45. (d) Jami, A. K.; Kishore, P. V. V. N.; Baskar, V. *Polyhedron* **2009**, *28*, 2284.

(20) (a) Hou, Y. L.; Xiong, G.; Shi, P. F.; Cheng, R. R.; Cui, J. Z.; Zhao, B. *Chem. Commun*. **2013**, *49*, 6066. (b) Shi, P. F.; Zheng, Y. Z.; Zhao, X. Q.; Xiong, G.; Zhao, B.; Wan, F. F.; Cheng, P. *Chem.–Eur. J*. **2012**, *18*, 15086.

(21) a) Zheng, Y. Z.; Zhou, G. J.; Zheng, Z. P.; Winpenny, R. E. P. *Chem. Soc. Rev*. **2014**, *43*, 1462. (b) Evangelisti, M.; Brechin, E. K. *Dalton Trans*. **2010**, *39*, 4672. (c) Sessoli, R. Angew. Chem., Int. Ed. 2012, 51, 43.

(22) Dubrovina, N. V.; Tararov, V. I.; Monsees, A.; Kadyrov, R,; Fischera, C.; Börner, A. *Tetrahedron: Asymmetry*, **2003**, *14*, 2739.

(23) (a) *SAINT Software Reference manuals*, Version 6.45; Bruker Analytical X-ray Systems, Inc.: Madison, WI, 2003. (b) Sheldrick, G. M. *SHELXS-97, Program for Crystal Structure Solution;* University of Göttingen: Göttingen, Germany, 1997. (c) Sheldrick, G. M. *Acta Crystallogr., Sect. A: Fundam. Crystallogr*. **2008**, *64*, 112. (d) Sheldrick, G. M. *Acta Crystallogr., Sect. C: Cryst. Struct. Commun*. **2015**, *71*, 3.

(24) (a) Alvarez, S.; Alemany, P.; Casanova, D.; Cirera, J.; Llunell, M.; Avnir, D. *Coord. Chem. Rev*. **2005**, *249*, 1693. (b) Casanova, D.; Llunell, M.; Alemany, P.; Alvarez, S. *Chem. –Eur. J*. **2005**, *11*, 1479.

(25) Chilton, N. F.; Anderson, R. P.; Turner, L. D.; Soncini, A.; Murray, K. S. *J. Comput. Chem*. **2013**, *34*, 1164 –1175.

(26) (a) Das, C.; Vaidya, S.; Gupta, T.; Frost, J. M.; Righi, M.; Brechin, E. K.; Affronte, M.; Rajaraman, G.; Shanmugam. M. *Chem. –Eur. J.* **2015**, *21*, 15639. (b) Lin, S. Y. ; Li, X.-L.; Ke, H.; Xu. Z. *CrystEngComm*. **2015**, *17*, 9167.

(27) Brunet, G.; Habib, F.; Korobkov, I.; Murugesu, M. *Inorg. Chem*., **2015**, *54*, 6195-6202. (b) Comba, P.; Großhauser, M.; Klingeler, R.; Koo, C.; Lan, Y.; Muller, D.; Park, J.; Powell, A; Riley, M. J.; Wadepoh, H. *Inorg. Chem*., **2015**, *54*, 11247.

(28) a) Upadhyay, A.; Singh, S. K.; Das, C.; Mondol, R.; Langley, S. K.; Murray, K. S.; Rajaraman, G.; Shanmugam, M. *Chem. Commun*., **2014**, *50*, 8838. (b) Cucinotta, G.; Perfetti, M. Luzon, J.; Etienne, M.; Car, P.-E; Caneschi, A.; Calvez, G.; Bernot, K.; Sessoli, R. *Angew. Chem., Int. Ed*., **2012**, *51*, 1606-1610.

(29) Rinehart, J. D.; Long, R. *Chem. Sci*., **2011**, 2, 2078.

(30) Langley, S. K.; Wielechowski, D. P.; Vieru, V.; Chilton, N. F.; Moubaraki, B.; Abrahams, B. F.; Chibotaru, L. F.; Murray, K. S. *Angew. Chem., Int. Ed*., **2013**, *52*, 12014.

(31) Xu, L.-Y.; Zhao, J.-P.; Liu, T.; Liu, F.-C. *Inorg. Chem*., **2015**, *54*, 5249.

(32) (a) Lorusso, G.; Sharples, J. W.; Palacios, E.; Roubeau, O.; Brechin, E. K.; Sessoli, R.; Rossin, A.; Tuna, F.; McInnes, E. J. L.; Collison, D.; Evangelisti, M. *Adv. Mater*., **2013**, *25*, 4653. (b) Evangelisti, M.; Roubeau, O.; Palacios, E.; Camon, A.; Hooper, T. N.; Bre-chin, E. K.; Alonso, J. J. *Angew. Chem. Int. Ed*., **2011**, *50*, 6606.

(33) Upadhyay, A.; Das, C.; Shanmugam, M.; Langley, S. K.; Murray, K. S.; Shanmugam, M. *Eur. J. Inorg. Chem*., **2014**, 4320.

(34) Upadhyay, A.; Komatireddy, N.; Ghirri, A.; Tuna, F.; Langley, S. K.; Srivastava, A. K.; Sañudo, E. C.; Moubaraki, B.; Murray, K. S.; McInnes, E. J. L.; Affronte, M.; Shanmugam, M. *Dalton Trans*., **2014**, *43*, 259.

(35) (a) Zheng, Y. Z.; Evangelisti, M.; Tuna, F.; Winpenny, R. E. P. *J. Am. Chem. Soc*., **2012**, *134*, 1057. (b) Chen, Y.-C.; Prokleš k, J.; Xu, W.-J.; Liu, J.-L.; Liu, J.; Zhang, W.-X.; Jia, J.-H.; Sechovsky, V.; Tong, M.-L. *J. Mater. Chem. C*., **2015**, *3*, 12206.

(36) (a) Gass, I. A.; Brechin, E. K.; Evangelisti. M. *Polyhedron*, **2013**, *52*, 1177-1180. (b) M.-J. Martínez-Pérez, O. Montero, M. Evangelisti, F. Luis, J. Sesé, S. Cardona-Serra, E. Coronado, *Adv. Mater*., **2012**, *24*, 4301.

Triketone Assisted Self-Assembly of Lanthanide oxo/hydroxo Clusters: Synthesis, Structure and Magnetic Measurments

CHAPTER 4

Tetranuclear Ln(III) clusters **4.1-4.2** $[Ln_4(\mu_3\text{-}OH)_2(phpt)_6(MeOH)_2].6CHCl_3$ {Ln=Dy(**4.1**) and Ho(**4.2**)} and $[Dy_4(\mu_3\text{-}OH)_2(hfht)_6(MeOH)_2].2Et_3N.4CH_3OH$ (**4.3**) have been isolated from the reaction of triketones 1,5-diphenylpentane-1,3,5-trione(H_2phpt) or 1,1,1,7,7,7-Hexafluoroheptane-2,4,6-trione(H_2hfht) with $Ln(NO_3)_3.6H_2O$ (Ln(III) = Dy and Ho) in presence of triethylamine as base. Using acetylacetone (acac) as co-ligand along with H_2hfht also resulted in the isolation of a tetranuclear cluster **4.4** $\{[Dy_4(\mu_3\text{-}OH)_2(acac)_4(hfht)_6].2CHCl_3\}$ which is structurally similar to **4.1-4.3**. This chapter presents a detailed description of structural characterization and magnetic properties of above mentioned metal clusters.

4.1 Introduction

There has been a continued interest in the synthesis and structural elucidation of polynuclear lanthanide complexes due to their potential applications in luminescence,[1] catalysis[2] and magnetic properties.[3] Recently, lanthanide complexes that function as single ion magnets (SIMs),[4] single chain magnets (SCMs)[5] and single molecule magnets (SMMs)[6] have been synthesised and their magnetic properties have been studied. SMMs are considered as an interesting class of molecules in the field of molecular magnetism. The presence of energy barrier to the reorientation of magnetization is the fundamental characteristic of SMMs, which mainly depends on large uniaxial anisotropy (D) and a large ground state spin (S). Lanthanides are the unique elements suitable for the synthesis of high energy barrier SMMs due to their large unquenched orbital angular momentum combined with ligand field effects and spin-orbit coupling. Since the discovery of double-deckar mononuclear phthlocyanin [LnPc2][7] complexes (Ln = Tb(III), Dy(III) and Ho(III)), large number of lanthanide based SMMs have been reported. In case of 4f metal ions, intermolecular effects often lead to quantum tunnelling of magnetization (QTM). Due to this fast QTM, only a few 4f based SMMs exhibit large effective energy barrier (U_{eff}) in absence of external magnetic field. Recently Long and co-workers have shown that cluster exhibiting decreased QTM is possible by introducing azide radical which lead to the observation of a hysteresis loop upto a blocking temperature of 14K.[8] In 4f metal chemistry, the coordination compounds of Dy(III) have been extensively studied as SMMs because of large Ising-type magnetic anisotropy and large magnetic moment of Kramers ground state ($^6H_{15/2}$). To date, there are a large number of Dy based SMMs which have been reported with nuclearity ranging from mono,[9] di,[10] tri,[11] tetra,[12] penta[13] and polynuclear.[14] Among varying nuclearity based SMMs, tetranuclear Dy-SMMs have received special attention since they seemed to be exhibiting high energy barrier for magnetic relaxation pathways. A centrosymmetric defect-dicubane [$Dy_4(\mu_3\text{-}OH)_2(bmh)_2(msh)_4Cl_2$][12] has been found to exhibit a large anisotropy barrier of 170 K. Recently Winpenny *et. al*, reported record highest energy barrier of 842K for a potassium doped oxo centered dysprosium cluster [$Dy_4K_2O(O\text{-}tBu)_{12}$].[12] Most of the lanthanide oxo-hydroxo clusters have been synthesized by utilizing flexible ligand systems like aminoacids,[15] β-diketones,[16] alkoxides,[17] carboxylates,[18] Schiff bases[19] and o-vanillin based Schiff bases.[20] β-diketones are well known for their bidentate chelating ability

which provides suitable ligand field for lanthanide complexes to study their magnetic anisotropy. Some *β*-diketone based Dy(III)-clusters have shown excellent magnetic properties. For example acetylacetone (acac) ligating Dy(III) complex $[Dy(acac)_3(H_2O)_2].H_2O.C_2H_5OH$ behaves as SMM with an energy barrier of 64.3 K.[21] *β*-diketones with different auxiliary ligands have been reported to result in higher effective energy barriers.[22] In all these compounds the geometry around Dy(III) ion shows approximate D_{4d} local symmetry, which is belived to be the most suitable geometry to exhibit SMM behaviour. Recently the use of mixed ligand systems for the isolation of lanthanide oxo-hydroxo clusters have been explored and some of these complexes have shown interesting structural and magnetic properties. For example, *β*-diketones with *o*-nitrophenols and peptides result in pentanuclear $[Ln_5(OH)_4(Ph_2acac)_7(o\text{-}O_2N\text{-}C_6H_4\text{-}O)_3Cl]^-$ $HNEt_3^+$ (Ln = Er, Tm; *o*-O_2N-C_6H_4O = o-nitro-phenolate)[23] and novel pentadecanuclear lanthanide hydroxyl cluster $[\{Ln_{15}(\mu_3\text{-}OH)_{20}(PepCO_2)_{10}(DBM)_{10}Cl\}Cl_4]$ (Ln = Y, Eu, Tb, Dy; PepCO2 = 2-[{3-(((tert-butoxycarbonyl)amino)methyl)benzyl}amino]acetate)[24] respectively. With amino acids and Schiff-bases, these *β*-diketones resulted in the isolation of pentanuclear $[Y_5(OH)_5(\alpha\text{-}AA)_4\text{-}(Ph_2acac)_6]$ (Ph_2acac = dibenzoylmethane; α-AA = D-phenyl glycine, L-proline, L-valine, and L-tryptophan),[25] tetra and penta nuclear lanthanide clusters $\{[Ln_4(\mu_3\text{-}OH)_2(L)(HL)(acac)_5(H_2O)](HNEt_3)(NO_3)\cdot 2(Et_2O)\}$, $\{[Dy_5(\mu_3\text{-}OH)_2(L)_3(DBM)_4(MeOH)_4]\cdot 4(MeOH)\}$.[26] In yet another interesting report by Murray *et al*, use of triethanolamine and 6-chloro-2-hydroxo pyridine as ligands resulted in the isolation of hexanuclear lanthanide cluster $\{[Ln_6(teaH)_2(teaH_2)_2(CO_3)(NO_3)_2(chp)_7(H_2O)]^+$ (Ln = Gd, Dy, Tb. tea = triethanolamine, chp = 6-chloro-2-hydroxypyridine)}.[27] Recently Tang and co-workers[28] used H_2hfht triketone with phenanthroline as co-ligand and structurally characterized a dinuclear Ln(III) cluster as well as studied its magnetism in detail. The dysprosium analogue exhibits SMM behaviour with an energy barrier of 86.8 K. As a logical extension to the ample work reported with β-diketones and in the backdrop of very few reports with triketones as ligands, the reactivity of different triketones was systematically investigated by reaction with Ln(III) ions in presence of a base. The synthesized products were thoroughly characterized by standard analytical and spectroscopic techniques. Replacing the co-ligand phenanthroline in Tang's study with β-diketone resulted in the isolation of a tetranuclear cluster as opposite to their dinuclear cluster reported.

4.2 Experimental Section

4.2.1 General Information and Instrumentation:

All the reagents used were of analytical grade and used as received without further purification. Lanthanum salts [$Ln(NO_3)_3.6H_2O$] were synthesized by neutralizing the corresponding oxides with concentrated HNO_3 followed by evaporation to dryness. 1,1,1,7,7,7-Hexafluoroheptane-2,4,6-trione (H_2hfht) and 1,5-diphenylpentane-1,3,5-trione (H_2phpt) were synthesized according to the literature procedure.[29] Infra-Red spectra of all the complexes were recorded on a JASCO-5300 FT-IR spectrometer as KBr pellets. Elemental analysis was performed on a flash EA series 1112 CHNS analyzer. Magnetic measurements were performed on polycrystalline samples with a Quantum Design MPMS-XL SQUID magnetometer equipped with a 7 T magnet.

4.2.2 General synthetic procedure:

To a methanolic solution of H_2L (H_2hfht or H_2phpt), $Ln(NO_3)_3.6H_2O$ was added followed by the addition of triethylamine. The mixture was stirred for 12 hr at ambient temperature. It resulted in the formation of a yellow precipitate which was collected and washed with methanol and redissolved in a 1:1 mixture of $CHCl_3$/MeOH. Slow evaporation of the solvent mixture resulted in isolation of X-ray quality single crystals in a week's time.

Compound **4.1**: H_2phpt (0.1g, 0.375 mmol), $Dy(NO_3)_3.6H_2O$ (0.171g, 0.375 mmol), Et_3N (0.154 ml, 1.125 mmol). Yield: 0.420 g 62.2 % (based on Dy). Mp: 178 °C. IR (KBr) cm^{-1}: 3473(br), 3051(w), 1594(s), 1566(s), 1511(w), 1468(s), 1408(m), 1282(m), 1189(m), 1079(s), 991(s), 887(s), 778(s). Anal. Calcd for $C_{106}H_{80}O_{22}Cl_6Dy_4$: C, 49.57; H 3.14. Found: C, 49.65; H 3.06%.

Compound **4.2**. H_2phpt (0.1 g, 0.375 mmol), $Ho(NO_3)_3.6H_2O$ (0.172 g, 0.375 mmol), Et_3N (0.154 ml, 1.125 mmol). Yield: 0.480 g, 65.3 % (based on Ho). Mp: 175°C. IR (KBr) cm^{-1}: 3419(br), 3057(w), 2926(w), 1605(s), 1561(s), 1517(s), 1457(s), 1402(m), 1254(m), 1183(m), 1073(m), 1024(s), 997(w), 897(s), 805(m), 695(s). Anal. Calcd for $C_{108}H_{82}O_{22}Cl_{12}Ho_4$: C, 46.05; H 2.93. Found: C, 46.15; H 2.86%.

Compound **4.3**. H_2hfht (0.1 g, 0.406 mmol), $Dy(NO_3)_3.6H_2O$ (0.185 g, 0.406 mmol), Et_3N (0.168 ml, 1.218 mmol). Yield: 0.430 g, 63.8% (based on Dy). Mp: 182°C. IR (KBr) cm^{-1}: 3480(br), 2957(w), 1638(s), 1556(s), 1484(w), 1402(m), 1271(m), 1199(m), 1128(s),

991(s), 887(s), 827(s) 613(s). Anal. Calcd for $C_{60}H_{60}O_{26}F_{36}N_2Dy_4$: C, 23.16; H 2.36. Found: C, 23.15; H 2.26%.

Compound **4.4**. The procedure used was similar to **4.1**-**4.3**, except that acac was also added along with H_2hfht. The stoichiometry of reagents is as follows, H_2hfht (0.1 g, 0.406 mmol), acac (0.041 ml, 0.406 mmol), $Dy(NO_3)_3.6H_2O$ (0.185 g, 0.406 mmol), Et_3N (0.225 ml, 1.624 mmol). Yield: 0.325 g, 59.7% (based on Dy). Mp: 179°C. IR (KBr) cm^{-1}: 3539(br), 3002(w), 2705(m), 1627(s), 1610(s), 1556(m), 1517 (m), 1484(m), 1308(m), 1287(m), 1200(m), 1117(s), 1013(m), 898(s), 821(s), 756(m) 663(s). Anal. Calcd for $C_{48}H_{36}O_{22}F_{24}Dy_4$: C, 27.84; H 1.75. Found: C, 27.71; H 1.83%.

4.2.3 X ray Crystallography

Single crystal X-ray diffraction data for all the complexes was recorded at 100K on a Bruker Smart Apex-II CCD area detector system (λ (Mo Kα) = 0.71073 Å) with a graphite monochromator. The data integration and reduction was carried out by using *SAINT* program. XPREP was used to determine the space group. The structures were solved by the direct methods using SHELXL-97 and refined using SHELXL-2014/7 program package.[30] All non-hydrogen atoms were refined anisotropically, hydrogen atoms were fixed by using riding model on the respective carbon atoms. Structure refinement parameters for **4.1**-**4.4** are summarized in Table 4.1 The disordered solvent molecules in the asymmetric unit **4.1**, **4.2** and **4.4** were removed using SQUEEZE option in PLATON.[31] The total electron count removed by SQUEEZE corresponds to 618 with a void volume of 2369.4 $Å^3$ (21.1%) per unit cell in **4.1**, 301 with a void volume of 1077.3 $Å^3$ (9.6%) per unit cell in **4.2** and 86 with a void volume of 553.8 $Å^3$ (9.6%) per unit cell in **4.4**.

4.3 Results and Discussion

The reaction of $Ln(NO_3)_3.6H_2O$ (Ln = Dy, Ho) with H_2phpt /H_2hfht or H_2hfht along with acac in presence of triethylamine as base in MeOH gave yellow precipitate which upon crystallization from $CHCl_3$/MeOH (1:1 v/v) gave yellow crystals of **4.1**-**4.4** which were characterized as $[Ln_4(\mu_3\text{-}OH)_2(phpt)_6(MeOH)_2].6CHCl_3$ {Ln=Dy(**4.1**) and Ho(**4.2**)}, $[Dy_4(\mu_3\text{-}OH)_2(hfht)_6(MeOH)_2].2Et_3N.4CH_3OH$ (**4.3**) and $[Dy_4(\mu_3\text{-}OH)_2(acac)_4(hfht)_4].2CHCl_3$ (**4.4**). All the compounds were characterized by standard analytical and spectroscopic techniques. IR spectra of **4.1**-**4.4** shows a broad peak around 3400-3600 cm^{-1} indicating the presence of hydroxyl group in the structure.

4.3.1 Description of the Crystal Structure for 4.1-4.4:

Single crystal X-ray analysis revealed that complexes **4.1-4.3** are isostructural. Hence **4.1** is used to describe the solid state structure of clusters. Single crystal X-ray studies confirmed the formation of a neutral tetranuclear [figure 4.1(a)] dysprosium hydroxo cluster $[Dy_4(\mu_3\text{-}OH)_4(phpt)_6(MeOH)_2].6CHCl_3$, which crystallized in monoclinic space group

C2/c. Asymmetric unit consists of a dysprosium dimer coordinated to three triketones, one coordinated MeOH molecule and three $CHCl_3$ solvent molecules. Dy2 is connected to Dy1 via μ_3-OH ion and μ_2-O2 of a triketonate ligand. On a whole, the metallic core is made up of four Dy(III) ions, which lie on the same plane and exhibit a planar butterfly type structural topology [figure 4.1(b)]. The metal centre Dy1 is symmetry equivalent to Dy1* defining the hinge or body of the butterfly and Dy2 is symmetry equivalent to Dy2*, defining the wing tips of butterfly motif. The two parts (body and wingtips) of butterfly core are connected through two μ_3-OH bridges (O10 and O10*) which are located on opposite sides of the Dy_4 plane and are displayed out of the plane by 0.895 Å. The hydroxo group forms a symmetrical triple bridge, with Dy-O10 distances of 2.339(3), 2.331(3), 2.415(3) Å and the Dy-O10-Dy angles of 97.90(12), 110.25(15) and 111.15(13) °. The peripheral part of the metal hydroxo core is surrounded by six triketonate ligands bound via a bridging mode to four Dy(III) ions. Two MeOH molecules are present to satisfy coordination geometry around Dy2 and Dy2* ions. Dy-$O_{(triketonate)}$ bond lengths are of the order of 2.236(4) to 2.407(4) Å and the shortest intramolecular Dy…Dy distances are in the range of 3.522(4) to 3.894(5) Å. All Dy(III) ions are octacoordinated and SHAPE[32] analysis reveals that the 8-coordinated Dy1 ion exhibits closest resemblance to distorted square-antiprismatic geometry (Figure 4.2 and Table 4.2).

4.3.2 Description of crystal structure of 4.4:

Compound **4.4** $[Dy_4(\mu_3\text{-}OH)_2(hfht)_4(acac)_4].2CHCl_3$ crystallizes in triclinic space group *P-1* with asymmetric unit containing half of the cluster which lies on an inversion centre. Crystal structure of **4.4** is depicted in figure 4.1(c). The asymmetric unit consists of dysprosium dimer coordinated to two (L) triketonate ligands via bridging mode, one μ_3-OH ion, one chelating acac, one bridging acac and a disordered $CHCl_3$ solvent molecule in the crystal lattice. The metallic core of **4.4** is made up of four Dy(III) ions and exhibits a planar butterfly type structural topology which is similar to the core in compound **4.1- 4.3**.

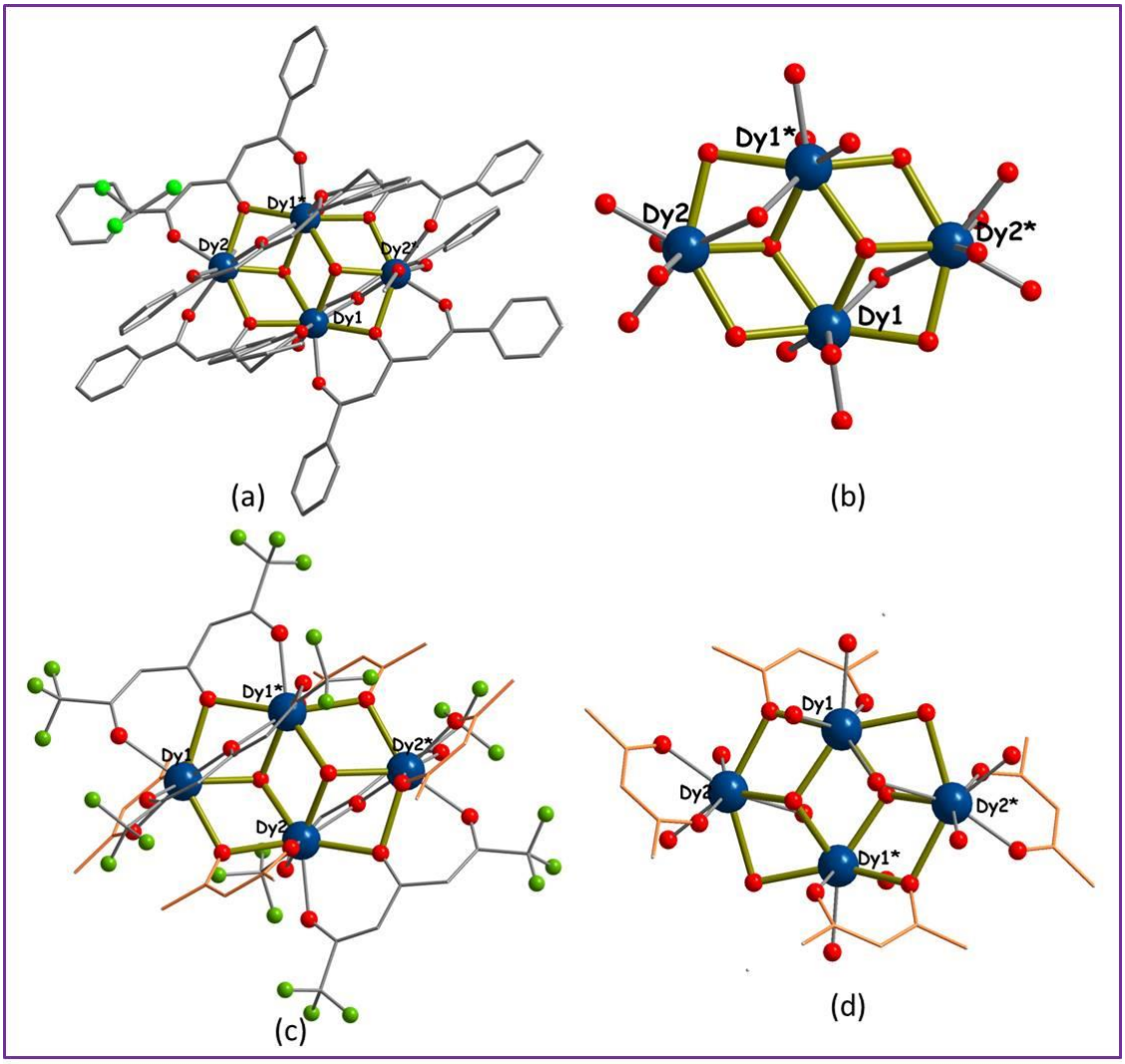

Figure 4.1. (a) Molecular structure of compound **4.1** (b) core of the cluster (c) molecular structure of compound **4.4** (d) core of the cluster along with acac ligands.

Two μ_3-hydroxide ligands (O11, O11*) bridge the central body ions (Dy1 and Dy1*) to the outer wingtip ions (Dy2 and Dy2*) and are displayed out of plane by 0.838 Å. The hydroxo group forms a symmetrical triple bridge with the Dy-O11 distances 2.332(2), 2.325(2), 2.326(2) Å and the Dy-O11-Dy angles 108.06(9), 103.54(9) and 111.65(9)° which are consistent with the reported tetranuclear butterfly complexes.[12] The peripheral part of the core is bridged by four triketonate ligands and by two acac ligands. There are also two chelating acac ligands which are bound to Dy1 and Dy1*. Each triketone ligand bridges a body part to a wing ion via μ_2-O5 and μ_2-O2, acac ligands also bridge the body of the cluster to the wing tip ions by μ_2-O9. Dy-$O_{(triketonate)}$ bond lengths are of the order of 2.269(3) to 2.457(2) Å and Dy-$O_{(acac)}$ bond lengths are of the order of 2.294(3) to 2.457(2)

Å. Shortest inter nuclear Dy...Dy distances are in the range of 3.76-3.85 Å. Dy1 ion is octacoordinated. Systematic analysis of the coordination geometries around the metals using SHAPE 2.1[32] reveals that all of the 8-coordinated Dy(III) ions exhibit closest resemblance to distorted square-antiprismatic geometry (Figure **4.2** and Table 4.2). Selected bond lengths and bond angles for all the complexes are shown in Table 4.3-4.6.

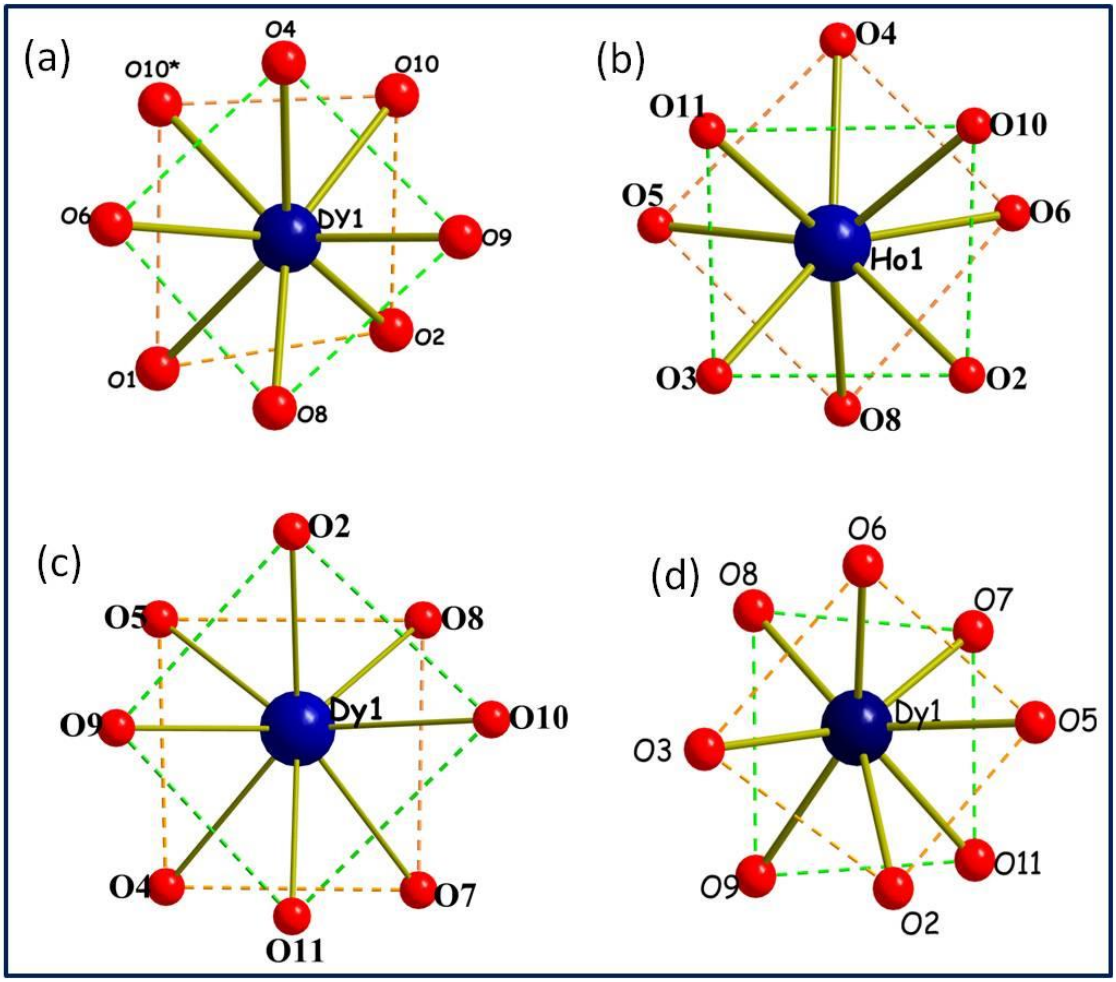

Figure 4.2. Coordination geometry around metal ion for compound **4.1-4.4**.

4.4 Magnetic Properties

4.4.1 Static Magnetic Properties of 4.1-4.4:

Variable temperature dc magnetic susceptibility data was collected on polycrystalline samples of complexes **4.1-4.4** under an applied dc field of 1000 Oe in the temperature range of 1.8 to 300 K as shown in Figure 4.3. At room temperature, the observed $\chi_M T$ values for complexes **4.1-4.4** are 63.51, 63.19, 50.65 and 54.08 cm^3 K mol^{-1} which are slightly larger than the expected theoretical values in case of **4.1** and **4.2**. In case of **4.3**,

the $\chi_M T$ value is lower than the expected value and in **4.4** the experimental value nearly equals the theoretical value {Dy(III), $^6H_{15/2}$, S = 5/2, L = 5, g = 4/3, C = 14.17 and 56.68 cm^3 K mol^{-1}, Ho(III), $^5I_8$, S = 2, L = 6, g = 5/4, C = 14.08 and 56.28 cm^3 K mol^{-1}} for four non- interacting Ln(III) ions. As temperature decreases, the $\chi_m T$ value for **4.1** undergoes a gradual reduction from 63.19 cm^3 K mol^{-1} at 300 K to 32.36 cm^3 K mol^{-1} at 2K. Similarly the $\chi_m T$ value for **4.2**, **4.3** and **4.4** undergoes a gradual reduction from 63.43 cm^3 K mol^{-1} at 300 K to 28.10 cm^3 K mol^{-1} at 2 K for **4.2**, 50.65 cm^3 K mol^{-1} at 300 K to 30.55 cm^3 K mol^{-1} at 2 K for **4.3** and 54.08 cm^3 K mol^{-1} at 300 K, undergoing a gradual reduction up to 44.75 cm^3 K mol^{-1} at 5K and below which there is a slight increase in $\chi_m T$ value up to 46.478 at 2 K for **4.4**. This increase in $\chi_m T$ value at low temperature suggests weak ferromagnetic interaction between Dy(III) ions in case of **4.4**. The decrease in $\chi_m T$ value as temperature decreases may be attributed to depopulation of the stark sub levels.

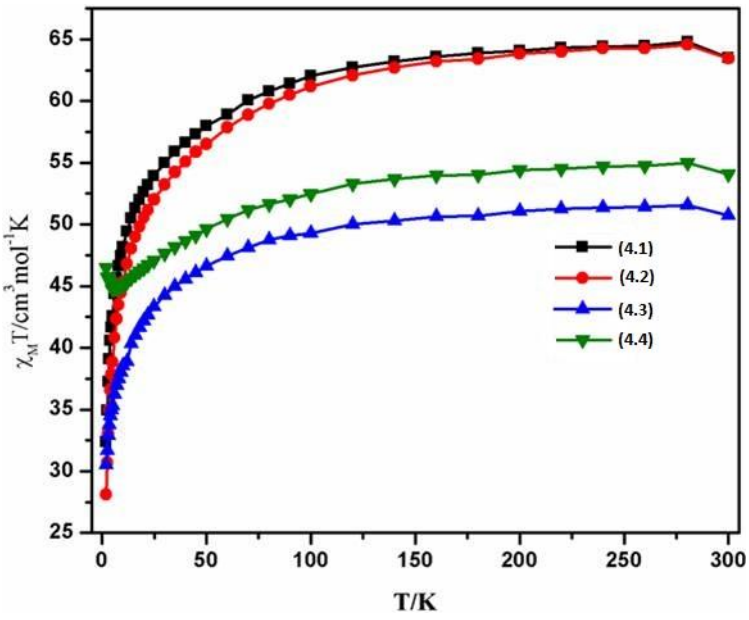

Figure 4.3. Plots of $\chi_M T$ vs T for compounds **4.1- 4.4** under 1000 Oe dc field.

The field dependence of magnetization plotted as *M* vs *H* is shown in figure 4.4 from 0 to 7 T for **4.1-4.4** at low temperature (1.8 K, 3K, 5K and 8K). It shows that at low fields, magnetization increases rapidly and reaches values of 24.17, 25.01, 20.35 and 20.74 Nμ_B at 7 T without clear saturation. These values are lower than the expected theoretical values for four non-interacting Dy(III) and Ho(III) ions. The lack of saturation suggests the presence of magnetic anisotropy or the lack of well-defined ground state. In poly-crystalline samples, low values of saturation are expected for Dy(III) and Ho(III).

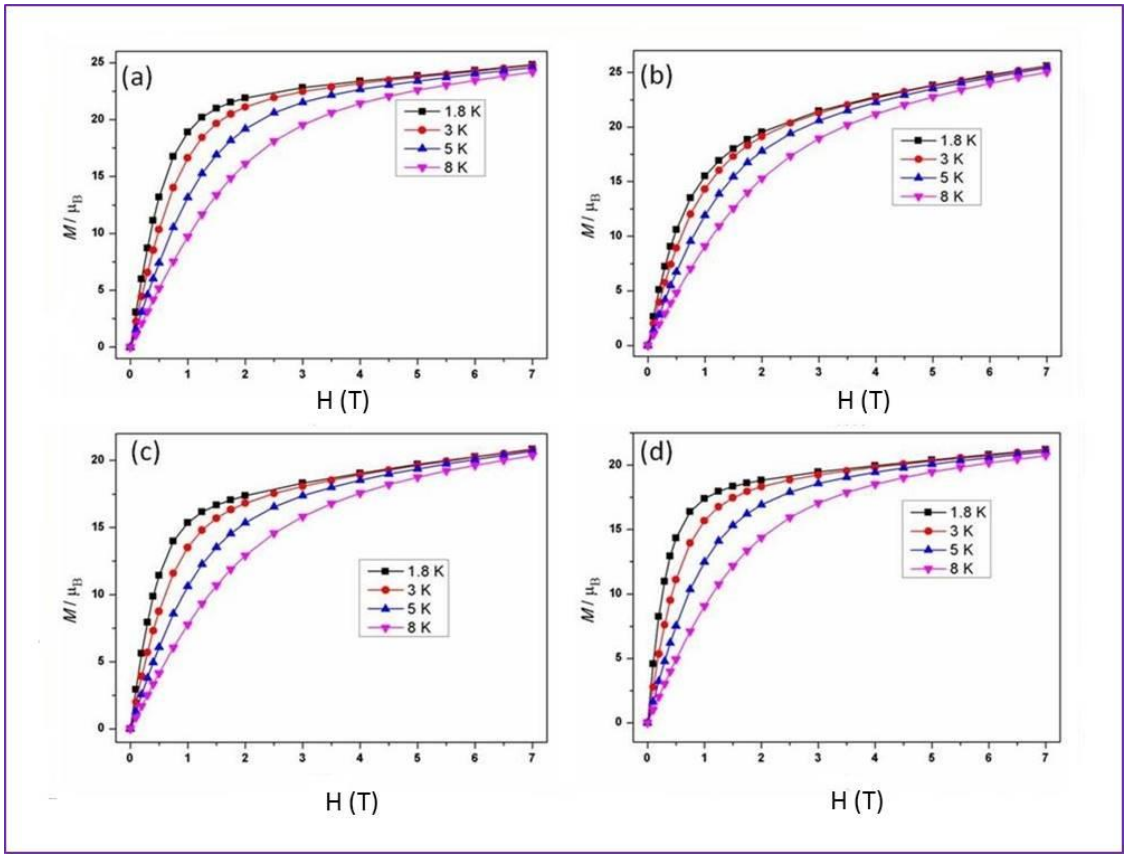

Figure 4.4. Detailed isothermal field dependant magnetization measurement of **4.1-4.4** measured from 0-7 Tesla at the indicated temperatures.

4.4.2 Dynamic Magnetic Properties:

As a result of the observed magnetic anisotropy, **4.1-4.4** were probed for dynamic magnetic behaviour using ac susceptibility measurements. The frequency dependence of ac magnetic susceptibility was measured for all the clusters, **4.3** and **4.4** were measured in the temperature range of 1.8 to 10 K and 1.8 to 5.5 K under an applied field as shown in figure 4.5. Below 5K, the imaginary components exhibit obvious peak values that vary with frequency as temperature increases under an applied magnetic field. This indicates the onset of field induced slow magnetic relaxation for **4.3**. Complex **4.1** and **4.2** do not show any sign of slow relaxation of the magnetization under zero field or under an applied field suggesting the absence of retention of magnetization for these complexes.

The magnetization plot in the form of lnT vs 1/T, derived from ac measurements is shown in figure **4.6** (for **4.3** and **4.4**). Fitting the data by using Arrhenius law provided the energy barrier of 10.2 K with a relaxation time (τ_0) 4.373 x 10^{-6} s for **4.3**, while in case of

compound **4.4** it gave an energy barrier value of 14.9 K with a relaxation time of (τ_0) 7.831 x 10^{-7} s. These parameters are similar to those reported for similar planar Dy_4 compounds in the literature (Table 4.**7**).

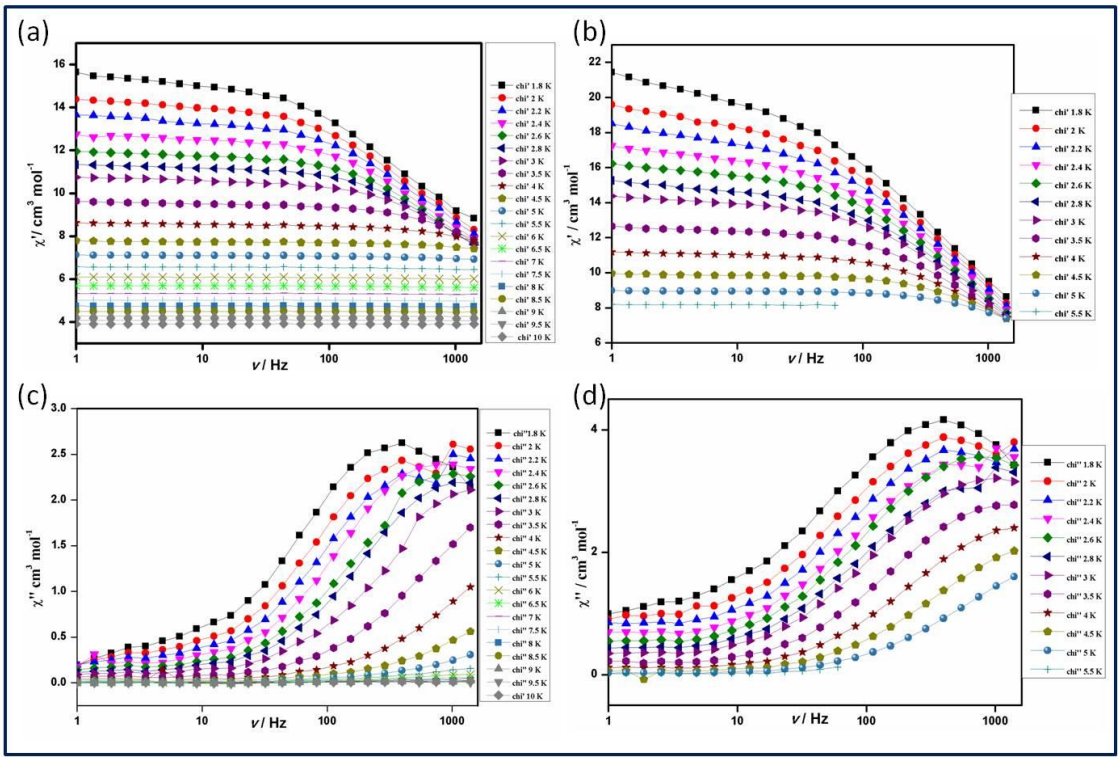

Figure 4.5. Alternating current magnetic susceptibility measurement performed on polycrystalline samples of **4.3** and **4.4** showing the frequency dependent in-phase (χ_M') [(a) and (b)] and out-of-phase susceptibility signals (χ_M'') in applied magnetic field of 1000 Oe [(c) and (d)].

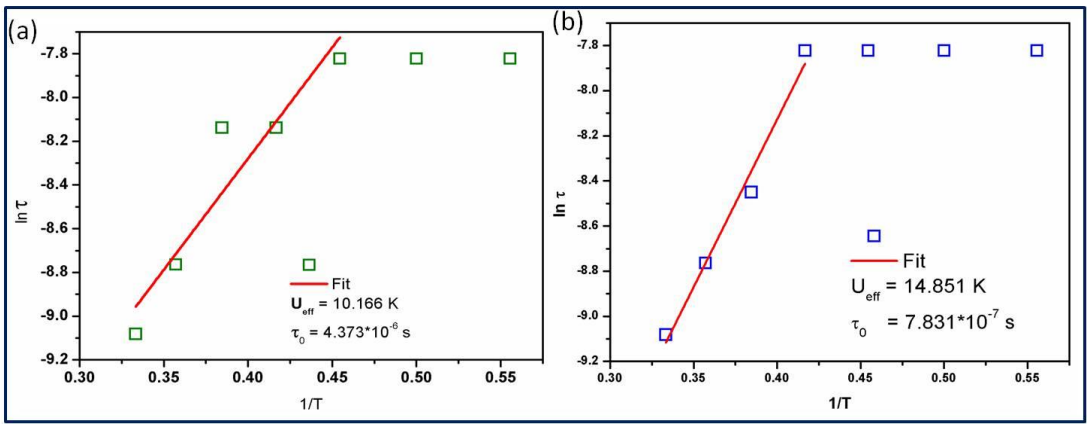

Figure 4.6. Arrhenius plot for compounds **4.3** and **4.4**

4.5 Conclusion

To summarize, a new family of tetranuclear lanthanide oxo/hydroxo clusters was synthesized and structurally characterized by using triketones as ligands. Clusters **4.3** and **4.4** exhibit SMM behaviour with an energy barrier of 10.166 K and 14.851 K under an applied external magnetic field. Employing triketones as flexible ligand systems in presence/absence of co-ligands provides a promising route towards the synthesis of newer families of lanthanide clusters with interesting magnetic properties.

Table 4.1. Crystal data and structure refinement for **4.1-4.4**

	4.1	**4.2**	**4.3**	**4.4**
Empirical formula	C_{106} H_{80} Cl_6 O_{22} Dy_4	C_{108} H_{82} Cl_{12} O_{22} HO_4	C_{60} H_{60} F_{36} N_2 O_{26} Dy_4	C_{48} H_{36} F_{24} O_{22} Dy_4
Fw.g mol^{-1}	2568.40	2816.85	2559.10	2070.77
Crystal system	Monoclinic	Monoclinic	Triclinic	Triclinic
Space group	C 2/c	C 2/c	P-1	P-1
a/Å	32.013(3)	32.078(4)	12.172(3)	13.425(3)
b/Å	14.5495(14)	14.5468(18)	12.396(3)	13.668(3)
c/Å^3	24.088(2)	24.116(3)	15.584(3)	14.118(3)
α (°)	90	90	96.853(12)	92.879
β (°)	92.551(2)	92.952(2)	103.071(12)	115.697(2)
γ (°)	90	90	110.734(12)	117.191
v/Å	11208.6(19)	11238(2)	2090.2(8)	9560.0(17)
Z	4	4	1	1
ρ_c/Mg m^{-3}	1.522	1.665	2.033	1.742
μ/mm^{-1}	2.843	3.137	3.687	3.856
F(000)	5032	5512	1230	980
θ range(°)	1.273 to 25.067	1.537 to 25.140	2.360 to 27.694	2.787 to 27.670
reflections collected	51810	50542	171609	144789
Completeness to θ (%)	99.7	98.9	99.9	99.8

independent reflections/R_{int}	9920/ 0.0586	9955/0.0719	9695/0.0757	9175/0.0655
GooF(F^2)	1.079	1.058	1.048	1.069
Final R indices (I>2σ(I))	R_1 = 0.0424 wR_2 = 0.0923	R_1 = 0.0577 wR_2 = 0.1298	R_1 = 0.0273 wR_2 = 0.0655	R1 = 0.0272 wR2 = 0.0692
R indices (all data)	R_1 = 0.0527 wR_2 = 0.0961	R_1 = 0.0722 wR_2 = 0.1365	R1 = 0.0351 wR2 = 0.0696	R1 = 0.0296 wR2 = 0.0705

Table 4.2. Summary of **SHAPE** analysis for complex **4.1- 4.4**.

S.No.	**Geometry**	CShM values for Dy1 in **4.1**	CShM values for Ho1 in **4.2**	CShM values for Dy1 in **4.3**	CShM values for Dy1 in **4.4**
1	Octagon(D8h)	30.361	30.268	29.702	29.957
2	Heptagonal pyramid(C7v)	20.851	21.821	22.108	23.442
3	Hexagonal bipyrami(D6h)	14.813	16.749	16.770	15.996
4	Cube(Oh)	9.009	10.009	10.215	8.708
5	**Square antiprism(D4d)**	**0.829**	**0.504**	**0.434**	**0.820**
6	Triangular dodecahedron(D2d)	1.974	2.045	2.319	1.462
7	Johnson gyrobifastigium J26(D2d)	15.026	16.313	16.247	16.165
8	Johnson elongated triangular bipyramid J14(D3h)	27.334	28.326	28.094	28.352
9	Biaugmented trigonal prism J50(C2v)	2.487	2.949	2.893	2.664
10	Biaugmented trigonal prism(C2v)	2.165	2.037	2.162	2.112
11	Snub diphenoid J84(D2d)	4.646	5.110	5.189	4.604
12	Triakis tetrahedron(Td)	9.621	10.737	10.820	9.477
13	Elongated trigonal bipyramid(D3h)	23.034	23.884	23.760	24.332

Table 4.3. Selected Bond distances (Å) and Bond angles (°) for **4.1**

Dy(1)-O(9)	2.236(4)	O(9)-Dy(1)-O(6)	118.59(12)
Dy(1)-O(8)	2.253(4)	O(8)-Dy(1)-O(6)	73.62(13)
Dy(1)-O(10)	2.332(3)	O(10) -Dy(1)-O(6)	71.73(12)
Dy(1)-O(4)	2.379(3)	O(4) -Dy(1)-O(6)	68.21(12)
Dy(1)-O(2)	2.391(3)	O(2)-Dy(1)-O(6)	148.76(12)
Dy(1)-O(10)	2.415(3)	O(10)-Dy(1)-O(6)	133.06(12)
Dy(1)-O(6)	2.419(4)	O(7)-Dy(2)-O(5)	79.34(13)
Dy(1)-O(1)	2.482(4)	O(7)-Dy(2)-O(3)	83.02(13)
Dy(2)-O(7)	2.205(4)	O(5)-Dy(2)-O(3)	83.27(13)
Dy(2)-O(5)	2.255(4)	O(7)-Dy(2)-O(10)	140.57(12)
Dy(2)-O(3)	2.316(4)	O(5)-Dy(2)-O(10)	136.33(13)
Dy(2)-O(10)	2.340(3)	O(3)-Dy(2)-O(10)	112.43(12)
Dy(2)-O(6)	2.385(3)	O(7)-Dy(2)-O(6)	74.78(13)
Dy(2)-O(4)	2.387(4)	O(5)-Dy(2)-O(6)	119.25(12)
Dy(2)-O(2)	2.407(3)	O(3)-Dy(2)-O(6)	143.73(13)
Dy(2)-O(11)	2.476(4)	O(10)-Dy(2)-O(6)	72.20(12)
O(9)-Dy(1)-O(8)	79.54(13)	O(7)-Dy(2)-O(4)	114.55(13)
O(9)-Dy(1)-O(10)	138.81(12)	O(5)-Dy(2)-O(4)	74.32(13)
O(8)-Dy(1)-O(10)	137.95(13)	O(3)-Dy(2)-O(4)	147.63(12)
O(9)-Dy(1)-O(4	75.62(13)	O(10)-Dy(2)-O(4)	72.06(12)
O(8)-Dy(1)-O(4)	115.12(12)	O(6)-Dy(2)-O(4)	68.63(12)
O(10) -Dy(1)-O(4)	72.34(12)	O(7)-Dy(2)-O(2)	147.55(13)
O(9)-Dy(1)-O(2)	84.95(13)	O(5)-Dy(2)-O(2)	79.23(12)
O(8)-Dy(1)-O(2)	92.64(12)	O(3)-Dy(2)-O(2)	70.51(12)
O(10) -Dy(1)-O(2)	104.98(12)	O(10)-Dy(2)-O(2)	69.48(12)
O(4) -Dy(1)-O(2)	141.80(12)	O(6)-Dy(2)-O(2)	137.43(12)
O(9)-Dy(1)-O(10)	77.64(12)	O(4)-Dy(2)-O(2)	82.40(12)
O(8)-Dy(1)-O(10)	151.45(13)	O(7)-Dy(2)-O(11)	79.35(13)
O(10) -Dy(1)-O(10)	69.75(15)	O(5)-Dy(2)-O(11)	145.70(14)

Table 4.4. Selected Bond distances (Å) and Bond angles (°) for **4.2**

Ho(1)-O(7)	2.236(6)	O(10)-Ho(1)-O(10)	68.8(2)
Ho(1)-O(9)	2.244(5)	O(6)-Ho(1)-O(10)	75.36(17)
Ho(1)-O(10)	2.305(5)	O(2)-Ho(1)-O(10)	68.39(17)
Ho(1)-O(6)	2.374(5)	O(7)-Ho(1)-O(4)	118.81(19)
Ho(1)-O(2)	2.387(5)	O(9)-Ho(1)-O(4)	73.56(19)
Ho(1)-O(10)	2.395(5)	O(5)-Ho(2)-O(8)	79.08(19)
Ho(1)-O(4)	2.409(5)	O(5)-Ho(2)-O(3)	81.8(2)
Ho(1)-O(1)	2.468(6)	O(8)-Ho(2)-O(3)	83.15(18)
Ho(1)-O(7)	2.236(6)	O(5)-Ho(2)-O(10)	141.21(18)
Ho(2)-O(5)	2.209(5)	O(8)-Ho(2)-O(10)	135.84(19)
Ho(2)-O(8)	2.246(5)	O(3)-Ho(2)-O(10)	113.47(18)
Ho(2)-O(3)	2.321(6)	O(5)-Ho(2)-O(6)	114.86(19)
Ho(2)-O(10)	2.334(5)	O(8)-Ho(2)-O(6)	74.33(18)
Ho(2)-O(6)	2.369(5)	O(3)-Ho(2)-O(6)	148.07(17)
Ho(2)-O(4)	2.370(5)	O(10) -Ho(2)-O(6)	71.46(18)
Ho(2)-O(2)	2.390(5)	O(5)-Ho(2)-O(4)	75.28(19)
Ho(2)-O(11)	2.448(6)	O(8)-Ho(2)-O(2)	79.61(18)
O(7)-Ho(1)-O(9)	79.3(2)	O(3)-Ho(2)-O(2)	70.76(19)
O(7)-Ho(1)-O(10)	138.73(18)	O(10) -Ho(2)-O(2)	69.34(17)
O(9)-Ho(1)-O(10)	138.3(2)	O(6) -Ho(2)-O(2)	82.97(18)
O(7)-Ho(1)-O(6)	76.28(18)	O(4)-Ho(2)-O(2)	137.65(18)
O(9)-Ho(1)-O(6)	114.93(18)	O(5)-Ho(2)-O(11)	79.2(2)
O(10)-Ho(1)-O(6)	71.88(18)	O(8)-Ho(2)-O(11)	145.81(19)
O(7)-Ho(1)-O(2)	83.97(19)	O(3)-Ho(2)-O(11)	67.85(18)
O(9)-Ho(1)-O(2)	92.87(18)	O(10) -Ho(2)-O(11)	74.9(2)
O(10)-Ho(1)-O(2)	105.37(18)	O(6-Ho(2)-O(11)	139.32(18)
O(6)-Ho(1)-O(2)	141.49(17)	O(4)-Ho(2)-O(11)	79.77(19)
O(7)-Ho(1)-O(10)	78.34(18)	O(2)-Ho(2)-O(11)	105.92(18)
O(9)-Ho(1)-O(10)	152.1(2)	O(5)-Ho(2)-Ho(1)	117.29(14)

Table 4.5. Selected Bond distances (Å) and Bond angles (°) for **4.3**

Dy(1)-O(4)	2.280(3)	O(10)-Dy(1)-O(8)	70.10(8)
Dy(1)-O(1)	2.289(3)	O(11)-Dy(1)-O(8)	111.09(9)
Dy(1)-O(7)	2.321(3)	O(4)-Dy(1)-O(5)	74.03(9)
Dy(1)-O(10)	2.325(2)	O(1)-Dy(1)-O(5)	112.71(9)
Dy(1)-O(11)	2.383(3)	O(7)-Dy(1)-O(5)	149.01(9)
Dy(1)-O(8)	2.400(2)	O(6)-Dy(2)-O(3)	78.99(9)
Dy(1)-O(5)	2.439(2)	O(6)-Dy(2)-O(9)	77.08(9)
Dy(1)-O(2)	2.448(2)	O(3)-Dy(2)-O(9)	146.35(9)
Dy(2)-O(6)	2.293(3)	O(6)-Dy(2)-O(10)	138.31(9)
Dy(2)-O(3)	2.297(3)	O(3)-Dy(2)-O(10)	137.39(8)
Dy(2)-O(9)#1	2.338(3)	O(9) -Dy(2)-O(10)	74.77(8)
Dy(2)-O(10)	2.351(2)	O(6)-Dy(2)-O(8)	90.75(9)
Dy(2)-O(8)#1	2.378(2)	O(3)-Dy(2)-O(8)	85.85(9)
Dy(2)-O(10)#1	2.392(2)	O(9) -Dy(2)-O(8)	71.22(9)
Dy(2)-O(2)	2.442(2)	O(10)-Dy(2)-O(8)	108.25(9)
Dy(2)-O(5)	2.444(2)	O(6)-Dy(2)-O(10)	150.29(9)
O(4)-Dy(1)-O(1)	74.60(10)	O(3)-Dy(2)-O(10)	77.79(9)
O(4)-Dy(1)-O(7)	82.07(10)	O(9) -Dy(2)-O(10)	114.44(9)
O(1)-Dy(1)-O(7)	78.54(9)	O(10)-Dy(2)-O(10)	70.77(9)
O(4)-Dy(1)-O(10)	141.28(9)	O(8) -Dy(2)-O(10)	69.37(8)
O(1)-Dy(1)-O(10)	136.19(9)	O(6)-Dy(2)-O(2)	116.04(9)
O(7)-Dy(1)-O(10)	121.06(9)	O(3)-Dy(2)-O(2)	74.96(8)
O(4)-Dy(1)-O(11)	79.86(10)	O(9) -Dy(2)-O(2)	137.40(8)
O(1)-Dy(1)-O(11)	145.72(9)	O(10)-Dy(2)-O(2)	69.75(8)
O(7)-Dy(1)-O(11)	75.60(10)	O(8) -Dy(2)-O(2)	142.44(8)
O(10)-Dy(1)-O(11)	77.30(9)	O(10) -Dy(2)-O(2)	75.11(8)
O(4)-Dy(1)-O(8)	148.22(9)	O(6)-Dy(2)-O(5)	74.54(9)
O(1)-Dy(1)-O(8)	81.62(9)	O(3)-Dy(2)-O(5)	114.52(9)
O(7)-Dy(1)-O(8)	72.66(9)	O(9) -Dy(2)-O(5)	81.25(9)

Table 4.6. Selected Bond distances (Å) and Bond angles (°) for **4.4**

Dy(1)-O(8)	2.269(3)	O(1)-Dy(1)-O(9)	77.37(9)
Dy(1)-O(6)	2.291(3)	O(11)-Dy(1)-O(9)	69.32(8)
Dy(1)-O(7)	2.294(3)	O(8)-Dy(1)-O(2)	155.90(9)
Dy(1)-O(1)	2.305(2)	O(6)-Dy(1)-O(2)	105.08(9)
Dy(1)-O(11)	2.332(2)	O(7)-Dy(1)-O(2)	129.90(9)
Dy(1)-O(9)	2.457(2)	O(3)-Dy(2)-O(4)	76.86(9)
Dy(1)-O(2)	2.501(2)	O(3)-Dy(2)-O(11)	79.62(9)
Dy(1)-O(5)	2.513(2)	O(4)-Dy(2)-O(11)	148.56(9)
Dy(2)-O(3)	2.303(2)	O(3)-Dy(2)-O(11)	138.92(8)
Dy(2)-O(4)	2.317(2)	O(4)-Dy(2)-O(11)	138.55(9)
Dy(2)-O(11)	2.325(2)	O(11) -Dy(2)-O(11)	71.94(9)
Dy(2)-O(11)	2.326(2)	O(3)-Dy(2)-O(10)	146.98(9)
Dy(2)-O(10)	2.331(2)	O(4)-Dy(2)-O(10)	78.56(9)
Dy(2)-O(9)	2.356(2)	O(11) -Dy(2)-O(10)	112.75(8)
Dy(2)-O(5)	2.414(2)	O(11)-Dy(2)-O(10)	73.10(8)
Dy(2)-O(2)	2.457(2)	O(3)-Dy(2)-O(9)	83.88(9)
O(8)-Dy(1)-O(6)	80.55(10)	O(4)-Dy(2)-O(9)	85.70(9)
O(8)-Dy(1)-O(7)	73.38(10)	O(11) -Dy(2)-O(9)	71.22(8)
O(6)-Dy(1)-O(7)	85.10(10)	O(11)-Dy(2)-O(9)	113.00(8)
O(8)-Dy(1)-O(1)	85.65(10)	O(10) -Dy(2)-O(9)	72.57(9)
O(6)-Dy(1)-O(1)	78.48(10)	O(3)-Dy(2)-O(5)	111.87(9)
O(7)-Dy(1)-O(1)	155.24(10)	O(4)-Dy(2)-O(5)	74.10(9)
O(8)-Dy(1)-O(11)	121.36(9)	O(11) -Dy(2)-O(5)	134.90(8)
O(6)-Dy(1)-O(11)	139.43(9)	O(11)-Dy(2)-O(5)	72.43(8)
O(7)-Dy(1)-O(11)	71.67(9)	O(10) -Dy(2)-O(5)	81.74(9)
O(1)-Dy(1)-O(11)	132.09(8)	O(9) -Dy(2)-O(5)	150.04(8)
O(8)-Dy(1)-O(9)	82.25(9)	O(3)-Dy(2)-O(2)	74.75(8)
O(6)-Dy(1)-O(9)	151.23(9)	O(4)-Dy(2)-O(2)	116.07(8)
O(7)-Dy(1)-O(9)	111.72(9)	O(9) -Dy(2)-O(2)	144.12(8)

Table 4.7. Butterfly shaped tetranuclear compounds and their energy barriers

S. No	Formula of Dy4 compound	Energy barrier/K	Pre-exponential factor
1.	$[Dy_4(\mu_3\text{-}OH)_2(hmmpH)_2(hmmp)(N_3)_4]$[20a]	7.0	3.8×10^{-5}
2.	$[Dy_4(\mu_3\text{-}OH)_2(mdeaH)_2(piv)_8]$[12c]	6.2	2.4×10^{-5}
3.	$[Dy_4(\mu_3\text{-}OH)_2(ampdH_4)_2(piv)_{10}]$[12g]	5.4	1.1×10^{-5}
4.	$[Dy_4(\mu_3\text{-}OH)_2(ovn)(piv)_4(NO_3)_2]$[12j]	6.25	3.75×10^{-5}
5.	$[Dy_4(\mu_3\text{-}OH)_2(L7)_4(HL7)_2]$[12k]	3.7	4.8×10^{-5}
6.	$[Dy_4(\mu_3\text{-}OH)_2(L)_8(acac)_6]$[12l]	22	3.66×10^{-6}

4.6 References

(1) a) Eliseeva, S. V.; Bunzli, J.-C. G. *Chem. Soc. Rev*. **2010**, *39*, 189. (b) Heffern, M. C.; Matosziuk, L. M.; Meade, T. J. *Chem. Rev*. **2014**, *114*, 4496.

(2) (a) Anwander, R. *Lanthanides: Chemistry and Use in Organic Synthesis*; Springer: Berlin, Heidelberg, **1999**. (b) Shibasaki, M.; Yamada K.-I.; Yoshikawa, N. Lanthanide Lewis Acids Catalysis. In *Lewis Acids in Organic Synthesis*; Wiley-VCH Verlag GmbH: Weinheim, **2008**, 911. (c) Roesky, P. W. *Molecular Catalysis of Rare-Earth Elements*; Springer: Berlin, Heidelberg, **2010**. (d) Anastasiadis, N. C.; Granadeiro, C. M.; Klouras, N.; Cunha-Silva, L.; Raptopoulou, C. P.; Psycharis, V.; Bekiari, V.; Balula, S. S.; Escuer A.; Perlepes, S. P. *Inorg. Chem.* **2013**, *52*, 4145. (e) Robinson, J. R.; Gu, J.; Carroll, P. J.; Schelter E. J.; Walsh, P. J. *J. Am. Chem. Soc*. **2015**, *137*, 7135. (f) Roesky, P. W.; Canseco-Melchor G.; Zulys, A. *Chem. Commun*. **2004**, 738.

(3) a) Woodruff, D. N.; Winpenny R. E. P.; Layfield, R. A. *Chem. Rev*. **2013**, *113*, 5110. b) Neville, S. M.; Halder, G. J.; Chapman, K. W.; Duriska, M. B.; Moubaraki, B.; Murray K. S.; Kepert, C. J. *J. Am. Chem. Soc*. **2009**, *131*, 12106. c) Ungur, L.;

Langley, S. K.;. Hooper, T. N.; Moubaraki, B.; Brechin, E. K.; Murray K. S.; Chibotaru, L. F. *J. Am. Chem. Soc*. **2012**, *134*, 18554. d) Le Roy, J. J.; Ungur, L.; Korobkov, L.; . Chibotaru L. F.; Murugesu, M. *J. Am. Chem. Soc.* **2014**, *136*, 8003. e) Chilton, N. F.; Collison, D.; McInnes, E. J. L.; Winpenny R. E. P.; Soncini A. *Nat. Commun*. **2013**, *4*, 2551. f) Chandrasekhar, V.; Bag P.; Colacio, E. *Inorg. Chem*. **2013**, *52*, 4562. g) Chandrasekhar, V.; Dey, A.; Das, S.; Rouzières, M.; Clérac, R. *Inorg. Chem*. **2013**, *52*, 2588. h) Goura, J.; Walsh, J.P. S.; Tuna F.;. Chandrasekhar, V. *Inorg. Chem*. **2014**, *53*, 3385. i) Goura, J.; Mereacre, V.; Novitchi, G.; Powell A. K.; Chandrasekhar, V. *Eur. J. Inorg. Chem*. **2015**, 156. j) Baniodeh, A.; Mereacre, V.; Magnani, N.; Lan, Y.; Wolny, J. A.; Schünemann, V.; Anson C. E.; Powell, A. K. *Chem. Commun*. **2013**, *49*, 9666. i) Baniodeh, A.; Magnani, N.; Bräse, S.; Anson C. E.; Powell, A. K. *Dalton Trans*. **2015**, *44*, 6343.

(4) Ishikawa, N.; Sugita, M.; Ishikawa, T.; Koshihara S.;. Kaizu, Y. *J. Am. Chem. Soc*. **2003**, *125*, 8694. (b) Takamatsu, S.; Ishikawa, T.; Koshihara S.; Ishikawa, N. *Inorg. Chem*. **2007**, *46*, 7250. (c) AlDamen, M. A.; Cardona-Serra, S. Clemente-Juan, J. M.; Coronado, E.; Gaita-AriÇo, A.; Martí-Gastaldo, C.; Luis, F. Montero, O. *Inorg. Chem*. **2009**, *48*, 3467 . (d) Jiang, S.-D.; Liu, S.-S.; Zhou, L.-N.; Wang, B.-W.; Wang Z.-M.; Gao, S. *Inorg. Chem*. **2012**, *51*, 3079. (e) Jiang, S.-D.; Wang, B.-W.; Sun, H.-L.; Wang, Z.-M.; Gao, S. *J. Am. Chem. Soc.* **2011**, *133*, 4730. (f) Cucinotta, G.; Perfetti, M.; Luzon, J.; Etienne, M.; Car, P.-E.; Caneschi, A.; Calvez, G.; Bernot K.; Sessoli, R. *Angew. Chem. Int. Ed*. **2012**, *124*, 1638. *Angew. Chem. Int. Ed.* **2012**, *51*, 1606. (g) Ungur, L.; Le Roy, J. J.; Korobkov, I.; Murugesu, M.; . Chibotaru, L. F.; *Angew. Chem. Int. Ed.* **2014**, *53*, 4413. (h) Zhu, J.; Wang, C.; Luan, F.; Liu, T.; Yan P.; Li, G. *Inorg. Chem*. **2014**, *53*, 8895.

(5) a) Clérac, R.; Miyasaka, H.; Yamashita M.; Coulon, C. *J. Am. Chem. Soc*. **2002**, *124*, 12837. (b) Miyasaka, H.; Julve, M.; Yamashita M.; Clerac, R. *Inorg. Chem*. **2009**, *48*, 3420. (c) Bernot, K.; Bogani, L.; Caneschi, A.; Gatteschi, D.; Sessoli, R. *J. Am. Chem. Soc*. **2006**, *128* , 7947. (d) Bogani, L.; Sangregorio, C.; Sessoli, R.; Gatteschi, D. *Angew. Chem. Int. Ed*. **2005**, *117*, 5967 . (e) Bernot, K.; Bogani, L.; Sessoli R.; Gatteschi, D. *Inorg. Chem. Acta*. **2007**, *360*, 3807. (g) Li, X-L.; Chen, C-L.; Xiao, H-P.; Wang, A-L.;. Liu, C-M.; Zheng, X.; Gao, L-J.; Yanga X-G., Fang, S-M. *Dalton Trans*., **2013**, *42*, 15317.

(6) (a) Sessoli, R.; Gatteschi, D.; Caneschi A.; Novak, M. A.; *Nature*. **1993**, *365*, 141; (b) Murrie, M. *Chem. Soc. Rev*. **2010**, *39*, 1986. (c) Woodruff, D. N.; Winpenny R. E. P.; Layfield, R. A.; *Chem. Rev*. **2013**, *113*, 5110. (d) Zhang, P.; Guo Y.-N.; Tang, J. *Coord. Chem. Rev*. **2013**, *257*, 1728. (e) Ishkawa, N.; Sugita, M.; Ishikawa, T.; Koshihara S.; Kaizu, Y. *J. Am. Chem. Soc*. **2003**, *125*, 8694. (f) Branzoli, F.; Carretta, P.; Filibian, M.; Zoppellaro, G.; Graf, M. J.; Galan-Mascaros, J. R.; Fuhr, O.; Brink S.; Ruben, M.; *J. Am. Chem. Soc*. **2009**, *131*, 4387. (g) Gonidec, M.; Amabilino D.; Veciana, J. *Dalton Trans*. **2012**, *41*, 13632. (h) Ishikawa, N.; Sugita, M.; Tanaka, N.; Ishikawa, T.; Koshihara S.; Kaizu, Y. *Inorg. Chem*. **2004**, *43*, 5498.

(7) Ishikawa, N.; Sugita, M.; Ishikawa, T.; Koshihara S.-Y.; Kaizu, Y. *J. Am. Chem. Soc*. **2003**, *125*, 8694.

(8) (a) Rinehart, J. D.; Fang, M.; Evans W. J.; Long, J. R. *J. Am. Chem. Soc*. **2011**, *133*, 14236.

(9) (a) Fortea-Pérez, F. R.; Vallejo, J.; Julve, M.; Lloret, F.; De Munno, G.; Armentano D.; Pardo, E. *Inorg. Chem*. **2013**, *52*, 4777. (b) Zhang, S.; Ke, H.; Sun, L.; Li, X.; Shi, Q.; Xie, G.; Wei, Q.; Yang, D.; Wang W.; Chen, S. *Inorg. Chem*. **2016**, *55*, 3865. (c) Jiang, Z.-X.; Liu, J.-L.; Chen, Y.-C.; Liu, J.; Jia J.-H.; Tong M.-L. *Chem. Commun*. **2016**, *52*, 6261. (d) Zhang, X.-J.; Liu, K.; Bing, Y.-M.; Xu, N.; Shi W.; Cheng P. *Dalton Trans*. **2015**, *44*, 7757. (e) Liu, J.-L.; Chen, Y.-C.; Zheng, Y.-Z.; Lin, W.-Q.; Ungur, L.; Wernsdorfer, W.; Chibotaru, L. F.; Tong, M.-L. *Chem. Sci*. **2013**, ***4***, 3310. (f) Campbell, V. E.; Bolvin, H.; Rivière, E.; Guillot, R.; Wernsdorfer W.; Mallah, T. *Inorg. Chem*. **2014**, *53*, 2598. (g) Zhu, J.; Wang, C. Z.; Luan, F.; Liu, T. Q.; Yan P. F.; Li, G. M. *Inorg. Chem*. **2014**, *53*, 8895. (h) Gao, F.; Cui, L.; Song, Y.; Li, Y.-Z.; Zuo, J.-L. *Inorg. Chem*. **2014**, *53*, 562.(i) Wang, Y.; Li, X. L.; Wang, T. W.; Song, Y.; You, X. Z. *Inorg. Chem*. **2010**, *49*, 969.

(10) (a) Long, J.; Habib, F.; Lin, P.-H.; Korobkov, I.; Enright, G.; Ungur, L.; Wernsdorfer, W.; Chibotaru L. F.; Murugesu, M. *J. Am. Chem. Soc*. **2011**, *133*, 5319. (b) Han, T.; Shi, W.; Zhang, X. P.; Li, L. L.; Cheng, P. *Inorg. Chem*. **2012**, *51*, 13009. (c) Wang, W.-M.; Zhang, H.-X.; Wang, S.-Y.; Shen, H.-Y.; Gao, H.-L.; Cui J.-Z.; Zhao, B. *Inorg. Chem*. **2015**, *54*, 10610. (d) Wang, Y.-L.; Han, C.-B.; Zhang, Y.-Q.; Liu, Q.-Y.; Liu C.-M.; Yan, S.-G. *Inorg. Chem*. **2016**, *55*, 5578.(e) Feng, M.; Pointillart, F.; Lefeuvre, B.; Dorcet, V.; Golhen, S.; Cador O.; Ouahab, L. *Inorg. Chem*. **2015**, *54*,

4021. (f) Brunet, G.; Habib, F.; Korobkov, I.; Murugesu, M.; *Inorg. Chem*. **2015**, *54*, 6195.

(11) a) Shen, S.; Xue S.; Lin, S.-Y.; Zhao L.; Tang, J. *Dalton Trans*. **2013**, *42*, 10413. (b) Lin, S.-Y.; Zhao, L.; Guo, Y.-N.; Zhang, P.; Guo Y.; Tang, J. *Inorg. Chem*. **2012**, *51*, 10522. (c) Hewitt, I. J.; Tang, J.; Madhu, N. T.; Anson, C. E.; Lan, Y.; Luzon, J.; Etienne, M.; Sessoli R.; Powell, A. K. *Angew. Chem., Int. Ed*. **2010**, *49*, 6352. (d) Luzon, J.; Bernot, K.; Hewitt, I. J.; Anson, C. E.; Powell A. K.; Sessoli, R. *Phys. Rev. Lett*. **2008**, *100*, 247205; (e) Tang, J.; Hewitt, I.; Madhu, N. T.; Chastanet, G.; Wernsdorfer, W.; Anson, C. E.; Benelli, C.; Sessoli, R.; Powell, A. K. *Angew. Chem., Int. Ed*. **2006**, *45*, 1729.

(12) a) McLellan, R.; Palacios, M. A.; Beavers, C. M.; Teat, S. J.; Brechin E. K.; Dalgarno, S. J. *Chem. Commun*. **2013**, *49*, 9552. (b) Hewitt, I. J.; Lan, Y.; Anson, C. E.; Luzon, J.; Sessoli R.; Powell, A. K. *Chem. Commun*. **2009**, 6765. (c) Abbas, G.; Lan, Y.; Kostakis, G. E.; Wernsdorfer, W.; Anson C. E.; Powell, A. K. *Inorg. Chem*. **2010**, *49*, 8067. (d) Guo, Y.-N.; Xu, G.-F.; Gamez, P.; Zhao, L.; Lin, S.-Y.; Deng, R.; Tang J.; Zhang, H.-J. *J. Am. Chem. Soc*. **2010**, *132*, 8538. (e) Lin, S.-Y.; Zhao, L.; Ke, H.; Guo, Y.-N.; Tang, J.; Guo Y.; Dou, J. *Dalton Trans*. **2012**, *41*, 3248. (f) Ke, H.; Xu, G.-F.; Guo, Y.-N.; Gamez, P.; Beavers, C. M.; Teat S. J.; Tang, J. *Chem. Commun*. **2010**, *46*, 6057. (g) Abbas, G.; Kostakis, G. E.; Lan Y.; Powell, A. K. *Polyhedron* **2012**, *41*, 1. (h) Langley, S. K.; Chilton, N. F.; Gass, I. A.; Moubaraki B.; Murray, K. S. *Dalton Trans*. **2011**, *40*, 12656.(i) Gass, I. A.; Moubaraki, B.; Langley, S. K.; Batten, S. R.; Murray, K. S. *Chem. Commun*. **2012**, *48*, 2089. (J) Langley, S. K.; Chliton, N. F.; Gass, I. A.; Moubaraki, B. ; Murray, K. S. *Dalton Trans*. **2011**, *40*, 12656. (K) Mondal, K. C.; Kostakis, G. E.; Lan, Y. H.; Powell, A. K. *Polyhedron* **2013**, *66*, 268. (l) Yan, P. F.; Lin, P. H.; Habib, F.; Aharen, T.; Murugesu, M.; Deng, Z. P.; Li, G. M.; Sun, W. B. *Inorg. Chem*. **2011**, *50*, 7059.

(13) a) Tian, H.; Zhao, L.; Lin, H.; Tang, J.; Li, G. *Chem. - Eur. J*. **2013**, *19*, 13235. b) Yadav, M.; Mondal, A.; Mereacre, V.; Jana, S. K.; Powell, A. K.; Roesky, P. W. *Inorg. Chem*. **2015**, *54*, 7846. c) Thielemann, D. T.; Wagner, A. T.; Lan, Y.; Anson, C. E.; Gamer, M. T.; Powell A. K.; Roesky, P. W. *Dalton Trans*. **2013**, *42*, 14794. d) Peng, J.-B.; Kong, X.-J.; Ren, Y.-P.; Long, L.-S.; Huang R.-B.; Zheng, L.-S. *Inorg.Chem*. **2012**, *51*, 2186.

(14) (a) Blagg, R. J.; Muryn, C. A.; McInnes, E. J. L.; Tuna F.; Winpenny, R. E. P. *Angew. Chem., Int. Ed*. **2011**, *50*, 6530. (b) Das, S.; Hossain, S.; Dey, A.; Biswas, S.; Sutter J.-P.; Chandrasekhar, V. *Inorg. Chem.* **2014**, *53*, 5020. (c) Lin, S.-Y.; Wernsdorfer, W.; Ungur, L.; Powell, A. K.; Guo, Y.-N.; Tang, J.; Zhao, L.; Chibotaru L. F.; Zhang, H.-J. *Angew. Chem., Int. Ed*. **2012**, *51*, 12767. (d) Sharples, J. W.; Zheng, Y.-Z.; Tuna, F.; McInnes E. J. L.; Collison, D. *Chem. Commun*. **2011**, *47*, 7650.

(15) (a) Wang, R.; Liu, H.; Carducci, M. D.; Jin, T.; Zheng C.; Zheng, Z. *Inorg. Chem*. **2001**, *40*, 2743. (b) Wang, R.; Carducci M. D.; Zheng, Z. *Inorg. Chem*. **2000**, *39*, 1836. (c) Wang, R.; Zheng, Z.; Jin T.; Staples, R. J. *Angew. Chem., Int. Ed.* **1999**, *38*, 1813. (d) Wang, R.; Selby, H. D.; Liu, H.; Carducci, M. D.; Jin, T.; Zheng, Z.; Anthis J. W.; Staples, R. J. *Inorg. Chem*. **2002**, *41*, 278. (e) Kong, X.-J.; Wu, Y.; Long, L.-S.; Zheng L.-S.; Zheng, Z. *J. Am. Chem. Soc*. **2009**, *131*, 6918. (f) Zheng, Z. *Chem. Commun*. **2001**, 2521.

(16) (a) Andrews, P. C.; Deacon, G. B.; Frank, R.; Fraser, B. H.; Junk, P. C.; MacLellan, J. G.; Massi, M.; Moubaraki, B.; Murray K. S.; Silberstein, M.; *Eur. J. Inorg. Chem*. **2009**, *6*, 744. (b) Baskar V.; Roesky, P. W.; *Z. Anorg. Allg. Chem.* **2005**, *631*, 2782. (c) Baskar V.; Roesky, P. W.; *Dalton Trans*. **2006**, 676. (d) Roesky, P. W.; CansecoMelchor G.; Zulys, A. *Chem. Commun*. **2004**, 738 (e) Bürgstein, M. R.; Gamer M. T.; Roesky, P. W. *J. Am. Chem. Soc*. **2004**, *126*, 5213. (f) Bürgstein M. R.; Roesky, P. W. *Angew. Chem., Int. Ed*. **2000**, *39*, 549. (g) Andrews, P. C.; Beck, T.; Fraser, B. H.; Junk, P. C.; Massi, M.; Moubaraki, B.; Murry K. S.; Silberstein, M. *Polyhedron* **2009**, *28*, 2123. (h) Petit, S.; Baril-Robert, F.; Pilet, G.; Reber C.; Luneau, D. *Dalton Trans*. **2009**, 6809. (i) Gamer, M. T.; Lan, Y.; Roesky, P. W.; Powell A. K.; Clerac, R. *Inorg. Chem*. **2008**, *47*, 6581. (k) Hubert-Pfalzgraf, L. G.; Meile-Pajot, N.; Papiernik R.; Vaissermann, J. *J. Chem. Soc., Dalton Trans*. **1999**, 4127. (l) Xu, G.; Wang, Z. M.; He, Z.; Lu, Z.; Liao C. S.; Yan, C. H. *Inorg. Chem*. **2002**, *41*, 6802. (m) Addamo, M.; Bombieri, G.; Foresti, E.; Grillone, M. D.; Volpe, M. *Inorg. Chem*. **2004**, ***43***, 1603. (n) Bombieri, G.; Clemente, D. A.; Foresti, E.; Grillone M. D.; Volpe, M. *J. Alloys Compd*. **2004**, *374*, 382. (o) Andrews, P. C.; Beck, T.; Forsyth, C. M.; Fraser, B. H.; Junk, P. C.; Massi M.; Roesky, P. W. *Dalton Trans*. **2007**, 5651. (p) Barash, E. H.; Coan, P. S.; Lobkovsky, E. B.; Streib W. E.; Caulton, K. G. *Inorg. Chem*. **1993**, *32*, 497. (q) Xiong, R.-G.; Zuo, J.-L.; Yu, Z.; You X.-Z.; Chen, W. *Inorg. Chem. Commun.* **1999**, *2*, 490. (r) Wang, R.; Song D.; Wang, S. *Chem. Commun*. **2002**, 368. (s) Wu, Y.;

Morton, S.; Kong, X.; Nichol G. S.; Zheng, Z. *Dalton Trans*. **2011**, *40*, 1041. (t) Andrews, P. C.; Gee, W. J.; Junk P. C.; MacLellan, J. G. *Dalton Trans*. **2011**, *40*, 12169. (u) Andrews, P. C.; Gee, W. J.; Junk P. C.; MacLellan, J. G. *Polyhedron* **2011**, *30*, 2837. (v) Yadav, M.; Mondal, A.; Mereacre, V.; Jana, S. K.; Powell A. K.; Roesky, P. W. *Inorg. Chem*. **2015**, *54*, 7846. (w) Hui, Y.-C.; Meng, Y.-S.; Li, Z.; Chen, Q.; Sun, H.-L.; Zhangd Y.-Q.; Gao, S. *CrystEngComm.* **2015**, *17*, 5620. (x) Thielemann, D. T.; Wagner, A. T.; Lan, Y.; Oña-Burgos, P.; Fernãndez, I.; Rösch, E. S.; Kölmel, D. K.; Powell, A. K.; Bräse S.; Roesky, P. W. *Chem. -Eur. J.* **2015**, *21*, 2813.

(17) (a) Kritikos, M.; Moustiakimov, M.; Wijk M.; Westin, G. *Dalton Trans*. **2001**, 1931 . (b) Blagg, R. J.; Muryn, C. A.; McInnes, E. J. L.; Tuna F.; Winpenny, R. E. P. *Angew. Chem., Int. Ed*. **2011**, *50*, 6530. (c) kritikos, M.; Moustiakimov M.; Westin, G. *Inorg. Chim. Acta.* **2012**, *384*, 125.(d) Blagg, R. J.; Ungur, L.; Tuna, F.; Speak, J.; Comar, P.; Collison. D.; Wernsdorfer, W.; McInnes, E. J. L.; Chibotaru L. F.; Winpenny, R. E. P. *Nat. Chem*. **2013**, *5*, 673.

(18) (a) Das, M. C.; Ghosh, S. K.; Sanudo E. C.; Bharadwaj, P. K. *Dalton Trans*. **2009**, 1644. (b) Li, C.-J.; Lin, Z.-J.; Peng, M.-X.; Leng, J.-D.; Yang M.-M.; Tong, M.-L. *Chem. Commun*. **2008**, 6348. (c) Li, C.-J.; Peng, M.-X.; Leng, J.-D.; Yang, M.-M.;. Lin, Z.-J.; Tong, M.-L. *CrystEngComm* **2008**, *10*, 1645. (d) Gao, H.-L.; Yi, L.; Ding, B.; Wang, H.-S.; Cheng, P.; Liao D.-Z.; Yan, S.-P. *Inorg. Chem.* **2006**, *45*, 481. (e) Ghosh S. K.; Bharadwaj, P. K. *Eur. J. Inorg. Chem*. **2005**, 4886. (f) Zhao, X.-Q.; Zhao, B.; Shi, W.; Cheng, P. *Inorg. Chem*. **2009**, *48*, 11048. (g) Zhao, X.-Q.; Zhao, B.; Shi, W.; Cheng, P.; Liao D.-Z.; Yan, S.-P. *Dalton Trans*. **2009**, 2281. (h) Fang, S.-M.; Sañudo, E. C.; Hu, M.; Zhang, Q.; Ma, S. T.; Jia, L.-R.; Wang, C.; Tang J.-Y.; Liu, C.-S. *Cryst. Growth Des*. **2011**, *11*, 811.

(19) (a) Yang, X.; Jones R. A.; Wong, W.-K. *Dalton Trans*. **2008**, 1676. (b) Tian, H.; Guo, L.; Zhao, Y.-N.; Tang J.; Liu, Z. *Inorg. Chem*. **2011**, *50*, 8688. (c) Ke, H.; Xu, G.-F.; Zhao, L.; Tang, J.; Zhang X.-Y.; Zhang, H.-J. *Chem. – Eur. J*. **2009**, *1*, 10335. (d) Zhao, L.; Xue, S.; Tang, J. *Inorg. Chem.* **2012**, *51*, 5994. (e) Lin, P.-H.; Burchell, T. J.; Clérac R.; Murugesu, M.; *Angew. Chem. Int. Ed*. **2008**, *47*, 8848. (f) Xue, S.; Zhao, L.; Guo, Y.-N.; Zhang P.; Tang, J. *Chem. Commun*. **2012**, *48*, 8946. (g) Chandrasekhar, V.; Hossain, S.; Das, S.; Biswas S.; Sutter, J.-P. *Inorg. Chem*. **2013**, *52*, 6346. (h). Lin, P.-H.; Burchell, T. J.; Ungur, L.; Chibotaru, L. F.; Wernsdorfer W.;

Murugesu, M. *Angew. Chem. Int. Ed*. **2009**, *48*, 9489. (i) Tian, H.; Zhao, L.; Lin, H.; Tang J.; Li, G. *Chem. – Eur. J.* **2013**, *19*, 13235. (j) Tian, H.; Wang, M.; Zhao, L.; Guo, Y.-N.; Guo, Y.; Tang J.; Liu, Z. *Chem. – Eur. J.* **2012**, *18*, 442. (k) Tian, H.; Zhao, L.; Guo, Y.; Guo, Y.-N.; Tang J.; Liu, Z. *Chem. Commun*. **2012**, *48*, 708. (l) Das, S.; Dey, A.; Kundu, S.; Biswas, S.; Narayanan, R. S.; Padilla, S. T.; Lorusso, G.; Evagelisti, M.; Coalcio E.; Chandrasekhar, V. *Chem.-Eur. J.* **2015**, *21*,1.

(20) (a) Zheng, Y.-Z.; Lan, Y.; Anson C. E.; Powell, A. K. *Inorg. Chem*. **2008**, *47*, 10813. (b) Lin, P.-H.; Burchell, T. J.; Clérac R.; Murugesu, M. *Angew. Chem., Int. Ed.* **2008**, *47*, 8848. (c) Hewitt, I. J.; Lan, Y.; Anson, C. E.; Luzon, J.; Sessoli R.; Powell, A. K. *Chem Commun.* **2009**, 6765. (d) Guo, Y.-N.; Xu, G.-F.; Gamez, P.; Zhao, L.; Lin, S.-Y.; Deng, R.; Tang J.; Zhang, H.-J. *J. Am. Chem. Soc.* **2010**, *132*, 8538. (e) Gao, Y.; Xu, G.-F.; Zhao, L.; Tang J.; Liu, Z. *Inorg. Chem.* **2010**, *48*, 11495. (f) Habib, F.; Lin, P.-O.; Long, J.; Korobkov, I.; Wernsdorfer W.; Murugesu, M. *J. Am. Chem. Soc.* **2011,** *133*, 8830. (g) Zou, L.; Zhao, L.; Chen, P.; Guo, Y. – N.; Guo, Y.; Li Y.-H.; Tang, J. *Dalton Trans.* **2012**, *41*, 2966. (h) Jami, A. K.; Baskar V.; Sañudo, E. C. *Inorg. Chem.* **2013,** *52*, 2432.

(21) (a) Jiang, S. D.; Wang, B. W.; Su, G.; Wang Z. M.; Gao, S. *Angew. Chem. Int. Ed*. **2010**, *122*, 7610. *Angew. Chem. Int. Ed*. **2010**, *49*, 7448. (b) Chen, G.-J.; Gao, C.-Y.; Tian, J.-L.; Tang, J.; Gu, W.; Liu, X.; Yan, S.-P.; Liao D.-Z.; Cheng, P. *Dalton Trans*. **2011**, *40*, 5579 .

(22) Bi, Y.; Guo, Y.-N.; Zhao, L.; Guo, Y.; Lin, S.-Y.; Jiang, S. D.; Tang, J.; Wang B. W.; Gao, S. *Chem. Eur. J*. **2011**, *17*, 12476.

(23) Datta, S.; Baskar, V.; Li H.; Roesky, P. W.; *Eur. J. Inorg. Chem*. **2007**, 4216.

(24) Thielemann, D. T.; Wagner, A. T.; Rösch, E.; Kölmel, D. K.; Heck, J. G.; Rudat, B.; Neumaier, M.; Feldmann, C.; Schepers, U.; Bräse S.; Roesky, P. W. *J. Am. Chem. Soc*. **2013**, *135*, 7454 .

(25) Thielemann, D. T.; Fernández I.; Roesky, P. W. *Dalton Trans*. **2010**, *39*, 6661.

(26) Yadav, M.; Mondal, A.; Mereacre, V.; Jana, S. K.; Powell A. K.; Roesky, P. W. *Inorg. Chem*. **2015**, *54*, 7846.

(27) Longley, S. K.; Moubaraki B.; Murray, K. S. *Inorg. Chem.* **2012**, ***51***, 3947.

(28) Wang, C.; Lin, S. Y.; Wu, J. F.; Yuan S. W.; Tang, J. *Dalton Trans*. **2015**, *44*, 4648.

(29) a) Sevenard, D. V.; Kazakova, O.; Chizhov D. L.; Röschenthaler, G.-V.; *J. Fluorine Chem.* **2006**, *127*, 983. b) Knight, J. D.; Metz, C. R.; Beam, C. F.; Pennington W. T.; Vanderveer, D. G. *Syn Commun*. **2008**, *38*, 2465.

(30) (a) *SAINT Software Reference manuals*, Version 6.45; Bruker Analytical X-ray Systems, Inc.: Madison, WI, 2003. (b) Sheldrick, G. M. *SHELXS-97, Program for Crystal Structure Solution;* University of Göttingen: Göttingen, Germany, 1997. (c) Sheldrick, G. M. *Acta Crystallogr. Sect. A: Fundam. Crystallogr*. **2008**, *64*, 112. (d) Sheldrick, G. M. *Acta Crystallogr. Sect. C: Cryst. Struct. Commun*. **2015**, *71*, 3.

(31) (a) Spek, A. L. Single-crystal structure validation with the program PLATON, *J. Appl. Crystallogr*. **2003**, *36*, 7; (b) Spek, A. L. Structure validation in chemical crystallography, *Acta Crystallogr., Sect. D*: *Biol. Crystallogr*. **2009**, *65*, 148.

(32) (a) Alvarez, S.; Alemany, P.; Casanova, D.; Cirera, J.; Llunell M.; Avnir, D. *Coord. Chem. Rev*. **2005**, *249*, 1693. (b) Casanova, D.; Llunell, M.; Alemany P.; Alvarez, S. *Chem. –Eur. J.* **2005**, *11*, 1479.

Unprecedented Octanuclear Ln(III) Clusters: Synthesis, Structure and Magnetic Measurements

CHAPTER 5

A set of three isostructurally similar and novel Ln(III) clusters represented as $[Ln_8(\mu_2\text{-}\eta^1\text{:}\eta^1 cyc PO_2)12(NO_3)_6(OH)_2]4OH$ where Ln = Gd(**5.1**), Dy(**5.2**) and Y(**5.3**) have been synthesized and unambiguously characterized by single crystal X-ray diffraction studies. Reaction of 1,1,2,3,3-pentamethyltrimethylenephosphinic acid [$cyc PO_2H.2H_2O$] with $Ln(NO_3)_3.6H_2O$ in presence of base under refluxing conditions resulted in the isolation of **5.1-5.3** which represent the first examples of organophosphinate based Ln(III) clusters. Synthesis, structural elucidation and magnetic properties are discussed in this chapter.

5.1 Introduction

Lanthanide polynuclear clusters have been the centre of immense interest in last few decades. These molecular entities bestowed with complex structural features and topologies find numerous applications in various technological fields.[1] Among their multidimensional utilities, their usage in the field of molecular magnetism in general and magneto caloric effect (MCE)[2] in particular has received considerable attention in past few years owing to their environment friendly nature and energy efficiency compared to their analogous conventional refrigerants which are presently used.[3] The property of cooling called as magnetic caloric effect (MCE) is based on the change in magnetic entropy ($-\Delta S_m$) or change in adiabatic temperature (ΔT_{ad}) with respect to change in applied magnetic field. The phenomenon of cooling is attributed to magnetic demagnetization. Systems having negligible anisotropy, large spin ground state S, low-lying excited spin states and dominant ferromagnetic interactions have been found to display excellent MCE properties, thus making Gd(III), high spin Mn(II) and Fe(III) based complexes as promising candidates for molecular refrigerants.[4] Very weak magnetic exchange interactions between Gd-Gd due to efficient shielding of 4f orbitals, negligible anisotropy and high spin degeneracy makes Gd(III) as the best candidate for magnetic cooling applications. In addition, complexes with larger mass ratio of metal to non-metal (high magnetic density) and heterometallic systems where light weight 3d metals like Fe(III), Mn(II), Cr(III), Cu(II) exhibiting weak ferromagnetic interactions are deployed along with Gd, have been found to be appropriate for enhancing the magnetic cooling properties.[5] To date, many 3d, 3d-Gd(III) and Gd(III) complexes have been extensively studied and among these Gd(III) containing complexes have been found to exhibit large MCE values.[6] Various small ligand systems like hydroxides, carbonates, oxalates and acetates have been used for synthesis of Gd(III) based molecular clusters and these small ligands are efficient in controlling magnetic density.[7] Phosphorous based ligands are also considered to be the excellent candidates to procure large MCE values on account of their property to interpose weak exchange coupling between isotropic ions like Gd(III).[8] Recently Murugavel and co-workers reported an organophosphate based Gd(III) complex for which MCE property has been studied in detail.[9] To the best of our knowledge no such report exists for phosphinic acid ligand systems. In this chapter the reaction of Ln(III) ions with a cyclicphosphinic

acid in presence of a base was investigated and its synthesis, structure and magnetic properties are discussed in detail.

5.2 Experimental Section

5.2.1 General information:

All the general reagents and solvents were purchased commercially and used as received. 1,1,2,3,3-pentamethyltrimethylenephosphinic acid [*cyc*$PO_2H.2H_2O$] was prepared according to the literature procedure.[10] Hydrated lanthanum nitrates were prepared from their corresponding oxides by neutralizing with concentrated HNO_3, followed by evaporation to dryness.

5.2.2 Synthesis:

To a methanolic solution of *cyc*$PO_2H.2H_2O$, $Ln(NO_3)_3.6H_2O$ was added and stirred at room temperature for 10 minutes. To this solution, triethylamine was added dropwise and the mixture was refluxed for 3h resulting in a clear solution. Methanol was removed under reduced pressure and the residue was re-dissolved in DMF/MeOH for crystallization. Colourless crystals suitable for X-ray diffraction studies were obtained by slow evaporation of solvent mixture.

Compound **5.1**: *cyc*$PO_2H.2H_2O$ (0.100 g, 0.471 mmol), $Gd(NO_3)_3.6H_2O$ (0.212 g, 0.471 mmol), Et_3N (0.195 mL, 1.413 mmol). Yield: 0.283 g, 43.80% (based on Gd). Mp: 210 ˚C (dec). IR (KBr) cm^{-1}: 2959(s), 2865(w), 2832(m), 1551(m), 1470(s), 1386(m), 1308(s), 1128(s), 1081(s), 1040(s), 931(m), 828(m), 761(s). Anal. Calcd for $C_{96}H_{198}N_6O_{48}P_{12}Gd_8$ (3834.23): C, 30.07; H, 5.20; N, 2.19. Found: C, 29.65; H, 4.95; N, 2.09%.

Compound **5.2**: *cyc*$PO_2H.2H_2O$ (0.100 g, 0.471 mmol), $Dy(NO_3)_3.6H_2O$ (0.215 g, 0.471 mmol), Et_3N (0.195 mL, 1.413 mmol). Yield: 0.270 g, 42.12% (based on Dy). Mp: 215 ˚C (dec). IR (KBr) cm^{-1}: 2967(m), 2894(w), 2863(m), 1670(m), 1577(m), 1458(s), 1443(m), 1391(m), 1263(s), 1133(s), 1081(s), 1040(s), 931(m), 854(m), 756(s). Anal. Calcd for $C_{96}H_{198}N_6O_{48}P_{12}Dy_8$ (3876.23): C, 29.75; H, 5.15; N, 2.17. Found: C, 29.65; H, 4.9; N, 2.07%.

Compound **5.3**: *cyc*$PO_2H.2H_2O$ (0.100 g, 0.471 mmol), $Y(NO_3)_3.6H_2O$ (0.212 g, 0.471 mmol), Et_3N (0.195 mL, 1.413 mmol). Yield: 0.400 g, 41.23% (based on Y). Mp: 210˚C (dec). IR (KBr) cm^{-1}: 2970(s), 2855(w), 2842(m), 1541(m), 1469(s), 1366(m), 1328(s), 1118(s), 1065(s), 1035(s), 913(m), 818(m), 741(s). Anal. Calcd for $C_{96}H_{198}N_6O_{48}P_{12}Y_8$

(3287.51): C, 35.07; H, 6.07; N, 2.56. Found: C, 35.65; H, 4.85%. ^{1}H NMR (400 MHz, $CDCl_3$, δ, ppm): 1.253 (S, 24H), 1.721 (S, 96H), 2.923 (S, 12H); ^{31} P NMR (162 MHz, $CDCl_3$, δ, ppm): 40.01.

5.2.3 Instrumentation:

Infrared spectra were recorded on a JASCO-5300 FT-IR spectrometer as KBr pellets. Elemental analysis was performed on a Flash EA Series 1112 CHNS analyzer. The solution phase ^{1}H and ^{31}P NMR spectra were recorded on a Bruker AVANCE^{III} 400 MHz instrument. Magnetic measurements were carried out using a Quantum Design MPMS-Xl SQUID magnetometer equipped with a 7 T magnet. Data was corrected for the diamagnetic contributions using Pascal constants. Single crystal X-ray data for compounds **5.1**-**5.3** was collected on a Bruker Smart Apex CCD area detector system with a graphite monochromator at 100(2) K. Data reduction was accomplished by using *SAINTPLUS* and the structures were solved and refined by using *SHELXS*-**97** and *SHELXL-2014/7* program respectively.[11] All non-hydrogen atoms were refined anisotropically and hydrogen atoms were fixed at calculated positions and refined as riding model. Details of the data collection and refinement parameters for **5.1**-**5.3** are given in Table 5.1. The disordered carbon atoms were constrained using EADP, ISOR, DELU instructions in SHELXL-2014/7. Disordered solvent accessible voids present in the asymmetric unit were removed by using the SQUEEZE[12] command in PLATON.[13]

5.3 Results and discussion

Synthetic procedure was adopted from literature reports. The hydrated lanthanum nitrates, *cyc*$PO_2H.2H_2O$ and triethylamine were reacted in methanol in 1:1:1 ratio under refluxion, yielding a clear solution which upon crystallization afforded colourless crystals. The product were characterized by standard analytical and spectroscopic techniques. The IR spectrum of **5.1**-**5.3** shows a characteristic band at around 2969 cm^{-1} corresponding to the Sp^3C-H stretching of the ligand and a peak around 1458cm^{-1} can be attributed to the nitrate anion. Further ^{31}P-NMR spectrum of **5.3** shows a signal at 40 ppm which corresponds to the presence of phosphorous atom in a unique environment.

Single crystal X-ray analysis of the crystals carried out at 100 K reveals that complexes **5.1**-**5.3** are structurally identical, crystallizes in monoclinic space group P2(1)/n. Due to their structural similarity, compound **5.1** (figure 5.1) is considered for detailed structural description. The structure can be visualized as follows; the eight Gd atoms can be

visualized to be present in the vertices of a cube connected through phosphinates and nitrates. To be more specific , if we can visualize the cube as sliced into two halves, four phosphinate ligands bridge the Ln(III) ions present in a square base. The two square faces are linked together by two sets of two phosphinates each along with NO_3 ions holding up the octanuclear cluster core. Six NO_3 ions are present in the cluster, one in each square face of the cube linking up the Gd(III) ions using a (μ_4- η^2: η^2: η^1) mode of bonding.

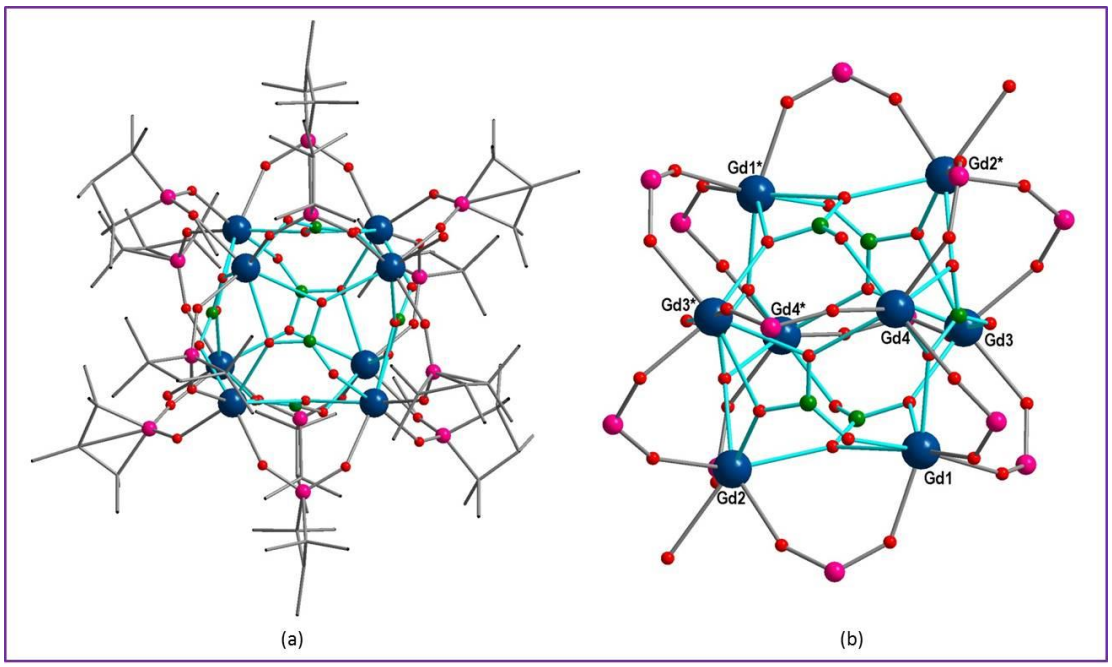

Figure 5.1. (a) Molecular structure of compound **5.1** (b) represents core of the cluster

The molecular structure can also be explained as follows: asymmetric unit consists of four Gd(III) ions bridged by four cyclic phosphinic acid molecules and a central nitrate anion (μ_4- η^2: η^2: η^1). Two more nitrate anions are present which bridge Gd2 with Gd3 and Gd3 with Gd4. In addition to this, two more cyclic phosphinic acids are present one each at Gd1 and Gd4 and a hydroxide ion is present at Gd2. All Gd(III) ions are hepta-coordinated by three oxygen atoms from two cyclic phosphinic acid and four oxygens from nitrate anions except for Gd2, which is coordinated by three oxygens from two cyclic phosphinic acid, three from nitrate anions and one hydroxide ion. For charge neutrality, oxygen atoms present outside the cluster core are considered as hydroxide anions. By doing the operation 1-x,-y+2,-z on O19, generates the complete molecule. Important bond metric parameters are listed as follows; Gd-$O_{(cycPO2H)}$, Gd-$O_{(nitrate)}$ and Gd-$O_{(OH^-)}$ distances are of the order of 2.24-2.31, 2.25-2.58 and 2.591 Å respectively. The Gd-O-Gd angles are in the range of 126.4-132.2° and the shortest intranuclear Gd…Gd distances are in the range of 4.28-4.60

Å. The coordination geometry around Gd(III) ions was calculated by using SHAPE 2.1 software[14] which is close to capped octahedron as shown in figure 5.2(b) (Table 5.2). Selected Bond distances (Å) and Bond angles (°) for **5.1** to **5.3** are given in Table 5.3-5.6

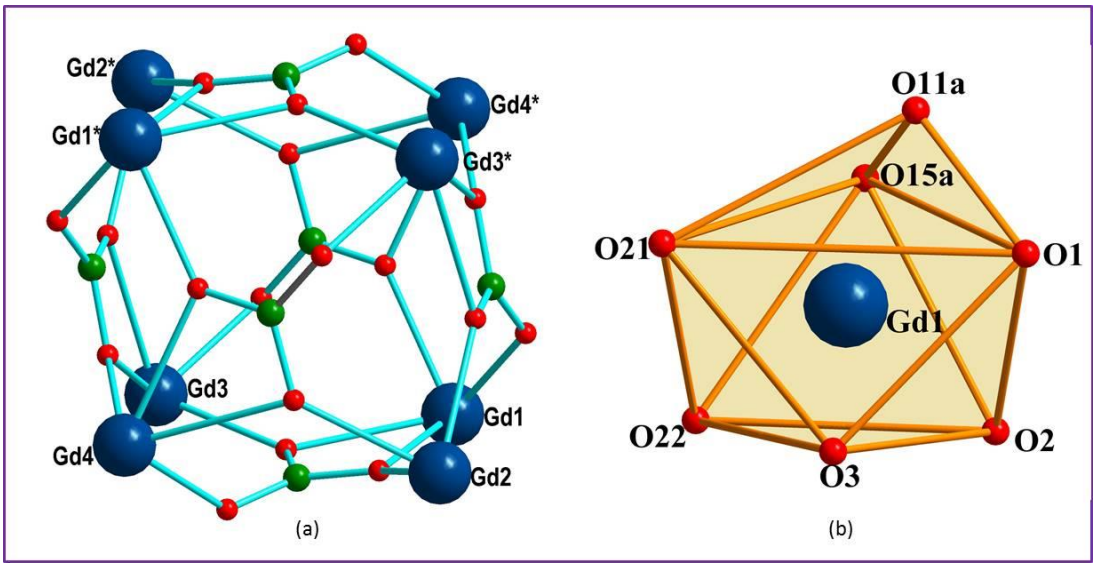

Figure 5.2. (a) Represents cubane core of **5.1** (b) coordination geometry around Gd1

5.4 Magnetic Measurements

Magnetic susceptibility of complexes **5.1** and 5.**2** were measured in an applied magnetic field of 1000 Oe over the temperature range of 300-2 K. The $\chi_M T$/8 Vs T plots are shown in figure 5.3. The observed $\chi_M T$ values are 7.75 and 14.15 cm^3 K mol^{-1} for **5.1** and **5.2** which are close to the theoretical value for one free Gd(III) ion (7.88 cm^3 K mol^{-1}; g = 2.0; S = 7/2; L = 0, $^8S_{7/2}$) and one Dy(III) ion (14.17 cm^3 K mol^{-1}; g = 4/3; S = 5/2; L = 5; $^6H_{15/2}$ for **2)** respectively. The $\chi_M T$ value remains constant for **5.1** up to 50 K and then decreases suddenly to 7.0 cm^3 K mol^{-1} at 2 K. In case of **5.2**, $\chi_M T$ value starts decreasing slowly up to 150 K and then decreases suddenly to 9.34 cm^3 K mol^{-1} at 2 K. The decrease at low temperature suggests antiferromagnetic interactions between adjacent metal ions.

$$\chi_{(\text{per Gd ion})} = [N\beta^2/3k(T-\theta)]S_{Gd}(S_{Gd}+1) \qquad (5.1)$$

where θ takes count of inter Gd-Gd interactions.

The temperature dependence of molar susceptibility for **5.1** is well fitted by Curie-Weiss law and the very small negative value of θ (-0.21 K) indicates antiferromagnetic interactions between Gd(III) ions. The observed antiferromagnetic interactions are most likely due to intermolecular interactions.

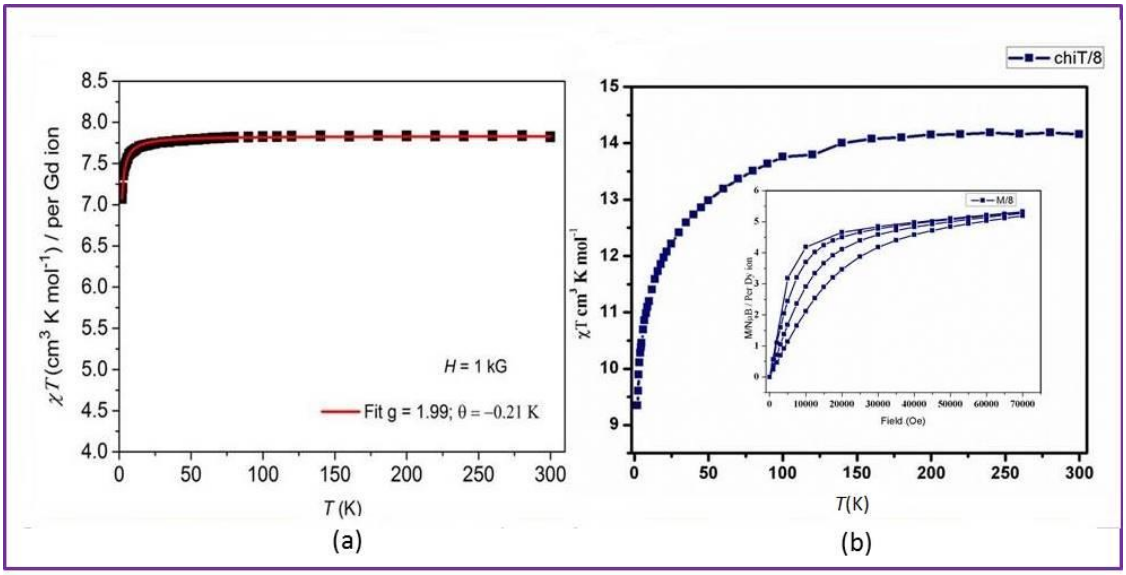

Figure 5.3. (a) and (b) Temperature dependence of the product of magnetic susceptibility and temperature for **5.1** and **5.2**

The M Vs H data for **5.1** and **5.2** was measured. The magnetization of **5.1** slowly increases and approaches 6.8 $N_{\mu B}$ at 70 KG which is close to the theoretical value 7 $N\mu_B$. Experimental magnetization superpose with Brillouin function which further supports antiferromagnetic interactions between metal ions [figure 5.4(a)]. In case of **5.2**, magnetization reaches a maximum of 5.3 $N\mu_B$ at 7.0 Tesla [figure 5.3(b) inset], which is significantly lower than the expected value 10 $N\mu_B$ per Dy(III) ion and is attributed to anisotropy associated with the metal ion.

Due to the presence of anisotropy in **5.2**, in order to check the magnetization relaxation dynamics, ac susceptibility measurements were performed. But this cluster does not show any sign of slow relaxation of the magnetization under zero filed or under an applied field suggesting the absence of retention of magnetization for these complexes.

In order to understand MCE efficiency of complex **5.1**, detailed isothermal measurements were performed from T = 3 to 10 K at 1-7 T applied field. To evaluate MCE efficiency,

change in magnetic entropy (-ΔS_m) and change in adiabatic temperature (ΔT_{ad}) are the two key parameters.

$$\Delta S_m(\mathrm{T},\mathrm{H}) = \int_{\mathrm{H_i}}^{\mathrm{H_f}} \left[\frac{\partial \mathrm{M}\ (\mathrm{T},\mathrm{H})}{\partial \mathrm{T}}\right]_{\mathrm{H}} \mathrm{dH} \qquad (5.2)$$

By making use of Maxwell thermodynamic relation -ΔS_m value can be obtained from the experimental magnetization data and the curves of -ΔS_m are shown in figure 5.4(b). The -ΔS_m value extracted by using Maxwell relation is reaching a maximum of 32 J Kg^{-1} K^{-1} for ΔH = 7 T at 2 K. As shown in figure 4(b), with increase in field -ΔS_m value increase gradually and decreases with increase in temperature. The obtained magnetic entropy change of complex **5.1** is at par with the value reported for Gd8-cluster[15] but it is slightly lower than the expected theoretical value 36.095 J Kg^{-1} K^{-1} calculated using nRln(2s+1) = 17.3 J mol^{-1} K^{-1} = 29.28 J Kg^{-1} K^{-1} per mole of Gd(III) involved, hence for 8 Gd(III) ions it is 138.4 J mol^{-1} K^{-1} or 36.095 J Kg^{-1} K^{-1}. The weak magnetic interactions and high magnetic density (M_w/ N_{Gd} = 479.27) is responsible for high MCE value for this complex.

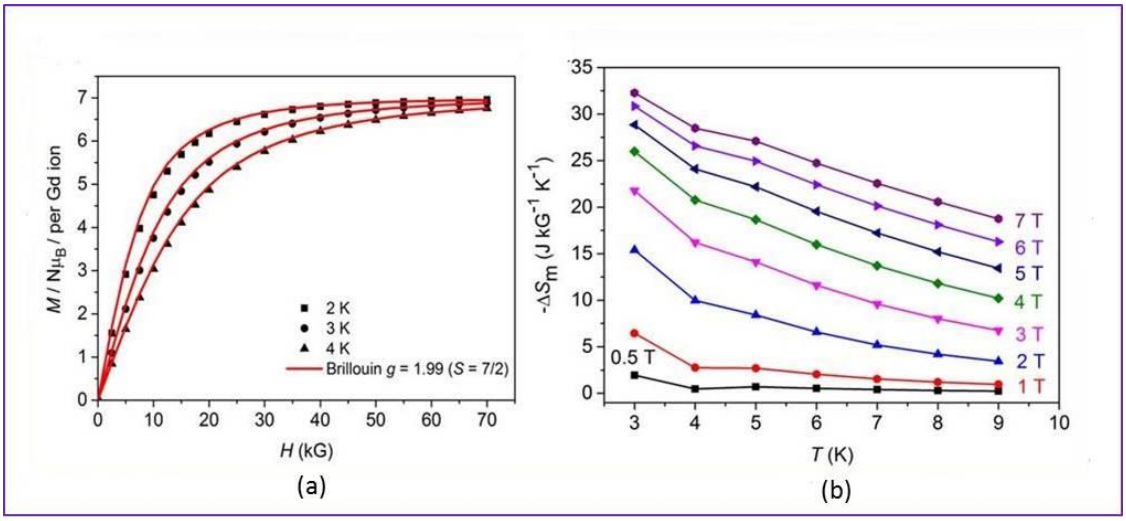

Figure 5.4. (a) Field dependence of magnetization for **5.1** (b) -ΔS_m calculated by using the magnetization data of **5.1** at different fields and temperatures.

5.5 Conclusion:

In conclusion, synthesis of three novel octanuclear organophosphinate lanthanide clusters was achieved successfully and the magnetic properties of Gd (**5.1**) and Dy(**5.2**) analogues were carried out. Magnetic studies reveal that **5.1** shows antiferromagnetic interactions and large MCE with -ΔS_m value 32 J Kg^{-1} K^{-1} for ΔH = 7 T at 2 K. Dynamics ac

susceptibility measurements reveal that Dy(III) analogue does not show any sign of slow relaxation of the magnetization under zero filed or under an applied field.The present study reveals that organophosphinate based lanthanide clusters possess significant potential to act as promising candidates for cryogenic magnetic refrigeration, which in turn necessitates further insights into this field .

Table 5.1. Crystal data and structure refinement for **5.1-5.3**

	5.1	**5.2**	**5.3**
Empirical formula	$C_{96}H_{198}N_6O_{48}P_{12}Gd_8$	$C_{96}H_{198}N_6O_{48}P_{12}Dy_8$	$C_{96}H_{198}N_6O_{48}P_{12}Y_8$
Fw.g mol^{-1}	3834.23	3876.23	3287.51
Crystal system	Monoclinic	Monoclinic	Monoclinic
Space group	P21/n	P21/n	P21/n
a/Å	17.891(3)	17.8216(13)	17.893(3)
b/Å	23.480 (3)	23.2829 (17)	23.443(4)
c/Å^3	18.511(3)	18. 4401(13)	18.448(3)
α (°)	90	90	90
β (°)	95.820(2)	95.9680(10)	95.351(6)
γ (°)	90	90	90
v/Å	7735.9(19)	7610.0(10)	7705(2)
Z	2	2	2
ρ_c/Mg m^{-3}	1.646	1.692	1.417
μ/mm^{-1}	3.574	4.074	3.173
F(000)	3784	3816	3384
θ range(°)	1.405 to 25.067	1.413 to 25.099	2.218 to 27.621
reflections collected	73925	73161	63745
Completeness to θ (%)	99.8	99.6	99.8
independent reflections/R_{int}	13684/ 0.0724	13481/0.1030	17108/0.0919
GooF(F^2)	1.079	1.061	1.071

Final R indices	R_1 = 0.0904	R_1 = 0.1009	R_1 = 0.1107
(I>2σ(I))	wR_2 = 0.1946	wR_2 = 0.2249	wR_2 = 0.2718
R indices (all data)	R_1 = 0.1180	R_1 = 0.1421	R1 = 0.1767
	wR_2 = 0.2113	wR_2 = 0.2497	wR2 = 0.3096

Table 5.2. Summary of **SHAPE** analysis for Gd1 in 5.**1**.

S. No.	Geometry	CShM value for Gd1
1	Heptagon (D7h)	31.708
2	Hexagonal pyramid (C6v)	21.069
3	Pentagonal bipyramid (D5h)	7.032
4	**Capped octahedron (C3v)**	**2.001**
5	Capped trigonal prism (C2v)	2.394
6	Johnson pentagonal bipyramid J13 (D5h)	10.357
7	Johnson elongated triangular pyramid J7 (C3v)	20.021

Table 5.3. Selected Bond distances (Å) and Bond angles (°) for **5.1**

Gd(1)-O(3)	2.244(10)	O(3)-Gd(1)-O(21)	83.7(6)	O(9)-Gd(2)-O(6)	131.0(4)
Gd(1)-O(21)	2.247(13)	O(3)-Gd(1)-O(2)	93.5(4)	O(22)-Gd(2)-O(6)	134.3(4)
Gd(1)-O(2)	2.275(10)	O(21)-Gd(1)-O(2)	172.1(4)	O(8)-Gd(3)-O(10)	82.7(6)
Gd(1)-O(1)	2.300(10)	O(3)-Gd(1)-O(1)	92.9(4)	O(8)-Gd(3)-O(13)	91.5(4)
Gd(1)-O(11)	2.341(16)	O(21)-Gd(1)-O(1)	82.9(4)	O(10)-Gd(3)-O(13)	173.2(6)
Gd(1)-O(15)	2.467(14)	O(2)-Gd(1)-O(1)	89.9(4)	O(8)-Gd(3)-O(12)	91.5(4)
Gd(1)-O(22)	2.557(12)	O(3)-Gd(1)-O(11)	157.2(6)	O(10)-Gd(3)-O(12)	85.4(7)
Gd(1)-N(2)	2.939(19)	O(21)-Gd(1)-O(11)	75.1(7)	O(13)-Gd(3)-O(12)	91.3(4)
Gd(2)-O(5)	2.239(12)	O(2)-Gd(1)-O(11)	106.4(6)	O(8)-Gd(3)-O(15)	160.0(4)
Gd(2)-O(7)	2.241(10)	O(1)-Gd(1)-O(11)	76.3(6)	O(10)-Gd(3)-O(15)	81.3(7)
Gd(2)-O(4)	2.281(10)	O(3)-Gd(1)-O(15)	115.9(5)	O(13)-Gd(3)-O(15)	103.7(5)
Gd(2)-O(9)	2.360(12)	O(21)-Gd(1)-O(15)	112.8(5)	O(12)-Gd(3)-O(15)	75.5(4)
Gd(2)-O(22)	2.396(11)	O(2)-Gd(1)-O(15)	75.1(4)	O(8)-Gd(3)-O(20)	113.1(4)
Gd(2)-O(19)	2.400(11)	O(1)-Gd(1)-O(15)	147.7(4)	O(10)-Gd(3)-O(20)	113.1(6)
Gd(2)-O(6)	2.603(14)	O(2)-Gd(1)-O(22)	109.4(4)	O(16)-Gd(4)-O(17)	82.4(6)
Gd(3)-O(8)	2.250(9)	O(1)-Gd(1)-O(22)	159.1(4)	O(16)-Gd(4)-O(18)	176.0(6)
Gd(3)-O(10)	2.271(19)	O(3)-Gd(1)-N(2)	97.6(5)	O(17)-Gd(4)-O(18)	93.6(4)
Gd(3)-O(13)	2.279(11)	O(21)-Gd(1)-N(2)	95.6(5)	O(16)-Gd(4)-O(14)	85.4(5)
Gd(3)-O(12)	2.301(11)	O(2)-Gd(1)-N(2)	92.1(5)	O(17)-Gd(4)-O(14)	92.3(4)
Gd(3)-O(15)	2.333(14)	O(1)-Gd(1)-N(2)	169.2(5)	O(18)-Gd(4)-O(14)	95.4(4)
Gd(3)-O(20)	2.417(11)	O(5)-Gd(2)-O(7)	115.0(5)	O(16)-Gd(4)-O(20)	76.1(6)
Gd(3)-O(19)	2.563(12)	O(5)-Gd(2)-O(4)	108.0(5)	O(17)-Gd(4)-O(20)	154.8(4)
Gd(4)-O(16)	2.233(14)	O(7)-Gd(2)-O(4)	107.0(4)	O(18)-Gd(4)-O(20)	107.9(4)
Gd(4)-O(17)	2.260(9)	O(5)-Gd(2)-O(9)	74.4(5)	O(14)-Gd(4)-O(20)	73.3(4)
Gd(4)-O(18)	2.275(11)	O(7)-Gd(2)-O(9)	93.3(6)	Gd(1)-O(11)-Gd(4)	126.0(8)
Gd(4)-O(14)	2.308(14)	O(4)-Gd(2)-O(9)	155.3(4)	Gd(3)-O(20)-Gd(4)	128.9(4)
Gd(4)-O(20)	2.433(10)	O(5)-Gd(2)-O(22)	91.1(4)	Gd(3)-O(15)-Gd(1)	126.6(6)
Gd(4)-O(11)	2.54(2)	O(7)-Gd(2)-O(22)	150.4(4)	Gd(2)-O(22)-Gd(1)	131.7(5)
Gd(4)-O(9)	2.743(19)	O(4)-Gd(2)-O(22)	75.4(4)	Gd(2)-O(19)-Gd(3)	128.7(5)
Gd(4)-N(3)	2.90(3)	O(5)-Gd(2)-O(19)	152.1(5)	Gd(2)-O(9)-Gd(4)	128.5(7)

Table 5.4. Selected Bond distances (Å) and Bond angles (°) for **5.2**

Dy(1)-O(21)	2.167(15)	O(21)-Dy(1)-O(1)	84.3(5)	O(13)-Dy(3)-O(22)	89.3(5)
Dy(1)-O(1)	2.254(13)	O(21)-Dy(1)-O(3)	81.0(6)	O(15)-Dy(3)-O(22)	76.7(6)
Dy(1)-O(3)	2.257(12)	O(1)-Dy(1)-O(3)	93.1(5)	O(10)-Dy(3)-O(20)	113.6(7)
Dy(1)-O(2)	2.267(12)	O(21)-Dy(1)-O(2)	170.4(5)	O(8)-Dy(3)-O(20)	114.9(6)
Dy(1)-O(11)	2.32(3)	O(1)-Dy(1)-O(2)	88.5(5)	O(13)-Dy(3)-O(20)	74.9(6)
Dy(1)-O(15)	2.460(19)	O(3)-Dy(1)-O(2)	93.0(5)	O(15)-Dy(3)-O(20)	81.5(7)
Dy(1)-O(12)	2.541(15)	O(21)-Dy(1)-O(11)	77.2(8)	O(15)-Dy(3)-O(19)	108.6(6)
Dy(1)-N(2)	2.944(19)	O(21)-Dy(1)-O(15)	114.5(6)	O(22)-Dy(3)-O(19)	159.4(5)
Dy(2)-O(5)	2.191(13)	O(1)-Dy(1)-O(15)	146.9(6)	O(20)-Dy(3)-O(19)	49.6(6)
Dy(2)-O(7)	2.220(12)	O(21)-Dy(1)-N(2)	95.9(5)	O(16)-Dy(4)-O(17)	82.8(5)
Dy(2)-O(4)	2.244(11)	O(1)-Dy(1)-N(2)	170.1(5)	O(16)-Dy(4)-O(18)	175.9(5)
Dy(2)-O(9)	2.327(17)	O(3)-Dy(1)-N(2)	96.7(5)	O(17)-Dy(4)-O(18)	93.3(5)
Dy(2)-O(19)	2.370(13)	O(2)-Dy(1)-N(2)	92.2(5)	O(16)-Dy(4)-O(14)	84.4(5)
Dy(2)-O(12)	2.387(15)	O(5)-Dy(2)-O(7)	115.7(6)	O(17)-Dy(4)-O(14)	92.8(5)
Dy(2)-O(6)	2.561(16)	O(5)-Dy(2)-O(4)	107.9(5)	O(18)-Dy(4)-O(14)	94.4(5)
Dy(3)-O(10)	2.176(19)	O(7)-Dy(2)-O(4)	107.8(5)	O(16)-Dy(4)-O(20)	76.6(7)
Dy(3)-O(8)	2.230(11)	O(5)-Dy(2)-O(9)	73.0(6)	O(17)-Dy(4)-O(20)	157.1(6)
Dy(3)-O(13)	2.265(13)	O(7)-Dy(2)-O(9)	94.2(6)	O(18)-Dy(4)-O(20)	106.9(6)
Dy(3)-O(15)	2.284(19)	O(4)-Dy(2)-O(9)	154.1(5)	O(14)-Dy(4)-O(20)	75.4(6)
Dy(3)-O(22)	2.288(15)	O(5)-Dy(2)-O(19)	152.1(5)	O(20)-Dy(4)-O(9)	107.1(6)
Dy(3)-O(20)	2.41(2)	O(7)-Dy(2)-O(19)	73.4(5)	O(14)-Dy(4)-O(9)	157.9(5)
Dy(3)-O(19)	2.556(15)	O(4)-Dy(2)-O(19)	92.8(5)	O(18)-Dy(4)-O(11)	79.9(7)
Dy(4)-O(16)	2.167(16)	O(9)-Dy(2)-O(19)	80.3(5)	Dy(1)-O(11)-Dy(4)	127.6(13)
Dy(4)-O(17)	2.246(14)	O(5)-Dy(2)-O(12)	91.2(6)	Dy(3)-O(15)-Dy(1)	126.8(9)
Dy(4)-O(18)	2.265(15)	O(9)-Dy(2)-O(6)	130.2(5)	Dy(2)-O(12)-Dy(1)	131.0(6)
Dy(4)-O(14)	2.297(16)	O(10)-Dy(3)-O(8)	83.7(6)	Dy(2)-O(19)-Dy(1)	128.2(6)
Dy(4)-O(20)	2.41(2)	O(10)-Dy(3)-O(13)	171.3(6)	Dy(4)-O(20)-Dy(3)	129.3(9)
Dy(4)-O(11)	2.50(3)	O(8)-Dy(3)-O(13)	91.1(4)	Dy(2)-O(9)-Dy(4)	129.3(7)

Table 5.5. Selected Bond distances (Å) and Bond angles (°) for **5.3**

Y(1)-O(5)	2.169(9)	O(5)-Y(1)-O(16)	84.3(5)	O(1)-Y(3)-O(18)	92.0(4)
Y(1)-O(16)	2.216(7)	O(5)-Y(1)-O(4)	81.0(6)	O(14)-Y(3)-O(18)	154.7(3)
Y(1)-O(4)	2.255(8)	O(16)-Y(1)-O(4)	93.1(5)	O(12)-Y(3)-O(8)	92.0(3)
Y(1)-O(9)	2.264(8)	O(5)-Y(1)-O(9)	170.4(5)	O(1)-Y(3)-O(8)	149.0(3)
Y(1)-O(20)	2.306(9)	O(16)-Y(1)-O(9)	88.5(5)	O(14)-Y(3)-O(8)	74.9(3)
Y(1)-O(21)	2.456(10)	O(4)-Y(1)-O(9)	93.0(5)	O(18)-Y(3)-O(8)	80.0(4)
Y(1)-O(8)	2.551(9)	O(5)-Y(1)-O(20)	77.2(8)	O(12)-Y(3)-O(23)	151.5(3)
Y(1)-N(3)	2.937(9)	O(16)-Y(1)-O(20)	114.5(6)	O(1)-Y(3)-O(23)	73.1(3)
Y(2)-O(17)	2.135(10)	O(4)-Y(1)-O(20)	146.9(6)	O(7)-Y(4)-O(11)	82.7(3)
Y(2)-O(2)	2.211(6)	O(9)-Y(1)-O(20)	95.9(5)	O(7)-Y(4)-O(10)	175.2(3)
Y(2)-O(19)	2.250(8)	O(5)-Y(1)-O(21)	113.9(3)	O(11)-Y(4)-O(10)	93.1(3)
Y(2)-O(3)	2.266(9)	O(16)-Y(1)-O(21)	116.8(4)	O(7)-Y(4)-O(15)	84.8(3)
Y(2)-O(21)	2.298(8)	O(17)-Y(2)-O(2)	84.0(4)	O(11)-Y(4)-O(15)	92.2(3)
Y(2)-O(6)	2.451(11)	O(17)-Y(2)-O(19)	170.4(4)	O(10)-Y(4)-O(15)	93.0(3)
Y(2)-O(23)	2.555(9)	O(2)-Y(2)-O(19)	90.5(3)	O(7)-Y(4)-O(6)	77.7(4)
Y(2)-N(1)	2.926(9)	O(17)-Y(2)-O(3)	82.2(4)	O(11)-Y(4)-O(6)	158.1(3)
Y(3)-O(12)	2.197(7)	O(2)-Y(2)-O(3)	91.4(3)	O(10)-Y(4)-O(6)	105.9(3)
Y(3)-O(1)	2.220(7)	O(19)-Y(2)-O(3)	90.1(3)	O(15)-Y(4)-O(6)	76.3(4)
Y(3)-O(14)	2.227(7)	O(17)-Y(2)-O(21)	80.4(4)	O(7)-Y(4)-O(20)	104.8(4)
Y(3)-O(18)	2.311(8)	O(2)-Y(2)-O(21)	161.3(3)	O(11)-Y(4)-O(20)	117.7(3)
Y(3)-O(8)	2.342(8)	O(19)-Y(2)-O(21)	103.4(3)	O(10)-Y(4)-O(20)	79.2(4)
Y(3)-O(23)	2.370(7)	O(4)-Dy(2)-O(19)	92.8(5)	Y(2)-O(23)-Y(2)	128.3(4)
Y(3)-O(13)	2.509(9)	O(19)-Y(2)-O(23)	107.7(3)	Y(1)-O(11)-Y(4)	127.6(13)
Y(4)-O(7)	2.183(9)	O(3)-Y(2)-O(23)	159.6(3)	Y(4)-O(6)-Y(2)	128.2(4)
Y(4)-O(11)	2.215(6)	O(21)-Y(2)-O(23)	108.0(4)	Y(1)-O(20)-Y(4)	125.2(5)
Y(4)-O(10)	2.257(9)	O(12)-Y(3)-O(1)	114.9(3)	Y(3)-O(8)-Y(1)	131.2(4)
Y(4)-O(15)	2.290(10)	O(12)-Y(3)-O(14)	108.6(3)	Y(3)-O(18)-Y(4)	125.2(5)

5.6 References

(1) (a) Sessoli, R.; Gatteschi, D.; Caneschi, A.; Novak, M. A. *Nature* **1993**, *365*, 141. (b) Murrie, M. *Chem. Soc. Rev*. **2010**, *39*, 1986. (c) Woodruff, D. N.; Winpenny, R. E. P.; Layfield, R. A. *Chem. Rev*. **2013**, *113*, 5110. (d) Zhang, P.; Guo Y.-N.; Tang, J.

Coord. *Chem. Rev*. **2013**, *257*, 1728. (e) Ishkawa, N.; Sugita, M.; Ishikawa, T.; Koshihara, S. Kaizu, Y. *J. Am. Chem. Soc*. **2003**, *125*, 8694. (f) Branzoli, F.; Carretta, P.; Filibian, M. Zoppellaro, G.; Graf, M. J.; Galan-Mascaros, J. R.; Fuhr, O.; Brink, S.; Ruben, M. *J. Am. Chem. Soc*. **2009**, 131, 4387. (g) Gonidec, M.; Amabilino, D.; Veciana, J. *Dalton Trans*. **2012**, *41*, 13632 (h) Ishikawa, N.; Sugita, M.; Tanaka, N.; Ishikawa, T.; Koshihara, S.; Kaizu, Y. *Inorg. Chem*. **2004**, *43*, 5498. (i) Veits, G. K.; Read de Alaniz, J. *Tetrahedron* **2012**, ***68***, 2015. (j) Eliseeva, S. V. Bunzli, J.-C. *Chem. Soc. Rev*. **2010**, *39*, 189. (k) Heffern, M. C.; Matosziuk, L. M.; Meade, T. J. *Chem. Rev*. **2014**, *114*, 4496.

(2) (a) Chang, L.-X.; Xiong, G.; Wang, L.; Cheng, P.; Zhao, B. *Chem. Commun*. **2013**, *49*, 1055. (b) Biswas, S.; Adhikary, A.; Goswami, S.; Konar, S. *Dalton Trans*. **2013**, *42*, 13331. (c) Yang, Y.; Zhang, Q.-C.; Pan, Y.-Y.; Long, L.-S.; Zheng, L.-S. *Chem. Commun*. **2015**, *51*, 7317. (d) Adhikary, A.; Sheikh, J. A.; Biswas, S.; Konar, S. *Dalton Trans*. **2014**, *43*, 9334. (e) Peng, J.-B.; Kong, X.-J.; Zhang, Q.-C.; Orendáč, M.; Prokleška, J.; Ren, Y.-P.; Long, L.-S.; Zheng, Z.; Zheng, L.-S. *J. Am. Chem. Soc*. **2014**, *136*, 17938 (f) Biswas, S.; Jena, H. S.; Adhikary, A.; Konar, S. *Inorg. Chem*. **2014**, *53*, 3926. (g) Roubeau, O.; Lorusso, G.; Teat, S. J.; Evangelisti, M. *Dalton Trans*. **2014**, *43*, 11502. (h) Liu, S.-J.; Zhao, J.-P.; Tao, J.; Jia, J.-M.; Han, S.-D.; Li, Y.; Chen, Y.-C.; Bu, X.-H. *Inorg. Chem*. **2013**, *52*, 9163. (i) Liu, S.-J.; Xie, C.-C.; Jia, J.-M.; Zhao, J.-P.; Han, S.-D.; Cui, Y.; Li, Y.; Bu, X.-H. *Chem. – Asian J*. **2014**, 9, 1116.

(3) (a) Meng, Y.; Chen, Y.-C.; Zhang, Z.-M.; Lin, Z.-J.; Tong, M.-L. *Inorg. Chem*. **2014**, *53*, 9052. (b) Sharples, J. W.; Zheng, Y.-Z.; Tuna, F.; McInnes, E. J. L.; Collison, D. *Chem*. *Commun*. **2011**, *47*, 7650.

(4) a) Torres, F.; Hernndez, J. M.; Bohigas, X.; Tejada, J. *Appl. Phys. Lett*. **2000**, ***77***, 3248. b) Manoli, M.; Johnstone, R. D. L.; Parsons, S.; Murrie, M.; Affronte, M.; Evangelisti, M.; Brechin, E. K. *Angew. Chem. Int. Ed*., **2007**, *119*, 4540; Angew. Chem. Int. Ed. 2007, **46**, 4456. c) Manoli, M.; Collins, A.; Parsons, S.; Candini, A.; Evangelisti, M.; Brechin, E. K.; J. *Am. Chem. Soc*. **2008**, *130*, 11129. d) Nayak, S.; Evangelisti, M.; Powell, A. K.; Reedijk, J.; *Chem. Eur. J*. **2010**, *16*, 12865. b) Evangelisti, M.; Candini, A.; Ghirri, A.; Affronte, M.; Brechin, E. K.; McInnes, E. J. L. *Appl. Phys. Lett*. **2005**, *87*, 072504. e) Shaw, R.; Laye, R. H.; Jones, L. F.; Low, D. M.; Talbot-Eeckelaers, C.; Wei, Q.; Milios, C. J.; Teat, S.; Helliwell, M.; Raftery, J.;

Evangelisti, M.; Affronte, M.; Collison, D.; Brechin, E. K.; McInnes, E. J. *Inorg. Chem.* **2007**, *46*, 4968. f) Evangelisti, M.; Roubeau, O.; Palacios, E.; Camon, A.; Hooper, T. N.; Brechin, E. K.; Alonso, J. J. *Angew. Chem.* **2011**, *123*, 6736; *Angew. Chem. Int. Ed.* **2011**, *50*, 6606. g) Guo, F. S.; Leng, J. D.; Liu, J. L.; Meng, Z. S.; Tong, M. L. *Inorg. Chem.* **2012**, *51*, 405. h) Sharples, J. W.; Zheng, Y. Z.; Tuna, F.; McInnes, E. J.; Collison, D. *Chem. Commun*. **2011**, *47*, 7650. i) Sedláková, L.; Hanko, J.; Orendáčová, A.; Orendáč, M.; Zhou, C. L.; Zhu, W. H.; Wang, B. W.; Wang, Z. M.; Gao, S. *J. Alloys Compd*. **2009**, *487*, 425. j) Lorusso, G.; Palacios, M. A.; Nichol, G. S.; Brechin, E. K.; Roubeau, O.; Evangelisti, M. *Chem. Commun*. **2012**, *48*, 7592.

(5) a) Cremades, E.; Gomez-Coca, S.; Aravena, D.; Alvarez, S.; Ruiz, E. *J. Am. Chem. Soc*. **2012**, *134*, 10532. (b) Hooper, T. N.; Schnack, J.; Piligkos, S.; Evangelisti, M.; Brechin, E. K. *Angew. Chem. Int. Ed*. **2012**, *51*, 4633. (c) Karotsis, G.; Evangelisti, M.; Dalgarno, S. J.; Brechin, E. K. *Angew. Chem. Int. Ed*. **2009**, *121*, 10112. (d) Karotsis, G.; Kennedy, S.; Teat, S. J.; Beavers, C. M.; Fowler, D. A.; Morales, J. J.; Evangelisti, M.; Dalgarno, S. J.; Brechin, E. K. *J. Am. Chem. Soc*. **2010**, *132*, 12983. (e) Birk, T.; Pedersen, K. S.; Thuesen, C. A.; Weyhermuller, T.; Schau-Magnussen, M.; Piligkos, S.; Weihe, H.; Mossin, S.; Evangelisti, M.; Bendix, J.; *Inorg. Chem*. **2012**, *51*, 5435. (f) Langley, S. K.; Chilton, N. F.; Moubaraki, B.; Hooper, T.; Brechin, E. K.; Evangelisti, M.; Murray, K. S. *Chem. Sci*. **2011**, *2*, 1166. b) Leng, J. D.; Liu, J. L.; Tong, M. L. *Chem. Commun*. **2012**, *48*, 5286.

(6) (a) Biswas, S.; Adhikary, A.; Goswami, S.; Konar, S. *Dalton Trans*. **2013**, *42*, 13331. (b) Chen, Y.-C.; Guo, F.-S.; Zheng, Y.-Z.; Liu, J.-L.; Leng, J.-D.; Tarasenko, R.; Orendáč, M.; Prokleška, J.; Sechovský, V.; Tong, M.-L. *Inorg. Chem. Front*. **2013**, *19*, 13504. (c) Hou, Y.-L.; Xiong, G.; Shi, P.-F.; Cheng, R.-R.; Cui, J.-Z.; Zhao, B. *Chem. Commun*. **2013**, *49*, 6066. (d) Lorusso, G.; Sharples, J. W.; Palacios, E.; Roubeau, O.; Brechin, E. K.; Sessoli, R.; Rossin, A.; Tuna, F.; McInnes, E. J. L.; Collison, D.; Evangelisti, M. *Adv. Mater*. **2013**, *25*, 4653. (e) Han, S.-D.; Miao, S.-H.; Liu, S.-J.; Bu, X.-H. *Inorg. Chem. Front*. **2014**, *1*, 549. (f) Chen, Y.-C.; Qin, L.; Meng, Z.-S.; Yang, D.-F.; Wu, C.; Fu, Z.; Zheng, Y.-Z.; Liu, J.-L.; Guo, F.-S.; Tarasenko, R.; Orendáč, M.; Prokleška, J.; Sechovsk, V.; Tong, M.-L. *J. Mater. Chem*. **2014**, *A2*, 9851.

(7) (a) Guo, F.-S.; Leng, J.-D.; Liu, J.-L.; Meng, Z.-S.; Tong, M.-L. *Inorg. Chem*. **2011**, *51*, 405. (b) Guo, F.-S.; Leng, J.-D.; Liu, J.-L.; Meng, Z.-S.; Tong, M.-L. *Inorg. Chem*. **2011**, *51*, 405. (c) Lorusso, G.; Palacios, M. A.; Nichol, G. S.; Brechin, E. K.;

Roubeau, O.; Evangelisti, M. *Chem. Commun*. **2012**, *48*, 7592. (d) Evangelisti, M.; Roubeau, O.; Palacios, E.; Camón, A.; Hooper, T. N.; Brechin, E. K.; Alonso, J. J. *Angew. Chem., Int. Ed*., **2011**, *123*, 6736. (e) Liu, S.-J.; Zhao, J.-P.; Tao, J.; Jia, J.-M.; Han, S.-D.; Li, Y.; Chen, Y.-C.; Bu, X.-H. *Inorg. Chem*. **2013**, *52*, 9163. (f) Guo, F.-S.; Chen, Y.-C.; Liu, J.-L.; Leng, J.-D.; Meng, Z.-S.; Vrabel, P.; Orendac, M.; Tong, M.-L. *Chem. Commun*. **2012**, *48*, 12219. (g) Chang, L.-X.; Xiong, G.; Wang, L.; Cheng, P.; Zhao, B. *Chem. Commun*. **2013**, *49*, 1055. (h) Zangana, K. H.; Pineda, E. M.; Schnack, J.; Winpenny, R. E. P. *Dalton Trans*. **2013**, *42*, 14045. (i) Lorusso, G.; Sharples, J. W.; Palacios, E.; Roubeau, O.; Brechin, E. K.; Sessoli, R.; Rossin, A.; Tuna, F.; McInnes, E. J. L.; Collison, D.; Evangelisti, M. *Adv. Mater*. **2013**, *25*, 4653.

(8) Tolis, E. I.; Engelhardt, L. P.; Mason, P. V.; Rajaraman, G.; Kindo, K.; Luban, M.; Matsuo, A.; Nojiri, H.; Raftery, J.; Scroder, C.; Timco, G. A.; Tuna, F.; Wernsdorfer, W.; Winpenny, R. E. P. *Chem. – Eur*. J. **2006**, *12*, 8961.

(9) Gupta, S. K.; Dar, A. A.; Rajeshkumar, T.; Kuppuswamy, S.; Langley, S. K.; Murray, K. S.; Rajaraman, G.; Murugavel, R. *Dalton Trans*. **2015**, *44*, 5961.

(10) McBride, J. J.; Jungermann, E.; Killheffer, J. V.; Clutter, R. J. *J. Org. Chem*. **1962**, *27*, 1833.

(11) (a) *SAINT Software Reference manuals*, Version 6.45; Bruker Analytical X-ray Systems, Inc.: Madison, WI, 2003. (b) Sheldrick, G. M. *SHELXS-97, Program for Crystal Structure Solution;* University of Göttingen: Göttingen, Germany, **1997**. (c) Sheldrick, G. M. *Acta Crystallogr., Sect. A: Fundam. Crystallogr*. **2008**, *64*, 112. (d) G. M. Sheldrick, *Acta Crystallogr., Sect. C: Cryst. Struct. Commun*. **2015**, *71*, 3.

(12) Van der Sluis, P.; Spek, A. L. BYPASS: an effective method for the refinement of crystal structures containing disordered solvent regions, *Acta Crystallogr*., *Sect. A*: Fundam. Crystallogr., **1990**, *46*, 194.

(13) (a) Spek, A. L. Single-crystal structure validation with the program PLATON, *J. Appl*. *Crystallogr*. **2003**, *36*, 7 (b) Spek, A. L.; Structure validation in chemical crystallography, *Acta Crystallogr*. *Sect. D*: *Biol. Crystallogr*. **2009**, *65*, 148.

(14) (a) Alvarez, S.; Alemany, P.; Casanova, D.; Cirera, J.; Llunell, M.; Avnir, D. *Coord. Chem. Rev*. **2005**, *249*, 1693. (b) Casanova, D.; Llunell, M.; Alemany, P.; Alvarez, S.; *Chem. –Eur. J*. **2005**, *11*, 1479.

(15) Zangana, K. H.; Pineda, E. M.; Schnack, J.; Winpenny, R. E. P. *Dalton Trans*. **2013**, *42*,14045.

Future Scope of the Thesis

This Thesis demonstrates the synthesis, structural characterization and magnetic properties of lanthanide oxo/hydroxo clusters resulting from functionalized β-diketones (in presence/absence of coligands), triketones and phosphinic acid with lanthanide metal salts.

Chapter 2. Treatment of ortho-substituted β-diketone with lanthanum halides resulted in isolation of novel hexanuclear clusters templated by carbonate anion. This study offers new pathways for designing novel carbonate bridged lanthanum clusters by introducing varying functionality at ortho position of β-diketones. It would also be interesting to study lanthanide based systems which could be used to reversibly bind CO_2 or HCO_3^- ions. This in turn can have profound impact on keeping a check over increasing levels of CO_2 in atmosphere.

Chapter 3. Di and tetranuclear (distorted cubane type) lanthanide clusters were isolated and their magnetic properties were studied in detail. This study can be extended further by using different coligands with functionalized β-diketones.

Chapter 4. Use of triketones as ligands resulted in isolation of tetranuclear (defect dicubane core) lanthanide clusters. Present study can be exploited further by- changing substituents on triketones, introducing one more oxo group on triketone or by changing co-ligand and one more interesting variation would be to move towards cyclic polyketones. These variations can give rise to various novel lanthanide clusters for further studies.

Chapter 5. Isolation of novel octanuclear lanthanide clusters resulted by treating phosphinic acid with lanthanum nitrates is described. Magnetic studies reveal the MCE property of Gd(III) cluster. Scope of this study can be elaborated by using different phosphinic acids which can give rise to novel structural entities with diverse nuclearities and interesting magnetic properties.

In broader perspective, the work demonstrated here can be further elaborated to have deeper insights into the magnetic potential of new lanthanide clusters for their applications in SMMs and Magnetic refrigerants.

List of Publications

[1] Redox shield enfololding magnetic core
Pilli.V.V.N Kishore, **Amaleswari Rasamsetty**, E.C.Sañudo and V. Baskar. *Polyhedron* **2015**, *102*, 361.

[2] Hexanuclear Lanthanide Clusters Encapsulating a μ_6-CO_3^{2-} Ion Displaying an Unusual Binding Mode
Amaleswari Rasamsetty, E. Carolina Sañudo and V. Baskar *ChemistrySelect* **2016**, *1*, 3323.

[3] Effect of coordination geometry on the magnetic properties of a series of Ln_2 and Ln_4 hydroxo clusters
Amaleswari Rasamsetty, Chinmoy Das, E. Carolina Sañudo, Maheswaran Shanmugam and Viswanathan Baskar (*Manuscript to be submitted*).

[4] Triketone Assisted Self-Assembly of Lanthanide oxo/hydroxo Clusters: Synthesis, Structure and Magnetic measurements
Amaleswari Rasamsetty, Ana-Maria Ariciu, Floriana Tuna, and Viswanathan Baskar (*Manuscript under preparation*).

[5] Unprecedented Octanuclear Ln(III) Clusters: Synthesis, Structure and Magnetic measurements
Amaleswari Rasamsetty, Ana-Maria Ariciu, Floriana Tuna, and Viswanathan Baskar (*Manuscript under preparation*).

Poster and Oral Presentations / Workshops

[1] Presented Poster entitled "Hexanuclear lanthanide clusters encapsulating a μ_6-CO_3^{2-} ion displaying an unusual binding mode" at **Chemfest-2015**, 12th Annual In-House Symposium, February-2015, University of Hyderabad.

[2] Oral and Poster Presentation on "Effect of coordination geometry on the magnetic properties of a series of Di and Tetra nuclear clusters" at **Modern Trends in Molecular Magnets (MTMM)**, May-2016, IIT Bombay, India.

[3] Attended **Workshop on Electronic Structure of Coordination Complexes (WESCC)**, May-2016, IIT Bombay, India.